UNIVERSITY OF OKLAHOMA

GRADUATE COLLEGE

STATEWIDE ASSESSMENT OF CO2 STORAGE RESOURCES FOR THE LOWER PALEOZOIC STRATA, OKLAHOMA

A DISSERTATION

SUBMITTED TO THE GRADUATE FACULTY

In partial fulfillment of the requirements for the

Degree of

DOCTOR OF PHILOSOPHY

By

ANNA TURNINI

Norman, Oklahoma

2025

STATEWIDE ASSESSMENT OF CO2 STORAGE RESOURCES FOR THE LOWER PALEOZOIC STRATA, OKLAHOMA

A DISSERTATION APPROVED FOR THE
SCHOOL OF GEOSCIENCES

BY THE COMMITTEE CONSISTING OF

Dr. Matthew J. Pranter, Chair

Dr. Heather Bedle

Dr. Brett Carpenter

Dr Deepak Devegowda

©Copyright by Anna Turnini 2025 All Rights Reserved.

Acknowledgements

First and foremost, I would like to thank my advisor, Dr. Matt Pranter. Thank you for the guidance, advice, and willingness to work with me again for this PhD. Thank you for keeping me on track to graduate and for your patience with the seemingly endless dissertation drafts I have sent you. I would also like to thank my fellow committee members, Dr. Heather Bedle, Dr. Brett Carpenter, and Dr. Deepak Devegowda, for their contribution to this dissertation and my educational journey.

Additionally, I would like to acknowledge the many amazing geoscientists that I have worked with in my career who have also been a wealth of knowledge, encouragement, and support. They have all played a part in my journey towards this PhD. This includes Kathy Bridges, Robert Vick, Steve Ladner, William "Bill" Clement, Lloyd Scheidt, Greg Cwayna, Lori Bryan, John Drake, and Craig Peck.

I would also like to thank my family, especially my husband Jimmy, who has been my number one fan and my biggest supporter while working towards this PhD. Thank you for believing in me and encouragement over these last 4 years. I could not have done this without you.

I would also like to thank my children, Ella and Victor. May you always remember that you are never too old to go back to school. Education is a lifelong journey filled with opportunities. Never underestimate your potential and always strive for your dreams!

Table of Contents

Acknowledgements……...iv

Table of Contents……v

List of Figures……....x

List of Tables…….…….....xx

List of Units and Abbreviations……xxi

Abstract……..……..xxiii

Introduction……1

Chapter 1: Data Collection and Subsurface Mapping……..4

Chapter 2: The Statewide variability of mineralogy, pore volume, and CO_2 storage resources for the Timbered Hills and Arbuckle groups, Oklahoma

Abstract……..12

Introduction……13

Geologic Setting……15

Methods……18

Subsurface Mapping……18

Derived Petrophysical Logs……..20

3-D Modeling and CO_2 Storage Resources Estimation..……...22

Induced Seismicity Risk……25

Results……25

Structure, Thickness, and Lithology Trends……..25

Petrophysical Properties……29

CO_2 Storage Resources..……30

Induced Seismicity Risk……31

Discussion……..33

CO_2 Storage Resources Calculations……33

Areas of Interest……34

Conclusions……36

Figures……38

Tables…….57

Acknowledgements……59

References……..60

Chapter 3: The Statewide variability of mineralogy, pore volume, and CO_2 storage resources for the Viola Limestone and Simpson Group, Oklahoma

Abstract……..64

Introduction…….……...65

Geologic Setting……67

Methods……..70

Subsurface Mapping…….…….70

Derived Petrophysical Logs…….……..71

3-D Modeling and CO_2 Storage Resources Estimation..……...73

Results……76

Structure, Thickness, and Lithology Trends……..……76

Petrophysical Properties…….……79

CO_2 Storage Resources..…….....81

Discussion……..……82

CO_2 Storage Resources Calculations……82

Areas of Interest……83

Conclusions……..……..84

Figures……85

Tables…….....99

Acknowledgements…….…….101

References……..…..102

Chapter 4: The Statewide variability of mineralogy, pore volume, and CO_2 storage resources for the Hunton Group, Oklahoma

Abstract……104

Introduction…….....105

Geologic Setting……...107

Stratigraphy and Lithology……..107

Dolomite……..111

Porosity……..…..112

Methods……..…..112

Subsurface Mapping……....112

Machine Learning to generate Photoelectric (PEF) Logs……114

Derived Petrophysical Logs……114

3-D Modeling and CO_2 Storage Resources Estimation..…….116

Results……..119

Machine Learning……119

Structure, Thickness, and Lithology Trends……121

Petrophysical Properties……...123

CO_2 Storage Resources..……..124

Discussion……....125

CO_2 Storage Resources Calculations……...125

Areas of Interest……..126

Lower Paleozoic CO_2 Storage Resources Comparison……..127

Conclusions…….…….128

Figures……..…130

Tables…….…….149

Acknowledgements……..151

References……..…..…152

Conclusions……..……...155

Appendix……...…..158

Appendix A: Regional cross sections and oversized maps……..158

Appendix B: 3-D Model Parameters……..…..178

Appendix C: Arbuckle Core Description and Petrophysics ……187

List of Figures

Figure 1.1. Study area and wells with LAS used in the study. Purple circles are the wells with LAS available used in the study. Red squares are wells with full Arbuckle penetration, and LAS used in the study. Orange circles are all the Arbuckle Group tops from well log interpretation. Small, light blue well spots have well tops for the Mississippian. Geologic Provinces were modified from Northcutt and Campbell, 1995. The Ardmore basin, Marietta basin, and Hollis basin were not evaluated due to structural complexities. The Ozark Uplift was evaluated where depths were adequate. Locations for the Shad 4, KGS Wellington 1-32, and Arbuckle type log from Figure 1.6.

Figure 1.2. Generalized Stratigraphic Column of Oklahoma. Modified from Oklahoma Corporation Commission's General Geologic Sections of Oklahoma and Arkansas, 1975. The top of the Mississippian used for structural modeling is Meramecian in age, and marks the beginning of this stratigraphic column. Correlated formation tops and isopach zones used for structural modeling are labeled.

Figure 1.3. A) Dip angle co-rendered with dip azimuth for the Mississippian Structure. Faults are apparent where the dip magnitude is high (dark grey to black) and a change in dip azimuth align. B) Blue faults are the modified fault database, which contains the OGS fault database (Holloway et al., 2016) and faults identified by the author. 1,000 ft (305 m) contour interval with a 20 vertical exaggeration. Ames Hole, an Ordovician-aged meteor impact, can be seen in Major County, strike-slip faulting along the Cherokee platform, and the major fault systems have been labeled. NOTE. The Mississippian is present in northeastern Oklahoma but was outside of the modeled area and is therefore not shown on the maps.

Figure 1.4. A) Mississippian (MSSP zone), Woodford (WDFD zone), Hunton (Hunton zone), Sylvan (SVLN zone), Ordovician (Ordovician zone), and Arbuckle zone flattened on the Mississippian. The top of the Mississippian is an unconformity except in the deep Anadarko and Arkoma basins, across the Anadarko shelf, and the Cherokee platform. This map is the pre-Pennsylvanian unconformity subcrop map. The Mississippian is present across Oklahoma except in central Oklahoma. B) Same model as 1.4A and except that the Mississippian and Woodford have been lifted to reveal the lateral extent of the Hunton, Sylvan, Ordovician, and Arbuckle zones. This is the post-Hunton unconformity subcrop map. C) Arbuckle to Basement (Arbuckle zone) Isopach, 250 ft (76 m) contour interval.

Figure 1.5. A) Arbuckle Structure map with the modified fault database, which contains the OGS fault database (Holloway et al., 2016) and faults identified by the author. 1,000 ft (305 m) contour interval. The Arbuckle is present in the northeastern part of the state, but it is shallower than 2,000 ft (610 m) deep. B) Basement Structure map with the modified fault database. 1,000 ft (305 m) contour interval. Black arrows point to basement bulges that show slightly different dip orientations when compared to the Arbuckle structure in Figure 1.5A.

Figure 1.6. Arbuckle zone type log, Voise 1-10, UWI 35-103-24450. The top of the Arbuckle is denoted by the spread in RHOB and PHIN curve and low GR, indicating dolomite. The second-

to-last column shows the mineral percentage curves from the RHO_{maa} - U_{maa} analysis, color-filled by lithology. The right column corresponds to the dominant lithology at that depth and was used for the discrete lithology log for the lithology model. The lowest 10 ft (3.0 m) of the Arbuckle zone is the Reagan Sandstone. Location seen on Figure 1.1.

Figure 1.7. RHO_{maa} - U_{maa} plot colored by V_{sh} for the Arbuckle zone. The Arbuckle is predominantly dolomite with lesser amounts of shale, silica, and limestone.

Figure 1.8. A) Lithology Model for the Arbuckle, flattened on the top of the Arbuckle. B) Fence diagram of the lithology model for the Arbuckle. Flattened on the top of the Arbuckle with a 120 Vertical Exaggeration skipping every 75 lines (roughly 35 miles, 56 kilometers). The black arrow indicates where an increase in silica occurs. The red arrow points to the Southern Oklahoma Aulacogen, where the Arbuckle is predominantly limestone.

Figure 1.9. Arbuckle Lithology thickness for A) Limestone. 200 ft (61 m) contour interval, 1,000 ft (305 m) bold contour interval. Red arrow pointing to the SOA. B) Sandstone-Silica. 100 ft (30 m) contour interval, 500 ft (152 m) bold contour interval. Black arrows are pointing to silica-rich areas along the Cherokee platform. C) Dolomite. 250 ft (76 m) contour interval, 1,000 ft (305 m) bold contour interval. D) Shale. 100 ft (30 m) contour interval, 500 ft (152 m) bold contour interval.

Figure 1.10. Total Porosity Models. A) Total Porosity Model for the Arbuckle, flattened on the top of the Arbuckle. Black arrows point to increased porosity in central Oklahoma. B) Fence diagram of the total porosity model for the Arbuckle. Flattened on the top of the Arbuckle with a 120 Vertical Exaggeration skipping every 75 lines (roughly 35 miles, 56 kilometers). The red arrow points to the central Oklahoma increase in porosity, which is associated with the increase in silica in the region. C) Average total porosity for the Arbuckle zone draped on the Arbuckle structure. The black arrow points to the Cushing oilfield, where there has been significant porosity enhancement.

Figure 1.11. Temperature, Pressure, and CO_2 Density maps. A) Average Arbuckle Temperature map. 50°F (10°C) contour interval. B) Average Arbuckle Pressure map. 1,000 psi (6.89 MPa) contour interval. C) Average Density of CO_2 at reservoir temperature and pressure. 100 kg/m^3 contour interval.

Figure 1.12. CO_2 storage resources modeling workflow.

Figure 1.13. CO_2 storage resources models using the P_{50} E_{saline} values at the formation level. A) Arbuckle Model B) Arbuckle fence diagram C) Arbuckle net-mass map, in megatons CO_2 per mi^2

Figure 1.14. A) Arbuckle true vertical depth map. 2,000 ft (610 m) contour interval. B) CO_2 storage resources for the entire Arbuckle zone subdivided by 2,000 ft (610 m) intervals. For example, from 4,000 to 6,000 feet depth, the Arbuckle zone can store between 3,000-6,748 Mt of CO_2 using formation level E_{saline} values, which is 6% of all the storage resources in the evaluated area, highlighted by the dark purple colored contour interval on the map.

Figure 1.15. Induced Seismicity Risk Map. A) Arbuckle structure map with the risk map overlaid and at 50% opacity. All earthquakes above 3.0 magnitude (M) from 2011-2023 are shown. Modified fault database, which contains the OGS fault database (Holloway et al., 2016) and faults identified by the author, shown in blue. B) All seismic events that occurred in the basement, looking north with a vertical exaggeration of 10. C) All seismic events that occurred in the basement, looking south with a vertical exaggeration of 10.

Figure 1.16. Seismic events in and above the Arbuckle zone. A) All Seismic events that took place in the Arbuckle zone. 41 events took place, 4 between 4.0-5.0 M and 37 between 3.0-4.0 M. Basement structure map shown with 2,000 ft (610 m) contour interval and vertical exaggeration of 10. B) All seismic events that took place above the Arbuckle zone. 88 events, all less than 5.0 M. Arbuckle structure map with 2,000 ft (610 m) contour interval and vertical exaggeration of 10 shown.

Figure 1.17. Induced Seismic Risk map, central Oklahoma. Central Oklahoma showing the Arbuckle structure with 100 ft (61 m) contour interval co-rendered with seismic risk map, injection wells, and earthquakes. The red arrow points to mapped fault-earthquake relationships. Blue ellipse identifies a SW-NE trending earthquake swarm, with a short fault that likely extends in both directions. The green ellipse shows a non-faulted area with an earthquake swarm and SWD injection well. The largest fault systems, the Nemaha and Wilzetta, have no associated earthquake swarms and have injection wells close. Magnitude 5.0 and above earthquakes are labeled. Small, sub-parallel fault to the Wilzetta fault associated with the 2011 Prague earthquake highlighted by the blue, double arrow.

Figure 1.18. A) Seismic events greater than 3.0 M per month (orange dots) versus total wastewater injection volumes per month (blue histogram) and count of horizontal Mississippian well completions per month (red dots). B) All horizontal Mississippian wells and SWD injection wells from the Oklahoma Corporation Commission. Horizontal Mississippian wells colored by completion year.

Figure 1.19. A) Arbuckle true vertical depth map with 2,000 ft (610 m) contour interval and average total porosity for the Arbuckle zone. Areas in the red polygons show increased average porosity in the Arbuckle zone at depths less than 8,000 ft (2,438 m). B) Arbuckle net-mass map (using the P_{50} E_{saline} values at the formation level) in tons CO_2 per mi^2. This is the same map as Figure 1.14C but rescaled to show variations in CO_2 storage resources at shallower depths. Red polygons show the CO_2 storage resources to range between 200,000-1,000,000 tons of CO_2 for the areas with enhanced porosity. C) The seismic risk map (as seen in Figure 1.15A) with the two Arbuckle areas of interest for CCUS development.

Figure 2.1. Study area and wells with LAS used in the study. Green circles are the wells with LAS available in the Ordovician. Blue squares are wells with LAS that penetrate the entire Ordovician zone. Pink circles are all the Ordovician tops from well log interpretation. Small, light blue well spots have well tops for the Mississippian. Geologic Provinces were modified from Northcutt and Campbell, 1995. The Ardmore, Marietta, and Hollis basins were not

evaluated due to structural complexities. The Ozark Uplift was evaluated where depths were adequate. The Ordovician Type log location is shown.

Figure 2.2. Generalized Stratigraphic Column of Oklahoma. Modified from Oklahoma Corporation Commission's General Geologic Sections of Oklahoma and Arkansas, 1975. The top of the Mississippian used for structural modeling is Meramecian in age, and marks the beginning of this stratigraphic column. Correlated formation tops and isopach zones used for structural modeling are labeled.

Figure 2.3 A) Mississippian Structure map. Blue faults are the modified fault layer that contains the OGS fault database (Holloway et al., 2016) and faults identified by the author. 1,000 ft (305 m) contour interval with a 20 vertical exaggeration. B) Mississippian (MSSP zone), Woodford (WDFD zone), Hunton (Hunton zone), Sylvan (SVLN zone), Ordovician (Ordovician zone), and Arbuckle zone flattened on the Mississippian. The top of the Mississippian is an unconformity across the Anadarko shelf and the Cherokee platform. This map is the pre-Pennsylvanian unconformity subcrop map. The Mississippian is present across Oklahoma except in central Oklahoma. C) Same model as 2.3B except the Mississippian and Woodford have been lifted to reveal the lateral extent of the Hunton, Sylvan, Ordovician, and Arbuckle zones. This is the post-Hunton unconformity subcrop map.

Figure 2.4. A) Sylvan Shale Isopach with 25 ft (7.6 m) contour interval. B) Ordovician Structure map with 500 ft (152 m) contour interval co-rendered with di-azimuth and dip-magnitude. C) Ordovician zone isopach with 100 ft (30 m) contour interval.

Figure 2.5. RHO_{maa} - U_{maa} plot colored by V_{sh} for the Ordovician zone. The Ordovician is composed of dolomite, calcite (limestone), quartz (sandstone), and shale.

Figure 2.6. Ordovician zone type log, Karon 1, UWI 35-073-24496. The top of the Ordovician zone is the Viola Limestone. The second-to-last column shows the mineral percentage curves from the RHO_{maa} - U_{maa} analysis, color-filled by lithology. The right column corresponds to the dominant lithology at each depth and was used for the discrete lithology log used in modeling. Mud log sample descriptions are in the last track.

Figure 2.7. A) Lithology Model for the Ordovician, flattened on the top of the Ordovician. B) Fence Diagram of the lithology model for the Ordovician, flattened on the top of the Ordovician with a 120 vertical exaggeration skipping every 75 lines (roughly 35 miles/56 kilometers). The black arrow indicates the siltstone and dolomite stringers that are present across the top of the Ordovician. Blue arrows point to the Viola Limestone. Red arrows point to the Simpson Group Bromide sandstones.

Figure 2.8. Ordovician Lithology thickness for A) Limestone. 200 ft (61 m) contour interval, 1,000 ft (305 m) bold contour interval. B) Sandstone. 100 ft (30 m) contour interval, 500 ft (152 m) bold contour interval. C) Dolomite. 50 ft (15 m) contour interval, 250 ft (76 m) bold contour interval. D) Shale. 100 ft (30 m) contour interval, 500 ft (152 m) bold contour interval.

Figure 2.9. A) Average Sandstone Porosity for the Ordovician zone. 2% contour interval, 10% bold contour interval. The sandstone average porosity is higher across the Cherokee platform

than in the Anadarko and Arkoma basins. B) Ordovician Net Pore Thickness map. 10 ft (3.0 m) contour interval, 50 ft (15 m) bold contour interval. While sandstone porosity is greater across the Cherokee platform, sand thickness increases towards the Anadarko Basin and the southern Cherokee platform, leading to an increase in net-pore space.

Figure 2.10. Temperature, Pressure, and CO_2 Density maps. A) Average Arbuckle Temperature map. 50 °F (10 °C) contour interval. B) Average Arbuckle Pressure map. 1,000 psi (6.89 MPa) contour interval. C) Average Density of CO_2 at reservoir temperature and pressure. 100 kg/m^3 contour interval.

Figure 2.11. CO_2 storage resources modeling workflow.

Figure 2.12. CO_2 storage resources models using the P_{50} E_{saline} values at the formation level. A) Ordovician Model B) Ordovician fence diagram C) Ordovician sandstone net-mass map, in megatons CO_2 per mi^2

Figure 2.13. A) Ordovician true vertical depth Map. 2,000 ft contour interval (610 m). CO_2 storage resources for the Ordovician sandstones by 2,000 ft (610 m) depth intervals. For example, from 4,000 to 6,000 feet depth, the Ordovician sandstones can store between 744 - 2,391 Mt of CO_2 using formation level E_{saline} values, which is 11% of all the storage resources in the evaluated area, highlighted by the dark purple colored contour interval. B) CO_2 storage resources models using the P_{50} E_{saline} values at the formation level and TVD structure map. Red polygon highlights where the Ordovician sandstone CO_2 storage resources, net pore volume, and porosity are the highest, and at depths shallower than 10,000 ft (3,048 m).

Figure 2.14. Stacked Storage Resources. The total P_{50} CO_2 storage resources at the formation level for the Ordovician sandstone and Arbuckle zone, draped on their respective structural horizon. Note the color bar scale differences. The Ordovician sandstone is significantly thinner than the Arbuckle zone, where the entire zone is the reservoir. The ability to inject into both zones from a single wellbore increases storage resources at each site.

Figure 3.1. Study area and wells with LAS used in the study. Small orange dots are wells with Hunton tops, and the small blue dots are wells with Mississippian tops. Large orange circles are wells with LAS and no PEF logs, and the large green circles are wells with LAS and PEF logs. Wells with purple squares were used to train and predict PEF logs for the wells without. Anadarko and Arkoma basin type log locations are shown. Geologic Provinces were modified from Northcutt and Campbell, 1995.

Figure 3.2. Generalized Stratigraphic Column of Oklahoma. Modified from Oklahoma Corporation Commission's General Geologic Sections of Oklahoma and Arkansas, 1975. The top of the Mississippian used for structural modeling is Meramecian in age, and marks the beginning of this stratigraphic column. Correlated formation tops and isopach zones used for structural modeling are labeled.

Figure 3.3. Anadarko Basin type log and mudlog descriptions. The Hunton Group formations are labeled on the left. The first column shows GR, followed by the measured depth track. The third column shows RHOB, PHIN, PEF, and PHIT curves from petrophysical analysis. The 4th column shows the mineral percentage curves for each lithology, with the predominant lithology at each depth to the right. The last column is the mudlog sample descriptions.

Figure 3.4. Arkoma Basin type log and mudlog descriptions. The Hunton Group formations are labeled on the left. The first column shows the GR, followed by the measured depth track. The third column shows RHOB, PHIN, PEF, and PHIT curves from petrophysical analysis. The 4th column shows the mineral percentage curves for each lithology, with the predominant lithology at each depth to the right. The last column is the mudlog sample descriptions.

Figure 3.5. Pair plots for GR (0-150 API), PHIN (0-30%), RHOB (2.2-2.8 c/cc), and PEF (2.2-9 barnes) logs for the Hunton zone.

Figure 3.6. Box plots for well logs used in predicting PEF logs. A) GR B) RHOB C) PHIN D) PEF

Figure 3.7. A) Root mean square error (RMSE) for K-NN for 1-30 nearest neighbors. B) Coefficient of determination (R2) for 1-30 nearest neighbors. C) PEF vs Predicted PEF for K=10 nearest neighbors using a 15:85 test: train split. D) PEF vs Predicted PEF for the supervised Random Forest model using 5-fold cross validation, 100 estimators, maximum depth of 5, and minimum of 3 data points per leaf.

Figure 3.8. A) Mississippian (MSSP zone), Woodford (WDFD zone), Hunton, Sylvan (SVLN zone), Ordovician, and Arbuckle zones flattened on the Mississippian. The top of the Mississippian is an unconformity across the Anadarko shelf and the Cherokee platform. This map is the pre-Pennsylvanian unconformity subcrop map. The Mississippian is present across Oklahoma except in central Oklahoma. B) Same model as 3.8A except the Mississippian has been lifted to reveal the lateral extents of the Woodford Shale. The Woodford Shale and Hunton are not present in the Oklahoma panhandle, and there is a thinning across Noble, Osage, Tulsa, and Wagoner counties. C) Same model as 3.8A and 3.8B except the Woodford has also been lifted to reveal the lateral extent of the Hunton, Sylvan, Ordovician, and Arbuckle zones. This is the post-Hunton unconformity subcrop map.

Figure 3.9. A) Hunton zone Isopach. 100 ft (30 m) contour interval, 500 ft (152 m) bold contour interval. B) Hunton Structure map. 1,000 ft (305 m) contour interval, 5,000 ft (1,524 m) bold contour interval. C) Hunton Structure map co-rendered with dip angle and dip magnitude. Faults include the OGS Comprehensive Fault Database (Holloway et al., 2016) and faults identified in this study.

Figure 3.10. Hunton Isopach and all Hunton well completions. The Oklahoma City (OKC) oilfield is marked by the blue star, and the West-Edmond oilfield is marked by the purple star. The OKC oilfield has no Hunton present because it was eroded by the pre-Pennsylvanian unconformity. Blue dots are all vertical wells completed in the Hunton zone, and blue sticks are horizontal wells completed in the Hunton. Because the horizontal wells are hard to see, the

polygons highlight areas with recent (post-2000) horizontal Hunton completions. Note, the west Edmond was initially developed by vertical wells but was later drilled horizontally. This same concept was applied to the regions just north and west of the West-Edmond field, blue arrows. Lincoln and Seminole counties also had horizontal development, green arrows.

Figure 3.11. RHO_{maa} - U_{maa} plot colored by V_{sh} for the Hunton zone. The Hunton is predominantly calcite (limestone) with lesser amounts of dolomite, quartz (sandstone and silica), and shale.

Figure 3.12. A) Lithology Model for the Hunton zone, flattened on the top of the Hunton. Orange arrow pointing to the Misener Sandstone development. B) Fence diagram of the lithology model for the Hunton. Flattened on the top of the Hunton with a 400 vertical exaggeration, skipping every 75 lines (roughly 35 miles/56 kilometers). The orange arrow points to the Misener Sandstone development, and the green arrow points to the chert development within the Hunton zone.

Figure 3.13. Hunton zone lithology thickness for A) Limestone. 100 ft (30 m) contour interval, 500 ft (152 m) bold contour interval. B) Sandstone-Silica. 20 ft (6.1 m) contour interval, 100 ft (30 m) bold contour interval. The orange arrow points to the Misener Sandstone development, and the green arrow points to the chert development within the Hunton zone. C) Dolomite. 50 ft (15 m) contour interval, 200 ft (61 m) bold contour interval. Blue arrow pointing to the northwestern Oklahoma dolomite development. Red arrow pointing to the central Oklahoma dolomite development. D) Shale. 20 ft (6.1m) contour interval, 80 ft (24 m) bold contour interval.

Figure 3.14. A) Hunton zone average porosity. Red arrow pointing to a large area of increased porosity. Blue double-headed arrows point to increased porosity along the Hunton subcrop. Black polygons highlight areas of both vertical and horizontal hydrocarbon development. B) Hunton zone limestone average porosity. Black arrow indicating areas of increased limestone porosity. Black polygons highlight areas of both vertical and horizontal hydrocarbon development. C) Hunton zone silica-sandstone average porosity. The green arrow points to the Chert development area, and the orange arrow points to the Misener Sandstone development. Misener Sandstones have higher porosity than the chert. Black polygons highlight areas of both vertical and horizontal hydrocarbon development. D) Hunton zone dolomite average porosity. The blue arrow highlights the northwest Oklahoma dolomite trend, and the red arrow points to the central Oklahoma dolomite development. Black polygons highlight areas of both vertical and horizontal hydrocarbon development.

Figure 3.15. A) Average Hunton Temperature map. 50 °F (10 °C) contour interval. B) Average Hunton Pressure map. 1,000 psi (6.89 MPa) contour interval. C) Average density of CO_2 at reservoir temperature and pressure. 100 kg/m^3 contour interval.

Figure 3.16. CO_2 storage resources modeling workflow.

Figure 3.17. CO_2 storage resources models using the P_{50} E_{saline} values at the formation level. A) Hunton zone Model B) Hunton fence diagram. Blue arrow pointing to the northwest Oklahoma

dolomite development showing increased CO_2 storage resources. C) Hunton net-mass map, in tons CO_2 per mi^2. Blue arrow pointing to the northwest Oklahoma dolomite development showing increased CO_2 storage resources.

Figure 3.18. A) Hunton true vertical depth map. 2,000 ft (610 m) contour interval. B) CO_2 storage resources for the entire Hunton zone broken down by 2,000 ft (610 m) intervals. For example, from 4,000 to 6,000 feet depth, the Hunton zone can store between 44-105 Mt of CO_2 using formation level E_{saline} values, which is 3% of all the storage resources in the evaluated area, highlighted by the dark purple color.

Figure 3.19. A) CO2 storage resources for the Hunton zone, Ordovician zone sandstones, and Arbuckle zone, broken down by 2,000 ft (610 m) intervals using the P50 Esaline storage efficiency coefficients, giving a conservative estimate of CO2 storage resources. B) CO2 storage resources for the Lower Paleozoic reservoirs (Hunton zone, Ordovician zone sandstones, and Arbuckle zone) and the Lower Paleozoic composite TVD structure map from 2,000-10,000 ft. Depths deeper than 10,000 ft have been removed. 200 ft (61 m) contour interval, 1,000 ft (305 m) bold contour interval. Thick white outlines show Arbuckle areas of interest, thin white outline shows the Ordovician sandstone area of interest and the white dashed outlines highlight Hunton zone areas of interest. The red polygon shows location of stacked CO2 storage resource potential.

Figure A-1. A) Base map showing the regional cross sections A-A' (Figure A-2), B-B' (Figure A-3), C-C' (Figure A-4), D-D' (Figure A-5), E-E' (Figure A-6), and F-F’ (Figure A-7). Orange triangles are wells with LAS for the Hunton Group, green circles are wells with LAS for the Viola Limestone and Simpson Group, and purple squares are wells with LAS for the Timbered Hills and Arbuckle groups. B) Generalized Stratigraphic Column of Oklahoma. Modified from Oklahoma Corporation Commissions General Geologic Sections of Oklahoma and Arkansas, 1975. The top of the Mississippian used for structural modeling is Meramecian in age, and the beginning of this stratigraphic column.

Figure A-2. Cross Section A-A', location seen on Figure A-1. West-East cross section from Cimarron County to Osage County across northern Oklahoma, flattened on the Mississippian. The first track shows the color-filled GR from 0-150 API, measured depth track, followed by a track showing the PEF from 0-20 barnes and RHOB from 2.0-3.0 g/cc. Mineral percentage curves are seen in the next track, and the dominant lithology seen in the last track was generated from methods found in Chapters 2-4 of this study. Color-filled GR between wells.

Figure A-3. Cross Section B-B', location seen on Figure A-1. West-east cross section from western Washita County to Osage County, flattened on the Mississippian. The first track shows the color-filled GR from 0-150 API, measured depth track, followed by a track showing the PEF from 0-20 barnes and RHOB from 2.0-3.0 g/cc. Mineral percentage curves calculated are seen in the next track, and the dominant lithology seen in the last track was generated from methods found in Chapters 2-4 of this study. Color-filled GR interpolation between wells.

Figure A-4. Cross Section C-C', location seen on Figure A-1. West-east cross section from Canadian County to Tulsa County, flattened on the Mississippian. The first track shows the

color-filled GR from 0-150 API, measured depth track, followed by a track showing the PEF from 0-20 barnes and RHOB from 2.0-3.0 g/cc. Mineral percentage curves calculated are seen in the next track, and the dominant lithology seen in the last track was generated from methods found in Chapters 2-4 of this study. Color-filled GR interpolation between wells.

Figure A-5. Cross Section D-D', location seen on Figure A-1. Southwest-northeast cross section from southwestern McClain County to Okmulgee County, flattened on the Mississippian. The first track shows the color-filled GR from 0-150 API, measured depth track, followed by a track showing the PEF from 0-20 barnes and RHOB from 2.0-3.0 g/cc. Mineral percentage curves calculated are seen in the next track, and the dominant lithology seen in the last track was generated from methods found in Chapters 2-4 of this study. Color-filled GR interpolation between wells.

Figure A-6. Cross Section E-E', location seen on Figure A-1. Southwest-northeast cross section from southern Hughes County to McIntosh County, flattened on the Mississippian. The first track shows the color-filled GR from 0-150 API, measured depth track, followed by a track showing the PEF from 0-20 barnes and RHOB from 2.0-3.0 g/cc. Mineral percentage curves calculated are seen in the next track, and the dominant lithology seen in the last track was generated from methods found in Chapters 2-4 of this study. Color-filled GR interpolation between wells.

Figure A-7. Cross Section F-F', location seen on Figure A-1. Northwest-southeast cross section from Harpy County to Hughes County, flattened on the Woodford Shale. The first track shows the color-filled GR from 0-150 API, measured depth track, followed by a track showing the PEF from 0-20 barnes and RHOB from 2.0-3.0 g/cc. Mineral percentage curves calculated are seen in the next track, and the dominant lithology seen in the last track was generated from methods found in Chapters 2-4 of this study. Color-filled GR interpolation between wells.

Figure A-8. Mississippian Structure Map and well control. 200 ft contour interval, 1,000 ft bold contour interval.

Figure A-9. Mississippian Isopach and well control. 50 ft contour interval, 250 bold contour interval.

Figure A-10. Woodford Shale Structure Map and well control. 200 ft contour interval, 1,000 ft bold contour interval.

Figure A-11. Woodford Shale Isopach and well control. 25 ft contour interval, 125 bold contour interval.

Figure A-12. Hunton Group Structure Map and well control. 200 ft contour interval, 1,000 ft bold contour interval.

Figure A-13. Hunton Group Isopach and well control. 50 ft contour interval, 250 bold contour interval.

Figure A-14. Sylvan Shale Structure Map and well control. 200 ft contour interval, 1,000 ft bold contour interval.

Figure A-15. Sylvan Shale Isopach and well control. 25 ft contour interval, 125 bold contour interval.

Figure A-16. Viola Limestone (Ordovician) Structure Map and well control. 200 ft contour interval, 1,000 ft bold contour interval.

Figure A-17. Ordovician Isopach and well control. 50 ft contour interval, 250 bold contour interval.

Figure A-18. Arbuckle Group Structure Map and well control. 200 ft contour interval, 1,000 ft bold contour interval.

Figure A-19. Arbuckle Group Isopach and well control. 100 ft contour interval, 500 bold contour interval.

Figure A-20. Crystalline Basement Structure Map and well control (red squares). 200 ft contour interval, 1,000 ft bold contour interval. Faults shown are from the Comprehensive Fault Database (Holloway et al., 2016) for the state of Oklahoma from the OGS and additional faults interpreted by the author from this study. All Earthquakes from 2011-2013 above 2.0 M. High-rate Arbuckle SWD Injection wells shown.

List of Tables

Table 1.1. Definition of terms used to calculate the Saline Storage Capacity Efficiency, E_{saline}. From IEA Greenhouse Gas R&D Programme 2009.

Table 1.2. E_{saline} values at the Site-Specific and Formation level. From IEA Greenhouse Gas R&D Programme 2009.

Table 1.3. CO_2 Storage resources for the Arbuckle calculated with Site-Specific E_{saline} values, broken down by lithology.

Table 1.4. CO_2 Storage resources for the Arbuckle calculated with Formation level E_{saline} values, broken down by lithology.

Table 2.1. Definition of terms used to calculate the Saline Storage Capacity Efficiency, E_{saline}. From IEA Greenhouse Gas R&D Programme 2009.

Table 2.2. E_{saline} values at the Site-Specific and Formation level. From IEA Greenhouse Gas R&D Programme 2009.

Table 2.3. CO_2 Storage resources for the Ordovician calculated with Site-Specific E_{saline} values, broken down by lithology.

Table 2.4. CO_2 Storage resources for the Ordovician calculated with Formation level E_{saline} values, broken down by lithology.

Table 3.1. Definition of terms used to calculate the Saline Storage Capacity Efficiency, E_{saline}. From IEA Greenhouse Gas R&D Programme 2009.

Table 3.2. E_{saline} values at the Site-Specific and Formation level. From IEA Greenhouse Gas R&D Programme 2009.

Table 3.3. CO_2 Storage resources for the Hunton calculated with Site-Specific E_{saline} values, broken down by lithology.

Table 3.4. CO_2 Storage resources for the Hunton calculated with Formation level E_{saline} values, broken down by lithology.

Table 3.5. CO_2 storage resources for the Arbuckle zone, Ordovician zone sandstones, and Hunton zone broken down by 2,000 ft (610 m) intervals using both the site-specific and formation level E_{saline} storage efficiency coefficients.

List of Units and Abbreviations

g = gram

cc = cubic centimeter = cm^3

ft = foot

mi = mile

km = kilometer

lb = pound

kg = kilogram

Ton = metric ton = 1,000 kg

Mt = megaton = million metric tons = 10^6 metric tons

Gt = gigaton = 10^9 metric tons

M = Magnitude

psi = pounds per square inch

Pa = pascal

MPa = Megapascal

GR – Gamma ray log

RHOB – Bulk density log

PHIN – Neutron porosity log

PHIT – Total porosity log (calculated)

PEF – Photoelectric factor log

PHID – Density porosity log (calculated)

V_{sh} – Shale volume (calculated)

RHO_{maa} – Apparent matrix grain density (calculated)

U_{maa} – Apparent matrix volume cross-section

Abstract

To reach the Paris Agreement's goal to keep the rise in global surface temperature to below 2 °C above pre-industrial levels, carbon capture, utilization, and storage (CCUS) will be required for large quantities of CO_2. Oklahoma's unique history as an oil and gas producing state makes it an ideal location for CCUS. While the United States Geological Survey (USGS) completed and released a national assessment of geologic carbon dioxide storage resources (U.S. Geological Survey Geologic Carbon Dioxide Storage Resources Assessment Team, 2013) which is an initial assessment of storage resources on a regional basis, there have been no statewide assessments of CO_2 storage for individual reservoirs at the state level. This dissertation attempts to fill that void by determining the spatial distribution of lithology, pore volume, and CO_2 storage resources for the: 1) Arbuckle and Timbered Hills group (Arbuckle zone). 2) Simpson Group and Viola Limestone (Ordovician zone). 3) Hunton Group and Misener Sandstone (Hunton zone). Due to the historical correlation between wastewater injection and induced seismicity in the Arbuckle zone, Chapter 1 also includes areas of high risk for induced seismicity by integrating well data, wastewater injection volumes, basement-seated faults, and historical earthquake locations and magnitudes. Chapter 2 highlights specifically the distribution of the sandstone reservoir, which is the intended target for CCUS. Chapter 3 on the Hunton zone uses supervised machine learning methods to generate synthetic well logs so that lithology predictions could be made for additional wells in the dataset. Key findings include 1) Areas of enhanced porosity in the Arbuckle zone and areas at high risk of induced seismicity due to basement faulting and proximity to wastewater injection wells. 2) Areas with thick, high porosity Ordovician sandstone at depths above 10,000 ft, and 3) Areas where the high porosity dolomite develops within the Hunton zone, and where pressure depletion due to hydrocarbon production has the potential to

lead to increased storage resources. Overall, this is the most detailed study to date of lithology, pore space, and CO_2 storage resources for the state of Oklahoma.

Introduction

This study evaluates CO_2 storage resources for all reservoirs from the Devonian-age Hunton Group to the pre-Cambrian basement. Chapter one addresses the Arbuckle zone, which contains the Arbuckle and Timbered Hills groups. This zone is the deepest reservoir and sits directly above the basement. The second chapter addresses the Ordovician zone, which includes the Trenton-age Viola Limestone and the Simpson Group. The Sylvan Shale was also mapped but not modeled for storage because it is predominantly shale and considered a reservoir seal. The third chapter evaluates the Hunton zone, which includes the Hunton Group and Misener Sandstone if present.

In the first chapter, we explore the CO_2 storage resources for the Arbuckle and Timbered Hills group in Oklahoma. These reservoirs are the oldest and deepest reservoirs in the state and have historically been used for hydrocarbon production and oilfield wastewater storage. Using well log information from over 80,800 wells and the US Department of Energy (US-DOE) methodology, the CO_2 storage resources were determined (NETL, 2007 & 2008; IEA GHG, 2009). Because of the historical correlation between wastewater injection in the Arbuckle Group, basement-seated faults, and induced seismicity, this chapter also includes an induced seismicity risk map generated from the distance from Arbuckle wastewater injection wells, the distance to known basement faults, and the distance to previously induced earthquakes.

The second chapter explores the CO_2 storage resources for the Ordovician reservoirs in Oklahoma. The Ordovician reservoirs in Oklahoma are also hydrocarbon-producing reservoirs, and the Bromide sandstones are the thickest and most laterally continuous sandstones in Oklahoma. Using well log information from over 80,800 wells and the US-DOE methodology,

the CO_2 storage resources were determined for the Ordovician reservoirs. With the Bromide sandstones being the targeted injection zone, the sandstone distribution and CO_2 storage resources are also highlighted and reported.

The third chapter explores the CO_2 storage resources for the Hunton Group. The Hunton Group extends across much of Oklahoma is also a hydrocarbon-producing reservoir, and it has been developed with both vertical and horizontal wells across the state of Oklahoma. Like the previous two chapters, the study utilized well log information from over 80,800 wells and the US-DOE methodology to determine the CO_2 storage resources for the Hunton Group. This chapter also utilizes supervised machine learning to generate synthetic well logs where missing to give a more robust dataset for the spatial distribution of lithologies.

To determine the storage resources in each chapter, over 1,469 of the 80,800 wells were digitized in log ascii standard (LAS) format with modern log suites that include Gamma Ray (GR), Bulk Density (RHOB), Neutron Porosity (PHIN), and Photoelectric Factor (PEF). Using RHO_{maa} - U_{maa} analysis, the minerology was estimated for each zone, and the 3D spatial distribution (3D models) was modeled using commercial software. Total porosity was calculated from well logs, and a total porosity model was constrained to the lithology model. While little core data are available for porosity and permeability calculations, mudlogs with rock descriptions to confirm lithology for each zone were used.

To apply the US-DOE methodology, the density of CO_2 at reservoir temperature and pressure was required. The bottom hole depth and temperature from wellbore data across Oklahoma were available from the Southern Methodist University (SMU) Geothermal Lab, which is a part of the National Geothermal Data System (SMU Node of National Geothermal Data System, Heat Flow and Well Data, accessed March 2023). The total CO_2 storage resource

for each zone was determined using both site-specific and formation level saline storage efficiency coefficients (E_{Saline}) and reported for the entire study area, by lithology and by measured depth.

Together, these chapters give the reader a detailed description of the rock type, porosity, and CO_2 storage resources for the deepest and most laterally continuous reservoirs in the state of Oklahoma. Across much of the state, these reservoirs are all present, stacked upon each other and at an adequate depth to store CO_2. This leads to the potential of stacked storage, where one well would access all 3 reservoirs for storage, which would reduce the cost of field development by requiring fewer wells to be drilled, which also reduces the surface footprint of the facilities. This research indicates that Oklahoma is poised to be a Carbon Hub for years to come.

Chapter 1: Data Collection and Subsurface Mapping

The data used in this dissertation were interpreted and gathered over 4 years. Using GVERSE GeoGraphix, in conjunction with the Enverus database, the Oklahoma Corporation Commission (OCC) online database, and the Oklahoma City Geological Society log library, a GVERSE GeoGraphix project containing all the wells in Oklahoma, along with available well data, was built. The author's 18 years of experience in the petroleum industry, specifically the mid-continent with a focus on the Pennsylvanian and lower Paleozoic hydrocarbon reservoirs, was what initially led to this study. The author began her career drilling vertical, lower Paleozoic (Chesterian, Meramecian, Osagean, and Devonian age-Hunton Group) comingled hydrocarbon wells in the Anadarko Basin and subsequently saw each of these reservoirs developed by horizontal wells. The author has been a part of teams that have drilled successful horizontal Mississippian (Osage and Meramecian), Woodford Shale, and Hunton Group wells in addition to multiple, high-rate Arbuckle Group saltwater disposal wells (SWD) across central Oklahoma. The lower Paleozoic reservoirs (Mississippian, Woodford Shale, Hunton Group, Sylvan Shale, Viola Limestone, Arbuckle Group, and crystalline Basement) were all correlated together with regional cross sections (Figure A-1). Due to the size requirements to show detailed cross sections and maps, they are included in Appendix A.

The Mississippian formation (not including Chesterian strata) exists across nearly all (Figures A-8 and A-9) of Oklahoma and was the youngest formation correlated. The majority of wells in Oklahoma penetrate the Mississippian formation due to its history as a hydrocarbon-producing reservoir. Along the Anadarko shelf and northern Oklahoma, it is predominantly limestone with lesser amounts of chert (Figure A-2). Above the Mississippian lies the Pennsylvanian shales. The top of the Mississippian in this region is marked by the decrease, or

‘cleaning-up’ of the Gamma Ray (GR) log. It is generally very low and between 0-30 API, with low PHIN. Additionally, in north central Oklahoma, along the Nemaha uplift, the Mississippian formation develops tripolitic chert, informally called the “Mississippi-Chat” (Figure A-2, wells 7 and 8). While it typically presents at the top of the formation (Figure A-2, well 8), it can be lower within the section, with tighter limestones in between (Figure A-1, well 7). It is denoted by low Bulk Density (RHOB), high neutron porosity (PHIN), and typically very low resistivity. Porosity in the tripolitic chert can be incredibly high, over 30%, and is easy to identify on well logs. While the GR in the tripolitic chert is generally low (less than 30 API), it can also have stringers of high GR and can appear ‘ratty’ at the top (Figure A-2, well 7).

In the heart of the Anadarko Basin, the Mississippian is predominantly Meramecian in age and has more silica and clay present, which leads to higher GR than the Anadarko shelf (Figure A-4, wells 1 and 2, and Figure A-7, wells 4-6). In this region, cyclical cleaning upward sequences can be seen on the GR and Resistivity (RESD) well logs (Figures A-4, A-5, A-6, and A-7, blue dashed lines in the Mississippian formation). These repetitive cycles can be followed and correlated to southeastern Oklahoma, where the Mississippian is a hot shale with GR readings above 85 API (Figures A-5, A-6, and A-7). In the heart of the Anadarko and Arkoma basins, the Chester formation lies above the Mississippian formation. It is not present along the Anadarko shelf or central Oklahoma due to erosion from the Pennsylvanian unconformity and is not included in this study. The GR response in the Chester and Mississippian formations is similar and is not useful in determining the boundary between them. Instead, the RESD curve is used in conjunction with the PHIN and RHOB. The Chester formation has lower RESD than the Mississippian formation, and the RHOB and PHIN pull together in the lower Mississippian

formation. This also coincides with the top and last of the cyclical cleaning upwards sequences that can be followed across the state.

The Woodford Shale is generally identified by the increase in GR, directly below the Mississippian. In northwestern Oklahoma is not present (Figure A-2 wells 1-4, Figure A-11), and the Mississippian reservoirs sit directly above the Ordovician-aged Viola Limestone. The boundary is not easily defined in this area. Along the Anadarko shelf and the Cherokee platform, the Woodford Shale has higher GR, over 150 API. While the GR in the Woodford Shale can be incredibly high (over 300 API), the majority of the rasters used and digitized in this study had GR readings clipped at 150 API. Across northern Oklahoma, in Woodford, Major, and Grant counties, the base of the Mississippian, the GR gradually increases with depth instead of having a distinct boundary with the overlying Mississippian. This interval is typically described as the Kinderhook Shale (Figure A-2, wells 4 and 5, Figure A-3, wells 1 and 2). Determining the top of the Woodford can be difficult in this region when compared to the rest of Oklahoma where the base of the Mississippian is a limestone with low GR and a sharp contact with the higher GR Woodford Shale, this accounts for some of the 'bullseyes' seen on the Woodford Shale Isopach (Figure A-11). In this region, the author picked the top of the Woodford Shale when the GR went over 150 API. Across most of Oklahoma, the Woodford Shale has high GR (above 150 API), high PHIN (over 30%), and low RHOB (less than 2.2 g/cc).

There are two regional thickenings of the Woodford Shale (Figure A-11). In Canadian County, the Woodford Shale thickens drastically and can be seen having intervals with lower GR, with porosity development (Figure A-4, well 1). This thickening runs northwest-southeast from the northwestern corner of Canadian county into Grady and McLain, and it is locally removed along the central Oklahoma uplift, and then can be seen continuing into Pontotoc, Coal, and

Atoka counties. The second thickening also trends northwest-southeast and extends from southwestern Garfield County through Kingfisher, Logan, Lincoln, and Potawatomie counties, where the two trends merge into one (Figure A-6, wells 1 and 2).

Below the Woodford Shale is the Misener Sandstone, when present (Figure A-2, wells 4 and 5 and Figure A-6, wells 3 and 4) or the Hunton Group. Both the Misener Sandstone and the Hunton Group are denoted by the drastic decrease in GR to less than 20 API at the base of the Woodford Shale. The Hunton Group is predominantly limestone with lesser amounts of dolomite and chert. The entire interval is typically low GR (less than 30 API) with low PHIN (less than 3%) and high RHOB (2.7 g/cc) except in areas where dolomite is present (Figure A-4, wells 2 and 3, Figure A-5, well 3, Figure A-7, wells 2, 4 and 5). The top of the Hunton is an unconformity along the Anadarko shelf and central Oklahoma and is responsible for the thinning and eventual disappearance of the interval on each regional cross section and isopach (Figure A-13). In central Oklahoma County, the Hunton has been removed by the Pennsylvanian unconformity and is not present, this is also where the Oklahoma City oilfield is located. In Canadian County, there is a localized thinning of the Hunton Group that coincided with the thickening of the above Woodford Shale (Figure A-11). This is also the location of the "Cana Woodford Play" of central Oklahoma that has been extensively developed by horizontal wells.

The Sylvan Shale lies at the base of the Hunton Group. It is denoted on well logs by the sharp increase in GR at the base of the Hunton Group and an increase in PHIN. It is easily identifiable and regionally continuous (Figure A-15). The Sylvan Shale is the seal for the Ordovician reservoirs. It is predominantly described as a green, waxy shale on mud logs but can have siltstones and dolomites present at the base of the interval (Figure A-2 well 5, Figure A-3 well 3, Figure A-4 wells 1 and 2, Figure A-5 well 1, Figure A-7 wells 2, 3 and 4) This interval at

the base of the Sylvan shows a decrease in GR and PHIN, while the RHOB generally stays consistent with the overlying shale. It is not present along the Cherokee platform due to removal from the post-Hunton unconformity. It sits above the very low GR found in the Viola Limestone below. This interval develops well log porosity in northern Oklahoma and was included in the lower Ordovician reservoirs.

Across most of Oklahoma, the top of the Ordovician is the Viola Limestone. The post-Hunton unconformity that removed the Hunton Group across central Oklahoma also eroded and removed the Sylvan Shale, Viola Limestone, and Simpson Group across northcentral Oklahoma. The Viola Limestone has been completely removed West of Kay, Pawnee, and Payne counties (Figure A-2, wells 7 and 8, Figure A-3, wells 6 and 7, A-2, well 5). In this area, the lower Simpson Group sandstones are present at the top of the Ordovician reservoirs.

These Simpson Group sandstones, specifically the Bromide sandstones, are the most laterally continuous sandstones in Oklahoma and can be seen as a distinct sandstone package in the Ordovician reservoirs on each regional cross section. They develop below the Viola Limestone and the Simpson dolomite when present (Figure A-2 well 5, Figure A-4 wells 3 and 4, Figure A-5 wells 2-4, Figure A-7 wells 2 and 5). The base of these sandstones is denoted by a sharp increase in GR, which correlates to the lower Oil Creek Formation. The Oil Creek Formation are sandstones and shales that can be seen below the Bromide sandstones, and above the Arbuckle Group. Along the Anadarko shelf and Cherokee platform, the shale at the base of the Bromide sandstones is correlatable and continuous but disappears in the Anadarko and Arkoma basins where sand content increases (Figure A-5, wells 1, 2, and 3, Figure A-6, all wells). The higher GR shales seen in the Oil Creek Formation are the seal to the lower Arbuckle

Group. Well log quality over the lower Ordovician reservoirs is notoriously bad due to wellbore washout associated with the Oil Creek Formation.

Ordovician reservoirs are present across nearly all of Oklahoma, except the northeastern corner of the state, where it has been removed by the Pennsylvanian unconformity (Figure A-17). Localized highs along the Nemaha and Wilzetta fault systems, including the Oklahoma City and Cushing, are also bald of Ordovician reservoirs. In these areas, the Pennsylvanian shales sit directly above the Arbuckle Group. Additionally, Ames Hole in southeastern Major County shows a circular-shaped thickening associated with the Ordovician-aged meteor impact.

The top of the Arbuckle Group is denoted by the decrease in GR and an increase in PHIN. Across the Anadarko shelf and Cherokee platform, it is an unconformity surface related to the pre-Simpson unconformity. The GR in the Arbuckle is generally low (around 30 API) with streaks of hot GR. The PHIN and RHOB curves typically parallel/track each other with a consistent spread between curves. Below the Arbuckle Group is the Timbered Hills Group, which contains the Honey Creek limestone and the Reagan Sandstone, where present. The Reagan Sandstone in western Oklahoma is typically low GR with low PHIN (less than 2%), with RHOB around 2.5 g/cc (Figure A-2, wells 1 and 2). In central Oklahoma, the Reagan Sandstone is more arkosic, which leads to higher GR readings over 80 API (Figure A-3 wells 4 and 7, Figure A-4 well 2, Figure A-5 well 4, Figure A-6 well 1, and Figure A-7 well 4).

In general, the base of the Arbuckle shows an increase in GR to over 150 API, which denotes the top of the crystalline basement in Oklahoma. The mineral model used for the above Arbuckle zone is inaccurate in the basement. Across most of Oklahoma, the basement is described as pink rhyolite in samples. RHOB and PHIN readings vary greatly across the state, but the GR is consistently high. Most of the wells that penetrate the crystalline basement are

SWD wells. Before 2015 and the subsequent induced seismicity related to high-rate Arbuckle SWD wells, it was common practice to continue drilling into the crystalline basement as it was assumed to have porosity and storage capacity. There are 3 wells in this study Buford 1-11 (Figure A-3, well 3), Pale Moon SWD 1-3 (Figure A-6, well 2) and Fountian SWD 1-14 (Figure A-2 well 7, drilled by the author) that drilled deep enough into the basement to intersect intervals in the basement with low GR (around 35 API), high RHOB (2.9 g/cc) and high PHIN (17%) (Figure A-3 well 3 and Figure A-6 well). In the Fountain SWD 1-14 mud log descriptions indicated a color change from the pink rhyolite to a black and white unknown mineral. It did not react with hydrochloric acid and was magnetic. There was no further assessment done and the author no longer has access to the data, but these were interpreted to be dykes or sills in the basement.

The initial structure map generated for the state was for the Mississippian formation using a 500 ft x 500 ft grid and convergent krigging. Isopachs for the Mississippian, Woodford, Hunton, Sylvan, Ordovician, and Arbuckle were then generated from well control and subsequently subtracted from the Mississippian structure map to generate the Woodford, Hunton, Sylvan, Ordovician, Arbuckle, and Basement Structure maps. No faults were used in mapping. Faults seen on the shallowest Mississippian formation can also be seen on the deeper formations, increasing with offset at depth (Figure A-8, A-10, A-12, A-14, A-16, A-18, and A-20). In general, the lower Paleozoic structure maps look very similar, except for the basement structure map in Osage County (Figure A-20). There is a very apparent closed structural high on the basement structure map that is not present in the younger sedimentary formations above it. Additionally, the basement structure map (Figure A-20) also shows the earthquake hypocenter locations for all events greater than 2.0 from 2011-2023, all high-rate Arbuckle SWD wells, and basement well

penetrations. Earthquakes commonly align and illuminate basement-seated faults that can be identified from well log control (i.e., this study).

After the wells were correlated across the state, if log ascii standard (LAS) formats were available, they were downloaded and imported. Additional rasters for wells with modern well logs (GR, RHOB, PHIN, and PEF) were then digitized by hand to ensure coverage across the state. If a caliper log was present, wellbore washout was removed, but otherwise all LAS's were hand edited to remove washout where appropriate. The Pennsylvanian shales that develop above the Mississippian and the lower Ordovician shales typically have the most wellbore washout and erroneous readings and require the heaviest editing. GR and RHOB were normalized where needed, but in general were left unedited. The project was then migrated to Petrel for 3-D reservoir modeling.

Chapter 2: The Statewide variability of mineralogy, pore volume and CO2 storage resources for the Timbered Hills and Arbuckle groups, Oklahoma

Abstract

The Arbuckle and Timbered Hills groups (Arbuckle zone) exist across the state of Oklahoma at depths adequate for saline storage of CO_2. It is also a hydrocarbon-producing reservoir where structurally trapped and a saltwater disposal zone for oilfield wastewater across north-central Oklahoma. While localized, site-specific CO_2 storage resource studies of the Arbuckle Group in Oklahoma have been reported, there are no publicly documented regional studies.

Using information from 80,800 wells and over 403 wells with log ascii standard (LAS) format modern well logs, a detailed 3-D lithology model was generated for the Arbuckle zone across the state of Oklahoma. Total porosity was calculated from well logs, and the total porosity model was constrained to the lithology model. To determine CO_2 storage resources, the United States Department of Energy's (US-DOE) methodology was applied. The total CO_2 storage resources were determined using both site-specific and formation level saline storage efficiency coefficients (E_{Saline}) and reported for the entire study area, by lithology and by measured depth. Due to the historical use of the Arbuckle Group for oilfield wastewater injection and subsequent induced seismicity, this study also presents an induced seismicity risk map by integrating historical wastewater injection wells, basement-seated faults, and historical earthquake data.

Results include 1) The entire zone consists of reservoir rock, predominantly dolomite with average well log porosity at 7%. 2) Total CO_2 storage resource is between 50,673-118,436 Mt of CO_2 over 44,627 mi^2, and 30% of that storage resource is at depths between 2,000-10,000

ft. 3) Induced seismicity risk maps and evidence that induced seismicity can be mitigated by limiting injection volumes and banning disposal into the crystalline basement.

Introduction

In 2013, the United States Geological Survey (USGS) completed and released a national assessment of geologic carbon dioxide storage resources (U.S. Geological Survey Geologic Carbon Dioxide Storage Resources Assessment Team, 2013). The assessment evaluated 36 sedimentary basins across the USA and used a geology-based probabilistic assessment method to estimate the subsurface CO_2 storage resource of 3,000 Gt of CO_2 for the USA. The goal of the USGS study was to conduct an initial assessment of storage resources on a regional basis. Through this regional assessment, not all viable storage formations were individually assessed, and various formations were combined and evaluated as one reservoir; thus, the results provide regional storage resource trends. For example, the Arbuckle Group, Viola Limestone, and Simpson Group were combined as a single reservoir called “Lower Paleozoic” in the Anadarko basin and was reported to have between 11.8 to 37.0 Gt of CO_2 storage resources. Meanwhile, the Arkoma Basin was only evaluated for the “Ordovician Composite” and was reported to have between 3.2 to 11.0 Gt of CO_2 storage resources. While informative, given how the stratigraphic units in the separate basins were combined, it is not possible to compare total storage resources for a particular stratigraphic interval or Oklahoma. In addition, the studies report total storage resources and do not include information about the spatial variability of rock properties and storage resources across the basins. Further north in Kansas, a regional study to evaluate groundwater flow and CO_2 storage resources for the Arbuckle was done by Carr et al. (2005). Using large-scale relational databases with temperature, pressure, water geochemistry, and well

logs, a CO_2 storage resource per 5 mi^2 (12.9 km^2) grid was calculated. Storage capacities ranged from 0 to 540,000 tons CO_2 per mi^2.

There has been one recent publication (Miranda et al., 2023) that references a regional assessment of CO_2 storage resources for the "Arbuckle Formation" and "Simpson Sandstones" as part of developing a roadmap for carbon capture and storage in Oklahoma by assessing the viability of stacked storage. CO_2 storage resources were determined using Carbon Solutions LLC's SCO_2T^{PRO} software, which uses the US-DOE methodology to assess CO_2 storage resources, but there were no details as to the geologic inputs that were used. There were no reported total CO_2 storage resources reported either.

There have also been site-specific studies that evaluate the storage resources for the Arbuckle Group. Milad et al. (2023), based on subsurface interpretation and modeling of the Arbuckle, reported that the CO_2 storage resources for Osage County, Oklahoma, are between 60 to 360 Mt, using CO_2 storage efficiency factors of 1%, 2%, and 4% for the entire zone, independent of lithology. Using the minimum, median, and 90th percentile thicknesses, porosities, and the P_{10}, $P_{50,}$ and P_{90} storage efficiency values for dolomites developed by Goodman (2011), Caf (2022) reported that Wellington Field, Kansas, has CO_2 storage resources between 0.95 to 22.5 Mt. These site-specific studies do account for the spatial variability of rock properties and are valuable when site selection for CO_2 has already been determined.

Because a detailed statewide assessment of pore volume and CO_2 storage resources was lacking for the state of Oklahoma, this study utilizes data from more than 80,800 wells and other regional information for geological interpretation and to construct and analyze well-constrained 3-D geological models of the Arbuckle (Figure 1.1). The study especially incorporates detailed constraints on the stratigraphy and structure (e.g., depth, areal extent, thickness, mineralogy,

porosity). The results include a detailed structural, lithology, total porosity, temperature, and pressure models of the Arbuckle Group and are the most detailed assessments, to date, of pore volume and CO_2 storage resources for Oklahoma.

The Arbuckle Group has been historically used for oilfield wastewater injection and storage. High-rate saltwater disposal wells (SWD's) have been tied to induced seismicity along basement-seated faults (Keranen et al., 2013 & 2014, Walsh & Zoback, 2015). To identify areas with a higher risk of induced seismicity, locations of known faults, Arbuckle SWD wells, and historical earthquake locations and depths were compiled. High rate SWD wells and injection volumes were compiled by the Oklahoma Corporation Commission (OCC) (Arbuckle AOI Well – 1012D Reported Volumes). Earthquake data, including the date, location, depth, and magnitude of the event, was obtained from the Oklahoma Geological Survey (OGS) (Walter et al., 2020). The Comprehensive Fault Database for the state of Oklahoma from OGS was also used (Holloway et al., 2016).

Geologic Setting

The early Paleozoic in Oklahoma was a time of rifting. Laurentia, the North American Craton, was composed predominantly of epizonal and mesozonal granites with comagmatic rhyolites (Ham et al., 1964; Figure 1.2). The Southern Oklahoma Aulacogen (SOA) began rifting in the middle Cambrian and gave way to the ancestral Anadarko Basin. During this time, Oklahoma was covered by shallow seas, which brought the first sediments from the weathered basement complex and deposited the Reagan Sandstone. It was deposited across most of the state except in areas of local highs. The Reagan Sandstone grades upwards into the succession of shallow-water carbonates called the Honey Creek Limestone. The Honey Creek is a fossiliferous

limestone that grades into a sandy dolomite on the shelf and ranges in thickness from 100-200 ft (30-61 m). Together, the Reagan Sandstone and Honey Creek Limestone comprise the Timbered Hills Group, the oldest sedimentary units in Oklahoma and included in the study (Ham et al., 1964).

The Arbuckle Group that overlies the Honey Creek Limestone is the thickest sequence of lower Paleozoic strata in Oklahoma, with a maximum thickness of 6,700 ft (2,042 m) of limestone in the SOA. It thins and transitions to a dolomite outside of the aulacogen with thickness ranging from 1,000-4,000 ft (305-1,219 m) (Johnson, 1991). The term "Arbuckle Facies" is used commonly for both the Arbuckle Group and Timbered Hills Group. The Arbuckle Group outcrops in the Slick Hills of the Arbuckle Mountains and is described as cyclic arrangements of interbedded carbonate mudstones, intraclast calcarenite, oolitic calcarenite, stromatolites, and laminated dolomites that have been wholly or partly dolomitized (Johnson, 1991). Dolomitization is thought to have begun shortly after lithification and predates the Pennsylvanian orogeny. It is thought that during deposition, the center of the basin was precluded from dolomitization due to intense pressure solution while the edges of the basin were dolomitized (Ross, 1976; Donovan and Ragland, 1986).

Following deposition of the Arbuckle Group, differential uplift of the craton led to the well-documented pre-Simpson unconformity across the midcontinent. The pre-Simpson unconformity is a product of dissolution and fluvial erosion. Karst is recognized and documented in Kansas (Lee et al., 1948), Missouri, and Arkansas (Purdue and Miser, 1916; McKnight, 1935), Kentucky and Tennessee (Kyle, 1976; Anderson, 1991) and Texas (Wright 1965). Karstification of the Arbuckle Group in the midcontinent has been documented as far south as Latimer County, Oklahoma (Carpenter and Evans, 1991), but is absent in the SOA indicating that the rapidly

subsiding parts of the basin appear to have continuous deposition between the Arbuckle and overlying Simpson Groups (Johnson, 1991). The Arbuckle Group and Timbered Hills Group were combined in this assessment to comprise the Arbuckle zone (Figure 1.2).

After the pre-Simpson unconformity, the Ordovician reservoirs, including the Simpson Group, Viola Limestone, and Sylvan Shale, were deposited across Oklahoma. Continuous deposition occurred through the Devonian, depositing the Hunton Group. The end of the Hunton Group is marked by the post-Hunton orogeny, which led to uplift and erosion across most of Oklahoma (Amsden, 1980). The post-Hunton unconformity removed portions of the Hunton Group across north-central Oklahoma and additionally cut down into the Ordovician strata, removing the Sylvan Shale, Viola Limestone, Simpson Group, and Arbuckle Group.

After the post-Hunton orogeny, the Misener Sandstone, Woodford Shale, and Mississippian Formation were deposited across Oklahoma. The end of the Mississippian is marked by the pre-Pennsylvanian unconformity. The ancestral Anadarko basin was experiencing rifting until the end of the Mississippian, leading to extensional faults across Oklahoma. The later Pennsylvanian time is divided into 5 epochs and includes Morrowan (early), Atokan, Desmoinesian (middle), Missourian, and Virgilian (late), all of which had orogenic events associated with them. These orogenies reactivated and transformed the extensional faults into compressional thrust faults. It led to uplift along the Nemaha ridge and Cherokee platform and created the massive, regional pre-Pennsylvanian unconformity. The unconformity extends west of the Nemaha and along the Anadarko shelf but disappears in the Anadarko and Arkoma basins, where deposition of the Pennsylvanian sands was taking place.

The regional seal for the Arbuckle Group is the shale that develops in the Simpson Group. The Oil Creek Formation at the base of the Simpson Group is described as medium-to

coarse-grained with well-rounded to rounded, frosted quartz grains and variable amounts of silica or carbonate cement. It is overlain by the Oil Creek "shale" in Oklahoma, which is predominantly limestone and dolomite. It is the first incursion of significant quantities of clay into Oklahoma following the basal Oil Creek Formation deposition (Suhm, 1997). The shales that develop within the Oil Creek Formation act as seals for hydrocarbons present in the Oil Creek sandstones and the lower Arbuckle Group.

Methods

Subsurface Mapping

The stratigraphy of the Arbuckle Group and the rest of the lower Paleozoic reservoirs including the Mississippian (less Chesterian strata), Woodford Shale, Hunton Group, Sylvan Shale, Viola Limestone, Arbuckle Group and crystalline basement was developed by interpreting conventional well logs (e.g., gamma-ray, apparent porosity, bulk density, resistivity) and classified lithology logs (i.e. mudlogs or sample logs). Formation tops were interpreted by the author through means of dip- and strike-oriented cross sections.

Well-derived formation tops resulted in 80,800 tops for the Mississippian (less Chesterian strata), 62,000 tops for the Woodford Shale, 41,200 tops for the Hunton Group, 34,300 tops for the Sylvan Shale, 40,800 tops for the Viola Limestone (Ordovician), 5,591 tops for the Arbuckle Group and 257 tops for the crystalline basement (Figure 1.1). Based on the interpreted formations from well logs, structure maps were generated for the Mississippian, Woodford, Hunton, Sylvan Shale, the Viola (Ordovician), Arbuckle, and crystalline basement (Figure 1.2). Due to the significant well control, the Mississippian structure map was used as the initial reference surface to constrain the structure maps of deeper formations. A structure map was

generated from well tops using a 2,500 ft x 2,500 ft (762 m x 762 m) grid and convergent gridding. Isopach maps were generated for the interval from the Mississippian to the Woodford (MSSP zone), Woodford to the Hunton (WDFD zone), Hunton to Sylvan (Hunton zone), Sylvan to Viola (SLVN zone), Viola to Arbuckle (Ordovician zone) and Arbuckle to crystalline Basement (Arbuckle zone). The isopach map for the MSSP zone was subtracted from the Mississippian structure map to create the Woodford structure map. The isopach map for the WDFD zone was subtracted from the Woodford structure map to generate the Hunton zone structure map, and so forth until the structure for the crystalline basement was generated. Of the 5,591 Arbuckle Group penetrations, 403 wells have modern log suites imported or digitized into log ascii standard (LAS) format. Of the 403 wells with LAS, 82 are full penetrations of the Arbuckle zone, while 321 are partial penetrations (Figure 1.1).

Two wells with full Arbuckle cores were used: the Amoco Shad 4 core in Rogers County, Oklahoma, and the KGS Wellington 1-32 core from Sumner County, Kansas. The Shad 4 core was acquired in 1986 by Amoco to test a continuous wireline slim-hole coring system. A detailed core description by Derby (1991) and core photos were used. Because of the coring test purpose, the core is 2.5 in (6.4 cm) in diameter, and there are no well logs or core porosity and permeability data. The Shad 4 well is in an area where the Arbuckle Group is too shallow to store CO_2 as a supercritical fluid (less than 2,000 ft deep). There are no Ordovician reservoirs present in the wellbore; the Devonian Woodford Shale sits directly above the Arbuckle Group. The KGS Wellington 1-32 well has modern well logs, core porosity and permeability, and core photos.

Derived Petrophysical Logs

The conventional modern well logs and other parameters in GVERSE Geographix were used to calculate derived logs for total porosity (PHIT), density porosity (PHID), shale volume (V_{sh}), apparent matrix grain density (RHO_{maa}), apparent matrix volumetric cross-section (U_{maa}), and percent mineralogy/lithology.

Mineralogy logs were generated using the RHO_{maa} - U_{maa} mineralogy cross-plot methodology with a 4-mineral (calcite, dolomite, quartz, and shale) model. To evaluate mixed lithologies and to semi-quantitatively estimate mineral volumetric proportions, a cross plot of the apparent matrix grain density, RHO_{maa}, versus apparent matrix volumetric cross-section, U_{maa}, is generated (Doveton, 1994). To compute the apparent matrix properties, the apparent porosity (i.e., total porosity), PHIT, is calculated as follows.

$$PHIT = \frac{PHID+PHIN}{2} \qquad \text{Eq (1)}$$

Because the Arbuckle zone is predominantly dolomite, PHID was calculated from RHOB using a dolomite matrix (ρ_m = 2.85 g/cm^3) with saltwater (ρ_f = 1.02 g/cm^3):

$$PHID = \frac{\rho_m - \mathrm{RHOB}_B}{\rho_m - \rho_f} \qquad \text{Eq (2)}$$

Shale Volume (V_{sh}) was determined from GR with GR_{cl} = 20 API and GR_{sh} = 100 API for clean (non-shaley) and shale endmembers, respectively.

$$V_{sh} = \frac{GR - GR_{cl}}{GR_{sh} - GR_{cl}} \qquad \text{Eq (3)}$$

The apparent matrix grain density is computed as:

$$RHO_{maa} = \frac{RHOB - PHIT * RHO_{fl}}{1 - PHIT} \quad \text{Eq (4)}$$

Where RHO_{fl} is the flushed zone pore water density (RHO_{fl} = 1.0 g cm^{-3}). The apparent matrix volumetric cross-section, U_{maa}, is computed from the photoelectric factor log and bulk density log as:

$$U_{maa} = \frac{PEF * \rho_e - PHIT * U_f}{1 - PHIT} \quad \text{Eq (5)}$$

Where ρ_e is the electron density and U_f is the volumetric photoelectric absorption or volumetric cross section of the flushed zone pore space (U_f = 0.398 barnes cm^{-3}). The photoelectric index, ρ_e, must be converted to a volumetric measure by multiplying the electron density, which is defined as:

$$\rho_e = \frac{\rho_B + 0.1883}{1.0704} \quad \text{Eq (6)}$$

RHO_{maa} and U_{maa} are cross-plotted on an imposed ternary diagram with trend lines for quartz, calcite, and dolomite. Shale percentage was calculated from GR and the calcite, quartz, and dolomite percentages from cross plot analysis. Calcite in the Arbuckle zone is described and interpreted as limestone. Quartz, or silica in the Arbuckle Group, is described as both chert and siltstone. Additionally, the Timbered Hills Group contains the Reagan Sandstone, all of which are included in the Arbuckle zone. Therefore, this mineralogy is interpreted as both sandstone and silica.

Because the volume of shale was calculated from GR, it is indicative of clay mineralogy in the Arbuckle zone. To generate lithology logs from the mineralogy logs, it was assumed that the dominant mineralogy at each depth corresponds to limestone (for calcite), dolostone (for dolomite), sandstone-silica (for quartz), and shale (clay content).

3-D Modeling and CO_2 Storage Resource Estimation

Three-dimensional geological models of key properties were constructed to ultimately calculate pore volume and CO_2 storage resources for the Arbuckle zone. Using the 3-D models to determine the CO_2 storage resources, the U.S. Department of Energy (US-DOE) methodology (NETL, 2007 & 2008; IEA GHG, 2009) was used as follows:

$$G_{CO2} = A * h * \varphi * \rho_{CO2} * E_{saline} \quad \text{Eq (7)}$$

G_{CO2} is the mass of CO_2 stored in the reservoir, A is the area of reservoir, h is the thickness of reservoir, φ is the total porosity, ρ_{CO2} is the density of CO_2 (dependent on temperature and pressure; dependent on depth), and E_{saline} is the saline storage efficiency coefficient (dependent on lithology).

The 3-D stratigraphic and structural framework (3-D model grid) of the Arbuckle zone was generated using the structure maps that define the reservoir zones. The 3-D grid covers an area of approximately 44,627 mi^2 (115,583 km^2) with aerial cell dimensions of 2,500 ft x 2,500 ft (762 m x 762 m). The Arbuckle zone was divided stratigraphically into 400 proportional layers, each approximately 6 ft (1.8 m) thick. The resulting 3-D model grid has 60,312,430 cells.

To represent the spatial variability of lithologies for the Arbuckle zone, a 3-D lithology model was constructed with commercial software using sequential-indicator simulation (SIS). The model constraints include: 1) the stratigraphic and structural framework (3-D grid), 2) upscaled lithology logs, 3) variogram parameters by zone, 4) lithology percentages by zone, and 5) vertical lithology proportion curves. Lithology logs were upscaled to the 3-D model grid by

assigning a single lithology class to a cell based on the most abundant lithology within a cell. The target fractions of each lithology were obtained from the upscaled lithology logs.

A 3-D porosity model was generated to evaluate the distribution of total porosity (PHIT) within the study area. PHIT logs were biased to the lithology logs and upscaled using an arithmetic mean. The porosity model was generated using sequential-Gaussian simulation (SGS) and was constrained to: 1) a 3-D lithology model, 2) upscaled PHIT logs (biased to lithology), 3) porosity histograms by zone and lithology, and 4) variogram parameters by zone and lithology.

The density of CO_2 in the reservoir is dependent on the temperature and pressure of the reservoir. Bottom hole temperature and total depth from the wellbore data across Oklahoma are available from the Southern Methodist University Geothermal Lab, which is a part of the National Geothermal Data System funded by the U.S. DOE (SMU Node of National Geothermal Data System, Heat Flow and Well Data, accessed March 2023). A temperature gradient map was generated for the state, assuming a 60° F surface temperature to bottom hole temperature. Using the temperature gradient map and measured depths from the 3-D grid, a 3-D temperature model was calculated for Oklahoma. Pressure data acquired from oil and gas operators across Oklahoma indicate that the Arbuckle Group is normally pressured (Puckette, 1996). Using a pressure gradient of 0.44 psi/ft (9,953 Pa/m), a 3-D reservoir pressure model was generated using the measured depths from the 3-D grid. Lastly, using the ideal gas law, the temperature model and pressure model were used to calculate the 3-D CO_2 density model as follows:

$$\rho = \frac{p*M}{R*T} \qquad \text{Eq (8)}$$

Where ρ is the density (g/m^3) of CO_2 at temperature and pressure, p is the pressure (pascal; Pa), M is the molar mass of CO_2 = 44.01 g/mol, R is Avogadro's constant and equal to 8.31 (joule/mol*kelvin; J/mol*K) and T is temperature (kelvin; K).

Saline storage efficiency coefficient (E_{saline}) is the percentage of pore space that the CO_2 will occupy in the reservoir and is dependent on lithology. The 2009 International Energy Agency Greenhouse Gas Development of Storage Coefficients for CO_2 storage in deep saline reservoirs (IEA GHG, 2009) states that E_{saline} is a function of the lithology and depositional environment and is calculated as (see Table 1.1 for a description of the equation terms):

$$E_{Saline} = \frac{A_n}{A_t} * \frac{h_n}{h_g} * \frac{\emptyset_{eff}}{\emptyset_{tot}} * (E_A * E_I * E_g * E_d) \qquad \text{Eq (9)}$$

The last 4 terms define the pore volume immediately surrounding a single well CO_2 injector. E_A is the areal displacement efficiency, E_I is the vertical displacement efficiency, E_g is gravity, and Ed is the microscopic displacement efficiency. To calculate storage efficiencies, heterogeneous 3-D models were developed for various lithologies, depositional environments, and structures. Statistical distributions from a global database of hydrocarbon reservoir properties were used, including key parameters like porosity and permeability (IEA GHG, 2009). The ranges of storage coefficients for each lithology were derived based on 195 simulations. If the assessment of storage resource is over a small, localized area, then it is likely that the values of the A_n/A_t and h_n/h_g will be relatively high. Therefore when determining E_{saline} at the site-specific level A_n/A_t was fixed at .8 while h_n/h_g and $\emptyset_{eff}/\emptyset_{tot}$ ranges between .25-.75 and .6-.95 respectively (Table 1.1). Regionally, the geologic properties will vary spatially; For this reason, the P_{50} of the A_n/A_t and h_n/h_g terms were fixed to determine the formation level E_{saline} values. This leads to an overall lower storage coefficient for each lithology at the formation level. E_{saline} values are reported for

the P_{10}, $P_{50,}$ and P_{90} for clastics, dolomites, and limestones at the site-specific and formation level evaluations. P_{10} notation indicates that there is a 10% probability that the value is less than the P_{10} value, and the P_{90} notation indicates there is a 90% probability that the value is less than the P_{90} value. The total CO_2 storage resources for the model were calculated for both the site-specific and formation level E_{saline} values. Table 1.2 shows the E_{saline} values for each lithology. Because E_{saline} values were reported by lithology, they were also applied to the corresponding lithologies in the model, with the values for clastics being applied to both the sandstone-silica and shale lithologies.

Induced Seismicity Risk

To generate an induced seismicity risk map, the fault database, high-rate SWD injection wells, and earthquake locations from 2011 to 2023 were used. The distance from the epicenter of all earthquakes larger than 3.0 M, the distance from mapped faults (the OGS Comprehensive Fault Database and faults identified by this study), and the distance from the high-rate SWD injection wells were calculated. They were then summed and rescaled from 0 to 1 to give a general induced seismicity risk map for the Arbuckle zone. The closer the reservoir is to a fault, high-rate injection well, or earthquake, the higher the risk of induced seismicity.

Results

Structure, Thickness, and Lithology Trends

The lower Paleozoic reservoirs across Oklahoma are structurally complex and highly faulted in certain areas. The Mississippian structure map, which was used to constrain the deeper formations across Oklahoma, coincides with the massive, regional pre-Pennsylvanian unconformity (Figure 1.3A and 1.3B). The unconformity extends west of the Nemaha and along

the Anadarko shelf but disappears in the Anadarko Basin, where deposition of the Pennsylvanian sands was taking place. Faults can be identified on the Mississippian structure map where the dip magnitude is high (dark grey to black) and a change in dip azimuth aligns.

In central Oklahoma, there are localized areas where the Mississippian, Woodford Shale, Hunton Group, Sylvan Shale, and Ordovician have been removed due to the pre-Pennsylvanian unconformity and post-Hunton unconformities (Figure 1.4). In these areas, the Pennsylvanian shales sit directly above the Arbuckle zone; the Oklahoma City oilfield and Cushing oilfields are examples. The Pennsylvanian shales act as the hydrocarbon seal for the Arbuckle Group in these areas. In general, the sealing reservoir for the Arbuckle Group is the younger Ordovician-aged shales. They are present across most of the state, except northeastern Oklahoma, where the Ordovician reservoirs have been removed (Figure 1.4B). Where this occurs, the Woodford Shale is present and above the Arbuckle Group and acts as the seal for the Arbuckle Group.

Because the Paleozoic formations were subjected to the same Pennsylvanian orogenies, faults that penetrate the shallower Mississippian commonly penetrate the deeper strata. This is why the Mississippian, Arbuckle, and basement structural trends all look very similar (Figures 1.3A, 1.5A, 1.5B). The only difference is that offset along faults become greater with stratigraphic age. When comparing the Arbuckle structure map to the basement structure map, there are some slight differences. While the Arbuckle dips west-southwest in Osage, Pawnee, and Payne counties, the Basement structure map shows two bulges with localized changes in dip direction and a crest in Osage County (Figure 1.5B, arrows).

The modified fault database displayed on Figures 1.3B, 1.5A, and 1.5B is a combination of the OGS Comprehensive Fault Database along with additional faults identified from the Arbuckle structural model. The Nemaha fault and Wilzetta fault are the two most prominent

North-South trending faults in the study area. There are also areas with east-west trending faults that show strike-slip movement (e.g., Logan County). Faults are not limited to north-central Oklahoma. While the Comprehensive Fault Database shows minimal faulting across the Oklahoma panhandle, there are, in fact, many faults present. This study's structural model, generated from well-derived formation tops, agreed with nearly all of the faults in the Comprehensive Fault Database and identified many more, especially in the Oklahoma panhandle.

In the heart of the Anadarko basin, the Arbuckle zone ranges from 100-5,600 ft (30-1,707 m) thick (Figure 1.4C). It is the thickest in southern Oklahoma near the SOA. It thins as it comes out of the Anadarko and Arkoma basins. In north central Oklahoma and the Oklahoma panhandle, it is roughly 1,000 ft (305 m) thick, but thins over small, paleo-highs across the Cherokee platform. These thins are usually fault-related and localized. The Arbuckle is present in the northeastern corner of Oklahoma but is not at depths deep enough for CCUS (Figure 1.5A).

The Arbuckle zone is predominantly dolomite but does contain chert, sandstones, siltstones, and shales. A type-log for the Arbuckle zone (Figure 1.6) illustrates mineral percentage curves generated using the 4-mineral (limestone, dolomite, sandstone-silica, and shale) model. The last track shows the dominant lithology at each depth, which was used in the lithology modeling. The RHO_{maa} - U_{maa} plot shows that the dominant mineralogy is dolomite with lesser amounts of quartz and calcite (Figure 1.7). The Arbuckle zone encompasses the Reagan Sandstone when it is present. It develops directly above the basement and is the lowest 10 ft (3.0 m) of the type-log. The Reagan Sandstone is arkosic, and in the Shad 4 core is also shaley (Derby, 1991). While no well logs were run in the Shad 4 core, the Shad 1 well, roughly 30 ft (9.1 m) away, does have open hole well logs and was used for general correlation purposes.

Like other arkosic sandstones, the Reagan Sandstone has a high gamma-ray reading of above 150 API (Figure 1.6). Because the shale content in the model is a direct result of gamma-ray, the Reagan Sandstone appears as a shale. Wilson et al. (1991) also describe a high gamma-ray response in the Arbuckle as thin clastic intervals. Therefore, shale in the lithology model is likely a combination of Reagan Sandstone at the base of the zone and clastic layers within the Arbuckle Group.

The limestone present in the Arbuckle Group is predominantly in the SOA, where dolomitization was precluded due to intense pressure solution. There is some limestone outside of the SOA, but they are generally thin beds within the Arbuckle Group. In the Arbuckle zone, lithologies are predominantly dolomite (85%) with lesser amounts of shale (8%), silica (4%), and limestone (3%) (Figure 1.8).

The Arbuckle lithology model shows that the Arbuckle is a somewhat heterogeneous reservoir of predominantly dolomite with interbedded thin clastic layers (Figure 1.8B). There is an increase in limestone in the SOA (red arrow), and a slight increase in silica in mid-central Oklahoma (black arrow). The top of the Arbuckle is an unconformity (pre-Simpson unconformity) across much of the state. While predominantly dolomite at the top, the overlying Joins Formation is typically sandstone or limestone in the study area. At times, it can be hard to differentiate the contact between the Joins Formations and Arbuckle Group, leading to all 4 lithologies being present at the top of the zone.

The limestone isopach generated from the lithology model shows a thickening in the deep basin (Figure 1.9A, red arrow). Outside of the SOA, there is significantly less limestone present. The sandstone-silica and shale maps (Figure 1.9B and 1.9C) both show thickenings in the Anadarko Basin and also in central Oklahoma near Oklahoma, Logan, and Lincoln counties

(Figure 1.9B, black arrows). The dolomite isopach looks nearly identical to the Arbuckle zone's gross isopach (Figure 1.4C) because it is the overwhelmingly dominant lithology in the reservoir.

Petrophysical Properties

The Arbuckle average total porosity is 7% and ranges from 2-14%. Both the Shad 4 core and the KGS Wellington 1-32 core show large secondary vugular porosity omnipresent throughout the well. Vugs can be very large (greater than the core width of 2.5 inches) and interconnected at times. Visual approximations of porosity were approximated by Derby (1991), which show that the Shad 4 core has many zones with porosity between 10-20% and greater than 20%. While the cored wells do not have sonic logs, there are 59 wells with sonic logs in the data set. In carbonates with vugular and moldic porosity, this secondary porosity can be approximated by subtracting the sonic porosity from the total (neutron-density) porosity (PHIT) (Schlumberger, 1989). For the 59 wells with sonic logs, the average secondary porosity for the Arbuckle zone is 2%. Because of the lack of a core to confirm the secondary porosity, the total porosity for the storage calculations was used directly. Porosity in the Arbuckle Group has also been approximated from tidal strain analyses from shut-in Arbuckle SWD's (Perilla-Castillo, 2017). Perilla-Castillo used 6 shut-in Arbuckle SWDs to calculate a median value of 24% for porosity in the Arbuckle, with the minimum and maximum porosity of 7% and 52%, respectively. It should be noted that when the study was conducted, large volumes of water had already been disposed of, which could have altered rock properties and therefore affected these porosity values. Regardless, the results presented herein use a conservative approach with well log-based porosity values.

The total porosity (PHIT) model was constrained to the lithology model (Figure 1.10). Average total porosity is 7% except in areas across the Cherokee platform (Figure 1.10B and 1.10C, black arrows). The Cushing oilfield, where the Arbuckle sits directly under the pre-Pennsylvanian unconformity, has noticeably higher porosity. Average porosity in the Cushing oilfield is upwards of 12%. The multiple erosional events removed roughly 850 ft (259 m) of Mississippian through Ordovician-age rock and enhanced porosity in the Arbuckle zone.

Based on the 3-D models of temperature and pressure, temperature for the Arbuckle ranges from 75-525°F (24-274 °C) (Figure 1.11A). Pressure ranges from 500-16,000 psi (3.45-110 MPa) with a median value of 4,000 psi (27.6 MPa) (Figure 1.11B). The temperature and pressure 3-D models were used to calculate the CO_2 density model (Figure 1.11C). CO_2 density ranges from 100-1,000 kg/m^3 with a median of 350 kg/m^3.

CO_2 Storage Resources

The CO_2 storage resources for the Arbuckle zone using the site-specific and formation level E_{saline} values range from 129,013-307,421 Mt (Table 1.3) and 50,673-118,436 Mt, respectively (Table 1.4, Figure 1.12). The CO_2 storage resources at the formation level are reduced by 33% for limestone, 40% for sandstone, and 37-41% for dolomite, and are directly related to the reduction in E_{saline} values. The CO_2 storage resource model using the P_{50} E_{saline} values at the formation level (Figure 1.13) shows the highest storage resources in the deep Anadarko Basin. Note: All figures for CO_2 storage resources were generated using the P_{50} E_{saline} storage efficiency factors at the formation level, giving a conservative estimate of CO_2 storage resources.

Because the Arbuckle zone ranges from 2,000-36,000 ft (610-10,973 m) deep across the study area and the goal of CCUS is to store the most CO_2 for the least cost, and the cost to drill a well increases with depth, the CO_2 storage resources were summed across 2,000 ft (610 m) depth intervals (Figure 1.14A). For example, from 4,000-6,000 ft (1,291-1,829 m) depth, the purple-colored contour interval on the map can store between 3,000-17,998 Mt of CO_2, depending on the E_{saline} values used. This is also 6% of the total storage resources for the entire study area. CO_2 storage resources across the state have a very broad range between 0-6.0 Mt per square mile. Across most of north central Oklahoma, the CO_2 storage resources per square mile are less than 2.0 Mt with little variability.

Induced Seismicity Risk

From 2011 to 2023, Oklahoma experienced 3,005 earthquakes that registered at or above 3.0 M (Figure 1.15A). There were 2,858 earthquakes with hypocenters located in the basement (Figure 1.15B and 1.15C), 41 earthquakes in the Arbuckle zone (Figure 1.16A), and 88 earthquakes above the Arbuckle zone (Figure 1.16B). Most of the events in Oklahoma originate in the basement. The majority of earthquakes occurred across the Cherokee platform and at depths significantly deeper than the top of the basement. All the seismic events above 5.0 M originated in the basement. In and above the Arbuckle zone had significantly fewer and smaller seismic events than the basement (Figures 1.16A and 1.16B).

As anticipated, north-central Oklahoma and the Anadarko shelf have a higher risk of induced seismicity and have a higher density of SWD wells (Figure 1.17). Seismic events occur along mapped faults (Figure 1.17, red arrows). They also follow faults that are likely to extend farther than the mapped distance (Figure 1.17, blue ellipse). There are also areas where there are

no apparent faults in the basement, but SWD injection wells are present, and earthquake swarms have occurred (Figure 1.17, green ellipse).

Induced seismicity in Oklahoma is, in part, tied to SWD injection volumes, Figure 1.18. While wastewater injection volumes began to increase in 2011, it took until 2013 before Oklahoma experienced an increase in seismic events. By the middle of 2015, wastewater injection volumes and seismic activity peaked. In response to the increase in seismicity, the OCC began imposing regulations that required operators to reduce wastewater injection volumes in earthquake prone areas by approximately 800,000 barrels per day, and to confirm that wells were not injecting into the crystalline basement. At the time, there were 227 wells disposing in or in communication with the basement that the state required to be shut-in or plugged back to a total depth above the basement (Response to Oklahoma Earthquakes, accessed 2024). These regulations have succeeded in reducing the earthquake count to pre-2013 frequencies. It should be noted that there have been no reports of wastewater leakage at the surface for any of the earthquakes or SWD disposal wells.

There are areas across the Cherokee platform that appear to have a lower risk of induced seismicity, specifically Osage County (Figure 1.17). Osage County coincides with the Osage Nation, which means the EPA maintains authority over injection wells, while the OCC oversees the rest of the state. This is why there are no SWD wells shown in Osage County (Figures 1.17 and 1.18B). There are SWD wells in Osage County (Barbour et al., 2017); however, this study did not have access to records of SWD wells in Osage County because they are not managed by the OCC. The increase in wastewater volumes was a direct result of the increase in horizontal Mississippian wells, which produced large volumes of water along with hydrocarbons. The first wave of horizontal Mississippian wells drilled in Oklahoma, from 2010 to 2016, were drilled

across north-central Oklahoma and were associated with large volumes of produced saltwater that required disposal (Figure 1.18B, red, orange, and yellow horizontal wells). Interestingly, there are no horizontal Mississippian wells in Osage County, indicating there would not be a large increase in produced water or water disposal in this region. The second wave of horizontal Mississippian wells was drilled from 2016 to the present, were drilled in the Sooner Trend, Anadarko, Canadian, and Kingfisher (STACK) area (Figure 1.18B green and blue horizontal wells). While the STACK Mississippian wells still produce water along with hydrocarbons, there has been no increase in wastewater injection volumes associated with their development.

It has been proposed (Shah and Keller, 2017) that this lack of induced seismicity is partially related to the basement rock type. Large intrusions that are minimally fractured appear to impede seismicity, which is what underlies Osage County. This study proposes that the lack of seismicity in Osage County is also related to the lack of horizontal well development and therefore lack of SWD injection volumes.

Discussion

CO_2 Storage Resources Calculations

The CO_2 storage resources are controlled by porosity, depth (i.e., pressure), and thickness. As these variables increase, so does CO_2 storage resources. Interestingly, the areas of increased porosity do not show an increase in CO_2 storage resources per square mile (Figure 1.19). This indicates that the depth and thickness are the main drivers of CO_2 storage resources for the Arbuckle zone.

The US-DOE methodology says the first three terms used to determine E_{saline} are the Net-to-Total Area, Net-to-Gross Thickness, and Effective-to-Total Porosity ratio (Table 1.1). The site-

specific E_{saline} values, which are the highest used in this study, were determined by fixing the Net-to-Total Area to .8, the Net-to-Gross Thickness ranged between .25-.75, and the Effect-to-Total Porosity ranged between .6-.95 (Table 1.1, third column). All 3 of these factors are equal to 1 in this study. This means the most optimistic CO_2 storage resources reported in this study (i.e., the site-specific level) are still likely to be an underestimation of total CO_2 storage resources.

Areas of Interest

The area of enhanced porosity seen in Grant and Alfalfa counties shows the highest CO_2 storage resources between 700,000-900,000 tons of CO_2 per sq mile (Figure 1.19B) an average thickness of 1,200 ft (366 m) (Figure 1.4C) and between 6,000-7,000 ft (1,829-2,134 m) deep (Figure 1.19A). The area of enhanced porosity in Payne, Lincoln Creek, Okfuskee, and Okmulgee counties shows a much broader range of CO_2 storage resources due to the thinning of the Arbuckle zone (Figure 1.4). CO_2 storage resources in this region range from 200,000-1,000,000 tons of CO_2 per sq mi, with thickness ranging from 700-2,000 ft (213-610 m) at depths between 3,000-7,000 ft (914-2,134 m). Unfortunately, both of these areas overlap with areas of induced seismicity (Figure 1.8C). To avoid areas of known induced seismicity in Oklahoma, western Osage County and eastern Kay County would be the best location (Figure 1.19). There has been little to no Mississippian horizontal well development, which has led to fewer Arbuckle SWD volumes and less induced seismicity. The depth to the Arbuckle is between 3,000-5,000 ft deep, and it is over 1,000 ft thick. The lower Ordovician shales are present and act as a seal. The Bromide sandstones are not present in this region and would not be available as additional storage potential.

Localized areas with active Arbuckle saltwater disposal wells should be avoided, and areas with previous SWD disposal in the Arbuckle zone should be approached with caution due to the possibility of reservoir pressure anomalies. While critically stressed basement seated faults have been associated with induced seismicity (NRC 2012, McGarr et al 2002, Walsh & Zoback, 2015) the largest fault systems, the Nemaha and Wilzetta faults, do not show any significant earthquake trends with exception of the 2011 5.0 M Prague earthquake in southern Lincoln County (Figure 1.17).

The 2011 Prague earthquake and subsequent aftershocks were tied to the increase in SWD volumes (Keranen et al., 2013). Keranen used the initial event and subsequent aftershocks to illuminate and describe the faults that ruptured. The earthquakes delineate a major seismic zone, with narrow, steeply dipping planes in the sedimentary section and basement adjacent to the Wilzetta fault (Keranen et al., 2013). The initial event took place directly below the Wilzetta fault, but the aftershocks, along with many smaller events over the years, can be seen occurring in a linear pattern, sub-parallel to the Wilzetta fault southeast of the main event (Figure 1.17A, double-headed arrow). This fault, along with many others across north central Oklahoma, is below the resolution of this model (i.e., well log control) but can be illuminated by the earthquake hypocenter trends. Thanks to the combination of extreme well control and the Arbuckle Group's massive thickness (1,000-2,000 ft) across north central Oklahoma this study can confirm that if faults are present in the basement along these trends and they extend into the overlying Arbuckle Group they would have very little vertical closure and Arbuckle Group would be present on both sides of the fault. This scenario could allow for fluid flow across the fault and/or create smear along the fault, which would create an impermeable boundary leading to pressure compartmentalization.

The base of the Arbuckle across the state is either the Reagan Sandstone or the Honey Creek Limestone, which have very little clay or shale content, indicating there is no seal between the Arbuckle zone and the crystalline basement. The vast thickness of this reservoir, its lateral continuity over nearly every fault in the state and its full connection with a porous crystalline basement (Kibikas et al., 2020) is why it was able to store over 11.9 million barrels of water, or the equivalent of 20 Lake Hefner's (at full capacity) in the Arbuckle Group, from 2011-2023. Additionally, while fluid flow is likely continuous both laterally and with depth, the lack of seismic events above the Arbuckle Group is a testament to the sealing capabilities of the shales found in the Oil Creek Formation.

In 2015, it was predicted that reducing the volume of injected saltwater into the Arbuckle should reduce the amount of triggered seismicity (Walsh & Zoback, 2015). This study further confirms that induced seismicity can be mitigated by limiting wastewater volumes, injection rates, and banning wastewater injection into the crystalline basement. Doing so has brought the induced seismicity rate back down to pre-2012 levels. It has also been proven that if induced seismicity should occur, it can be remedied quickly.

Conclusions

The entire Arbuckle zone is a candidate for CO_2 injection. It is predominantly dolomite but does contain cherts, siltstones, and shales, which are all reservoir rocks. Approximately 30% of the total CO_2 storage resources for the Arbuckle zone can be reached at depths from 2,000-10,000 ft (610-3,048 m). Two areas in northern and central Oklahoma show enhanced porosity at reasonable depths (less than 8,000 ft) for CCUS. CO_2 storage resources in these regions are

generally less than 1,000,000 tons of CO_2 per square mile, with an average 8-10% porosity. These areas do overlap with where induced seismicity from wastewater injections has occurred.

The state of Oklahoma has observed a decrease in induced seismicity since it peaked in 2015 due to reduced injection rates, volume limits, and banning disposal into the crystalline basement. It is a normally pressured reservoir and is laterally continuous, even across most faults in the state. It has an average total porosity of 7% but has additional vugular porosity, which has been reported to be over 20% in some areas. The Arbuckle Group is the thickest and deepest reservoir suitable for CCUS in Oklahoma.

FIGURES

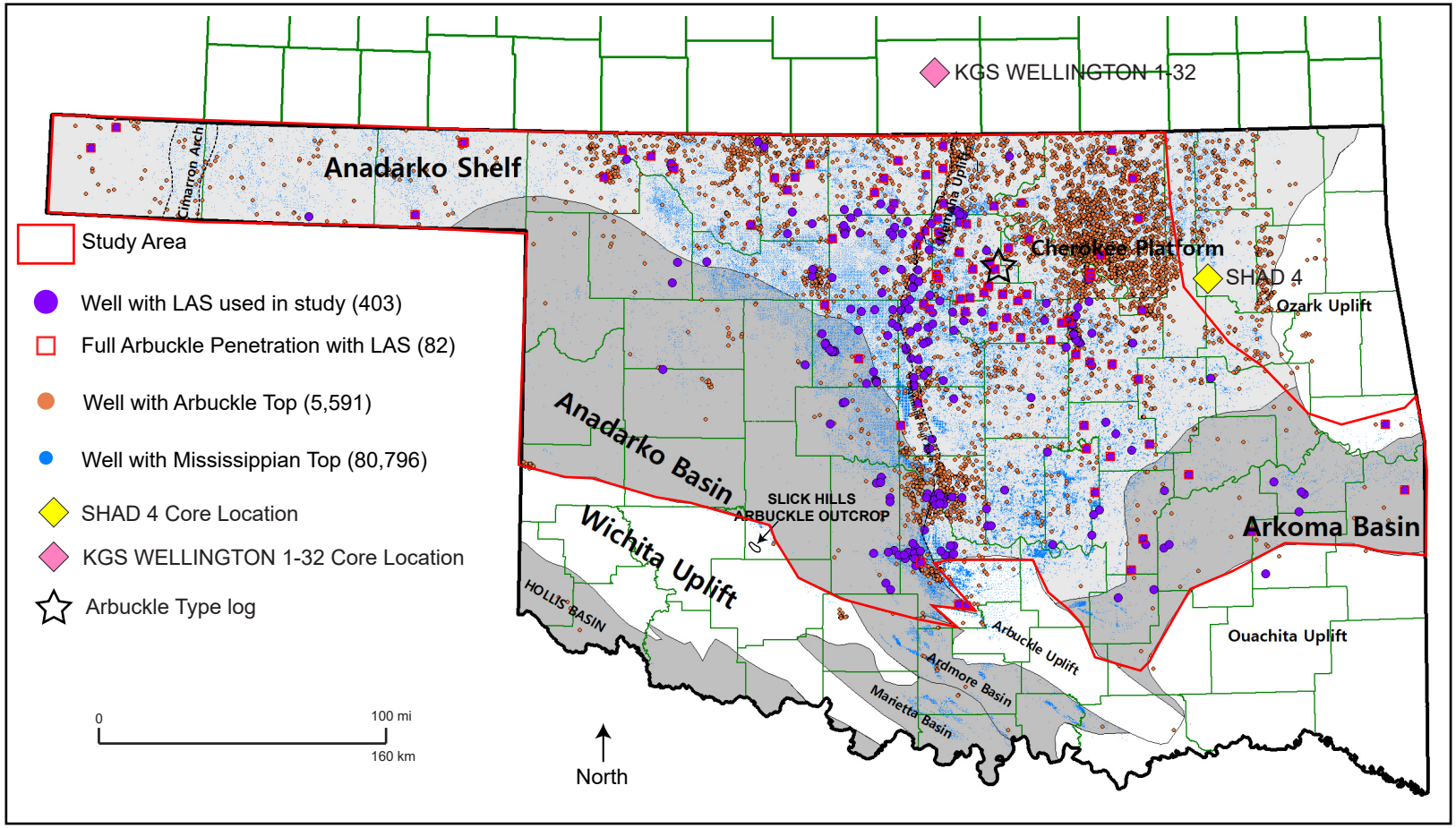


Figure 1.1. Study area and wells with LAS used in the study. Purple circles are the wells with LAS available used in the study. Red squares are wells with full Arbuckle penetration, and LAS used in the study. Orange circles are all the Arbuckle Group tops from well log interpretation. Small, light blue well spots have well tops for the Mississippian. Geologic Provinces were modified from Northcutt and Campbell, 1995. The Ardmore basin, Marietta basin, and Hollis basin were not evaluated due to structural complexities. The Ozark Uplift was evaluated where depths were adequate. Locations for the Shad 4, KGS Wellington 1-32, and Arbuckle type log from Figure 1.6.

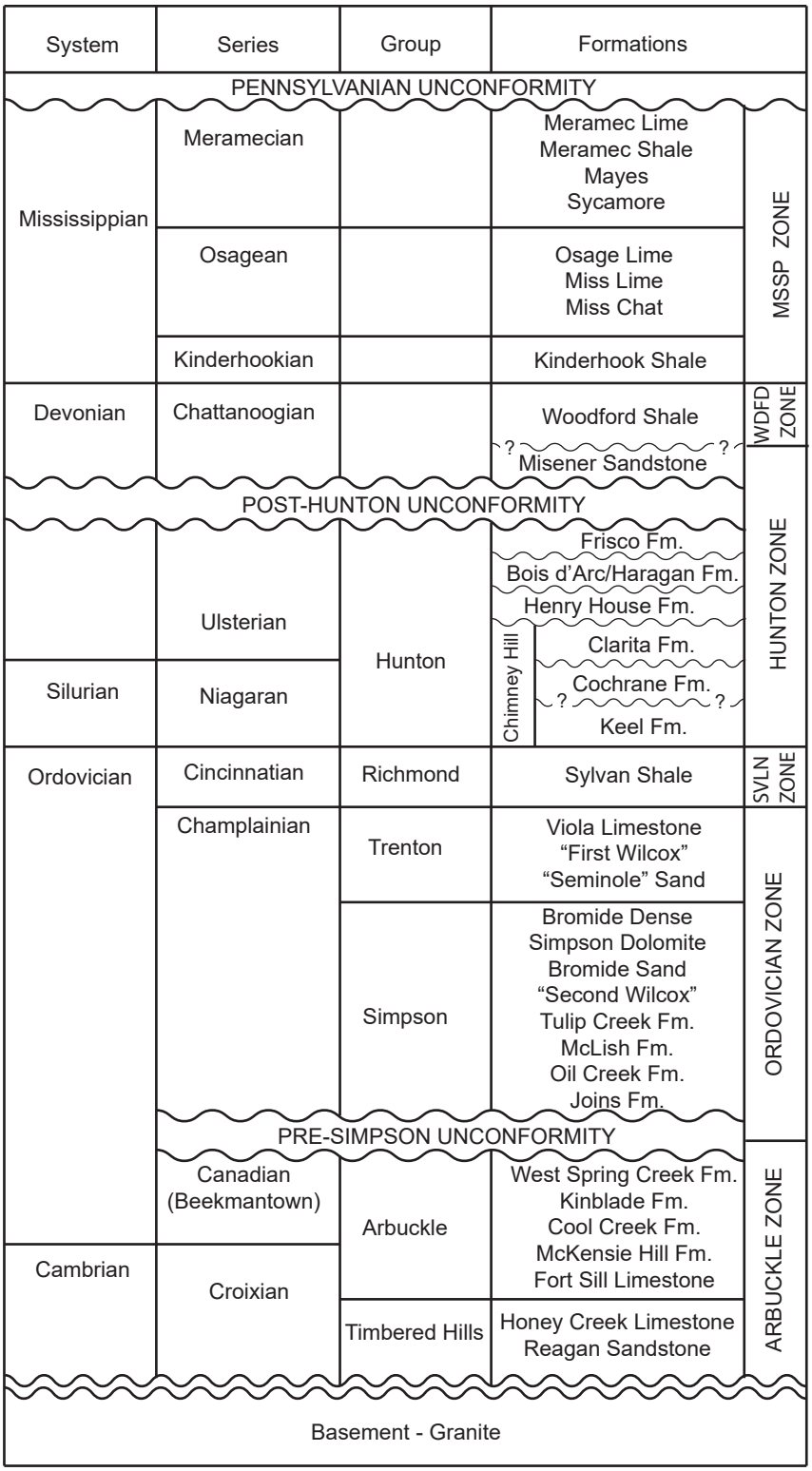


Figure 1.2. Generalized Stratigraphic Column of Oklahoma. Modified from Oklahoma corporation commissions General Geologic Sections of Oklahoma and Arkansas,1975. The top of Mississippian used for structural modeling is Meramecian in age, and the beginning of this stratigraphic column. Correlated formation tops and isopach zones used for structural modeling labeled.

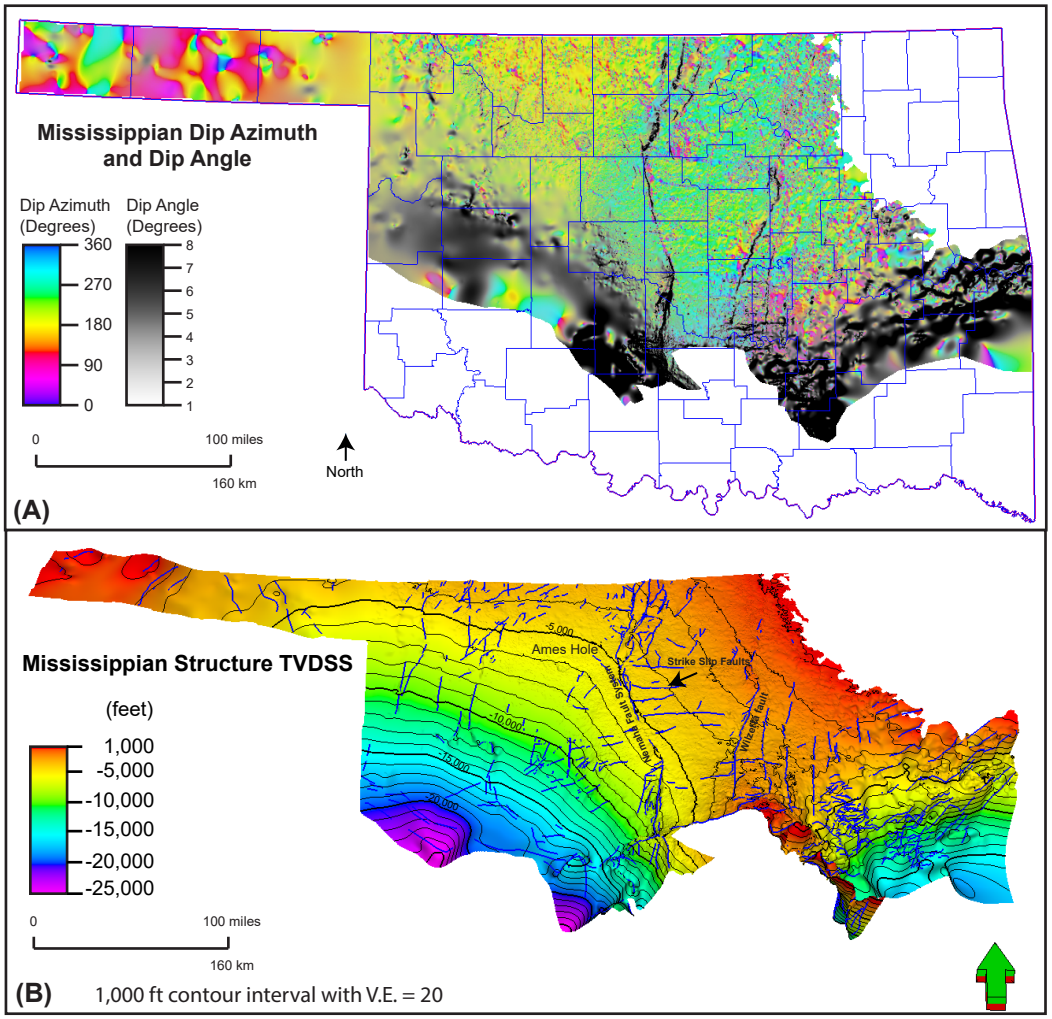


Figure 1.3. A) Dip angle co-rendered with dip azimuth for the Mississippian Structure. Faults are apparent where the dip magnitude is high (dark grey to black) and a change in dip azimuth align. B) Blue faults are the modified fault database, which contains the OGS fault database (Holloway et al., 2016) and faults identified by the author. 1,000 ft (305 m) contour interval with a 20 vertical exaggeration. Ames Hole, an Ordovician-aged meteor impact, can be seen in Major County, strike-slip faulting along the Cherokee platform, and the major fault systems have been labeled. NOTE. The Mississippian is present in northeastern Oklahoma but was outside of the modeled area and is therefore not shown on the maps.

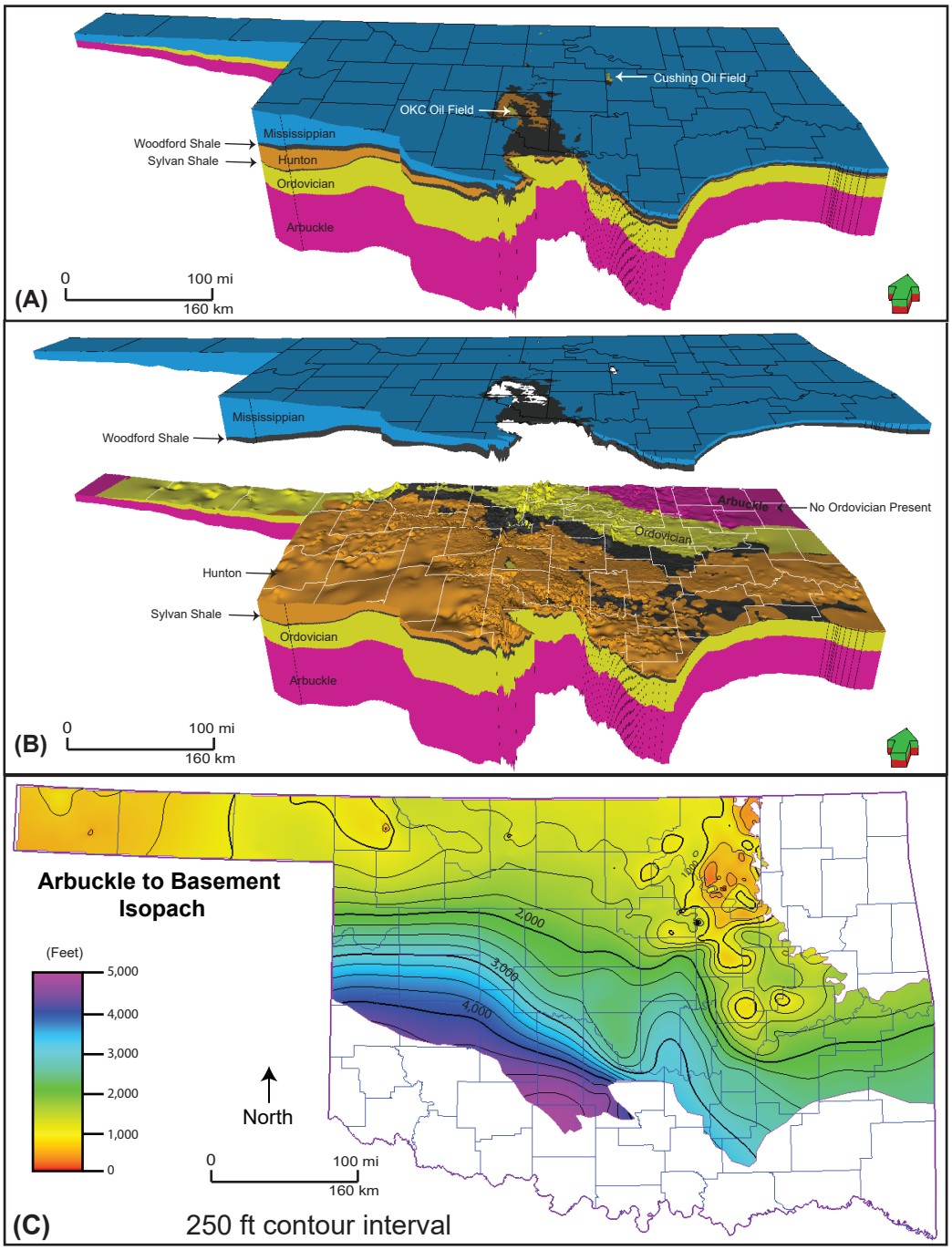


Figure 1.4. A) Mississippian (MSSP zone), Woodford (WDFD zone), Hunton (Hunton zone), Sylvan (SVLN zone), Ordovician (Ordovician zone), and Arbuckle zone flattened on the Mississippian. The top of the Mississippian is an unconformity except in the deep Anadarko and Arkoma basins, across the Anadarko shelf, and the Cherokee platform. This map is the pre-Pennsylvanian unconformity subcrop map. The Mississippian is present across Oklahoma except in central Oklahoma. B) Same model as 1.4A and except that the Mississippian and Woodford have been lifted to reveal the lateral extent of the Hunton, Sylvan, Ordovician, and Arbuckle zones. This is the post-Hunton unconformity subcrop map. C) Arbuckle to Basement (Arbuckle zone) Isopach, 250 ft (76 m) contour interval.

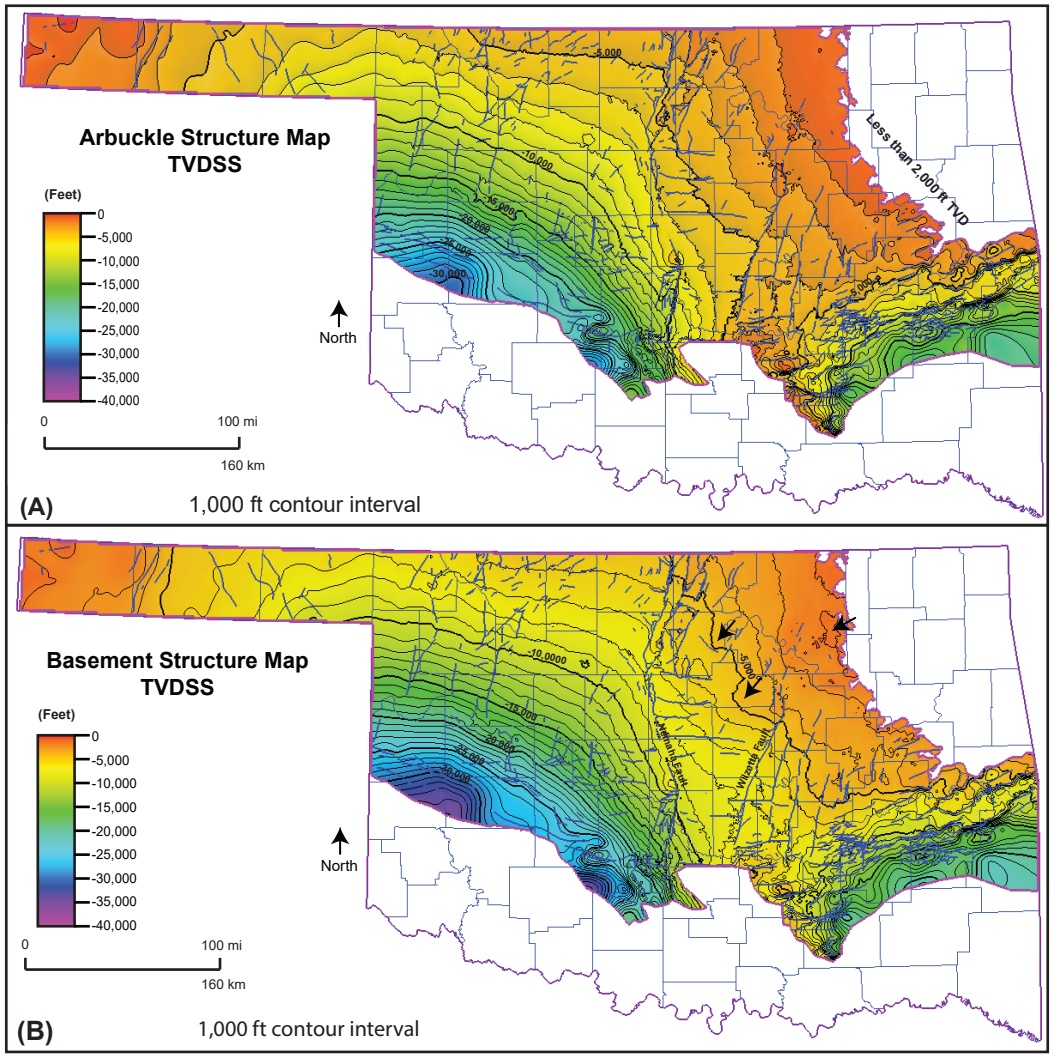


Figure 1.5. A) Arbuckle Structure map with the modified fault database, which contains the OGS fault database (Holloway et al., 2016) and faults identified by the author. 1,000 ft (305 m) contour interval. The Arbuckle is present in the northeastern part of the state, but it is shallower than 2,000 ft (610 m) deep. B) Basement Structure map with the modified fault database. 1,000 ft (305 m) contour interval. Black arrows point to basement bulges that show slightly different dip orientations when compared to the Arbuckle structure in Figure 1.5A.

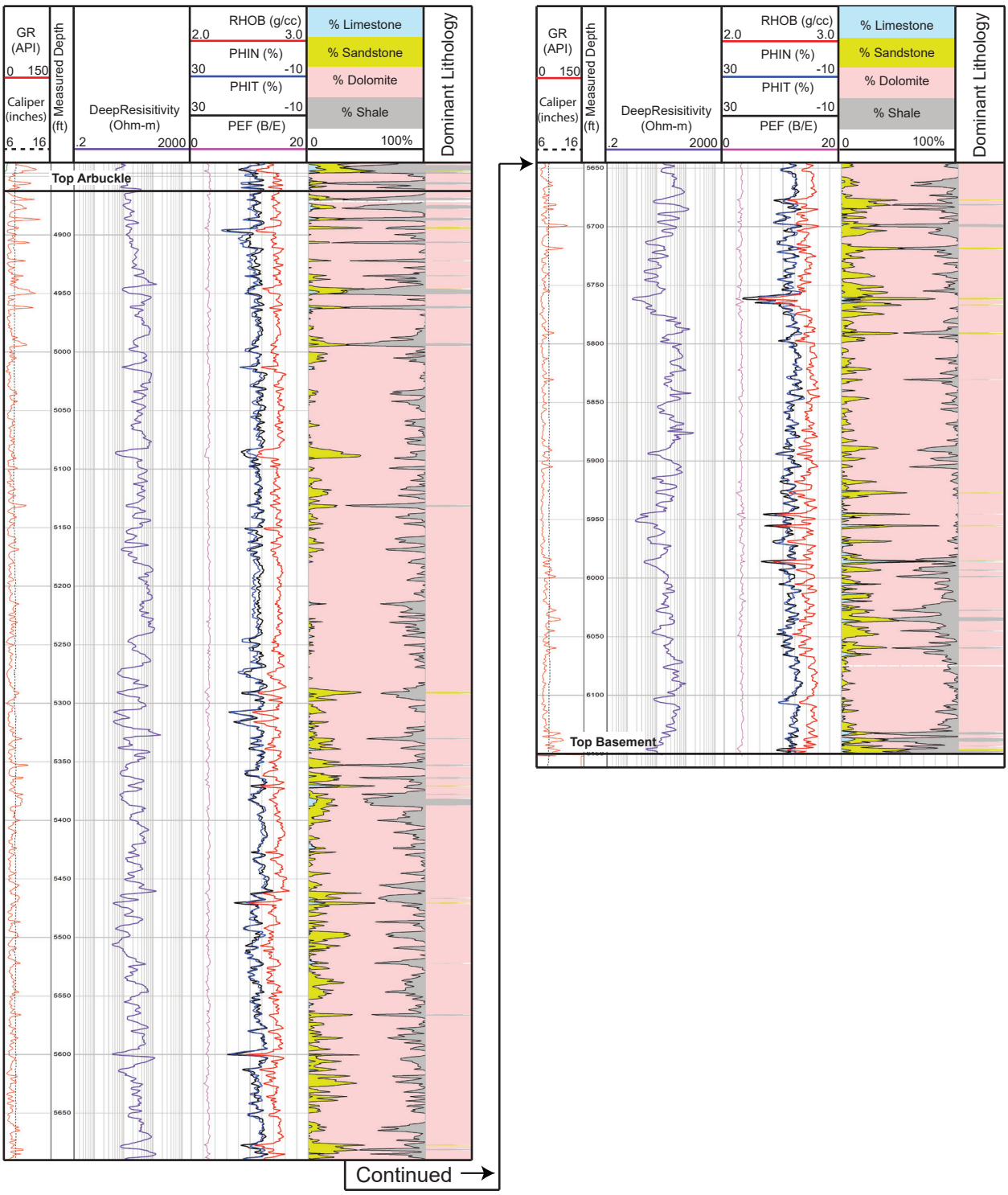


Figure 1.6. Arbuckle zone type log, Voise 1-10, UWI 35-103-24450. The top of the Arbuckle is denoted by the spread in RHOB and PHIN curve and low GR, indicating dolomite. The second-to-last column shows the mineral percentage curves from the RHOmaa - Umaa analysis, color-filled by lithology. The right column corresponds to the dominant lithology at that depth and was used for the discrete lithology log for the lithology model. The lowest 10 ft (3.0 m) of the Arbuckle zone is the Reagan Sandstone. Location seen on Figure 1.1.

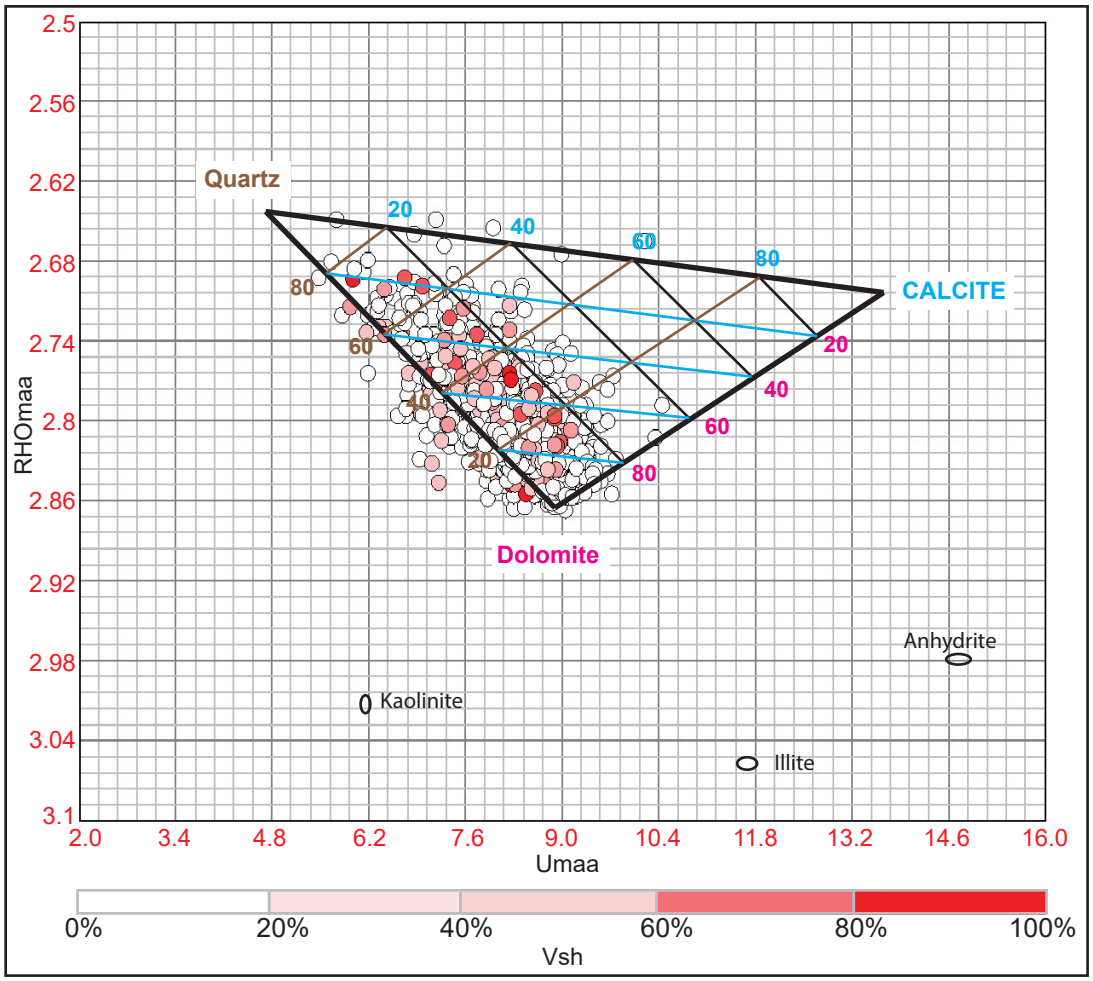


Figure 1.7. RHOmaa - Umaa plot colored by Vsh for the Arbuckle zone. The Arbuckle is predominantly dolomite with lesser amounts of shale, silica and limestone.

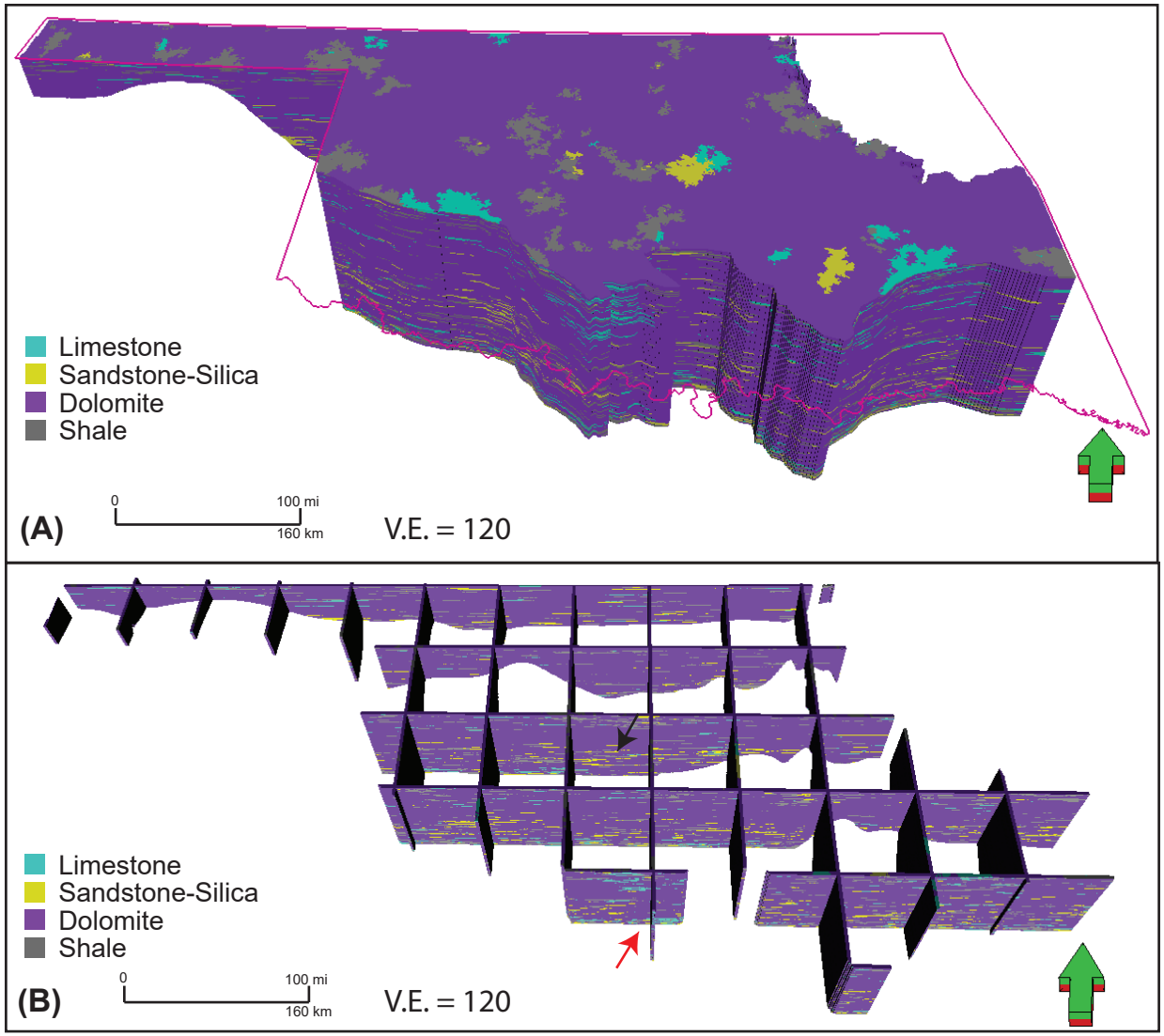


Figure 1.8. A) Lithology Model for the Arbuckle, flattened on the top of the Arbuckle. B) Fence diagram of the lithology model for the Arbuckle. Flattened on the top of the Arbuckle with a 120 Vertical Exaggeration skipping every 75 lines (roughly 35 miles, 56 kilometers). The black arrow indicates where an increase in silica occurs. The red arrow points to the Southern Oklahoma Aulacogen, where the Arbuckle is predominantly limestone.

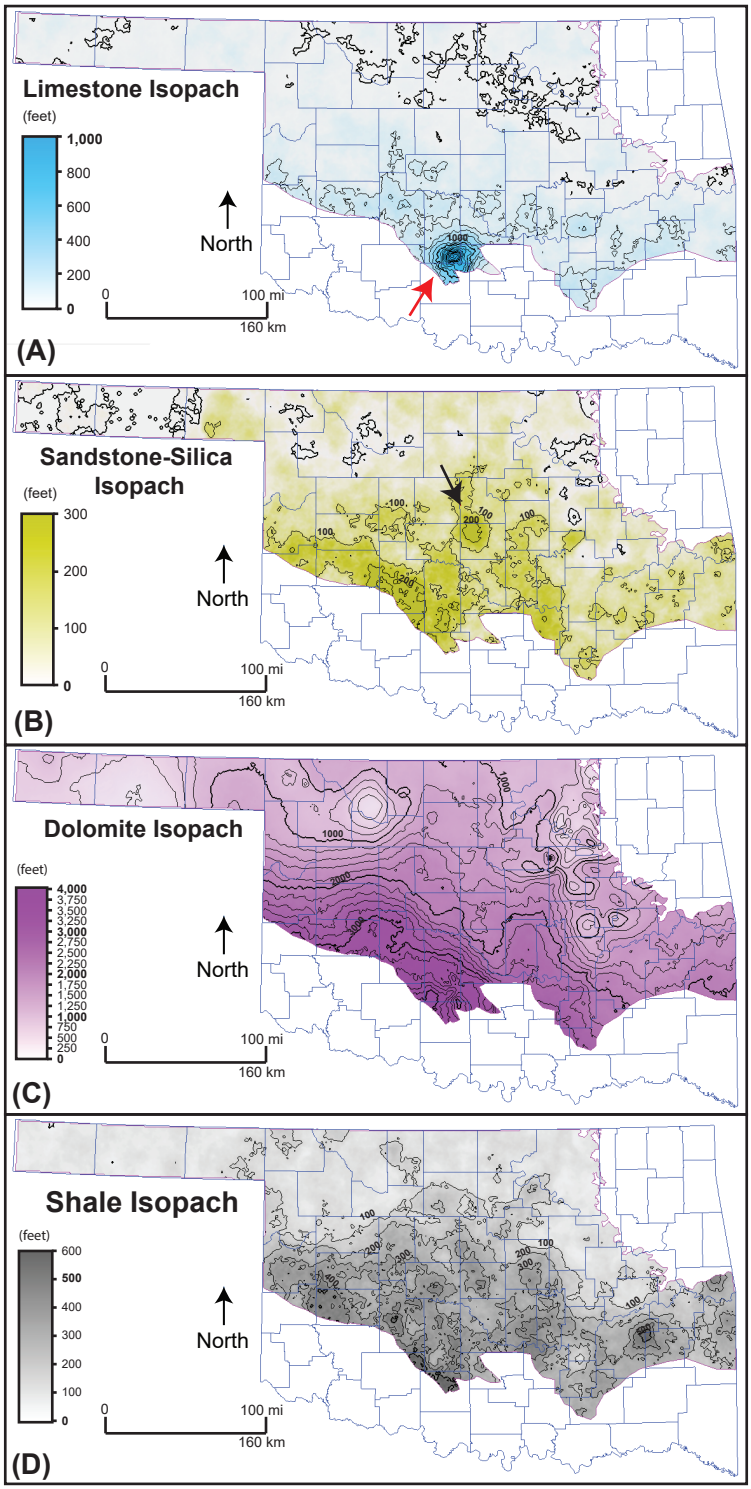


Figure 1.9. Arbuckle Lithology thickness for A) Limestone. 200 ft (61 m) contour interval, 1,000 ft (305 m) bold contour interval. Red arrow pointing to the SOA. B) Sandstone-Silica. 100 ft (30 m) contour interval, 500 ft (152 m) bold contour interval. Black arrows pointing to silica rich areas along the Cherokee platform. C) Dolomite. 250 ft (76 m) contour interval, 1,000 ft (305 m) bold contour interval. D) Shale. 100 ft (30 m) contour interval, 500 ft (152 m) bold contour interval.

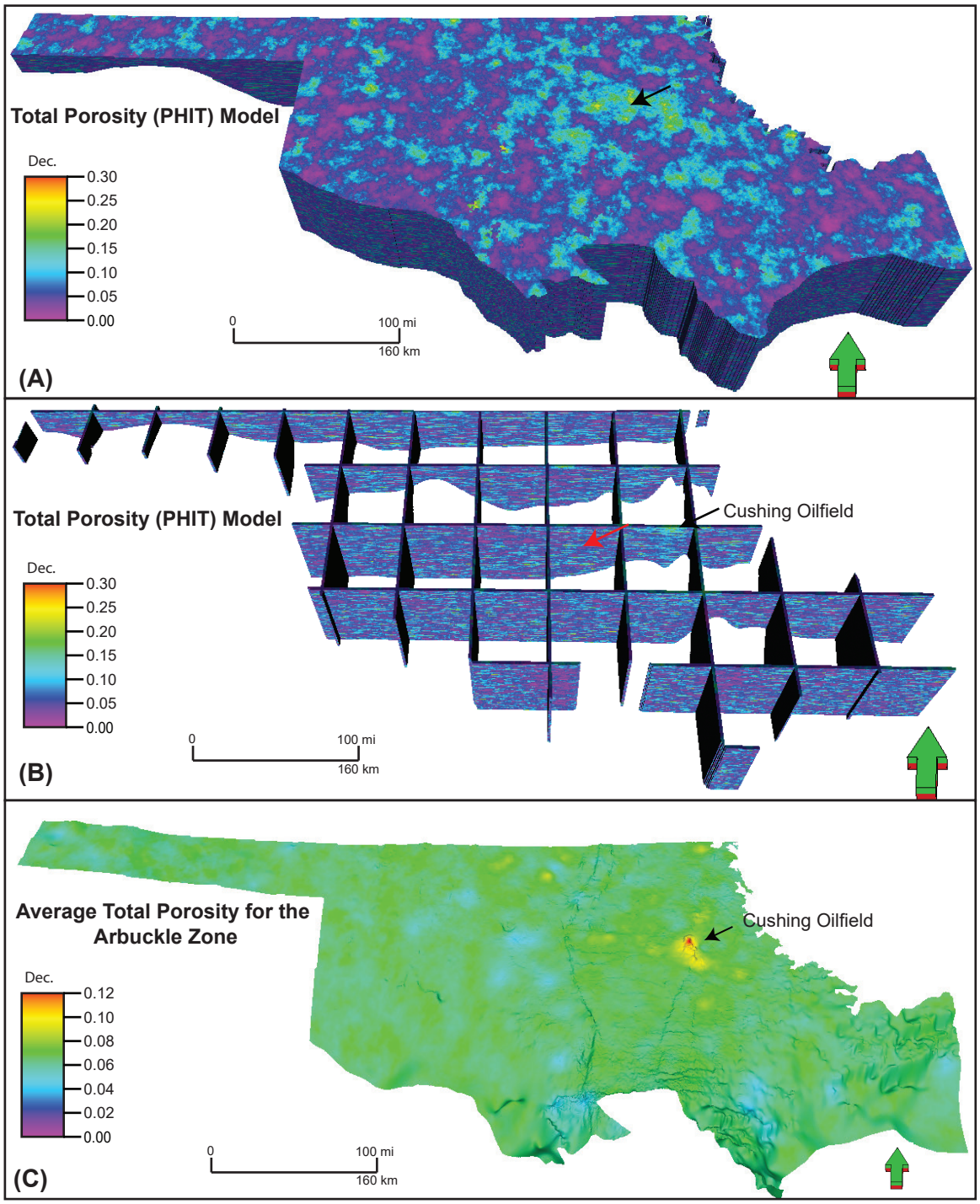


Figure 1.10. Total Porosity Models. A) Total Porosity Model for the Arbuckle, flattened on the top of the Arbuckle. Black arrows point to increased porosity in central Oklahoma. B) Fence diagram of the total porosity model for the Arbuckle. Flattened on the top of the Arbuckle with a 120 Vertical Exaggeration skipping every 75 lines (roughly 35 miles, 56 kilometers). Red arrow points to central Oklahoma increase in porosity which is associated with the increase in silica in the region. C) Average total porosity for the Arbuckle zone draped on the Arbuckle structure. Black arrow points to the Cushing oilfield where there has been significant porosity enhancement.

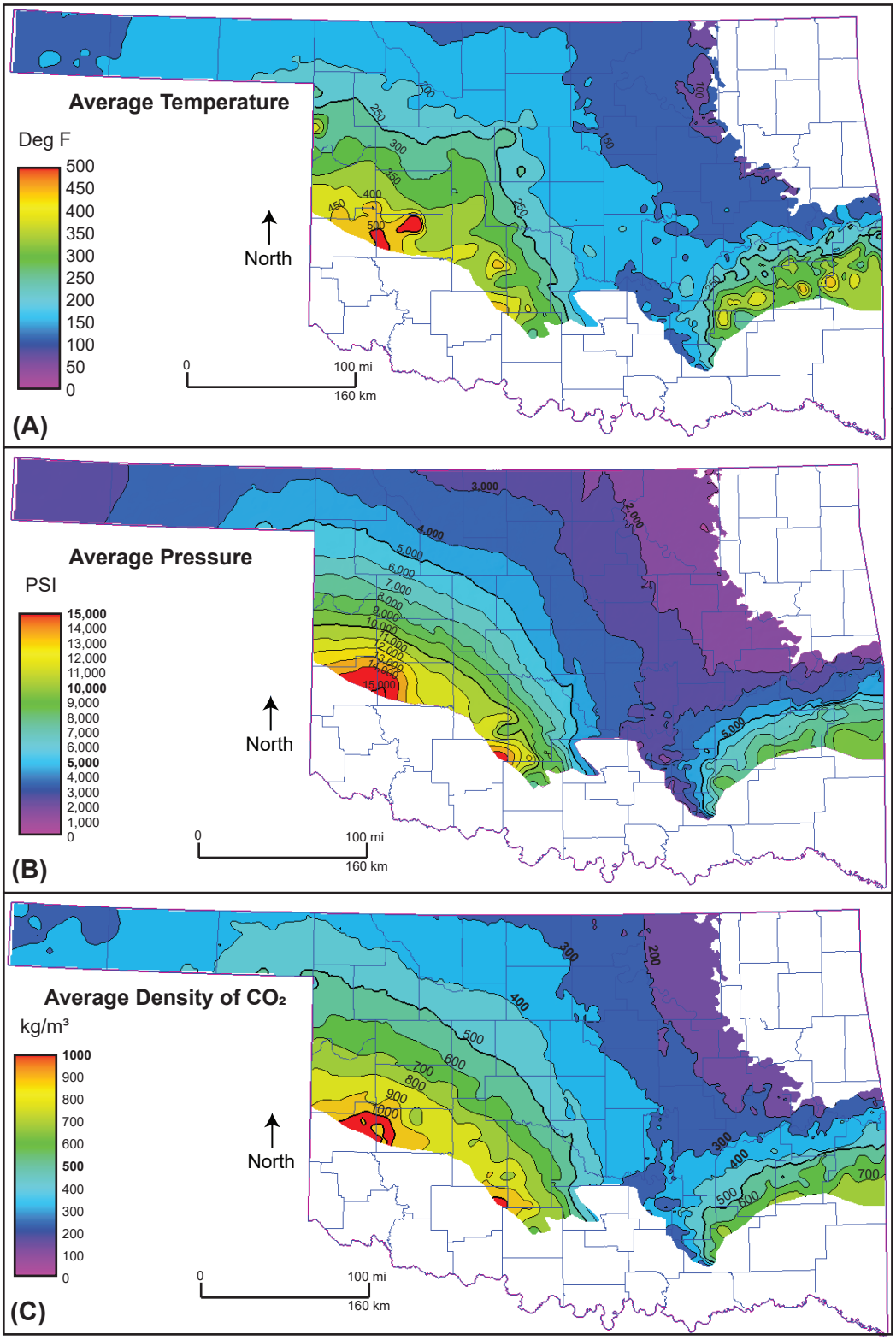


Figure 1.11. Temperature, Pressure and CO_2 Density maps. A) Average Arbuckle Temperature map. 50°F (10°C) contour interval. B) Average Arbuckle Pressure map. 1,000 psi (6.89 MPa) contour interval. C) Average Density of CO_2 at reservoir temperature and pressure. 100 kg/m³ (6.2 lb/ft³) contour interval.

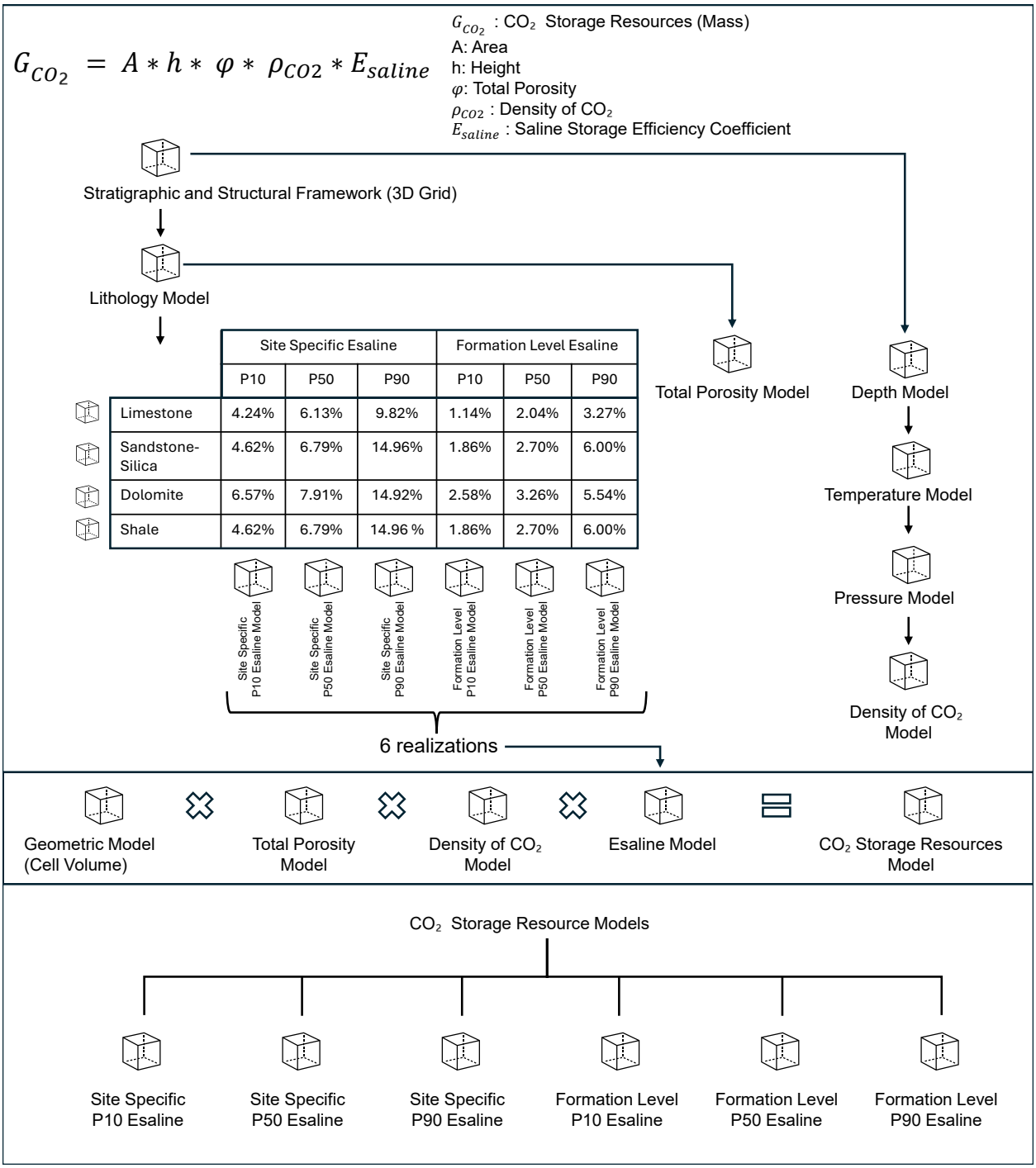


Figure 1.12. CO_2 storage resources modeling workflow.

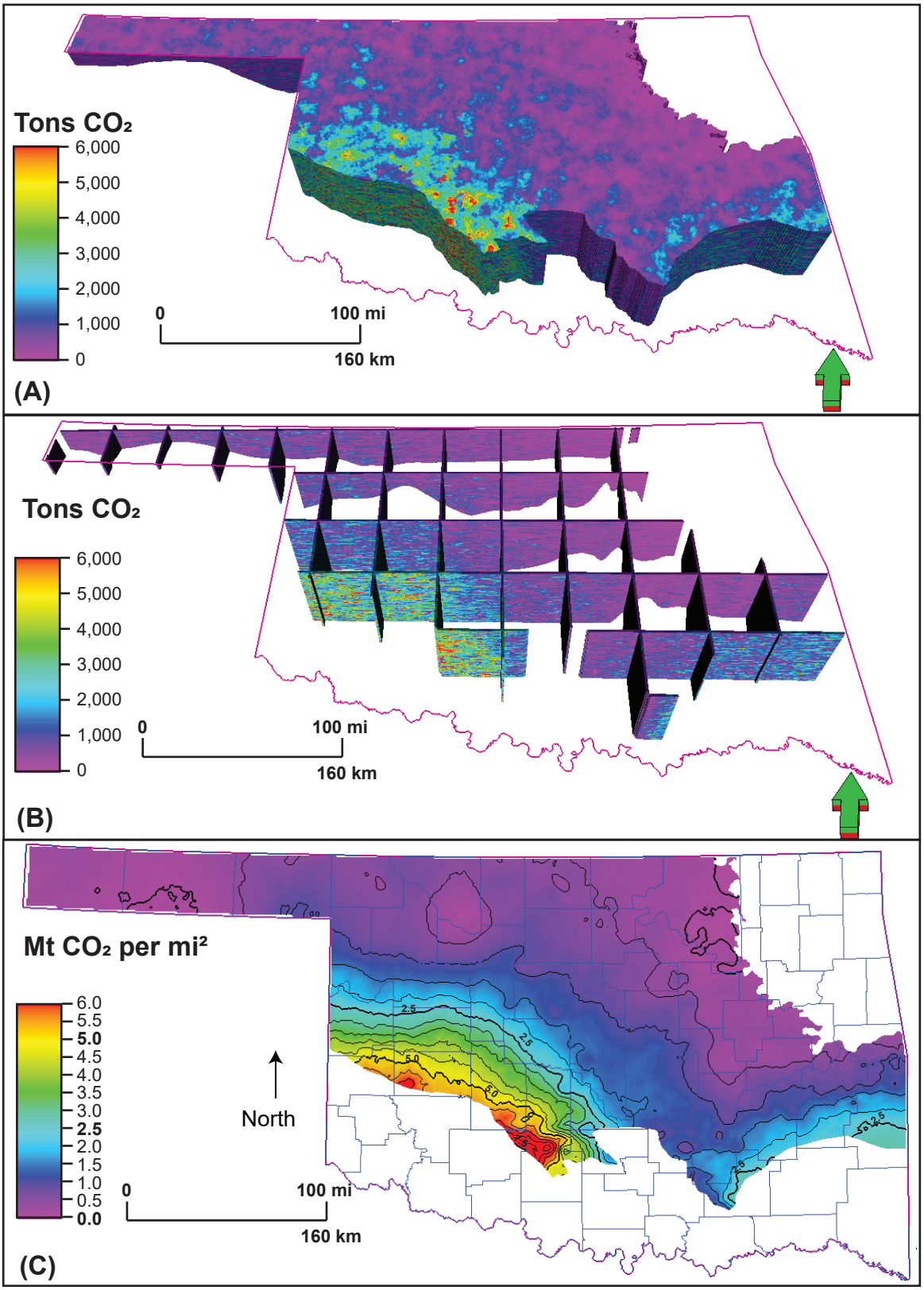
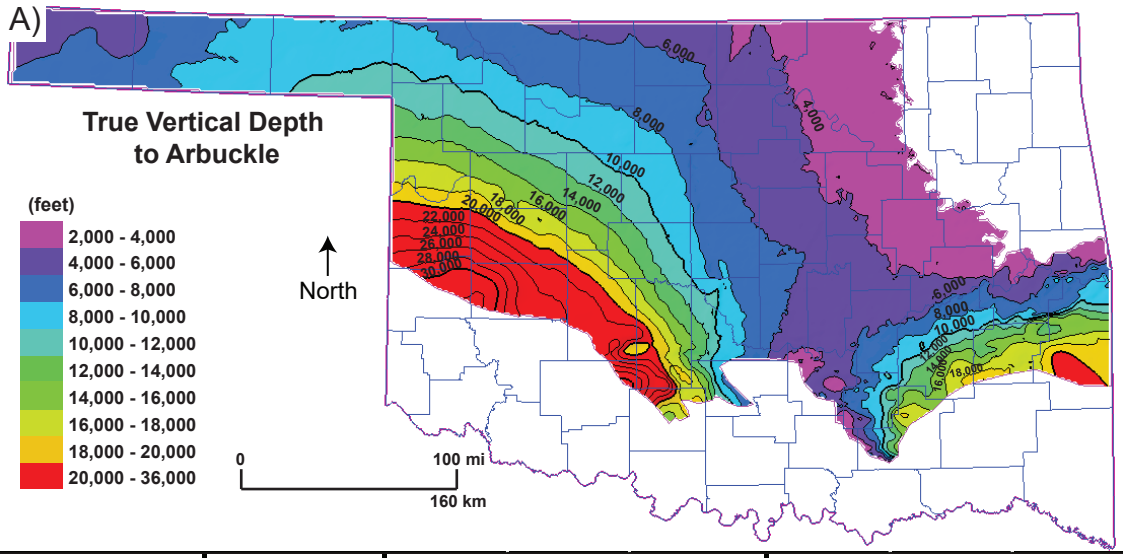


Figure 1.13. CO_2 storage resources model using the P_{50} Esaline values at the formation level. A) Arbuckle Model B) Arbuckle fence diagram C) Arbuckle net-mass map, in megatons CO_2 per mi^2

A)



B)

MD	% of total Storage Resources	Site Specific Mt CO_2			Formation Level Mt CO_2		
		P10	P50	P90	P10	P50	P90
2,000-4,000	2%	2,351	2,788	5,486	923	1,180	2,050
4,000-6,000	6%	7,631	9,385	17,998	3,000	3,847	6,748
6,000-8,000	11%	14,711	18,168	34,928	5,784	7,437	13,113
8,000-10,000	11%	13,903	17,234	33,203	5,465	7,045	12,481
10,000-12,000	7%	9,433	11,659	22,402	3,707	4,768	8,407
12,000-14,000	6%	7,777	9,630	18,500	3,054	3,933	6,943
14,000-16,000	7%	8,738	10,825	20,784	3,429	4,419	7,797
16,000-18,000	7%	9,370	11,618	22,298	3,675	4,738	8,363
18,000-20,000	7%	9,232	11,522	22,081	3,642	4,695	8,275
20,000-36,575	37%	45,808	58,938	109,742	17,994	23,239	41,260

Figure 1.14. A) Arbuckle true vertical depth map. 2,000 ft (610 m) contour interval. B) CO_2 storage resources for the entire Arbuckle zone subdivided by 2,000 ft (610 m) intervals. For example, from 4,000 to 6,000 feet depth the Arbuckle zone can store between 3,000-6,748 Mt of CO_2 using formation level Esaline values, which is 6% of all the storage resources in the evaluated area, highlighted by the dark purple colored contour interval on the map.

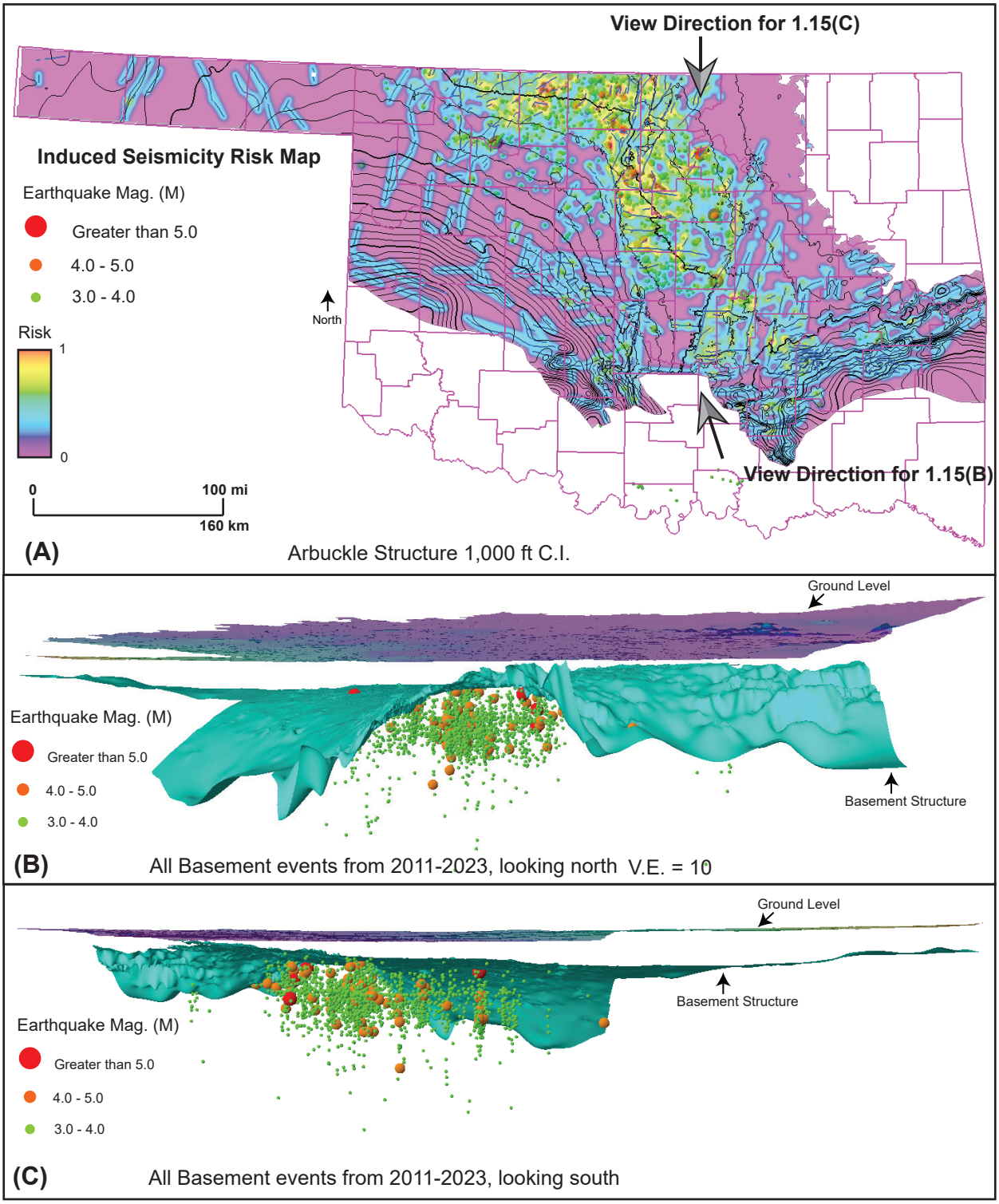


Figure 1.15. Induced Seismicity Risk Map. A) Arbuckle structure map with the risk map overlaid and at 50% opacity. All earthquakes above 3.0 magnitude (M) from 2011-2023 are shown. Modified fault database, which contains the OGS fault database (Holloway et al., 2016) and faults identified by the author, shown in blue. B) All seismic events that occurred in the basement, looking north with a vertical exaggeration of 10. C) All seismic events that occurred in the basement, looking south with a vertical exaggeration of 10.

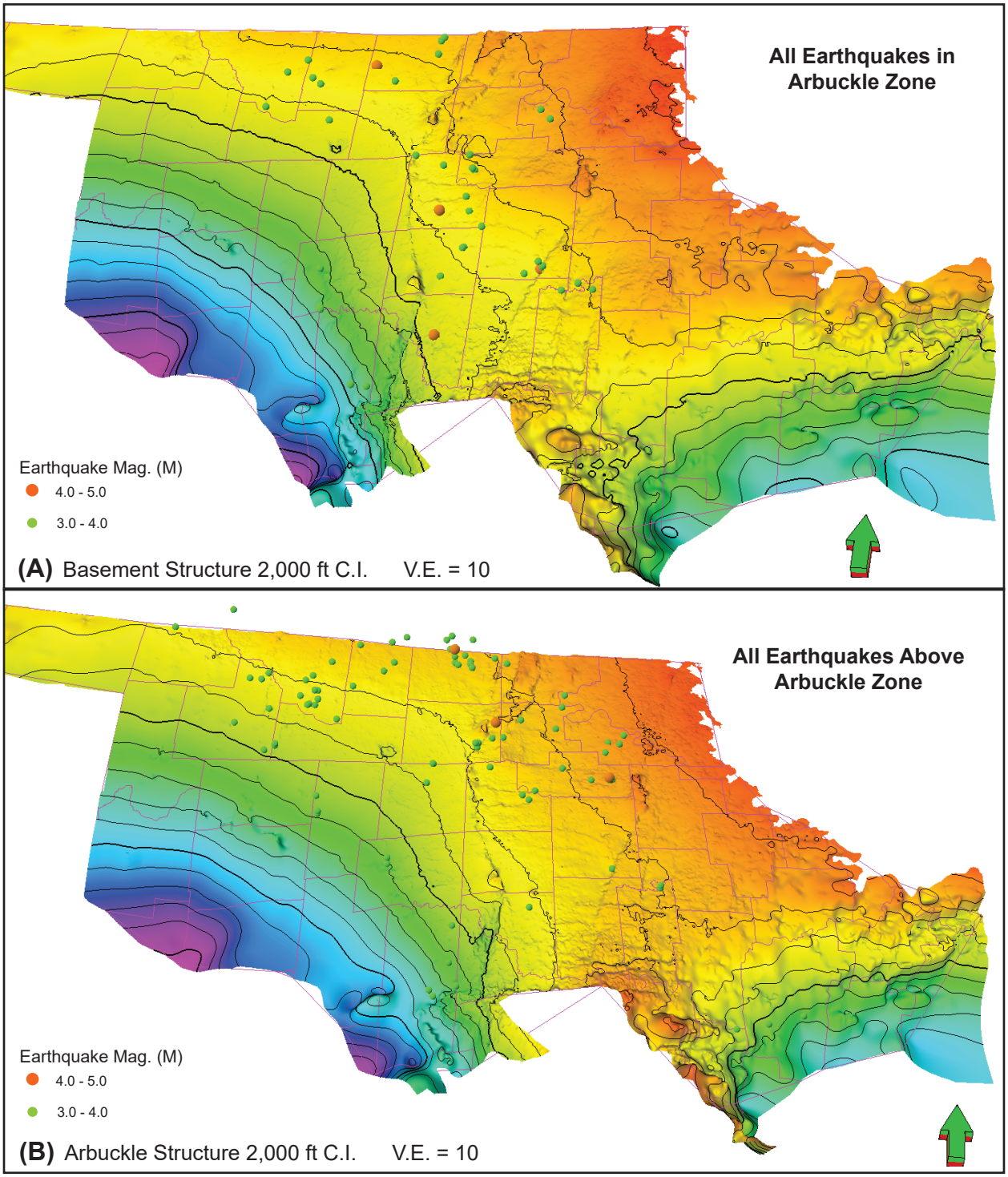


Figure 1.16. Seismic events in and above the Arbuckle zone. A) All Seismic events that took place in the Arbuckle zone. 41 events took place, 4 between 4.0-5.0 M and 37 between 3.0-4.0 M. Basement structure map shown with 2,000 ft (610 m) contour interval and vertical exaggeration of 10. B) All seismic events that took place above the Arbuckle zone. 88 events, all less than 5.0 M. Arbuckle structure map show with 2,000 ft (610 m) contour interval and vertical exaggeration of 10.

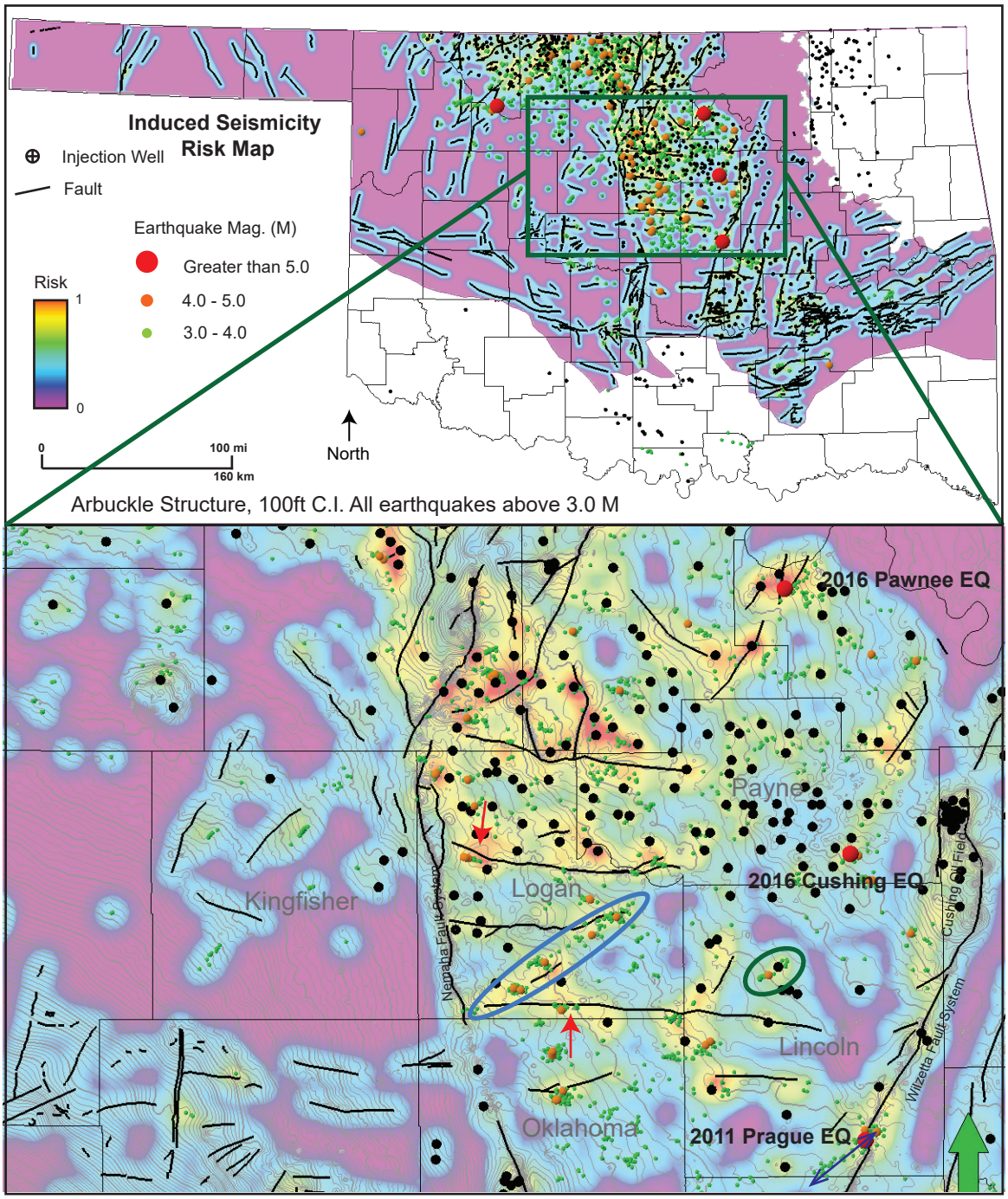


Figure 1.17. Induced Seismic Risk map, central Oklahoma. Central Oklahoma showing the Arbuckle structure with 100 ft (61 m) contour interval co-rendered with seismic risk map, injection wells, and earthquakes. The red arrow points to mapped fault-earthquake relationships. Blue ellipse identifies a SW-NE trending earthquake swarm, with a short fault that likely extends in both directions. The green ellipse shows a non-faulted area with an earthquake swarm and SWD injection well. The largest fault systems, the Nemaha and Wilzetta, have no associated earthquake swarms and have injection wells close. Magnitude 5.0 and above earthquakes are labeled. Small, sub-parallel fault to the Wilzetta fault associated with the 2011 Prague earthquake highlighted by the blue, double arrow.

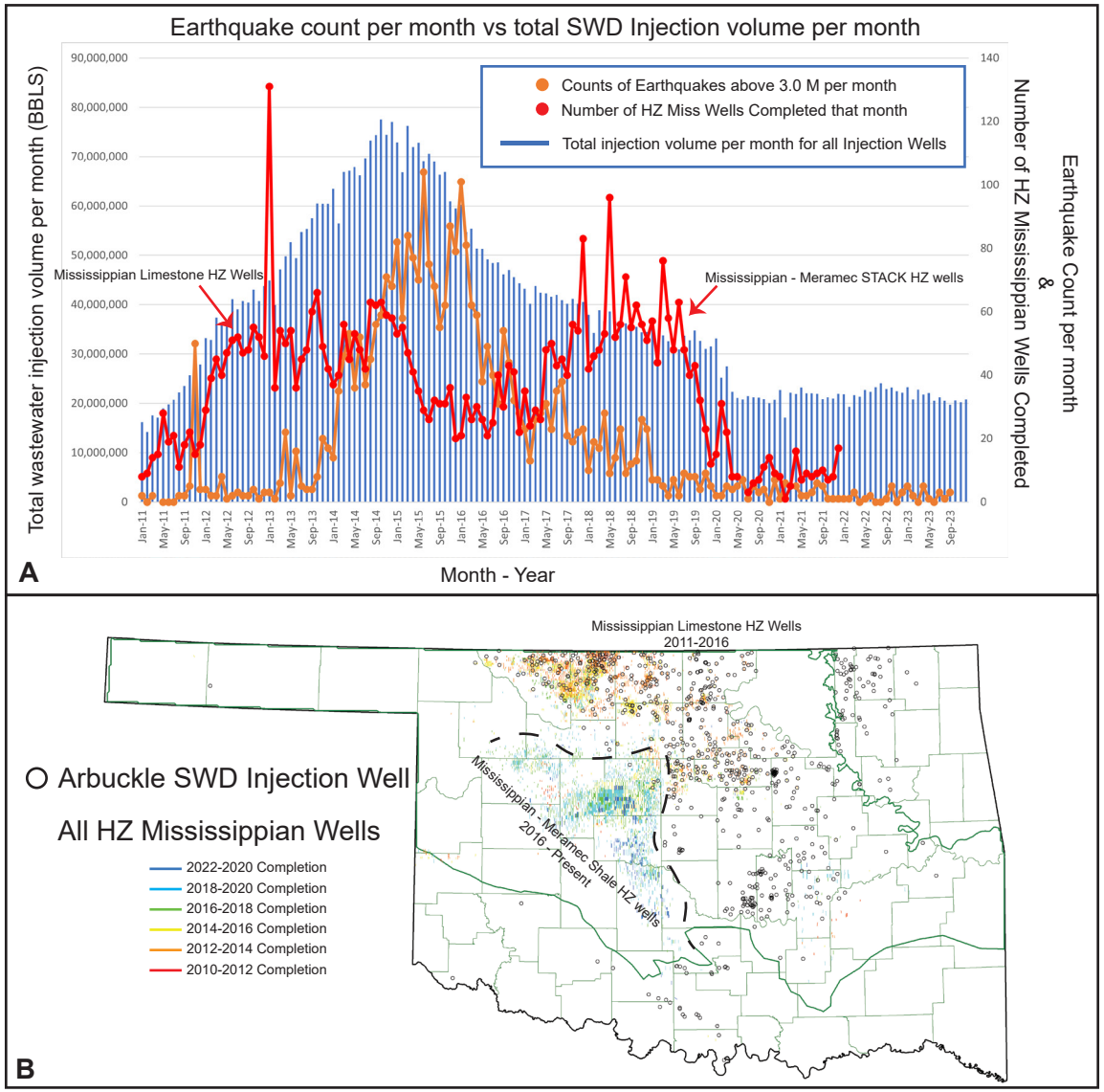


Figure 1.18. A) Seismic events greater than 3.0 M per month (orange dots) versus total wastewater injection volumes per month (blue histogram) and count of horizontal Mississippian well completions per month (red dots). B) All horizontal Mississippian wells and SWD injection wells from the Oklahoma Corporation Commission. Horizontal Mississippian wells colored by completion year.

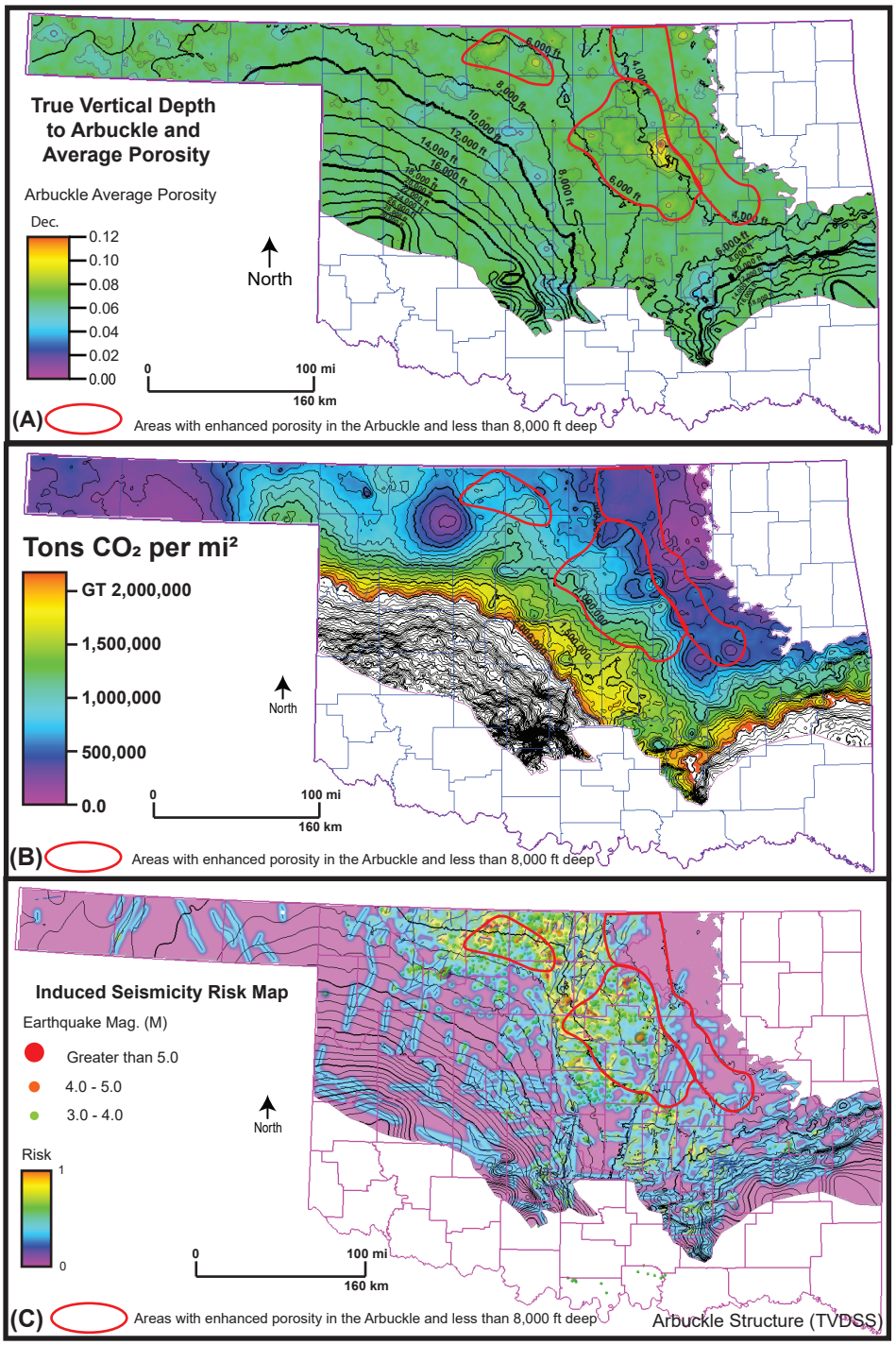


Figure 1.19. A) Arbuckle true vertical depth map with 2,000 ft (610 m) contour interval and average total porosity for the Arbuckle zone. Areas in the red polygons show increased average porosity in the Arbuckle zone at depths less than 8,000 ft (2,438 m). B) Arbuckle net-mass map (using the P_{50} Esaline values at the formation level) in tons CO_2 per mi2. This is the same map as Figure 1.14C but rescaled to show variations in CO_2 storage resources at shallower depths. Red polygons show the CO_2 storage resources to range between 200,000-1,000,000 tons of CO_2 for the areas with enhanced porosity. C) The seismic risk map (as seen in Figure 1.15A) with the two Arbuckle areas of interest for CCUS development.

Tables

Symbol	Term	Range	Description
Terms used to define the entire basin/region pore volume			
A_n/A_t	Net to total Area	0.2 - 0.8	Fraction of total basin/Region are that has a suitable formation present
h_n/h_g	Net to Gross Thickness	0.25 - 0.75	Fraction of total geologic unit that meets minimum porosity and permeability requirements for injection
$\emptyset_{eff}/\emptyset_{tot}$	Effective to Total Porosity Ratio	0.6 - .95	Fraction of total porosity that is effective, i.e. interconnected
Terms used to define the pore volume immediately surrounding a single-well CO_2 injector			
E_A	Areal Displacement Efficiency	0.5 - 0.8	Fraction of immediate area surrounding an injection well that can be contacted by CO_2
E_I	Vertical Displacement Efficiency	0.6 - .9	Fraction of vertical cross section with the volume defined by the area (A) that can be contacted by the CO_2 plume from a single well
E_g	Gravity	0.2 - 0.6	Fraction of net thickness that is contacted by CO_2 as a consequence of the density difference between CO_2 and in-situ brine.
E_d	Microscopic Displacement Efficiency	0.5 - 0.8	Portion of the CO_2 contacted, brine-filled pore volume that can be replaced by CO_2

Table 1.1. Definition of terms used to calculate the Saline Storage Capacity Efficiency, Esaline. From IEA Greenhouse Gas R&D Programme 2009.

Esaline	Site Specific			Formation Level		
	P10	P50	P90	P10	P50	P90
Limestone	4.24%	6.13%	9.82%	1.41%	2.04%	3.27%
Clastics	4.62%	6.79%	14.96%	1.86%	2.70%	6.00%
Dolomite	6.57%	7.91%	14.92%	2.58%	3.26%	5.54%

Table 1.2. Esaline values at the site Specific and Formation level. From IEA Greenhouse Gas R&D Programme 2009.

	SITE SPECIFIC Esaline Values		
	Arbuckle - Mt		
	P10	P50	P90
Limestone	2,287	3,307	5,297
Sandstone	4,846	7,112	15,649
Dolomite	111,768	134,564	253,817
Shale	10,113	14,863	32,659
Total	129,013	159,855	307,421

Table 1.3. CO_2 Storage resources for the Arbuckle calculated with Site Specific Esaline values, broken down by lithology.

	FORMATION LEVEL Esaline Values		
	Arbuckle - Mt		
	P10	P50	P90
Limestone	761	1,004	1,764
Sandstone	1,951	2,832	9,293
Dolomite	43,891	55,459	94,246
Shale	4,071	5,910	13,134
Total	50,673	65,204	118,436

Table 1.4. CO_2 Storage resouces for the Arbuckle calculated with Formation Level Esaline values, broken down by lithology.

Acknowledgements

I would like to thank Enverus for the well information and well logs, and GVERSE Geographix and Schlumberger's Petrel for the software used in this study. I would also like to thank Dr. Jake Walters at OGS for guidance with the earthquake data provided by the OGS. Lastly, I would like to thank my doctoral committee members, M. Pranter, H. Bedle, B. Carpenter, and D. Devegowda.

References

Amsden, T. W., 1980, Hunton Group (late Ordovician Silurian, and early Devonian) in the Arkoma Basin of Oklahoma: Oklahoma Geological Survey Bulletin 129.

Anderson, W. H., 1991, Mineralization and hydrocarbon emplacement in the Cambrian-Ordovician Mascot Dolomite of the Knox Group in south-central Kentucky: Kentucky Geological Survey Report of Investigations 4, Series 11, 29 p.

Arbuckle AOI Well - 1012D Reported Volumes - Oil and Gas Data files, n.d.: <https://oklahoma.gov/occ/divisions/oil-gas/oil-gas-data.html> (accessed January, 2023).

Barbour, A. J., J. H. Norbeck, and J. L. Rubinstein, 2017, The effects of varying injection rates in Osage County, Oklahoma, on the 2016 Mw 5.8 Pawnee earthquake: Seismological Research Letters, v. 88, no. 4, p. 1040–1053, doi:10.1785/0220170003.

Caf, A. B., 2022, Quantitative seismic interpretation and machine learning applications for subsurface characterization and modeling, dissertation, 119 p.

Carpenter, B. N. and Evans, M. C., 1991, Comparison of the Arbuckle Group at Wilburton Field, Latimer County, with the N.E. Alden Field, Caddo County, Oklahoma, in Johnson, K. S. (ed.), Arbuckle Group core workshop and field trip: Oklahoma Geological Survey Special Publication 91-3, p. 111-132.

Carr, T. R., D. F. Merriam, and J. D. Bartley, 2005, Use of relational databases to evaluate regional petroleum accumulation, groundwater flow, and CO2 sequestration in Kansas, AAPG Bulletin, 89 no. 12, 1607–1627, doi:10.1306/07190504086

Derby, J. R., 1991, Lithology, Stratigraphy and Age of the Arbuckle Group in the Amoco SHADS No. 4, a Continuous Core from Grassroots into Basement, Rogers County, Oklahoma: Oklahoma Geological Survey Special Publication, no. 91, p. 69–82.

Donovan, R. N., and D. A. Ragland, 1986, Paleozoic Stratigraphy of the Slick Hills, Southwestern Oklahoma: Oklahoma Geological Survey Guidebook, p. 1.

Doveton, J. H., 1994, Geologic log interpretation: Tulsa, OK, SEPM.

EPA, 2022, Inventory of U.S. Greenhouse Gas Emissions and Sinks: 1990-2022. U.S. Environmental Protection Agency, EPA 430-R-24-004.

General Geologic Sections of Oklahoma, 1975: <https://oklahoma.gov/content/dam/ok/en/occ/images/og/geocolumn-occ.pdf> (accessed October, 2022).

Goodman, A. et al., 2011, U.S. DOE methodology for the development of geologic storage potential for carbon dioxide at the national and regional scale: International Journal of Greenhouse Gas Control, v. 5, no. 4, p. 952–965, doi:10.1016/j.ijggc.2011.03.010.

Ham, W. E.; Denison, R. E.; and Merritt, C. A., 1964, Basement rocks and structural evolution of southern Oklahoma: Oklahoma Geological Survey Bulletin 95, 302 p.

Holloway, S., A. Holland, and R. Keller, 2016: Oklahoma Geological Survey-Oklahoma Fault Database: <https://www.ou.edu/ogs/data/fault> (accessed April 24, 2023).

IEA Greenhouse Gas R&D Programme (IEA GHG), "Development of Storage Coefficients for CO2 Storage in Deep Saline Formations", October 2009

IEA, 2022, Global Energy Review: CO2 Emissions in 2021- Global emissions rebound sharply to highest ever level: < https://iea.blob.core.windows.net/assets/c3086240-732b-4f6a-89d7-db01be018f5e/GlobalEnergyReviewCO2Emissionsin2021.pdf> (accessed January, 2023).

Johnson, K. S., 1991, Geologic Setting of the Arbuckle Group in Oklahoma: Oklahoma Geological Survey Special Publication 91-3; Arbuckle Group Core Workshop and Field Trip.

Keranen, K. M., Savage, H. M., Abers, G. A., & Cochran, E. S., 2013, Potentially induced earthquakes in Oklahoma, USA: Links between wastewater injection and the 2011 Mw 5.7 earthquake sequence. Geol. 41, 699-702

Keranen, K. M., M. Weingarten, G. A. Abers, B. A. Bekins, S. Ge, 2014, Sharp increase in central Oklahoma seismicity since 2008 induced by massive wastewater injection. Science 345, 448–451

Kibikas, W. M., B. M. Carpenter, and A. Ghassemi, 2020, Mechanical strength and physical properties of Oklahoma's igneous basement: Tectonophysics, v. 777, p. 228336, doi:10.1016/j.tecto.2020.228336.

Kyle, J. R., 1976, Brecciation, alteration, and mineralization in the central Tennessee zinc district: Economic Geology, v. 71, p. 892-903.

Lee, W.; Leatherock, C.; and Botinelly, T., 1948, The stratigraphy and structural development of the Salina basin of Kansas: Kansas Geological Survey Bulletin 74, 155p.

McGarr, A., D. Simpson, L. Seeber, 2002, Case histories of induced and triggered seismicity. *Int. Handb. Earthq. Eng. Seismol.* **81A**, 647–66.

McKnight, E. T., 1935, Zinc and lead deposits of Northern Arkansas: U.S. Geological Survey Bulletin 853, 311 p.

Milad, B., R. G. Moghanloo, and N. W. Hayman, 2023, Assessing CO2 geological storage in Arbuckle Group in Northeast Oklahoma: Fuel, v. 356, p. 129323, doi:10.1016/j.fuel.2023.129323.

Miranda, M. W., J. D. Ogland-Hand, J. M. Bielicki, R. G. Moghanloo, J. DaneshFar, and R. S. Middleton, 2023, Developing a roadmap for carbon capture, and storage in Oklahoma by assessing the viability of stacked storage: Greenhouse Gases: Science and Technology, v. 13, no. 6, p. 763–779, doi:10.1002/ghg.2244.

Northcutt, R. A., and J. A. Campbell, 1995, Geologic Provinces of Oklahoma: Oklahoma Geological Survey Open File Report 5. http://ogs.ou.edu/docs/openfile/OF5-95.pdf, accessed March 2022

NRC (National Research Council), *Induced Seismicity Potential in Energy Technologies* (The National Academies Press, Washington, DC, 2012)

Perilla-Castillo, P. J., 2017, Rock properties derived from analysis of Earth tide strain observed in continuous pressure monitoring of the Arbuckle Group of Oklahoma, thesis.

Puckette, J. O., 1996, Evaluation of underpressured reservoirs as potential repositories for liquid waste: Oklahoma State University unpublished Ph.D. thesis, 273 p.

Purdue, A. H.; and Miser, H. D., 1916, Description of the Eureka Springs and Harrison quadrangles (Arkansas-Missouri): U.S. Geological Survey, Geologic Atlas of the United States, Folio 202, 21 p.

Response to Oklahoma Earthquakes, n.d.: <https://oklahoma.gov/occ/divisions/oil-gas/induced-seismicity-and-uic-department/response-oklahoma-earthquakes.html> (accessed August, 2024, b), 25 p.

Ross, R. J., 1976, Ordovician Sedimentation in the Western United States: Rocky Mountain Association of Geologists, p. 109–133.

Schlumberger Log Interpretation principles, 1989: Houston, TX, Schlumberger Educational Services.

Shah, A. K., and G. R. Keller, 2017, Geologic influence on induced seismicity: Constraints from potential field data in Oklahoma: Geophysical Research Letters, v. 44, no. 1, p. 152–161, doi:10.1002/2016gl071808.

SMU Node of National Geothermal Data System, Heat Flow and Well Data, n.d.: <http://geothermal.smu.edu> (accessed March, 2023).

Suhm, R., 1997, Simpson Stratigraphy of the Southern Midcontinent: Oklahoma Geological Survey Circular 99, p. 3–38.

U.S. Department of Energy National Energy Technology Laboratory Office of Fossil Energy (NETL), 2007, Carbon sequestration atlas of the United States and Canada.

U.S. Department of Energy National Energy Technology Laboratory Office of Fossil Energy (NETL), 2008, Carbon sequestration atlas of the United States and Canada.

U.S. Geological Survey Geologic Carbon Dioxide Storage Resources Assessment Team, 2013, National assessment of geological carbon dioxide storage resources—Results (ver. 1.1, September 2013): U.S. Geological Survey Circular 1386, 41 p., <https://pubs.usgs.gov/circ/1386/>.

Walsh, F. R., and M. D. Zoback, 2015, Oklahoma's recent earthquakes and saltwater disposal: Science Advances, v. 1, no. 5, doi:10.1126/sciadv.1500195.

Walter, J. I., P. Ogwari, A. Thiel, F. Ferrer, I. Woelfel, J. C. Chang, A. P. Darold, and A. A. Holland (2020), The Oklahoma Geological Survey Statewide Seismic Network, Seismol. Res. Lett., 91 (2A): 611–621, doi:10.1785/0220190211

Wilson, J. L., R. D. Fritz, and P. L. Medlock, 1991, The Arbuckle Group - Relationship of Core and Outcrop Analyses to Cyclic Stratigraphy and Correlation: Oklahoma Geological Survey Special Publication 91-3, p. 133–144.

Wright, W. F., 1965, Petroleum geology of the Simpson Group, west Texas and southeast New Mexico, in Herndon, Thomas (ed.), Symposium on the Simpson: Tulsa Geological Society Digest, v. 33, p. 62-73.

Chapter 3: The Statewide variability of mineralogy, pore volume, and CO2 storage resources for the Viola Limestone and Simpson Group, Oklahoma

Abstract

Like the Arbuckle Group, the Ordovician reservoirs of Oklahoma exist over most of the state, at depths adequate for carbon capture, utilization, and storage (CCUS). The Ordovician reservoirs include the Viola Limestone and Simpson Group and lie above the Arbuckle Group. They are hydrocarbon-producing reservoirs where structurally trapped and have also been used as saltwater disposal reservoirs for oilfield wastewater. While there has been significant research on the reservoirs for hydrocarbon potential, there have been no regional studies showing the distribution of lithologies, pore volume, and their CO_2 storage resources.

Using well information from 80,800 wells for the structural model and over 1,126 wells with log ascii standard (LAS) format with modern well logs, a detailed 3-D lithology model was built for the Ordovician zone across the state of Oklahoma. Total porosity was then calculated from well logs, and the total porosity model was constrained to the lithology model. To determine the CO_2 storage resources, the United States Department of Energy's (US-DOE) methodology was applied. The total CO_2 storage resources for the Ordovician were then determined using both site-specific and formation level saline storage efficiency coefficients (E_{saline}) and reported for the entire study area, by lithology and by measured depth.

Results include 1) detailed lithology and porosity models, including maps of the distribution of the sandstone lithology and the intended CCUS target lithology. 2) Total CO_2 storage resources between 13,800-40,792 Mt, specifically 6,501-20,877 Mt for the sandstone

lithology over 44,627 mi^2 (115,583 km^2) of which 35% is accessible at depths shallower than 10,000 ft (3,048 m).

Introduction

Above the Arbuckle Group lie the Ordovician reservoirs of Oklahoma. While Ordovician reservoirs have been historically important in oil and gas production, there has been no detailed statewide assessment of pore volume or CO_2 storage resources. Ordovician formations in the state of Oklahoma include the Richmond-age Sylvan Shale, the Trenton-age Viola Limestone, and the Simpson-age Bromide, McLish, Oil Creek, and Joins formations. The Sylvan Shale is the seal for oil and gas production in the subsurface and is therefore assumed not to be a reservoir rock. The first reservoir lithology is the Viola Limestone, and the top of the Ordovician zone for this chapter. The bottom of the zone is the top of the Arbuckle Group. The target formation for CCUS is the highest porosity and the laterally continuous Simpson-age Bromide sandstones, commonly referred to as the "2nd Wilcox".

Due to their historical production of hydrocarbons, Ordovician reservoirs have been extensively researched across Oklahoma. The earliest published studies of the Simpson stratigraphy were done by Taff (1904) and Ulrich (1911), who described the Simpson rocks of eastern Oklahoma. Furthermore, C. E. Decker (Decker and Merritt, 1931; Decker, 1941) had a detailed investigation of the Simpson outcrops in the Criner Hills and Arbuckle Mountains. Cronenwett (1958) did a detailed study correlating the Simpson Group in the subsurface using electrical logs (Elogs) and sample logs. Schramm (1964) published a regional study of the Simpson Group across Oklahoma, which provided maps of the regional extent, thicknesses, and lithology for the Simpson Group. This study included several hundred Elogs, sample logs, and

outcrops. Statler (1965) further expanded the work of Shramm to clarify and simplify the Simpson stratigraphic nomenclature and identify localized areas deserving of more specialized attention. Nearly 30 years later, Suhm (1997) expanded this subsurface study to include over 3,500 wells across Oklahoma and western Arkansas thanks to funding from the Oklahoma Geological Survey and US-DOE.

While the Ordovician reservoirs have been extensively researched for hydrocarbon potential, there have been very few studies on the CO_2 storage resources for the zone. In 2013, the United States Geological Survey (USGS) completed and released a national assessment of geologic carbon dioxide storage resources (U.S. Geological Survey Geologic Carbon Dioxide Storage Resources Assessment Team, 2013). The assessment evaluated 36 sedimentary basins across the USA and used a geology-based probabilistic assessment method to estimate the subsurface CO_2 storage resource of 3,000 Gt of CO_2 for the USA. The goal of the USGS study was to conduct an initial assessment of storage resources on a regional basis. Through this regional assessment, not all viable storage formations were individually assessed, and various formations were combined and evaluated as one reservoir; thus, the results provide regional storage resource trends. For example, the Arbuckle Group, Viola Limestone, and Simpson Group were combined as a single reservoir called "Lower Paleozoic" in the Anadarko basin and was reported to have between 11.8 to 37.0 Gt of CO_2 storage resources. Meanwhile, the Arkoma Basin was only evaluated for the "Ordovician Composite" and was reported to have between 3.2 to 11.0 Gt of CO_2 storage resources. While informative, given how the stratigraphic units in the separate basins were combined, it is not possible to compare total storage resources for a particular stratigraphic interval or Oklahoma. In addition, the studies report total storage

resources and do not include information about the spatial variability of rock properties and storage resources across the basins.

There has been one recent publication (Miranda et al., 2023) that references a regional assessment of CO_2 storage resources for the "Arbuckle Formation" and "Simpson Sandstones" as part of developing a roadmap for carbon capture and storage in Oklahoma by assessing the viability of stacked storage. CO_2 storage resources were determined using Carbon Solutions LLC's SCO_2T^{PRO} software, which uses the US-DOE methodology to determine CO_2 storage resources, but there were no details as to the geologic inputs that were used. There were no reported total CO_2 storage resources reported either.

Because a detailed statewide assessment of pore volume and CO_2 storage resources was lacking for the state of Oklahoma, this study utilizes data from more than 80,800 wells and other regional information for geological interpretation and to construct and analyze well-constrained 3-D geological models of the Ordovician zone (Figure 2.1). The study especially incorporates detailed constraints on the stratigraphy and structure (e.g., depth, areal extent, thickness, mineralogy, porosity). The results include a detailed structural, lithology, total porosity, temperature, and pressure models of the Ordovician zone and are the most detailed assessments, to date, of pore volume and CO_2 storage resources for Oklahoma.

Geologic Setting

The Simpson Group deposition began at the end of the Canadian time and after the pre-Simpson unconformity (Figure 2.2). Its thickness is greatest in the Anadarko and Ardmore basins in Oklahoma at over 2,000 ft (610 m) thick. Formations of the Simpson Group include, in stratigraphically ascending order, Joins, Oil Creek, McLish, and Bromide formations.

The Joins Formation is composed of thin limestones and interbedded shales with a basal conglomerate and is typically inside the confines of the SOA; otherwise, the Arbuckle Group is overlain by sandstones of the Oil Creek Formation (Ragland and Donovan, 1991). The basal Oil Creek sandstone is described as medium-to coarse-grained with well-rounded to rounded, frosted quartz grains and variable amounts of silica or carbonate cement. It is overlain by the Oil Creek "shale" in Oklahoma, which is predominantly limestone and dolomite. It is the first incursion of significant quantities of clay into Oklahoma following the basal Oil Creek Formation deposition (Suhm, 1997).

The McLish Formation was deposited after the Oil Creek Formation and is present throughout Oklahoma except in the western and southern parts of the Anadarko and Ardmore basins and the Texas Arch. The base of the McLish Formation is composed of fine to medium-sized, rounded, frosted quartz grains cemented by variable amounts of silica or carbonate cement. It grades upward into limestones, dolomites, sandstones, and beds of green to gray glauconitic shale (Suhm, 1997). Above the McLish Formation are the Bromide sandstones. It is characterized as sublithographic to lithographic limestone and dolomites at the top and sandstones and shale at the base. The sandstone interval is commonly referred to as the "Second Wilcox" and is the most areally extensive of the Simpson Group sandstones (Suhm, 1997). The Bromide sandstones are medium-to-coarse grained with rounded and frosted quartz grains and varying types and amounts of cement. In Oklahoma, the Simpson Group sandstones exhibit geometries and sedimentary characteristics of a shallow-water subaqueous fan or marine-modified delta. It is believed to be the basinward equivalent of the Starved Rock Sandstone in Illinois, Iowa, Missouri, and on the western side of the Ozark dome in eastern Kansas (Suhm,

1997). Because of its thickness and lateral continuity across most of the state, the Bromide sandstones or "Second Wilcox" would be the primary target for CO_2 storage.

The Trenton Group, also called the Viola Limestone, overlies the Simpson Group. The top of the Viola is denoted by the sharp decrease in the gamma ray log at the base of the Sylvan Shale. The Viola Limestone in the Arbuckle Mountains and heart of the SOA are described as cherty, finely laminated lime mudstones and are organic-rich. These grade upwards into a crinoid-rich grainstone. Outside of the SOA, the Viola is predominantly composed of packstones and wackestones with fewer laminations (Denison, 1997). The youngest Ordovician formation in Oklahoma is the Sylvan Shale. In outcrop in eastern Oklahoma, it is described as dark green and fissile. Locally thin stringers of brown, dolomitic sandstone occur in the lower portion (Huffman, 1953). After the Sylvan Shale was deposited, the Hunton Group was deposited across the Anadarko Basin, Arkoma Basin, and southern Oklahoma. Post-Hunton deposition was marked by the post-Hunton orogeny, which led to uplift and erosion across much of the region (Amsden, 1980). The post-Hunton unconformity removed portions of the Hunton Group across north-central Oklahoma and also cut down into the Ordovician strata, removing the Sylvan Shale, Viola Limestone, Simpson Group, and Arbuckle Group. Both the top and bottom of the Ordovician zone are unconformities across north-central Oklahoma.

After the post-Hunton orogeny, the Misener Sandstone, Woodford Shale, and Mississippian Formation were deposited across Oklahoma. The end of the Mississippian across Oklahoma is marked by the pre-Pennsylvanian unconformity. The ancestral Anadarko basin was experiencing rifting until the end of the Mississippian, leading to extensional faults across Oklahoma. The later Pennsylvanian time is divided into 5 epochs and includes Morrowan (early), Atokan, Desmoinesian (middle), Missourian, and Virgilian (late), all of which had orogenic

events associated with them. These orogenies reactivated and transformed the extensional faults into compressional thrust faults. It led to uplift along the Nemaha ridge and Cherokee platform and created the massive, regional pre-Pennsylvanian unconformity. The unconformity extends west of the Nemaha and along the Anadarko shelf but disappears in the Anadarko Basin, where deposition of the Pennsylvanian sands was taking place.

Methods

Subsurface Mapping

The stratigraphy of the Ordovician zone and the rest of the lower Paleozoic reservoirs including the Mississippian (less Chesterian strata), Woodford Shale, Hunton Group, Sylvan Shale, Viola Limestone, Arbuckle Group and crystalline basement was developed by interpreting conventional well logs (e.g., gamma-ray, apparent porosity, bulk density, resistivity) and classified lithology logs (i.e. mudlogs or sample logs). Formation tops were interpreted by the author through means of dip- and strike-oriented cross sections.

Well-derived formation tops resulted in 80,800 tops for the Mississippian (less Chesterian strata), 62,000 tops for the Woodford Shale, 41,200 tops for the Hunton Group, 34,300 tops for the Sylvan Shale, 40,800 tops for the Viola Limestone (Ordovician), 5,591 tops for the Arbuckle Group and 257 tops for the crystalline basement (Figure 2.1). Based on the interpreted formations from well logs, structure maps were generated for the Mississippian, Woodford, Hunton, Sylvan Shale, the Ordovician (Viola Limestone or Simpson Group), Arbuckle, and crystalline basement (Figure 2.2). Due to the significant well control, the Mississippian structure map was used as the initial reference surface to constrain the structure maps of deeper formations. A structure map was generated from well tops using a 2,500 ft x 2,500 ft (762 m x

762 m) grid and convergent gridding. Isopach maps were generated for the interval from the Mississippian to the Woodford (MSSP zone), Woodford to the Hunton (WDFD zone), Hunton to Sylvan (Hunton zone), Sylvan to Viola (SLVN zone), Viola to Arbuckle (Ordovician zone) and Arbuckle to crystalline Basement (Arbuckle zone). The isopach map for the MSSP zone was subtracted from the Mississippian structure map to create the Woodford structure map. The isopach map for the WDFD zone was subtracted from the Woodford structure map to generate the Hunton zone structure map, and so forth until the structure for the crystalline basement was generated. Of the 40,800 Ordovician penetrations, 1,469 wells have modern log suites imported or digitized into log ascii standard (LAS) format. Of the 1,469 wells with LAS, 343 were full penetrations of the Ordovician zone, while 1,126 were partial penetrations (Figure 2.1). There were no cores available for the study, but of the 1,469 wells with modern well logs, 46 had mudlogs or sample logs with rock descriptions available.

Derived Petrophysical Logs

The conventional modern well logs and other parameters in GVERSE Geographix were used to calculate derived logs for total porosity (PHIT), density porosity (PHID), shale volume (V_{sh}), apparent matrix grain density (RHO_{maa}), apparent matrix volumetric cross-section (U_{maa}), and percent mineralogy/lithology.

Mineralogy logs were generated using the RHO_{maa} - U_{maa} mineralogy cross-plot methodology with a 4-mineral (calcite, dolomite, quartz, and shale) model. To evaluate mixed lithologies and to semi-quantitatively estimate mineral volumetric proportions, a cross plot of the apparent matrix grain density, RHO_{maa}, versus apparent matrix volumetric cross-section, U_{maa}, is generated (Doveton, 1994).

Because the Ordovician zone has sandstones, limestones, dolomites, and shales, PHID was calculated using a matrix density (ρ_m) of 2.68 g/cm^3 with saltwater (ρ_f = 1.02 g/cm^3):

$$PHID = \frac{\rho_m - \mathrm{RHOB}_B}{\rho_m - \rho_f} \quad \text{Eq (1)}$$

Because of the multiple lithologies present in the zone, PHIT was calculated using the cross-plot porosity method and Schlumberger's salt-water filled Formation Density vs CNL Compensated Neutron cross plot chart (Schlumberger, 1989).

Shale Volume (V_{sh}) was determined from GR with GR_{cl} = 20 API and GR_{sh} = 100 API for clean (non-shaley) and shale endmembers, respectively.

$$V_{sh} = \frac{GR - GR_{cl}}{GR_{sh} - GR_{cl}} \quad \text{Eq (2)}$$

The apparent matrix grain density is computed as:

$$RHO_{maa} = \frac{RHOB - PHIT * RHO_{fl}}{1 - PHIT} \quad \text{Eq (3)}$$

Where RHO_{fl} is the flushed zone pore water density (RHO_{fl} = 1.0 g cm^{-3}). The apparent matrix volumetric cross-section, U_{maa}, is computed from the photoelectric factor log and bulk density log as:

$$U_{maa} = \frac{PEF * \rho_e - PHIT * U_f}{1 - PHIT} \quad \text{Eq (4)}$$

Where ρ_e is the electron density and U_f is the volumetric photoelectric absorption or volumetric cross section of the flushed zone pore space (U_f = 0.398 barnes cm^{-3}). The photoelectric index, ρ_e, must be converted to a volumetric measure by multiplying the electron density, which is defined as:

$$\rho_e = \frac{\rho_B + 0.1883}{1.0704} \quad \text{Eq (5)}$$

RHO_{maa} and U_{maa} are cross-plotted on an imposed ternary diagram with trend lines for quartz, calcite, and dolomite. Shale percentage was calculated from GR and the calcite, quartz, and dolomite percentages from cross plot analysis. Calcite in the Ordovician zone is described and interpreted as limestone. Quartz is predominantly sandstone with minor amounts of chert, therefore, this mineralogy is interpreted as sandstone.

Because the volume of shale was calculated from GR, it is indicative of clay mineralogy in the Ordovician zone. To generate lithology logs from the mineralogy logs, it was assumed that the dominant mineralogy at each depth corresponds to limestone (for calcite), dolostone (for dolomite), sandstone (for quartz), and shale (clay content).

3-D Modeling and CO_2 Storage Resources Estimation

Three-dimensional geological models of key properties were constructed to calculate pore volume and CO_2 storage resources for the Ordovician zone in Oklahoma. Using the 3-D models to determine the CO_2 storage resources, the U.S. Department of Energy methodology (NETL, 2007 & 2008; IEA GHG, 2009) was used as follows:

$$G_{CO2} = A * h * \varphi * \rho_{CO2} * E_{saline} \quad \text{Eq (6)}$$

G_{CO2} is the mass of CO_2 stored in the reservoir, A is the area of reservoir, h is the thickness of reservoir, φ is the total porosity, ρ_{CO2} is the density of CO_2 (dependent on temperature and pressure; dependent on depth), and E_{saline} is the saline storage efficiency coefficient (dependent on lithology).

The 3-D stratigraphic and structural framework (3-D model grid) of the Ordovician zone was generated using the structure maps that define the reservoir zones. The 3-D grid covers an area of approximately 44,627 mi^2 (115,583 km^2) with aerial cell dimensions of 2,500 ft x 2,500 ft (762 m x 762 m). The Ordovician zone was divided stratigraphically into 160 proportional layers, each approximately 7 ft (2.1 m) thick. The resulting 3-D model grid has 21,771,462 cells.

To represent the spatial variability of lithologies for the Ordovician zone, a 3-D lithology model was constructed with commercial software using sequential-indicator simulation (SIS). The model constraints include: 1) the stratigraphic and structural framework (3-D grid), 2) upscaled lithology logs, 3) variogram parameters by zone, 4) lithology percentages by zone, and 5) vertical lithology proportion curves. Lithology logs were upscaled to the 3-D model grid by assigning a single lithology class to a cell based on the most abundant lithology within a cell. The target fractions of each lithology were obtained from the upscaled lithology logs.

A 3-D porosity model was generated to evaluate the distribution of total porosity (PHIT) within the study area. PHIT logs were biased to the lithology logs and upscaled using an arithmetic mean. The porosity model was generated using sequential-Gaussian simulation (SGS) and was constrained to: 1) a 3-D lithology model, 2) upscaled PHIT logs (biased to lithology), 3) porosity histograms by zone and lithology, and 4) variogram parameters by zone and lithology.

The density of CO_2 in the reservoir is dependent on the temperature and pressure of the reservoir. Bottom hole temperature and total depth from the wellbore data across Oklahoma are available from the Southern Methodist University Geothermal Lab, which is a part of the National Geothermal Data System funded by the U.S. DOE (SMU Node of National Geothermal Data System, Heat Flow and Well Data, accessed March 2023). A temperature gradient map was generated for the state, assuming a 60° F surface temperature to bottom hole temperature. Using

the temperature gradient map and measured depths from the 3-D grid, a 3-D temperature model was calculated for Oklahoma. Pressure data acquired from oil and gas operators across Oklahoma indicate that the Simpson Group is normally pressured (Puckette, 1996). Using a pressure gradient of 0.44 psi/ft (9,953 Pa/m), a 3-D reservoir pressure model was generated using the measured depths from the 3-D grid. Lastly, using the ideal gas law, the temperature model and pressure model were used to calculate the 3-D CO_2 density model as follows:

$$\rho = \frac{p*M}{R*T} \qquad \text{Eq (7)}$$

Where ρ is the density (g/m^3) of CO_2 at temperature and pressure, p is the pressure (pascal; Pa), M is the molar mass of CO_2 = 44.01 g/mol, R is Avogadro's constant and equal to 8.31 (joule/mol*kelvin; J/mol*K) and T is temperature (kelvin; K).

Saline storage efficiency coefficient (E_{saline}) is the percentage of pore space that the CO_2 will occupy in the reservoir and is dependent on lithology. The 2009 International Energy Agency Greenhouse Gas Development of Storage Coefficients for CO_2 storage in deep saline reservoirs (IEA GHG, 2009) states that E_{saline} is a function of the lithology and depositional environment and is calculated as (see Table 2.1 for a description of the equation terms):

$$E_{Saline} = \frac{A_n}{A_t} * \frac{h_n}{h_g} * \frac{\emptyset_{eff}}{\emptyset_{tot}} * (E_A * E_I * E_g * E_d) \qquad \text{Eq (8)}$$

The last 4 terms define the pore volume immediately surrounding a single well CO_2 injector. E_A is the areal displacement efficiency, E_I is the vertical displacement efficiency, E_g is gravity, and Ed is the microscopic displacement efficiency. To calculate storage efficiencies, heterogeneous 3-D models were developed for various lithologies, depositional environments, and structures. Statistical distributions from a global database of hydrocarbon reservoir properties were used,

including key parameters like porosity and permeability (IEA GHG, 2009). The ranges of storage coefficients for each lithology were derived based on 195 simulations. If the assessment of storage resource is over a small, localized area, then it is likely that the values of the A_n/A_t and h_n/h_g will be relatively high. Therefore when determining E_{saline} at the site-specific level A_n/A_t was fixed at .8 while h_n/h_g and $\emptyset_{eff}/\emptyset_{tot}$ ranges between .25-.75 and .6-.95 respectively (Table 2.1). Regionally, the geologic properties will vary spatially; For this reason, the P_{50} of the A_n/A_t and h_n/h_g terms were fixed to determine the formation level E_{saline} values. This leads to an overall lower storage coefficient for each lithology at the formation level. E_{saline} values are reported for the P_{10}, $P_{50,}$ and P_{90} for clastics, dolomites, and limestones at the site-specific and formation level evaluations. P_{10} notation indicates that there is a 10% probability that the value is less than the P_{10} value, and the P_{90} notation indicates there is a 90% probability that the value is less than the P_{90} value. The total CO_2 storage resources for the model were calculated for both the site-specific and formation level E_{saline} values. Table 2.2 shows the E_{saline} values for each lithology. Because E_{saline} values were reported by lithology, they were also applied to the corresponding lithologies in the model, with the values for clastics being applied to both the sandstone and shale lithologies.

Results

Structure, Thickness, and Lithology Trends

The lower Paleozoic reservoirs across Oklahoma are structurally complex and highly faulted in certain areas. The Mississippian structure map, which was used to constrain the deeper formations across Oklahoma, coincides with the massive, regional pre-Pennsylvanian unconformity (Figure 2.3A). The unconformity extends west of the Nemaha and along the

Anadarko shelf but disappears in the Anadarko Basin, where deposition of the Pennsylvanian sands was taking place. The major structural features of Oklahoma, including the Nemaha and Wilzetta fault systems, run north-south through central Oklahoma.

In central Oklahoma, there are localized areas where the Mississippian, Woodford Shale, Hunton Group, Sylvan Shale, and Ordovician have been removed due to the pre-Pennsylvanian unconformity and post-Hunton unconformities (Figure 2.3B and 2.3C). In these areas, the Pennsylvanian shales sit directly above the Arbuckle zone; the Oklahoma City oilfield and Cushing oilfields are examples. The Sylvan Shale is a seal for hydrocarbon reservoirs, and therefore a seal for CO_2 storage in Ordovician reservoirs. It ranges from 0-360 ft (0-110 m) thick and is present across much of central Oklahoma (Figure 2.3C and 2.4A). The Sylvan Shale is not present in Pawnee, Osage counties due to the post-Hunton unconformity, but the Woodford Shale is present and acts as a seal for the Ordovician reservoirs (Figure 2.3B). The Oklahoma panhandle does not have Sylvan Shale or Woodford Shale present to seal the Ordovician reservoirs. Instead, the Mississippian limestones sit directly above the Ordovician limestones. It can be incredibly hard to distinguish on older well logs where the base of the Mississippian limestones and the top of the Ordovician limestones begin. While there is no shale boundary to separate the Mississippian and Ordovician reservoirs, the Mississippian does have a large regional seal of Pennsylvanian shales above it, which are also hydrocarbon seals (Figure 2.3B).

Because the Paleozoic formations were subjected to the same Pennsylvanian orogenies, faults that penetrate the shallower Mississippian commonly penetrate the deeper strata. This is why the Mississippian and Ordovician structural trends all look similar (Figures 2.3A and 2.4B). The only difference is that offset along faults become greater with stratigraphic age. Faults

shown on Figure 2.3A are a combination of the OGS Comprehensive Fault database (Holloway et al., 2016) and faults identified from the structural model.

The Ordovician zone ranges from 0-2,800 ft (0-853 m) in thickness, with the thickest interval in southern Oklahoma (Figure 2.4C). Like the Sylvan Shale, the Ordovician zone is not present in the northeastern portion of Osage County due to the post-Hunton unconformity or the westernmost corner of the Oklahoma panhandle, due to non-deposition (Suhm, 2016). RHO_{maa} - U_{maa} cross-plots show the Ordovician zone is predominantly calcite, quartz, and shale with lesser amounts of dolomite (Figure 2.5). A type log for the Ordovician zone (Figure 2.6) illustrates mineral percentage curves generated using the 4-mineral (limestone, dolomite, sandstone, and shale) model in the second-to-last track. The last track shows the dominant lithology at each depth, which was used in the lithology modeling.

In general, the Viola Limestone is described as tan to creamy grey, very dense, hard, brittle, and low porosity with traces of translucent chert (Figure 2.6). The Bromide sandstones are described as clear to white in color, fine to medium grained, angular to rounded grains, well sorted, and well cemented with quartz. The Oil Creek shales are described as green, firm, and waxy, while the Oil Creek sandstone and McLish sandstones are described similarly as the Bromide sandstones. The 46 available mudlogs were used to confirm the petrophysical cutoffs used for the lithology model. The correlation between mudlog descriptions and the discrete lithology log used for the lithology model is very good.

Across much of Oklahoma, the top of the Ordovician zone is the Viola Limestone (Figure 2.7, blue arrows). Western Oklahoma has a large NW-SE trending area that indicates shale at the top of the Ordovician (Figure 2.7, black, double-headed arrow). This is because at the top of the Viola, the base of the Sylvan Shale has stringers of siltstones and dolomites. While these

siltstones and dolomites generally present with lower gamma-ray than the above Sylvan Shale, they still read around 40-50 API units, which presents as shale in the petrophysical model because the shale content is a direct reading of the gamma-ray. These siltstones can present with porosity and were included in the Ordovician zone. As expected, the Simpson-age Bromide sandstones are at the top of the reservoir in northeastern Oklahoma (Figure 2.7, red arrows) where the post-Hunton unconformity has removed the younger Sylvan Shale and Viola Limestone. These sandstones can also be seen as the large continuous sand bodies on the cross-sectional views (Figure 2.7B, red arrows).

The Ordovician is predominantly limestone (50%) and sandstone (30%) with lesser amounts of shale (16%) and dolomite (4%) (Figure 2.8). Limestone thickens to the south with the greatest thickness in the Anadarko Basin (Figure 2.8A). Sandstone also thickens towards the Anadarko and Arkoma basins and along the crest of the Cherokee platform just north of the Arbuckle uplift (Figure 2.8B). Shale thickness increases toward the Anadarko and Arkoma basins. Dolomite appears to thicken slightly in the Arkoma basin, but it is the thinnest of all the lithologies (Figure 2.8C). The shale in the Ordovician zone is predominantly described as waxy and green (Figure 2.6) and is a known hydrocarbon seal for the sandstones and dolomites within the zone when structurally trapped. The Simpson Group shales also act as the regional seal for the Arbuckle Group, which is a hydrocarbon-producing reservoir where structurally trapped, and an oilfield wastewater disposal zone.

Petrophysical Properties

The total porosity model (PHIT) for the Ordovician was constrained to the lithology model. The Ordovician zone shows that limestone average porosity is <4%. The limestone

interval is predominantly the Viola Limestone, which is a hydrocarbon-producing reservoir where structurally trapped and highly fractured. The sandstone lithology in the Ordovician has the highest porosity of all lithologies. On average, it is 10% but can be as high as 20% (Figure 2.9A). Across central and northern Oklahoma, the sandstone has an increased average porosity when compared to the deeper Anadarko and Arkoma basins. The net pore volume for the Ordovician sandstones is more dependent on lithology thickness than average porosity (Figure 2.9B), i.e., the Ordovician sandstone net pore thickness map (Figure 2.9B) and sandstone isopach (Figure 2.8B) look very similar.

The Simpson sandstones produce hydrocarbons on closed structural traps and are prolific producers. There are over 7,240 wells in Oklahoma that produce from the Simpson, Bromide, and "Wilcox" sandstones (Enverus, January 2021). Cumulative production from these wells and reservoirs is 320 million barrels of oil and 874 billion cubic feet (BCF) of gas. These same sandstones have also been used for saltwater injection wells (SWD). Dolomite is present in the Ordovician but accounts for 6.8% of the total rock volume with an average of 5% total porosity. These dolomites are not always laterally continuous and would not be the intended targets for CO_2 storage. While some of the shale in the model may have porosity development (i.e., the siltstones and dolomites that develop at the top of the Ordovician zone), the majority of the shale in the model is considered non-reservoir rock.

Based on the 3-D models of temperature and pressure, temperature for the Ordovician ranges from 100-525°F (24-274°C) (Figure 2.10A). Pressure ranges from 500-16,000 psi (3.45-110 MPa) with a median value of 4,000 psi (27.6 MPa) (Figure 2.10B). The temperature and pressure 3-D models were used to calculate the CO_2 density model. CO_2 density ranges from 100-1,000 kg/m^3 with a median of 325 kg/m^3 (Figure 2.10C).

CO_2 Storage Resources

The CO_2 storage resources for the Ordovician zone range from 35,973-105,560 Mt for the Ordovician zone at the site-specific level (Table 2.3, Figure 2.11) and 13,800-40,792 Mt at the formation level (Table 2.4) for all lithologies. The shale is not considered a reservoir lithology, and the limestone is generally low porosity and tight. The dolomite reservoirs are not as laterally continuous as the sandstones. The CO_2 storage resources model using the P_{50} E_{saline} values at the formation level (Figure 2.12) shows the highest storage resources in the deep Anadarko Basin. Note: All figures for CO_2 storage resources were generated using the P_{50} E_{saline} storage efficiency factors at the formation level, giving a conservative estimate of CO_2 storage resources.

Because the intended CCUS storage target is the sandstone lithology, Figure 2.12C shows the net-mass storage resources for the Ordovician sandstones in megatons CO_2 per mi^2. The CO_2 storage resources at the formation level are reduced by 33% for clastics, 40% for sandstone, and 37-41% for dolomite, and are directly related to the reduction in E_{saline} values (Table 2.2). Storage resources increase with depth, thickness, and porosity (Figures 2.13). Across much of north central Oklahoma, the CO_2 storage resources are around .25 Mt (250,000 Tons) per square mile (Figure 2.12). It is not until the deep Anadarko Basin that storage resources begin to increase.

Because the Ordovician zone ranges from 2,000-36,000 ft (610-10,973 m) deep across the study area and the goal of CCUS is to store the most CO_2 for the least cost, and the cost to drill a well increases with depth, the CO_2 storage resources were summed across 2,000 ft (610 m) depth intervals (Figure 2.13A). For example, the Ordovician sandstones from 4,000-6,000 ft

(1,200-1,800 m) have CO_2 storage resources between 1,874-6,028 Mt at the site-specific level and 753-2,421 Mt at the formation level. That equates to 11% of total storage resources for all sandstones in the Ordovician (Figure 2.13A). Approximately 35% of the total sandstone storage resources are accessible at depths from 2,000-10,000 ft (600-3,000 m) across north-central Oklahoma, predominantly across the Cherokee Platform.

Discussion

CO_2 Storage Resources Calculations

The US-DOE methodology says the first three terms used to determine E_{saline} are the Net-to-Total Area, Net-to-Gross Thickness, and Effective-to-Total Porosity ratio (Table 2.1). The site-specific E_{saline} values, which are the highest used in this study, were determined by fixing the Net-to-Total Area to .8, the Net-to-Gross Thickness ranged between .25-.75, and the Effect-to-Total Porosity ranged between .6-.95 (Table 2.1, third column). All 3 of these factors are equal to 1 in this study. This means the most optimistic CO_2 storage resources reported in this study (i.e., the site-specific level) are still likely to be an underestimation of total CO_2 storage resources.

The intended targets for CCUS are the Bromide sandstones due to their gross thickness and lateral continuity (Figures 2.6 & 2.2). The sandstones in this model include the Bromide sandstones and the lower Oil Creek, McLish sandstones. These sandstones are also suitable for CCUS, but they are not nearly as laterally continuous and cannot be correlated over long distances. The Bromide, Oil Creek, and McLish sandstones are separate reservoirs. Therefore, maps and calculations of the CO_2 storage resources for the Ordovician zone are not a direct measurement for the Bromide sandstones.

The Viola Limestone that sits above the Simpson Group is the thickest lithology found in the model (Figure 2.8A) and has CO_2 storage resources between 10,200-24,414 Mt at the site-specific level (Table 2.3), and 3,461 and 8,373 Mt at the formation level (Table 2.4). These storage resources are less than the Ordovician sandstones, but not significantly. Due to the low average well log porosity of less than 4%, it is not the intended injection target. It does have storage capacity, and sits directly above the intended injection target and with no regional shale to separate the two reservoirs. This is especially true along the Cherokee platform, where the entire Ordovician zone thins due to both deposition and the post-Hunton unconformity. Where the Ordovician zone thins, the total CO_2 storage resources will be both the limestone and sandstone lithologies acting as one reservoir.

Areas of Interest

Across most of north-central Oklahoma, the Ordovician reservoirs are between 2,000 and 10,000 ft (610 and 3,048 m) deep. This same region has laterally continuous sandstone bodies with enhanced porosity with large regional seals both above and at the base of the zone. The Ordovician zone is significantly thinner than the Arbuckle zone, which leads to much lower CO_2 storage resources; it still can store roughly 250,000 tons of CO_2 per square mile in the sandstones alone. Central Oklahoma is the most favorable location for CCUS in the Ordovician sandstones and the Arbuckle zone (Figure 2.14). Both the Arbuckle and Ordovician are present and at adequate depths for CCUS, giving the unique ability to store CO_2 in multiple reservoirs from one wellbore. This would decrease the cost of field development, increase total field storage resources, while reducing the surface footprint. Additionally, the Ordovician reservoirs have not been tied to induced seismicity from wastewater injection wells like the Arbuckle zone and

would give the operator an additional reservoir to store CO_2 that is not in communication with the crystalline basement.

Conclusions

The Ordovician reservoirs of Oklahoma, specifically the Bromide sandstones, are the most laterally continuous sandstone in the state. It is a normally pressured reservoir with an average porosity of 10%. Across much of north central Oklahoma, it is less than 10,000 ft (3,048 m) deep with 400 ft (122 m) of sandstone. The CO_2 storage resources range from 6,501-20,877 Mt for the Ordovician sandstone at the site-specific level and 16,182-52,003 Mt at the formation level. 35% of the storage resources are accessible at depths shallower than 10,000 ft (3,048 m). Using the P_{50} E_{saline} values at the formation level, the CO_2 storage resources are around 300,000 tons of CO_2 per square mile. While the Ordovician zone has significantly less CO_2 storage resources than the Arbuckle zone, it is still a viable target for CCUS that can be exploited. The unique ability to have multiple CCUS reservoirs accessible by one wellbore has Oklahoma poised to become one of the largest carbon hubs in North America.

FIGURES

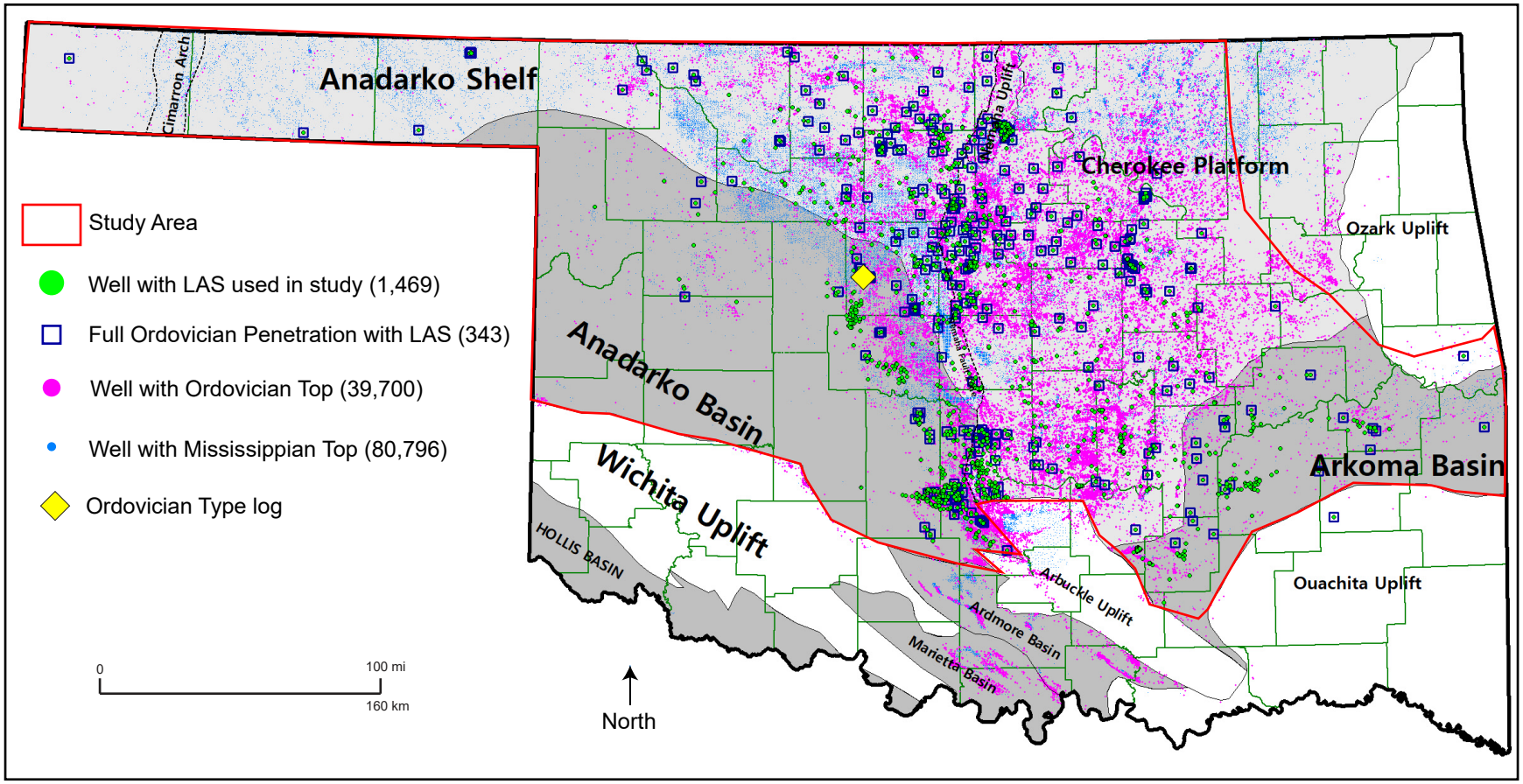


Figure 2.1. Study area and wells with LAS used in the study. Green circles are the wells with LAS available in the Ordovician. Blue squares are wells with LAS that penetrate the entire Ordovician zone. Pink circles are all the Ordovician tops from well log interpretation. Small, light blue well spots have well tops for the Mississippian. Geologic Provinces were modified from Northcutt and Campbell, 1995. The Ardmore, Marietta, and Hollis basins were not evaluated due to structural complexities. The Ozark Uplift was evaluated where depths were adequate. The Ordovician Type log location is shown.

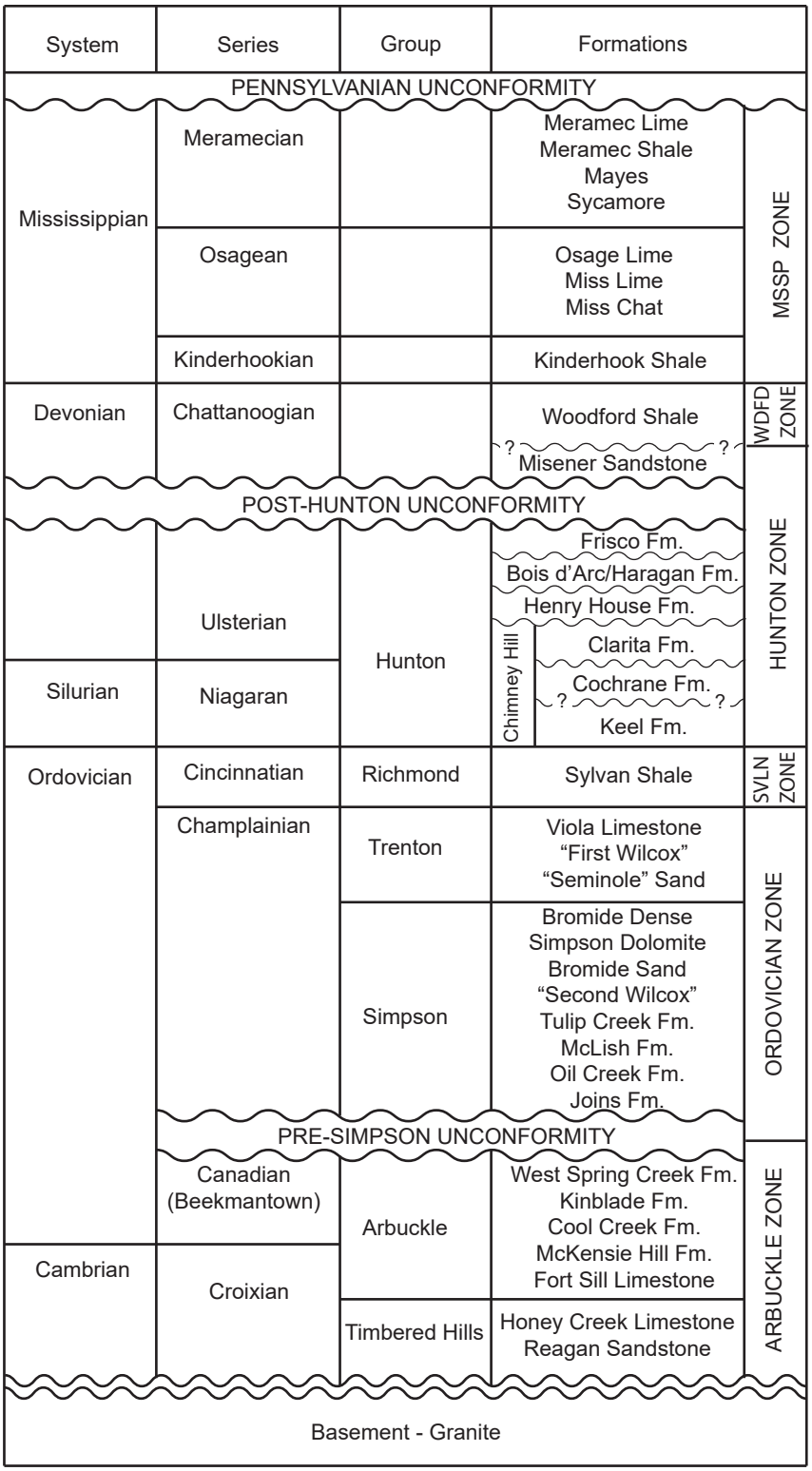


Figure 2.2. Generalized Stratigraphic Column of Oklahoma. Modified from Oklahoma Corporation Commission's General Geologic Sections of Oklahoma and Arkansas, 1975. The top of the Mississippian used for structural modeling is Meramecian in age, and marks the beginning of this stratigraphic column. Correlated formation tops and isopach zones used for structural modeling are labeled.

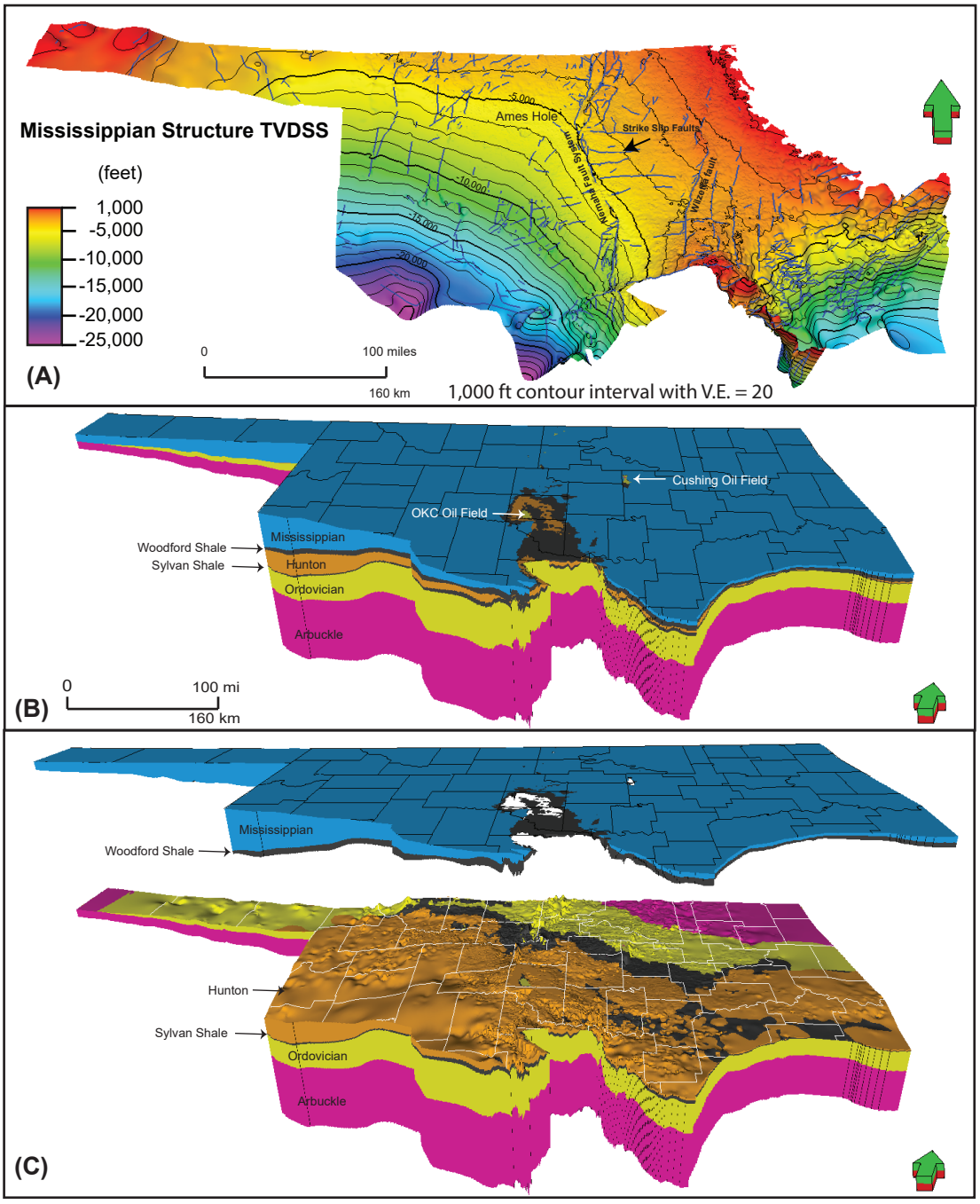


Figure 2.3 A) Mississippian Structure map. Blue faults are the modified fault layer that contains the OGS fault database (Holloway et al., 2016) and faults identified by the author. 1,000 ft (305 m) contour interval with a 20 vertical exaggeration. B) Mississippian (MSSP zone), Woodford (WDFD zone), Hunton (Hunton zone), Sylvan (SVLN zone), Ordovician (Ordovician zone), and Arbuckle zone flattened on the Mississippian. The top of the Mississippian is an unconformity across the Anadarko shelf and the Cherokee platform. This map is the pre-Pennsylvanian unconformity subcrop map. The Mississippian is present across Oklahoma except in central Oklahoma. C) Same model as 2.3B except the Mississippian and Woodford have been lifted to reveal the lateral extent of the Hunton, Sylvan, Ordovician, and Arbuckle zones. This is the post-Hunton unconformity subcrop map.

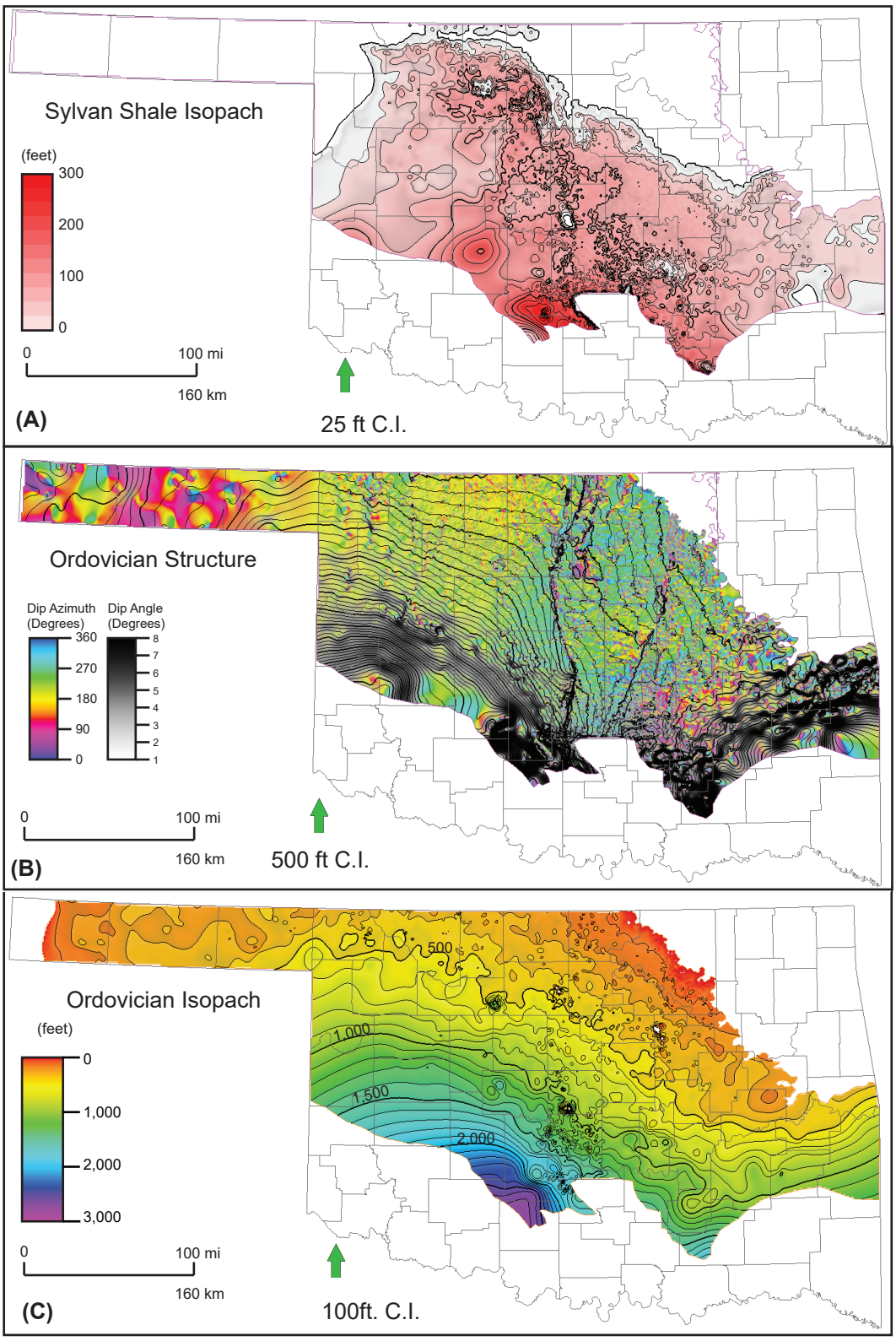


Figure 2.4. A) Sylvan Shale Isopach with 25 ft (7.6 m) contour interval. B) Ordovician Structure map with 500 ft (152 m) contour interval co-rendered with di-azimuth and dip-magnitude. C) Ordovician zone isopach with 100 ft (30 m) contour interval.

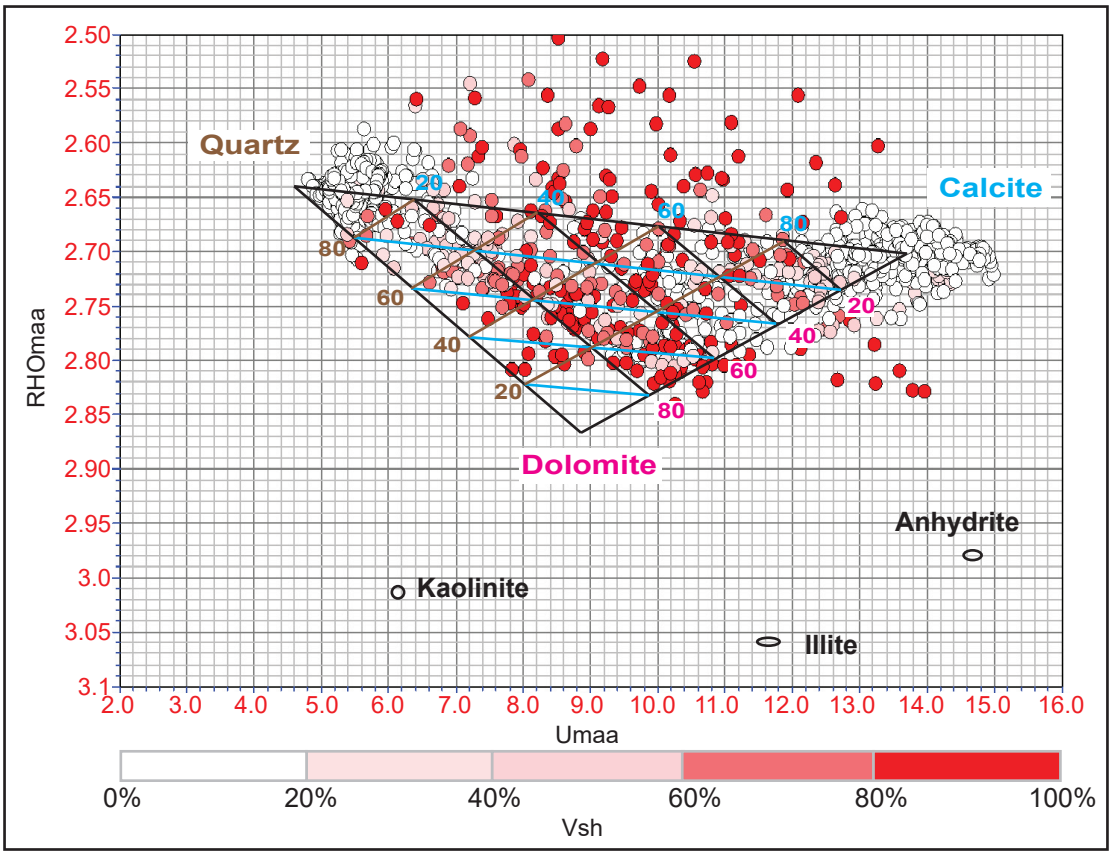


Figure 2.5. RHOmaa - Umaa plot colored by Vsh for the Ordovician zone. The Ordovician is composed of dolomite, calcite (limestone), quartz (sandstone), and shale.

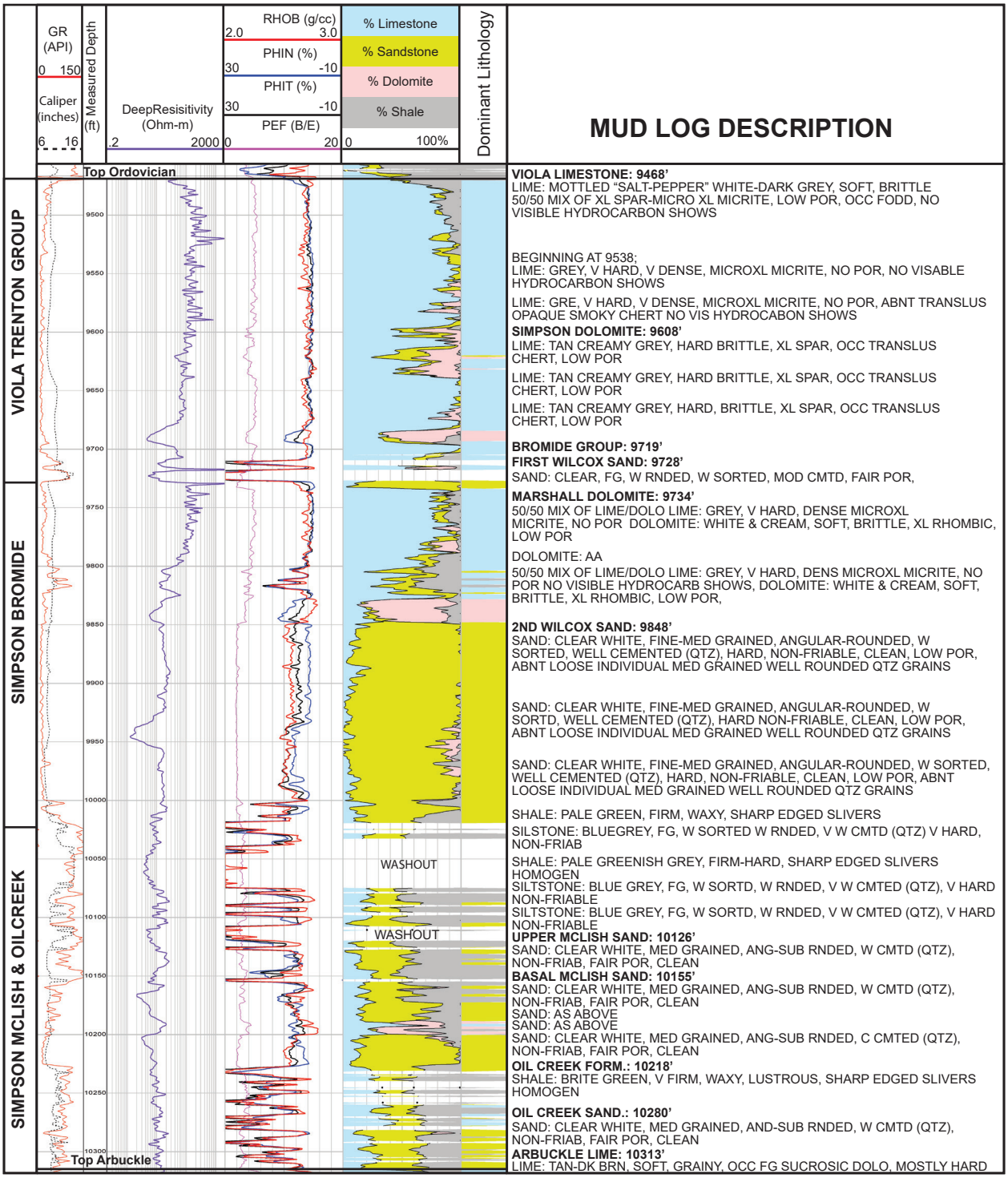


Figure 2.6. Ordovician zone type log, Karon 1, UWI 35-073-24496. The top of the Ordovician zone is the Viola Limestone. The second-to-last column shows the mineral percentage curves from the RHOmaa - Umaa analysis, color-filled by lithology. The right column corresponds to the dominant lithology at each depth and was used for the discrete lithology log used in modeling. Mud log sample descriptions are in the last track.

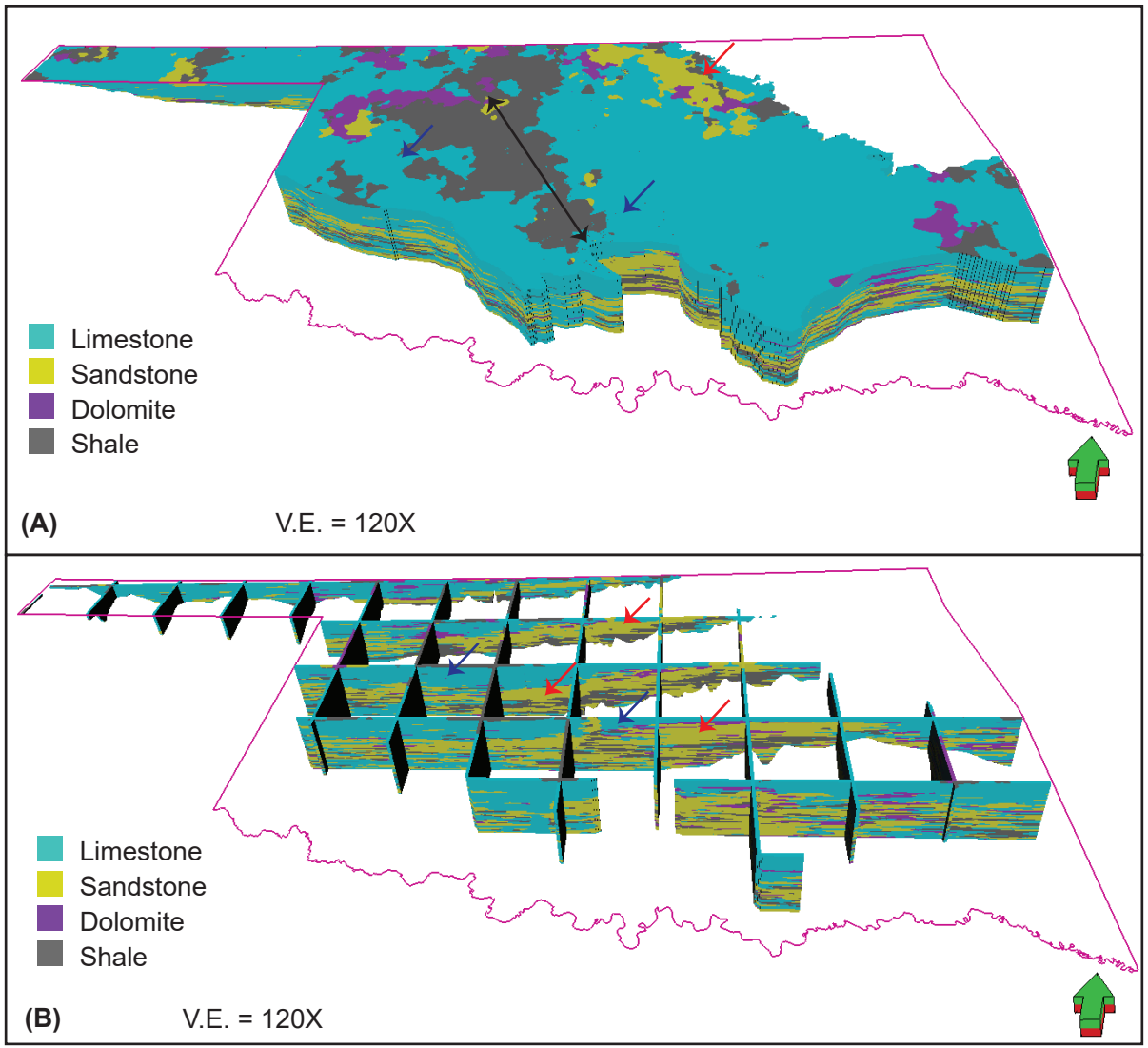


Figure 2.7. A) Lithology Model for the Ordovician, flattened on the top of the Ordovician. B) Fence Diagram of the lithology model for the Ordovician, flattened on the top of the Ordovician with a 120 vertical exaggeration skipping every 75 lines (roughly 35 miles/56 kilometers). The black arrow indicates the siltstone and dolomite stringers that are present across the top of the Ordovician. Blue arrows point to the Viola Limestone. Red arrows point to the Simpson Group Bromide sandstones.

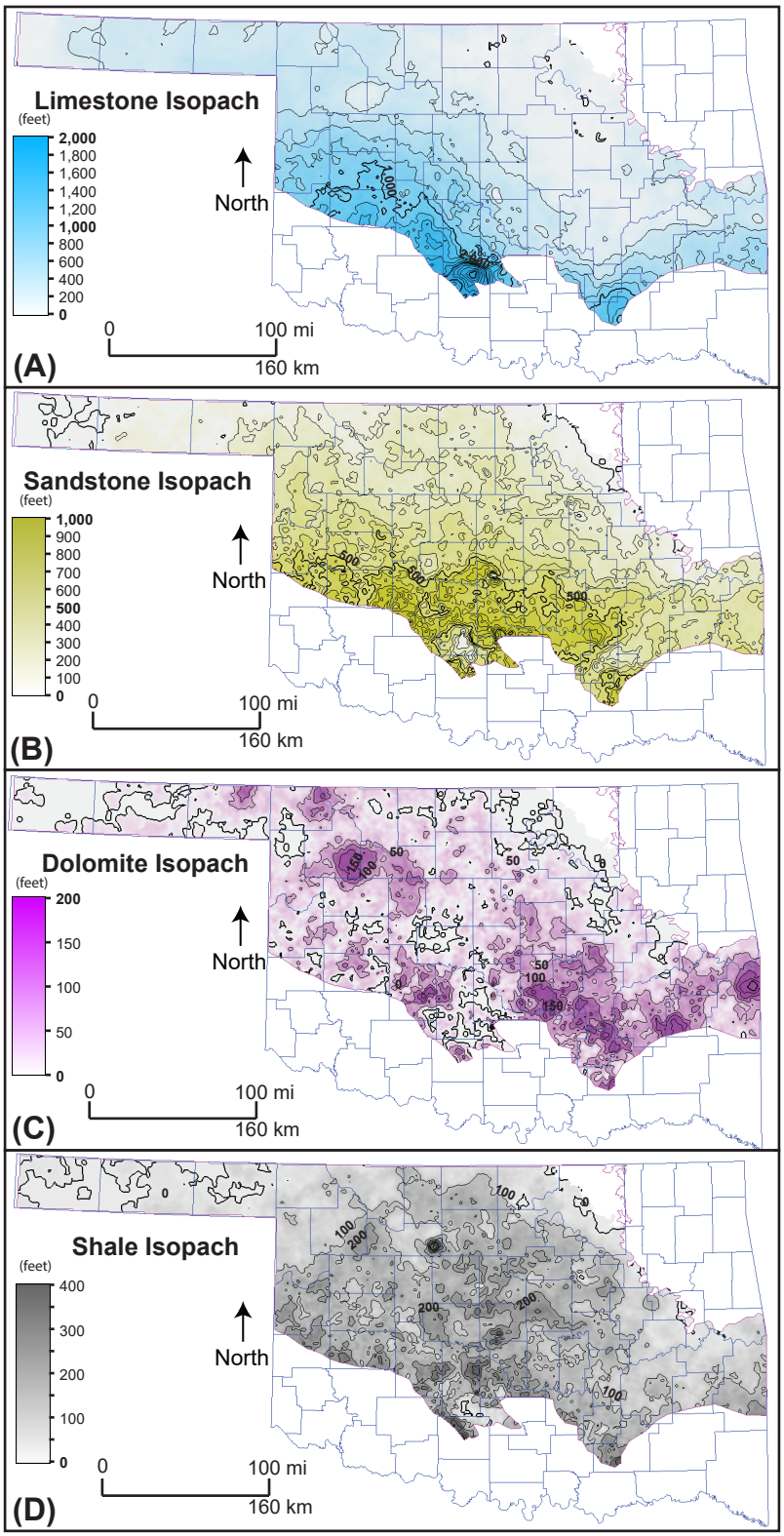


Figure 2.8. Ordovician Lithology thickness for A) Limestone. 200 ft (61 m) contour interval, 1,000 ft (305 m) bold contour interval. B) Sandstone. 100 ft (30 m) contour interval, 500 ft (152 m) bold contour interval. C) Dolomite. 50 ft (15 m) contour interval, 250 ft (73 m) bold contour interval. D) Shale. 100 ft (30 m) contour interval, 500 ft (152 m) bold contour interval.

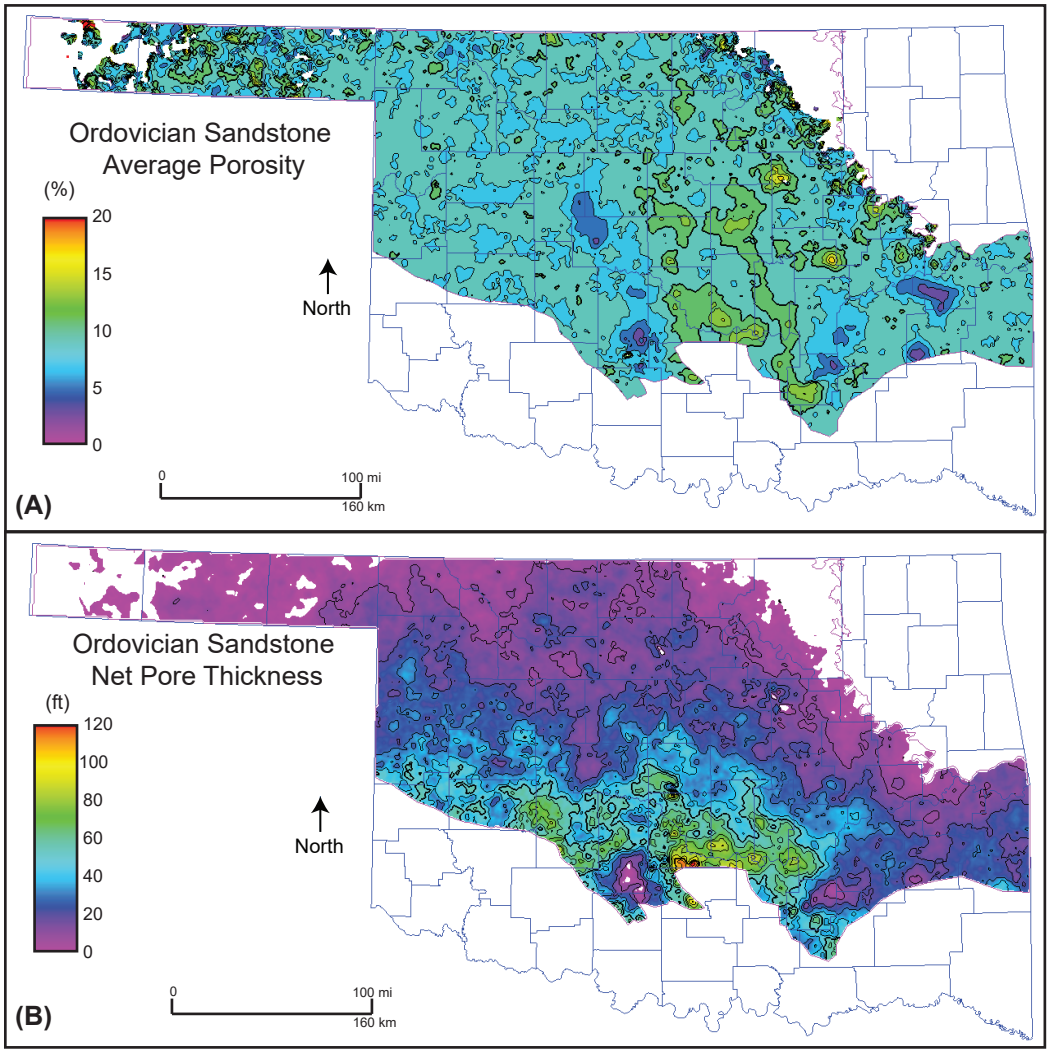


Figure 2.9. A) Average Sandstone Porosity for the Ordovician zone. 2% contour interval, 10% bold contour interval. The sandstones average porosity is higher across the Cherokee platform than in the Anadarko and Arkoma basins. B) Ordovician sandstone Net Pore Thickness map. 10 ft (3.0 m) contour interval, 50 ft (15 m) bold contour interval. While sandstone porosity is greater across the Cherokee platform, sand thickness increases towards the Anadarko Basin and the southern Cherokee platform, leading to the increase in net-pore space.

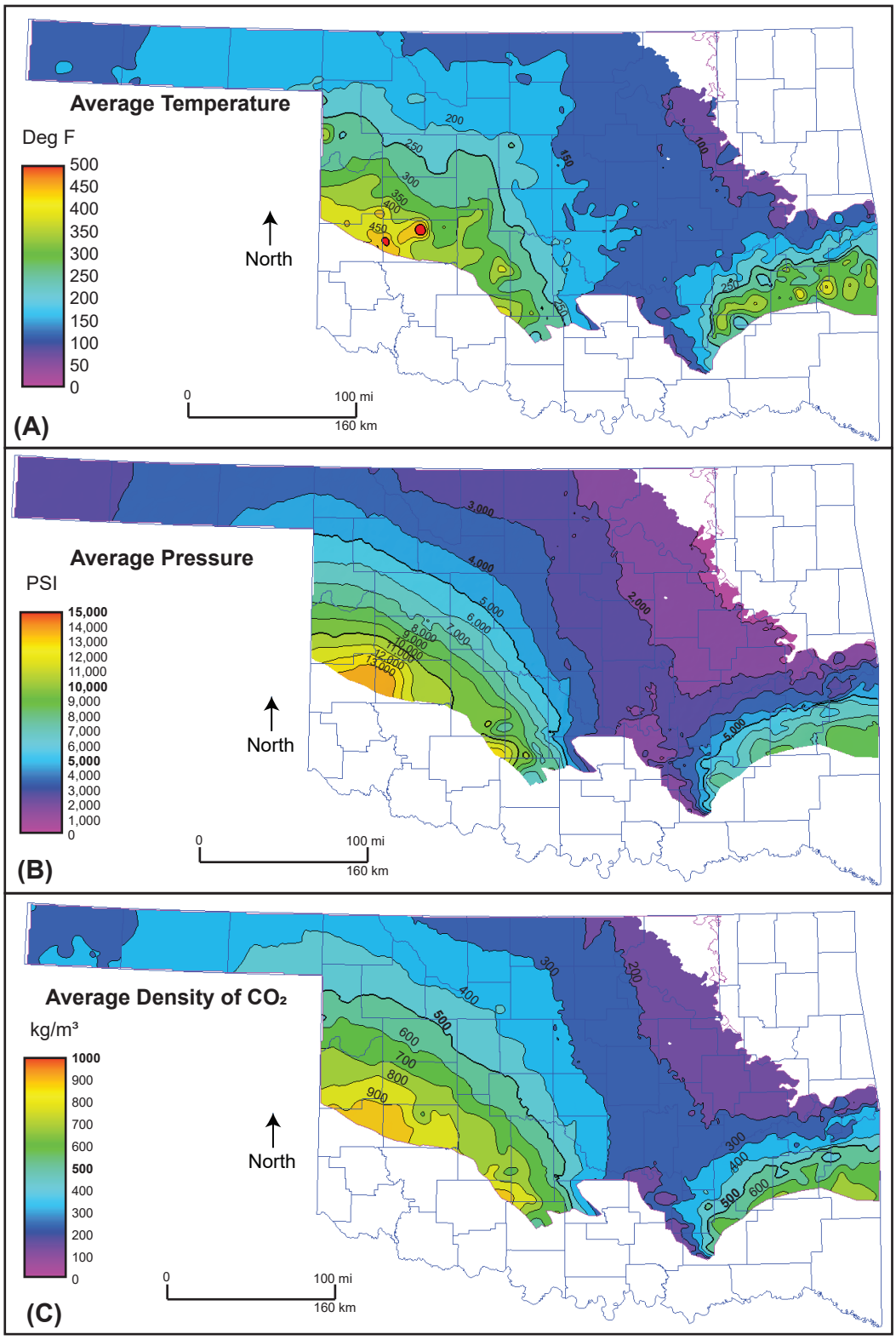


Figure 2.10. Temperature, Pressure and CO_2 Density maps. A) Average Ordovician Temperature map. 50 °F (10°C) contour interval. B) Average Ordovician Pressure map. 1,000 psi (6.89 MPa) contour interval. C) Average Density of CO_2 at reservoir temperature and pressure. 100 kg/m³ contour interval.

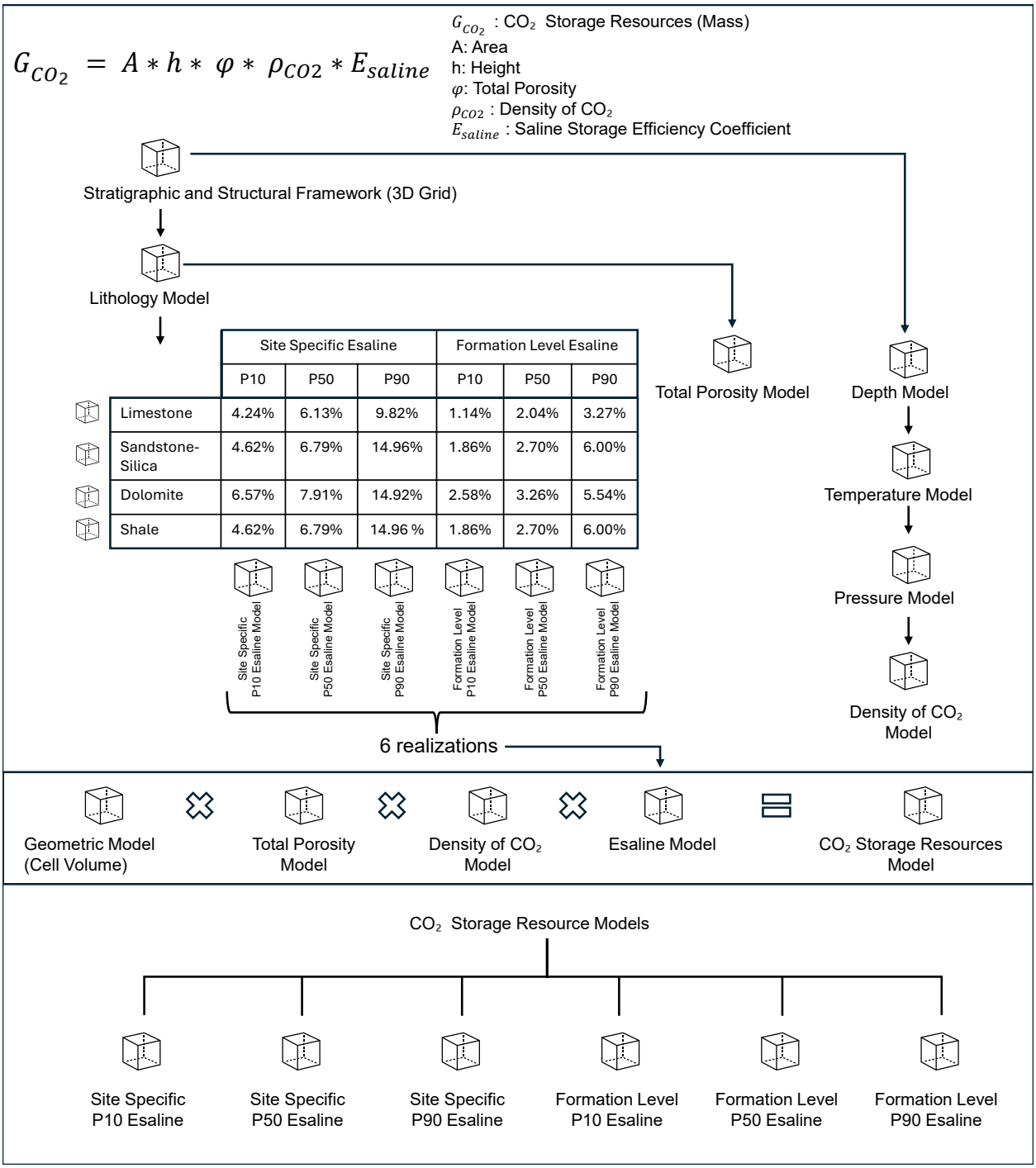


Figure 2.11. CO_2 storage resources modeling workflow.

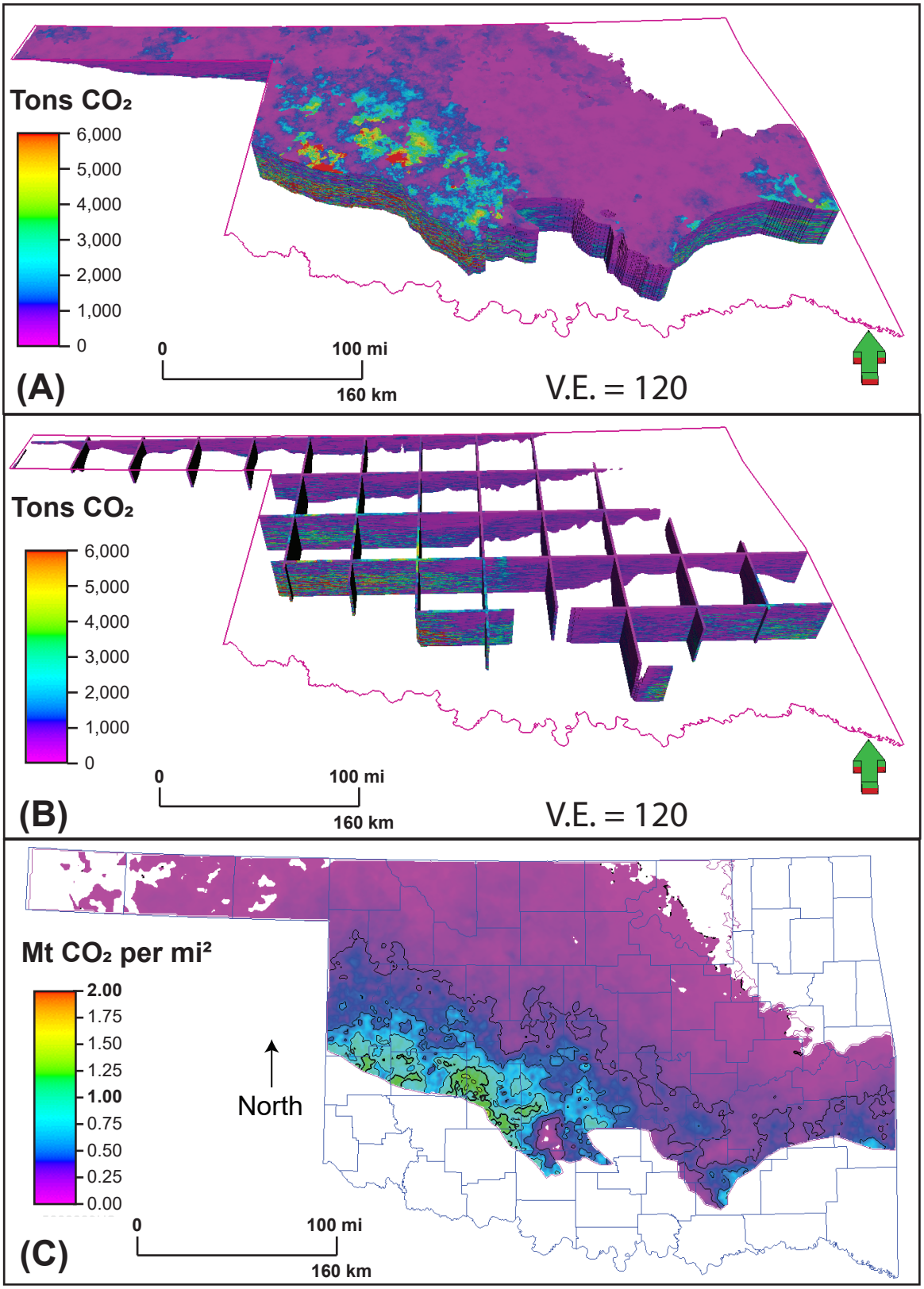
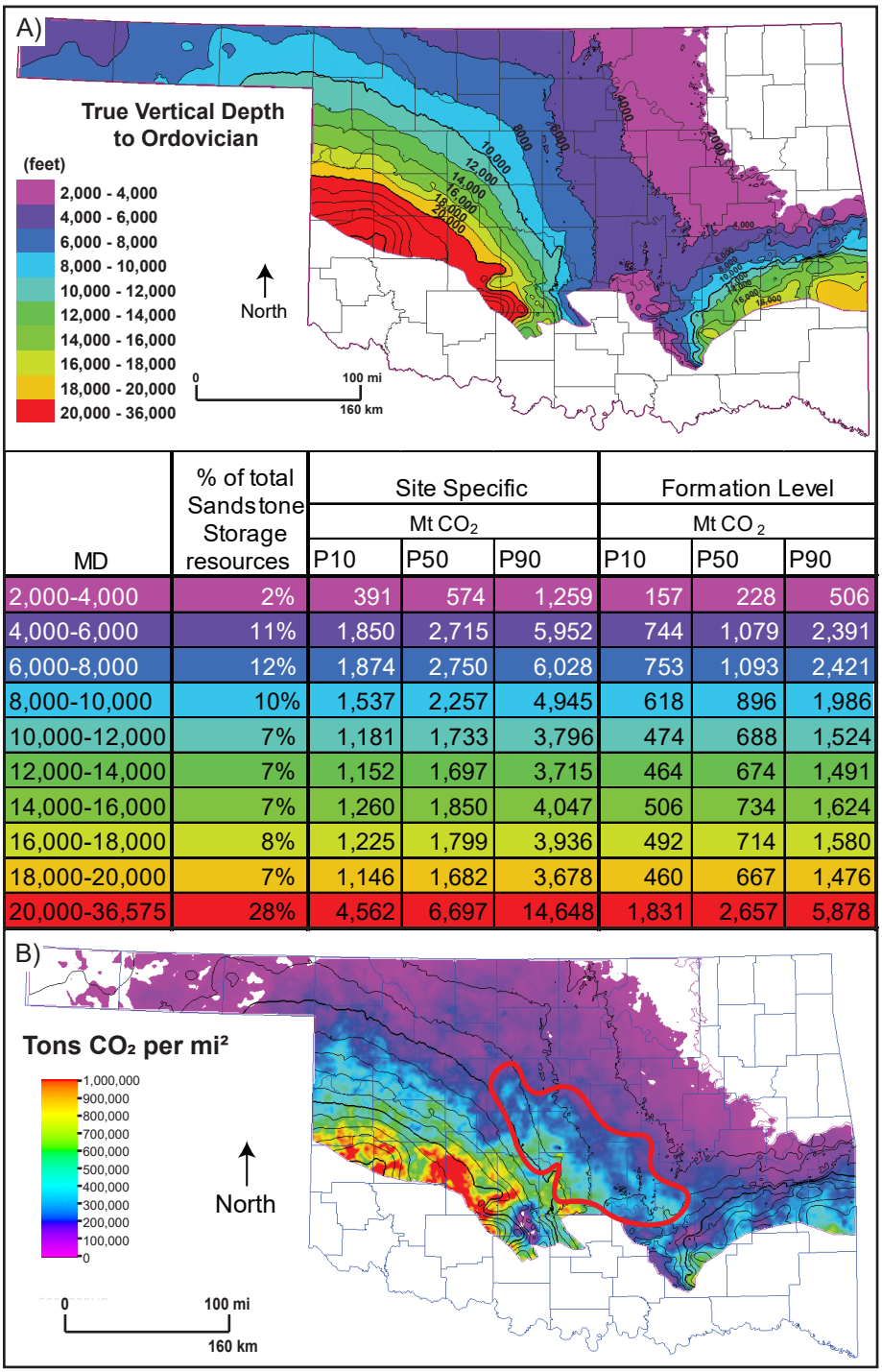


Figure 2.12. CO_2 storage resources models using the P_{50} Esaline values at the formation level. A) Ordovician Model B) Ordovician fence diagram C) Ordovician sandstone net-mass map, in megatons CO_2 per mi^2



MD	% of total Sandstone Storage resources	Site Specific Mt CO_2 P10	Site Specific Mt CO_2 P50	Site Specific Mt CO_2 P90	Formation Level Mt CO_2 P10	Formation Level Mt CO_2 P50	Formation Level Mt CO_2 P90
2,000-4,000	2%	391	574	1,259	157	228	506
4,000-6,000	11%	1,850	2,715	5,952	744	1,079	2,391
6,000-8,000	12%	1,874	2,750	6,028	753	1,093	2,421
8,000-10,000	10%	1,537	2,257	4,945	618	896	1,986
10,000-12,000	7%	1,181	1,733	3,796	474	688	1,524
12,000-14,000	7%	1,152	1,697	3,715	464	674	1,491
14,000-16,000	7%	1,260	1,850	4,047	506	734	1,624
16,000-18,000	8%	1,225	1,799	3,936	492	714	1,580
18,000-20,000	7%	1,146	1,682	3,678	460	667	1,476
20,000-36,575	28%	4,562	6,697	14,648	1,831	2,657	5,878

Figure 2.13. A) Ordovician true vertical depth Map. 2,000 ft contour interval (610 m). CO_2 storage resources for the Ordovician sandstones by 2,000 ft (610 m) depth intervals. For example, from 4,000 to 6,000 feet depth, the Ordovician sandstones can store between 744 - 2,391 Mt of CO_2 using formation level Esaline values, which is 11% of all the storage resources in the evaluated area, highlighted by the dark purple colored contour interval. B) CO_2 storage resources models using the P50 Esaline values at the formation level and TVD structure map. Red polygon highlights where the Ordovician sandstone CO_2 storage resources, net pore volume, and porosity are the highest, and at depths shallower than 10,000 ft (3,048 m).

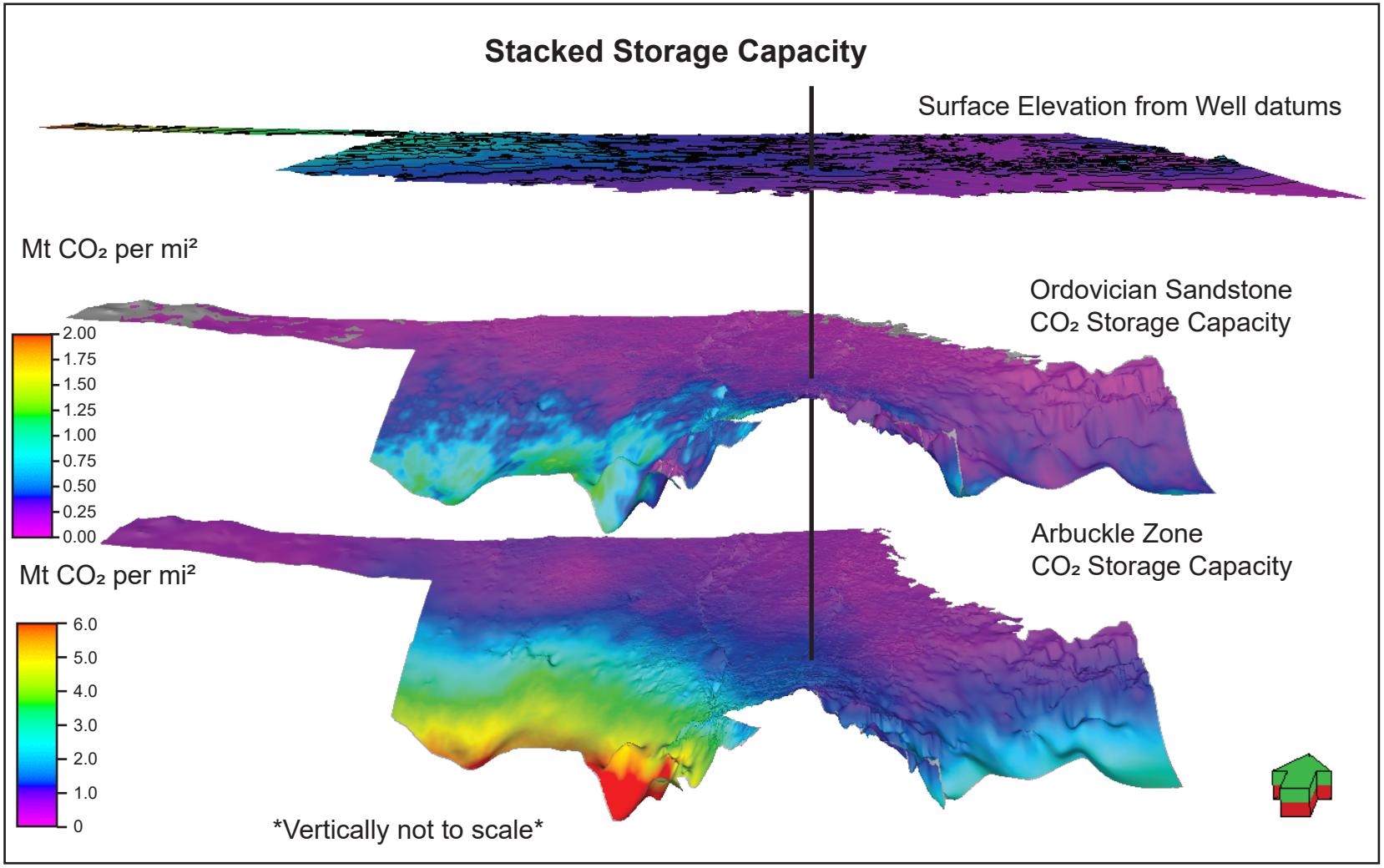


Figure 2.14. Stacked Storage Resources. The total P_{50} CO_2 storage capacity at the formation level for the Ordovician sandstone and Arbuckle zone, draped on their respective structural horizon. Note the color bar scale differences. The Ordovician sandstone is significantly thinner than the Arbuckle zone, where the entire zone is the reservoir. The ability to inject into both zones from a single wellbore increases storage resources at each site.

Tables

Symbol	Term	Range	Description
Terms used to define the entire basin/region pore volume			
A_n/A_t	Net to total Area	0.2 - 0.8	Fraction of total basin/Region are that has a suitable formation present
h_n/h_g	Net to Gross Thickness	0.25 - 0.75	Fraction of total geologic unit that meets minimum porosity and permeability requirements for injection
$\emptyset_{eff}/\emptyset_{tot}$	Effective to Total Porosity Ratio	0.6 - .95	Fraction of total porosity that is effective, i.e. interconnected
Terms used to define the pore volume immediately surrounding a single-well CO_2 injector			
E_A	Areal Displacement Efficiency	0.5 - 0.8	Fraction of immediate area surrounding an injection well that can be contacted by CO_2
E_I	Vertical Displacement Efficiency	0.6 - .9	Fraction of vertical cross section with the volume defined by the area (A) that can be contacted by the CO_2 plume from a single well
E_g	Gravity	0.2 - 0.6	Fraction of net thickness that is contacted by CO_2 as a consequence of the density difference between CO_2 and in-situ brine.
E_d	Microscopic Displacement Efficiency	0.5 - 0.8	Portion of the CO_2 contacted, brine-filled pore volume that can be replaced by CO_2

Table 2.1. Definition of terms used to calculate the Saline Storage Capacity Efficiency, Esaline. From IEA Greenhouse Gas R&D Programme 2009.

Esaline	Site Specific			Formation Level		
	P10	P50	P90	P10	P50	P90
Limestone	4.24%	6.13%	9.82%	1.41%	2.04%	3.27%
Clastics	4.62%	6.79%	14.96%	1.86%	2.70%	6.00%
Dolomite	6.57%	7.91%	14.92%	2.58%	3.26%	5.54%

Table 2.2. Esaline values at the Site Specific and Formation level. From IEA Greenhouse Gas R&D Programme 2009.

	SITE SPECIFIC Esaline Values		
	Ordovician - Mt		
	P10	P50	P90
Limestone	10,200	14,734	24,414
Sandstone	16,182	23,754	52,003
Dolomite	1,900	2,313	4,390
Shale	7,692	11,294	24,752
Total	35,973	52,095	105,560

Table 2.3. CO_2 Storage resources for the Ordovician calculated with Site Specific Esaline values, broken down by lithology.

	FORMATION LEVEL Esaline Values		
	Ordovician - Mt		
	P10	P50	P90
Limestone	3,461	5,000	8,337
Sandstone	6,501	9,430	20,877
Dolomite	746	949	1,636
Shale	3,092	4,486	9,942
Total	13,800	19,865	40,792

Table 2.4. CO_2 Storage resources for the Ordovician calculated with Formation Level Esaline values, broken down by lithology.

Acknowledgements

I would like to thank Enverus for the well information and well logs, and GVERSE Geographix and Schlumberger's Petrel for the software used in this study. I would also like to thank my doctoral committee members, M. Pranter, H. Bedle, B. Carpenter, and D. Devegowda.

References

Amsden, T. W., 1980, Hunton Group (late Ordovician Silurian, and early Devonian) in the Arkoma Basin of Oklahoma: Oklahoma Geological Survey Bulletin 129.

Cronenwett, C. E., 1958, A Subsurface Study of the Simpson Group in East-Central Oklahoma: Oklahoma City Geological Society Shale Shaker Digest II, v. VI–VIII.

Decker, C. A., 1941, Simpson Group of Arbuckle and Wichita Mountains of Oklahoma: American Association of Petroleum Geologists Bulletin, v. 25, no. 4, p. 650–667.

Decker, C. E., and C. A. Merritt, 1931, The Stratigraphy and Physical Characteristics of the Simpson Group: Oklahoma Geological Survey Bulletin 55.

Denison, R. E., 1997, Contrasting Sedimentation Inside and Outside the Southern Oklahoma Aulacogen Durin Middle and Late Ordovician: Oklahoma Geological Survey Circular 99, p. 39–47.

Doveton, J. H., 1994, Geologic log interpretation: Tulsa, OK, SEPM.

Enverus Database: <https://www.enverus.com/> (accessed August, 2021).

General Geologic Sections of Oklahoma, 1975: <https://oklahoma.gov/content/dam/ok/en/occ/images/og/geocolumn-occ.pdf> (accessed October, 2022).

Holloway, S., A. Holland, and R. Keller, 2016: Oklahoma Geological Survey-Oklahoma Fault Database: <https://www.ou.edu/ogs/data/fault> (accessed April 24, 2023).

Huffman, G. G., 1953, Sylvan Shale in Northeastern Oklahoma: Geologic Notes, v. 37, no. 2, p. 447–450.

IEA Greenhouse Gas R&D Programme (IEA GHG), “Development of Storage Coefficients for CO2 Storage in Deep Saline Formations”, October 2009

Miranda, M. W., J. D. Ogland-Hand, J. M. Bielicki, R. G. Moghanloo, J. DaneshFar, and R. S. Middleton, 2023, Developing a roadmap for carbon capture, and storage in Oklahoma by assessing the viability of stacked storage: Greenhouse Gases: Science and Technology, v. 13, no. 6, p. 763–779, doi:10.1002/ghg.2244.

Northcutt, R. A., and J. A. Campbell, 1995, Geologic Provinces of Oklahoma: Oklahoma Geological Survey Open File Report 5. http://ogs.ou.edu/docs/openfile/OF5-95.pdf, accessed March 2022

Puckette, J. O., 1996, Evaluation of under pressured reservoirs as potential repositories for liquid waste: Oklahoma State University unpublished Ph.D. thesis, 273 p

Ragland, D. A.; and Donovan, R.N., 1991, Sedimentology and Diagenesis of the Arbuckle Group in Outcrops of Southern Oklahoma: Oklahoma Geological Survey Special Publication 91-3.

Schlumberger Log Interpretation principles, 1989: Houston, TX, Schlumberger Educational Services.

Schramm, Jr, M., 1964, Paleogeologic and quantitative lithofacies analysis, Simpson Group, Oklahoma: AAPG Bulletin, v. 48, no. 7, p. 1164–1195.

SMU Node of National Geothermal Data System, Heat Flow and Well Data, n.d.: <http://geothermal.smu.edu> (accessed March, 2023).

Statler, A. T., 1965, Stratigraphy of the Simpson Group in Oklahoma: Tulsa Geological Society Digest, v. 33, p. 162–209.

Suhm, R., 1997, Simpson Stratigraphy of the Southern Midcontinent: Oklahoma Geological Survey Circular 99, p. 3–38.

Suhm, R. W., 2016, The Simpson Play (Including Parts of the Arbuckle and Viola) Stratigraphy and Petroleum Potential of the Simpson Group (Ordovician), Oklahoma: Oklahoma Geological Survey Open File Report 3-2016.

Taff, J.A., 1904, Preliminary report on the geology of the Arbuckle and Wichita Mountains in Indian Territory and Oklahoma, with an appendix on reported ore deposits of the Wichita Mountains by H.F. Bain: U.S. Geological Survey Professional Paper, 31, 97 p.

Ulrich, E.O., 1911, Revision of the Paleozoic systems: Geological Society of America Bulletin, v. 22, p. 281-680.

U.S. Department of Energy National Energy Technology Laboratory Office of Fossil Energy (NETL), 2007, Carbon sequestration atlas of the United States and Canada.

U.S. Department of Energy National Energy Technology Laboratory Office of Fossil Energy (NETL), 2008, Carbon sequestration atlas of the United States and Canada.

U.S. Geological Survey Geologic Carbon Dioxide Storage Resources Assessment Team, 2013, National assessment of geological carbon dioxide storage resources—Results (ver. 1.1, September 2013): U.S. Geological Survey Circular 1386, 41 p., <https://pubs.usgs.gov/circ/1386/>.

Chapter 4: The Statewide variability of mineralogy, pore volume and CO_2 storage resources for the Hunton Group, Oklahoma

Abstract

The Silurian-Devonian-aged Hunton Group in Oklahoma exists across much of Oklahoma and is at adequate depths for carbon capture, utilization, and storage (CCUS). It lies above the Sylvan Shale, which is the sealing reservoir for Ordovician reservoirs across Oklahoma. While there has been significant research on the Hunton Group for hydrocarbon potential, there have been no regional studies showing the distribution of lithologies, pore volume, and their CO_2 storage resources.

Using information from 80,800 wells and 500 wells with log ascii standard (LAS) format modern well logs, a detailed 3-D lithology model was generated for the Hunton Group across the state of Oklahoma. Because the Hunton Group has been well explored across the state for hydrocarbon potential, one well per township (6 mi x 6 mi) was used. Additionally, wells that did not have photoelectric logs available were predicted using machine learning methods to generate a more robust dataset. Total porosity was calculated from well logs, and the total porosity model was constrained to the lithology model. To determine CO_2 storage resources, the United States Department of Energy's (US-DOE) methodology was applied. The total CO_2 storage resources were determined using both site-specific and formation level saline storage efficiency coefficients (E_{saline}) and reported for the entire study area, by lithology and by measured depth.

Results include 1) The entire zone consists of reservoir rock, predominantly limestone and dolomite, with the dolomite having the best porosity at 7%. 2) Highlighted areas with historical hydrocarbon production from the zone across the state, both from vertical and

horizontal well development that has likely reduced reservoir pressures and could increase CO_2 storage resources, and 3) statewide pre-Pennsylvanian and post-Hunton subcrop maps.

Introduction

Above the Ordovician reservoirs in Oklahoma lies the Silurian-Devonian-aged Hunton Group. The Hunton Group is a series of shallow-water carbonates. It was deposited after the Ordovician-aged Sylvan Shale and is capped by the post-Hunton unconformity at the base of the Woodford Shale. It is a major oil and gas reservoir in the Anadarko basin that has been developed by both vertical and horizontal wells. It was named by J.A. Taff in 1902 after his work in the Atoka Quadrangle. Further stratigraphic and paleontological work was done by Amsden (1957) and Shannon (1962). The Hunton Group exists across much of Oklahoma, and at depth suitable for carbon capture, utilization, and storage (CCUS). It has a regional seal above the reservoir, the Woodford Shale, and below the reservoir, the Sylvan Shale. While extensive research has been done on the Hunton Group for hydrocarbon potential, there have been no studies on the CO_2 storage resources for the reservoir.

Due to its historical importance as a hydrocarbon-producing reservoir, there has been extensive research on the Hunton Group. In 1957, Amsden described and developed the stratigraphy and paleontology of the Hunton Group in the Arbuckle Mountain region. In 1962, Shannon expanded that framework to include the subsurface. In 1975, the Oklahoma Geological Survey (OGS) published Bulletin 121, Hunton Group (Late Ordovician, Silurian, and Early Devonian) in the Anadarko Basin of Oklahoma by Amsden, in which 125 cores were described and analyzed by thin section, chemical analyses, and porosity-permeability tests. Five years later, the OGS published Bulletin 129, Hunton Group (Late Ordovician Silurian and Early Devonian)

in the Arkoma by Amsden (1980), which detailed 90 well logs and 11 cores across the Arkoma Basin to give a sedimentary model for the Late Ordovician to Early Mississippian strata.

From 1982-1989, the Hunton Group was studied by employees and consultants of Masera Corporation as part of a commercial project. More than 10,000 wells were correlated and evaluated for reservoir potential. Many of the results were published in 1993 by the OGS as Special Publication 93-4, The Hunton Group workshop and Field Trip (Johnson, 1993). Topics covered in the publication included petroleum-reservoir characterization, deposition, diagenesis, facies, sequence stratigraphy, paleokarst, petroleum production, and interpretation of the Hunton Group geology based on petrologic, petrographic, and innovative subsurface studies. Subsequently, in 1994, Al-Shaieb et al published a study on formation pressures in the Anadarko basin, which determined that the Hunton Group was generally a normally pressured reservoir. Research continued through the 1990's which resulted in the 1996 OGS Circular 101, Platform Carbonates in the Southern Midcontinent (Johnson, 1996), which focused on limestones and dolomites deposited in shallow-marine platform (shelf) environments and 1999 OGS Circular 105, Silurian, Devonian and Mississippian Geology and Petroleum in the Southern Midcontinent (Johnson, 1999), which focused on the reservoirs, geologic events and petroleum rocks deposited during the Silurian, Devonian and Mississippian periods. Furthermore, in 2000, the OGS released Special Publication 2000-2, Hunton Play in Oklahoma (Rottman et al., 2000), which was prepared for a one-day workshop. The purpose of this publication was to further integrate and expand on the work done by Amsden in the Arkoma and eastern Anadarko basin, as the western Anadarko and deep Anadarko basin had not yet been included. It also further expanded on the Hunton-Woodford stratigraphic relationship. In conjunction with this Special publication, the OGS published Guidebook 33, Stratigraphy and Facies Relationships of the Hunton Group,

Northern Arbuckle Mountains and Lawrence Uplift (Stanley, 2001) to bridge the gap between subsurface well log correlations and surface outcrops. While these circulars, special publications, and bulletins were predominantly focused on hydrocarbon exploration, they contain important information about reservoir properties for the Hunton Group across Oklahoma.

Because a detailed statewide assessment of pore volume and CO_2 storage resources for the Hunton was lacking for the state of Oklahoma, this study utilizes data from more than 80,000 wells (Enverus, 2021) and other regional information for geological interpretation and to construct and analyze well-constrained 3-D geological models of the Hunton (Figure 3.1). The study incorporates detailed constraints on the stratigraphy and structure (e.g., depth, areal extent, thickness, mineralogy, porosity). The results include a detailed structural, lithology, total porosity, temperature, and pressure models of the Hunton Group and are the most detailed assessments, to date, of pore volume and CO_2 storage resources for Oklahoma.

Geologic Setting

Stratigraphy and Lithology

The Hunton Group was deposited in an epicontinental sea. It conformably overlies the Sylvan Shale. In contrast to the Ordovician, the Hunton was deposited during a time of low subsidence (Al-Shaieb et al., 1993). It is a series of shallow-water carbonates that are separated by disconformities. In ascending order, the Hunton Group includes the Keel Formation, Cochrane Formation, and the Clarita Formation. These three formations form the Chimney Hill Subgroup. The Chimney Hill Subgroup is unconformably overlain by the Henryhouse Formation, which is itself uncomformably overlain by the Haragan Formation, and then the Bois d'Arc Formation. Lastly, the Frisco Formation, which is a lithologically distinct package of

carbonate rocks, was deposited, ending the Hunton Group deposition (Amsden, 1957; Shannon, 1962).

The Keel formation is the oldest formation within the Hunton Group. It is an ooidic grainstone to packstone (Amsden, 1960). It represents a shoaling upward carbonate package. It is correlative with the Pettit Formation in the southern part of the Ozark uplift (Amsden, 1980). It is bounded by an unconformity in the Arbuckle Mountain region (Amsden, 1960; Manni, 1985). Post Keel deposition was the Cochrane Formation, which is described as a poorly sorted to well-sorted glauconitic grainstone (Stanley, 2001). Glauconite, while conspicuous, only makes up .5-2.0% of the total rock volume (Amsden, 1960). Chert is also present and occurs as bedded laminae or nodules. Some chert nodules exhibit a brecciated texture, which may be deposition or evidence for sub-aerial exposure (Amsden, 1960; Stanley, 2001). After the Cochrane Formation deposition, the Clarita Formation was deposited. It is characterized as an interval of well-laminated, dark gray or brown clay-shale that grades into a high argillaceous limestone, followed by fossiliferous mudstone to wackestone (Stanley, 2001). This shale at the bottom of the Clarita, i.e., the top of the Cochrane, is identifiable with gamma-ray logs in the subsurface.

The Henryhouse and Haragan formations are described as whole-fossil (to unfossiliferous) argillaceous mudstone to locally occurring wackestone (Amsden, 1960). Anhydrites are also present. Both the Henryhouse and Haragan formations were initially described and grouped together by Amsden (1957) as the Hunton marlstone, because there is little lithologic distinction between units. Further paleontological work confirmed distinct boundaries and periods of deposition. There is no way to distinguish the formations without comparing fossil fauna. Along with limestone, detrital quartz varying from 10-35% of the total rock volume can be found in this interval (Amsden, 1960). Marl is used to describe carbonate-

rich clay and silt in which the carbonate component accounts for less than 55-60% of the rock volume, which the Henryhouse-Haragan formations do not fall under. Because of this, the Henryhouse-Haragan formations are considered an argillaceous limestone (Stanley, 2001). The boundary between the Henryhouse and Haragan is not apparent on well logs in the subsurface.

Continuous deposition post-Haragan Formation led to the Bois d'Arc Formation. It is described as having basal, cherty mudstones and wackestones followed by an upper grainstone facies (Amsden, 1960). Although argillaceous at its base, it contains less detritus than the older Henryhouse-Haragan formations (Amsden 1957, 1960). Because of this, the gamma-ray response in the Bois d'Arc is slightly lower than the Haragan Formation, and the boundary can be determined in the subsurface. Chert in the Bois D'arc is described as a porous, brown, tripolitic chert or a dense, glassy, and bedded chert (Amsden 1957, 1960).

The last formation in the Hunton Group is the Frisco Formation, which was unconformably laid above the Bois d'Arc Formation. It consists of two distinct lithofacies, a mud-supported, crinoid-bryozoan floatstone to wackestone and a grain-supported, intermound, and capping bed facies formed by the reworking and washing of the mound facies by currents (Medlock, 1984; Fritz & Medlock, 1993).

Although the Hunton Group outcrop nomenclature has been used extensively with great accuracy, the subsurface use of names has been misapplied, and it has led to great confusion (Fritz & Medlock, 1993). While many of the formations found in the Hunton Group have slightly different well log responses, the multiple unconformities within the Group make large regional correlations difficult.

Post-Hunton Group deposition was marked by a regional transgressive sequence that led to one of the most prominent unconformities in the Midcontinent. As the seas transgressed and the Ozark Uplift took place, the older Simpson Group in northeastern Oklahoma was eroded. These reworked sandstones were then deposited as the Misener Sandstone directly on top of the Hunton Group (Lee, 1956; Amsden and Klapper, 1972; Kuykendall & Fritz,1993). The Misener Sandstone is a middle-to-late Devonian-aged sandstone, and its deposition is closely associated with the Hunton Group carbonates along the northern shelf of the Anadarko basin. The Misener Sandstone and Woodford Shale are parts of the same transgressive/regressive megacycle (Johnson et al., 1985; Mankin, 1987). In north central Oklahoma, the Misener Sandstone can be divided into an upper and lower unit. The upper unit is described as a fine-grained, poorly sorted sandstone containing abundant clay matrix, while the lower unit is predominantly sandstone with interbeds of shale and dolomitic zones (Kuykendall & Fritz,1993). The dolomitic zones contain shale laminae, chert nodules, and quartz grains. Because Misener Sandstone develops directly above the Hunton Group, develops porosity, and is a subsurface hydrocarbon reservoir that is trapped by the Woodford Shale, which is also the regional seal for the Hunton Group, it has been included in this study. After the Woodford Shale was deposited, the Mississippian Formation was deposited across the state.

The end of the Mississippian is marked by the pre-Pennsylvanian unconformity. The ancestral Anadarko basin was experiencing rifting until the end of the Mississippian, leading to extensional faults across Oklahoma. The later Pennsylvanian time is divided into 5 epochs and includes Morrowan (early), Atokan, Desmoinesian (middle), Missourian, and Virgilian (late), all of which had orogenic events associated with them. These orogenies reactivated and transformed the extensional faults into compressional thrust faults. It led to uplift along the Nemaha ridge and

Cherokee platform and created the massive, regional pre-Pennsylvanian unconformity. The unconformity extends west of the Nemaha and along the Anadarko shelf but disappears in the Anadarko Basin, where deposition of the Pennsylvanian sands was taking place.

Dolomite

While the Hunton Group is predominantly limestone, it also contains a significant amount of dolomite. The Henryhouse Formation is mostly dolomitized. Three different types of dolomite are present: hypersaline dolomite, mixed-water dolomite, and deep burial dolomite (Al-Shaieb et al., 1993). The Henryhouse Formation was deposited during supratidal conditions where anhydrite was precipitated, indicating evaporation was sufficient to generate hypersaline brines. It also indicates that dolomitizing brines moved downward and seaward from the supratidal zone dolomite (Al-Shaieb et al., 1993). Furthermore, the Henryhouse Formation's regressive, progradational deposition eventually led to exposure to brackish to meteoric water. These shoreline waters could have been saturated with respect to dolomite. Mixed-water mechanisms of dolomitization are supported by the clear overgrowth and their near-uniform distribution (Al-Shaieb et al., 1993). The final state of dolomitization in the Henryhouse Formation is the deep burial dolomite, which is described as white, cloudy, void-filling saddle dolomite. These crystals predominantly fill secondary vugs and fractures but rarely fill molds of fossil dolomite (Al-Shaieb et al., 1993).

Dolomite development in the Hunton also coincides with the thinning of Woodford Shale. Howery (1993) determined there was a Hunton dolomite porosity fairway across western Oklahoma into the Texas side of the Anadarko basin that also coincided with the regional thinning of the Woodford Shale.

Porosity

The four types of porosity found in the Hunton Group are moldic, vuggy, intercrystalline, and fracture. The two fabric-selective, moldic and intercrystalline, are responsible for most high-porosity zones. The moldic porosity is caused by the dissolution of fossil grains. Molds may also be filled by late baroque dolomite or calcite. Intercrystalline porosity developed in response to dissolution of non-dolomitized, cryptocrystalline calcite matrix (Al-Shaieb et al., 1993). The highest porosities found in the Hunton are the most dolomitized reservoir rocks. Porosity in oolitic grainstones is predominantly interooid and poorly developed because of early sedimentation by sparry calcite.

The most important nonfabric selective porosity is dissolution porosity. Shaieb reported solution-enlarged vugular porosity where the original fossil outline has been completely destroyed. Some of the largest vugs were created by the dissolution of incompletely replaced anhydrite nodules (Al-Shaieb et al., 1993). Solution enlarged fractures, joints, and channels play a significant role in karst-related porosity in the Hunton Group.

Methods

Subsurface Mapping

The stratigraphy of the Hunton Group and the rest of the lower Paleozoic reservoirs including the Mississippian (less Chesterian strata), Woodford Shale, Hunton Group, Sylvan Shale, Viola Limestone, Arbuckle Group and crystalline basement was developed by interpreting conventional well logs (e.g., gamma-ray, apparent porosity, bulk density, resistivity) and classified lithology logs (i.e. mudlogs or sample logs). Formation tops were interpreted by the author through means of dip- and strike-oriented cross sections. After the wells were correlated

across the state, if log ascii standard (LAS) formats were available, they were downloaded and imported. Additional rasters for wells with modern well logs, including Gamma Ray (GR), Bulk Density (RHOB), Neutron Porosity (PHIN), and Photoelectric Factor (PEF), were then digitized by hand to ensure coverage across the state.

Well-derived formation tops resulted in 80,800 tops for the Mississippian (less Chesterian strata), 62,000 tops for the Woodford Shale, 41,200 tops for the Hunton Group, 34,300 tops for the Sylvan Shale, 40,800 tops for the Viola Limestone (Ordovician), 6,050 tops for the Arbuckle Group and 257 tops for the crystalline basement (Figure 3.2). Due to the significant well control, the Mississippian structure map was used as the initial reference surface to constrain the structure maps of deeper formations. A structure map was generated from well tops using a 2,500 ft x 2,500 ft (762 m x 762 m) grid and convergent gridding. Isopach maps were generated for the interval from the Mississippian to the Woodford (MSSP zone), Woodford to the Hunton (WDFD zone), Hunton to Sylvan (Hunton zone), Sylvan to Viola (SLVN zone), Viola to Arbuckle (Ordovician zone) and Arbuckle to crystalline Basement (Arbuckle zone). The isopach map for the MSSP zone was subtracted from the Mississippian structure map to create the Woodford structure map. The isopach map for the WDFD zone was subtracted from the Woodford structure map to generate the Hunton zone structure map, and so forth until the structure for the crystalline basement was generated. 500 wells with LAS were used in the study. 156 of those wells did not have PEF logs available. Additionally, 16 of the 500 wells with LAS also had mud logs or sample reports with lithology descriptions (Figure 3.1). The dataset attempted to digitize one modern well log per township where available.

Machine Learning to generate Photoelectric (PEF) logs

Of the 500 wells with LAS, 156 wells did not have PEF logs run in the wellbore, which is required to determine lithology. To create a more robust dataset, PEF curves for the 156 wells were predicted using supervised machine learning methods, including K-Nearest Neighbor (K-NN) and Random Forest regression. 31 wells from across the state were used to train the model to predict PEF from GR, PHIN, and RHOB for the Hunton zone. Using both test-train and cross-fold validation in conjunction with hyperparameter optimization, PEF curves were predicted and then added to the dataset to generate lithology logs for the additional 156 wells.

Derived Petrophysical Logs

The conventional modern well logs and other parameters in GVERSE Geographix were used to calculate derived logs for total porosity (PHIT), density porosity (PHID), shale volume (V_{sh}), apparent matrix grain density (RHO_{maa}), apparent matrix volumetric cross-section (U_{maa}), and percent mineralogy/lithology.

Mineralogy logs were generated using the RHO_{maa} - U_{maa} mineralogy cross-plot methodology with a 4-mineral (calcite, dolomite, quartz, and shale) model. To evaluate mixed lithologies and to semi-quantitatively estimate mineral volumetric proportions, a cross plot of the apparent matrix grain density, RHO_{maa}, versus apparent matrix volumetric cross-section, U_{maa}, is generated (Doveton, 1994).

Because the Hunton zone is predominantly limestone, PHID was calculated using a limestone matrix density (ρ_m) of 2.71 g/cm^3 with saltwater (ρ_f = 1.02 g/cm^3):

$$PHID = \frac{\rho_m - \mathrm{RHOB}_B}{\rho_m - \rho_f} \qquad \text{Eq (1)}$$

To compute the apparent matrix properties, the apparent porosity (i.e., total porosity), PHIT, was calculated as follows:

$$PHIT = \frac{PHID+PHIN}{2} \quad \text{Eq (2)}$$

Shale Volume (V_{sh}) was determined from GR with GR_{cl} = 20 API and GR_{sh} = 100 API for clean (non-shaley) and shale endmembers, respectively.

$$V_{sh} = \frac{GR-GR_{cl}}{GR_{sh}-GR_{cl}} \quad \text{Eq (3)}$$

The apparent matrix grain density is computed as:

$$RHO_{maa} = \frac{RHOB-PHIT*RHO_{fl}}{1-PHIT} \quad \text{Eq (4)}$$

Where RHO_{fl} is the flushed zone pore water density (RHO_{fl} = 1.0 g cm^{-3}). The apparent matrix volumetric cross-section, U_{maa}, is computed from the photoelectric factor log and bulk density log as:

$$U_{maa} = \frac{PEF * \rho_e - PHIT * U_f}{1-PHIT} \quad \text{Eq (5)}$$

Where ρ_e is the electron density and U_f is the volumetric photoelectric absorption or volumetric cross section of the flushed zone pore space (U_f = 0.398 barnes cm^{-3}). The photoelectric index, ρ_e, must be converted to a volumetric measure by multiplying the electron density, which is defined as:

$$\rho_e = \frac{\rho_B+0.1883}{1.0704} \quad \text{Eq (6)}$$

RHO_{maa} and U_{maa} are cross-plotted on an imposed ternary diagram with trend lines for quartz, calcite, and dolomite. Shale percentage was calculated from GR and the calcite, quartz, and dolomite percentages from cross plot analysis. Calcite in the Hunton zone is described and interpreted as limestone, while dolomite is interpreted as dolostone. Because the Hunton zone contains the Misener Sandstone along with chert within the Hunton Group, quartz is interpreted as both sandstone and silica, depending on where it is found stratigraphically.

Because the volume of shale was calculated from GR, it is indicative of clay mineralogy in the Hunton zone. To generate lithology logs from the mineralogy logs, it was assumed that the dominant mineralogy at each depth corresponds to limestone (for calcite), dolostone (for dolomite), sandstone-silica (for quartz), and shale (clay content). The 16 wells with mud logs or sample logs were used to calibrate petrophysical cutoffs for lithology determination.

3-D Modeling and CO_2 Storage Resources Estimation

Three-dimensional geological models of key properties were constructed to ultimately calculate pore volume and CO_2 storage resources for the Hunton zone. Using the 3-D models to determine the CO_2 storage resources, the U.S. Department of Energy methodology (NETL, 2007 & 2008; IEA GHG, 2009) was used as follows:

$$G_{CO2} = A * h * \varphi * \rho_{CO2} * E_{saline} \qquad \text{Eq (7)}$$

G_{CO2} is the mass of CO_2 stored in the reservoir, A is the area of reservoir, h is the thickness of reservoir, φ is the total porosity, ρ_{CO2} is the density of CO_2 (dependent on temperature and pressure; dependent on depth), and E_{saline} is the saline storage efficiency coefficient (dependent on lithology).

The 3-D stratigraphic and structural framework (3-D model grid) of the Hunton zone was generated using the structure maps that define the reservoir zones. The 3-D grid covers an area of approximately 28,662 mi^2 with aerial cell dimensions of 2,500 ft x 2,500 ft (762 m x 762 m) with an approximate cell/layer thickness of 3.4 ft (1.0 m). The Hunton zone was divided stratigraphically into 100 proportional layers with resulting 3-D model grid having 9,318,792 cells.

To represent the spatial variability of lithologies for the Hunton, a 3-D lithology model was constructed with commercial software using sequential-indicator simulation (SIS). The model constraints include: 1) the stratigraphic and structural framework (3-D grid), 2) upscaled lithology logs, 3) variogram parameters by zone, 4) lithology percentages by zone, and 5) vertical lithology proportion curves. Lithology logs were upscaled to the 3-D model grid by assigning a single lithology class to a cell based on the most abundant lithology within a cell. The target fractions of each lithology were obtained from the upscaled lithology logs.

A 3-D porosity model was generated to evaluate the distribution of total porosity (PHIT) within the study area. PHIT logs were biased to the lithology logs and upscaled using an arithmetic mean. The porosity model was generated using sequential-Gaussian simulation (SGS) and was constrained to: 1) a 3-D lithology model, 2) upscaled PHIT logs (biased to lithology), 3) porosity histograms by zone and lithology, and 4) variogram parameters by zone and lithology.

The density of CO_2 in the reservoir is dependent on the temperature and pressure of the reservoir. Bottom hole temperature and total depth from the wellbore data across Oklahoma are available from the Southern Methodist University Geothermal Lab, which is a part of the National Geothermal Data System funded by the U.S. DOE (SMU Node of National Geothermal Data System, Heat Flow and Well Data, accessed March 2023). A temperature gradient map was

generated for the state, assuming a 60° F surface temperature to bottom hole temperature. Using the temperature gradient map and measured depths from the 3-D grid, a 3-D temperature model was calculated for Oklahoma. Pressure data acquired from oil and gas operators across Oklahoma indicate that the Hunton Group is normally pressured (Al-Shaieb et al., 1994). Using a pressure gradient of 0.44 psi/ft (9,953 Pa/m), a 3-D reservoir pressure model was generated using the measured depths from the 3-D grid. Lastly, using the ideal gas law, the temperature model and pressure model were used to calculate the 3-D CO_2 density model as follows:

$$\rho = \frac{p*M}{R*T} \qquad \text{Eq (8)}$$

Where ρ is the density (g/m^3) of CO_2 at temperature and pressure, p is the pressure (pascal; Pa), M is the molar mass of CO_2 = 44.01 g/mol, R is Avogadro's constant and equal to 8.31 (joule/mol*kelvin; J/mol*K) and T is temperature (kelvin; K).

Saline storage efficiency coefficient (E_{saline}) is the percentage of pore space that the CO_2 will occupy in the reservoir and is dependent on lithology. The 2009 International Energy Agency Greenhouse Gas Development of Storage Coefficients for CO_2 storage in deep saline reservoirs (IEA GHG, 2009) states that E_{saline} is a function of the lithology and depositional environment and is calculated as (see Table 3.1 for a description of the equation terms):

$$E_{Saline} = \frac{A_n}{A_t} * \frac{h_n}{h_g} * \frac{\emptyset_{eff}}{\emptyset_{tot}} * (E_A * E_I * E_g * E_d) \qquad \text{Eq (9)}$$

The last 4 terms define the pore volume immediately surrounding a single well CO_2 injector. E_A is the areal displacement efficiency, E_I is the vertical displacement efficiency, E_g is gravity, and Ed is the microscopic displacement efficiency. To calculate storage efficiencies, heterogeneous 3-D models were developed for various lithologies, depositional environments, and structures. Statistical distributions from a global database of hydrocarbon reservoir properties were used,

including key parameters like porosity and permeability (IEA GHG, 2009). The ranges of storage coefficients for each lithology were derived based on 195 simulations. If the assessment of storage resource is over a small, localized area, then it is likely that the values of the A_n/A_t and h_n/h_g will be relatively high. Therefore when determining E_{saline} at the site-specific level A_n/A_t was fixed at .8 while h_n/h_g and $\emptyset_{eff}/\emptyset_{tot}$ ranges between .25-.75 and .6-.95 respectively (Table 3.1). Regionally, the geologic properties will vary spatially; For this reason, the P_{50} of the A_n/A_t and h_n/h_g terms were fixed to determine the formation level E_{saline} values. This leads to an overall lower storage coefficient for each lithology at the formation level. E_{saline} values are reported for the P_{10}, $P_{50,}$ and P_{90} for clastics, dolomites, and limestones at the site-specific and formation level evaluations. P_{10} notation indicates that there is a 10% probability that the value is less than the P_{10} value, and the P_{90} notation indicates there is a 90% probability that the value is less than the P_{90} value. The total CO_2 storage resources for the model were calculated for both the site-specific and formation level E_{saline} values. Table 3.2 shows the E_{saline} values for each lithology. Because E_{saline} values were reported by lithology, they were also applied to the corresponding lithologies in the model, with the values for clastics being applied to both the sandstone-silica and shale lithologies.

Results

Machine Learning

To predict PEF logs for the 156 wells, 31 wells out of the 344 available were chosen. Careful effort was taken to identify 1 well per county that had good well log quality (i.e., minimal wellbore wash out through the Hunton zone, washouts, and bad hole data removed) across Oklahoma were chosen to train and predict (Figure 3.1). The top of the Hunton zone on

well logs is identified by the drastic decrease in GR immediately below the Woodford Shale (Figures 3.3 and 3.4). For the Hunton zone GR is typically low and below 40 API, PEF ranged between 4.0-6.0 barnes, PHIN was consistently low and less than 10% and RHOB ranged between 2.6-2.8 g/cc (Figures 3.3, 3.4 and 3.5) Both type logs (Figure 3.3 and 3.4) show the GR in the first column, a measured depth track followed by the RHOB, PHIN and PEF in the next column. GR, RHOB, and PHIN were used to train the model to predict PEF curves for the missing wells.

When looking at the individual well's input distribution, there are 2 wells that appear as outliers, 3503224760000 and 35081239270000 (Figure 3.6). These wells have a significant amount of Misener Sandstone present (included in the Hunton zone) when compared to the other wells used in the dataset. While these wells appear as outliers, they are accurate readings.

Using the K-NN algorithm for k = 1-30, nearest neighbors elbow plots indicate that k = 10 gives the lowest root mean square error (RMSE) and the highest coefficient of determination (R2). Using k=10 and a test-train split of 15:85, the training data sets R2=.517 while the test data sets R2=.409 (Figure 3.7C). Furthermore, applying k = 1-30 nearest neighbors and using a 5-fold cross validation for hyperparameter optimization determined that k = 30 would be the best fit for the data, which is similar to what Figures 3.7A and 3.7B show. Figures 3.7A and 3.7B show that the 'elbow' is roughly at k = 10, but k = 30 is still the lowest RMSE. K = 10 was determined to be the best choice.

Random Forest Regression was also used on the dataset to predict PEF. Hyperparameter optimization was run for 25, 50, and 100 estimators, a maximum depth of 5, 10, 15, and the minimum samples per leaf of 3 and 4 (Figure 3.7D). The Random Forest Regression model, with a cross-fold validation of 5 using 100 estimators, a max depth of 5 with a minimum number of 3

data points allowed per leaf node, was chosen as optimal (Figure 3.7D). Cross-validation score was low, at .18, with R2 of the test data set at .405. Error results were similar for both methods. K-NN was chosen to predict PEF logs for the 156 wells.

Structure, Thickness, and Lithology Trends

The lower Paleozoic strata across Oklahoma in general thin toward the Ozark Uplift in northeastern Oklahoma and thicken toward the Anadarko and Arkoma basins (Figure 3.8). The Mississippian is present across nearly all of Oklahoma, except central Oklahoma (Figure 3.8). In central Oklahoma, the Mississippian, Woodford, Hunton, Sylvan, and Ordovician reservoirs have been completely removed, and the Arbuckle Group sits directly below the Pennsylvanian shale. In Oklahoma County, the Hunton zone can be seen directly at the top of the pre-Pennsylvanian unconformity (Figure 3.8A, orange zone in Oklahoma County). In this region, the Hunton zone is sealed by the Pennsylvanian shales (instead of the Woodford Shale) and is associated with hydrocarbon production.

The Hunton Group ranges in thickness from 0-1,200 ft (0- 366m) thick (Figure 3.9A). Faults are apparent where the dip magnitude is high (dark grey to black) and a change in dip azimuth align, and present across the state (Figures 3.9B and 3.9C). Across northeastern Oklahoma, the Hunton pinches out as a result of the erosion, which creates a convenient up-dip trap for hydrocarbons across much of the state (Figure 3.10). Across Oklahoma, the Hunton thickness is related to both the post-Hunton unconformity and pre-Pennsylvanian unconformity, which saw uplift and erosion along major faults like the Nemaha fault system. For example, the Oklahoma City oilfield has no Hunton present (Figures 3.8, 3.9, and 3.10).

The Hunton Group is predominantly limestone with lesser amounts of dolomite, chert, and shale (Figure 3.11). The RHO_{maa} - U_{maa} mineralogy cross-plot for the Hunton Group shows it is predominantly calcite and dolostone, with very low V_{sh} and quartz. Type logs for the Hunton zone (Figures 3.3 and 3.4) illustrate mineral percentage curves generated using the 4-mineral (limestone, dolomite, sandstone-silica, and shale) model in the third track. The last track shows the dominant lithology at each depth, which was used in the lithology modeling. Mud log descriptions in the last column were used to confirm the lithology.

The Hunton lithology model is predominantly limestone (89%) with lesser amounts of dolomite (8%), silica-sandstone (2%), and shale (1%) (Figures 3.12 and 3.13). Northwestern Oklahoma in Major, Woodward, and Dewey counties is where the dolomite is the thickest (Figure 3.13C, blue arrow). This also coincides with the thinning of the Woodford Shale (Figure 3.8B) as described by Howery (1993). There is also an increase in dolomite west of the Nemaha in Lincoln, Okfuskee, and Seminole counties (Figure 3.13C, red arrow), which also coincides with the horizontal Hunton completions (Figure 3.10, green arrows). While sandstones do not develop in the Hunton Group, the Misener Sandstone does develop at the top of the Hunton zone. The Misener Sandstone and the Hunton Group are one reservoir in the subsurface according to the Oklahoma Corporation Commission (OCC) because there is no sealing reservoir between formations, the horizontal wells east of the Nemaha (Figure 3.10, green arrows) are considered to be completed in both the Misener Sandstone and the Hunton Group. The Misener Sandstone can be seen across north-central Oklahoma (Figure 3.12A and 3.12B, orange arrows). The other form of silica found in the model is chert (Figure 3.3). Chert development can be seen in northwestern Oklahoma (Figures 3.12B and 3.13B, green arrows). This chert development is deeper in the Hunton zone and stretches across Major, Woodward, Dewey, and Blaine counties, similarly to

the dolomite development area. Shale in the model is less than 1% and is typically found at the top of the Hunton zone, at the contact with the Woodford Shale and/or Misener Sandstone. It is considered insignificant in this study.

Petrophysical Properties

The Hunton zone's average well log total porosity (PHIT) is 3% but ranged between 0-14%. The average limestone porosity is 2%, the average sandstone-silica porosity is 5.5%, and the average dolomite porosity is 7% (Figure 3.14). While this study did not have cores, many studies across Oklahoma have reported porosity values for the Hunton Group. Al-Shaieb et al (1993) described 5 cores across the Anadarko basin and reported measured porosity values from 7-17%, 0-5%, 5-15%, 0-5%, and 0-15%, giving a good indication that well log porosity readings are reasonable. Vugs are commonly found in dolomitic zones and can be filled with calcite. The highest porosity is the dolomite, followed by Misener Sandstones and silica-rich chert zones (Figure 3.14). As expected, the average porosity for the entire Hunton zone is increased in areas with large percentages of dolomite, silica-sandstone, and along the unconformity.

The average porosity for the limestone in the Hunton is generally less than 2% except in Lincoln, Okfuskee, and Seminole counties (Figure 3.14B, black arrows), where it appears to have increased porosity in the 10% range. This area also has an increase in dolomite thickness (Figure 3.13C, red arrows) and an increased average dolomite porosity above 15% (Figure 3.14D, red arrow). In this area, the Hunton Group is primarily the lower Chimney Hill Formation, which has had significant alteration from the post-Hunton unconformity.

Porosity is also well developed in areas with Misener Sandstone present (Figure 3.13B and 3.14C, orange arrow). Average porosity for the Misener Sandstone can be upwards of 18%.

The chert-rich silica areas in northwestern Oklahoma also have increased porosity around 6-7%, but are generally less than the Misener Sandstone (Figures 3.13B and 3.14C, green arrow).

Based on the 3-D+ models of temperature and pressure, temperature for the Hunton ranges from 100-470°F (24-243°C) (Figure 3.15A). Pressure ranges from 800-13,000 psi (5.5-90 MPa) with an average of 5,200 (36 MPa) (Figure 3.15B). The temperature and pressure 3-D models were used to calculate the CO_2 density model (Figure 3.15C). CO_2 density ranges from 200-1,000 kg/m^3 with an average of 425 kg/m^3.

CO_2 Storage Resources

The CO_2 storage resources for the Hunton zone using the site-specific and formation level E_{saline} values range from 3,876-9,065 Mt (Table 3.3) and 1,331-3,094 Mt (Table 3.4), respectively (Figure 3.16). The CO_2 storage resources at the formation level are reduced by 33% for limestone, 40% for sandstone, and 37-41% for dolomite, and are directly related to the reduction in E_{saline} values. Increased CO_2 storage resources for the Hunton zone can be seen where the high porosity dolomite develops and as depth and thickness increase in the Anadarko Basin (Figure 3.17). Note: All figures for CO_2 storage resources were generated using the P_{50} E_{saline} storage efficiency factors at the formation level, giving a conservative estimate of CO_2 storage resources.

Because the Hunton zone ranges from 2,000-31,000 ft (610-9,756 m) deep across the study area and the goal of CCUS is to store the most CO_2 for the least cost, and the cost to drill a well increases with depth, the CO_2 storage resources were summed across 2,000 ft (610 m) depth intervals (Figure 3.18). For example, the Hunton zone from 4,000-6,000 ft (1,200-1,800 m) has CO_2 storage resources between 125-299 Mt at the site-specific level and 44-105 Mt at the

formation level. That equates to 3% of the total storage resources for the Hunton zone (Figure 3.18). Approximately 18% of the Hunton zone storage resources are accessible at depths from 2,000-10,000 ft (600-3,000 m) across Oklahoma.

Discussion

CO_2 Storage Resources Calculations

While this study assumes a normally pressured reservoir, the Hunton zone has been produced by both vertical and horizontal well development across much of the state (Figure 3.10). There are 3 areas west of the Nemaha with horizontal well development (Figure 3.10, blue arrows) and 2 areas east of the Nemaha (green arrows). The West Edmond field, just to the northeast, was discovered in 1942, which was the biggest discovery since the 1928 discovery of the Oklahoma City field. By 1945, the field reached peak production of 87,500 bbls/day. It was subsequently water-flooded. In the early 2000's horizontal wells were added across the structure to further increase field production (Miller, 2017). All 5 of these areas are likely to have reduced reservoir pressures.

The US-DOE methodology says the first three terms used to determine E_{saline} are the Net-to-Total Area, Net-to-Gross Thickness, and Effective-to-Total Porosity ratio (Table 3.1). The site-specific E_{saline} values, which are the highest used in this study, were determined by fixing the Net-to-Total Area to .8, the Net-to-Gross Thickness ranged between .25-.75, and the Effect-to-Total Porosity ranged between .6-.95 (Table 3.1, third column). All 3 of these factors are equal to 1 in this study. This means the most optimistic CO_2 storage resources reported in this study (i.e., the site-specific level) are still likely to be an underestimation of total CO_2 storage resources.

Areas of Interest

The northwestern dolomite trend has upwards of 300,000-400,000 tons of CO_2 per square mile, whereas the surrounding areas average 100,000 tons per square mile (Figure 3.17B and 3.17C, blue arrows). While the dolomite thickness isopach and Misener Sandstone also show increased porosity east of the Nemaha in the Lincoln, Okfuskee, and Seminole counties, the entire Hunton zone is significantly thinner (Figure 3.8A) than in the Anadarko basin. Because of these reasons, storage resources are fairly low at around 50 thousand metric tons of CO_2 per square mile in that region (Figure 3.17C). As expected, CO_2 storage resources also increase with depth, specifically in the deep Anadarko basin, where it reaches 1,000,000 tons of CO_2 per square mile.

Identifying the best places for CCUS development in the Hunton zone across Oklahoma is controlled by multiple factors. Where the Hunton zone is the shallowest, it has been extensively developed by hydrocarbon wells because of stratigraphic trapping (Figure 3.10). Anywhere hydrocarbons have been extensively produced would likely have reduced reservoir pressure that could aid in storage resources. Along much of the Hunton subcrop, the Hunton zone shows increased average porosity, which is also helpful (Figure 3.14A, blue double-headed arrow). Storing CO_2 along the subcrop is also ideal because it is a known subsurface trap.

Across Oklahoma, except for the deep Anadarko basin and Major County, the CO_2 storage resources are approximately 50,000 tons of CO_2 per square mile for the Hunton zone (Figure 3.17C). Major County has significant dolomite development, which led to a localized increase in CO_2 storage resources between 300,000-400,000 tons of CO_2 per square mile (Figure

3.17C, blue arrow). This area is less than 10,000 ft (3,048 m) deep and would make an ideal target for CCUS.

Lastly, while the Hunton zone is significantly thinner east of the Nemaha, it shows increased dolomite development, Misener Sandstone development, and porosity (Figure 3.10, green arrows). Thanks to hydrocarbon production, it likely has reduced reservoir pressure, which would increase CO_2 storage resources. This region is also shallower than Major County, between 4,000-6,000 ft (1,291-1,829 m) deep, which should decrease field development costs. Below the Hunton zone, the Simpson Group sandstones and Arbuckle Group are also present and suitable reservoirs for CCUS, allowing this region to store CO_2 in all three reservoirs.

Lower Paleozoic CO_2 Storage Resources Comparison

When comparing the Hunton zone to the Ordovician zone sandstones and the Arbuckle zone, the Hunton has the lowest storage resources (Table 3.5 and Figure 3.19). The Ordovician sandstones have the second highest storage resources, with the Arbuckle zone being the largest. The Arbuckle zone can store roughly 5 times more CO_2 than the Hunton zone and Ordovician sandstones combined. The lowest CO_2 storage resources by depth are between 2,000-4,000 ft (Figure 3.19). From 6,000-10,000 ft deep, there is an increase in the CO_2 storage resources, followed by a decrease at deeper depths. The spatial distribution of the total CO_2 storage resources for the lower Paleozoic reservoirs across Oklahoma at depths between 2,000 and 10,000 ft indicates central Oklahoma has the highest storage resources per square mile (Figure 3.19A).

Because the Arbuckle zone has the highest CO_2 storage resources, the main target zone for CCUS should be the Arbuckle zone, followed by the Ordovician zone, and then the Hunton

zone. The ideal areas for the Arbuckle zone (Figure 3.19B, thick white polygons) are further north in Oklahoma than the areas for the Ordovician zone (Figure 3.19B, thin white polygon). This is where the Arbuckle is the shallowest and has increased porosity. Unfortunately, in those areas, the Ordovician reservoirs are thin, and in Kay and Osage counties, they are not present. To have both reservoirs present, the ideal location would be central Oklahoma in Logan, Lincoln, and Okfuskee counties. Additionally, in central Oklahoma, the Hunton zone is present and is a potential third reservoir for CCUS(Figure 3.19B, red polygon). The Hunton zone in this region has also been heavily produced by hydrocarbons, indicating there could be reduced reservoir pressure, which could lead to higher CO_2 storage resources. Central Oklahoma is the ideal location for stacked, CCUS projects to be developed.

Conclusions

Across most of Oklahoma, the Hunton zone is present and at depths adequate for CCUS. It is predominantly limestone with lesser amounts of dolomite and chert with a negligible amount of shale. The Misener Sandstone is present at the top of the zone across central Oklahoma and the Anadarko shelf. On average, the zone has 3% porosity, but the dolomite, chert, and sandstones have increased porosity. Increased porosity can also be found along the stratigraphic pinch-out of the zone due to erosion. The subcrop region is also a known stratigraphic trap in the subsurface. Areas with a high volume of dolomite present have increased CO_2 storage resources, i.e., Major County. Major County shows the highest storage resources at depths shallower than 10,000 ft (3,048 m) and is the most ideal location for CCUS in the Hunton zone.

Any region where there has been significant hydrocarbon production is likely to have reduced reservoir pressure and increased CO_2 storage resources. East of the Nemaha is the

second-best region for CCUS development in the Hunton zone. It has less storage capacity per square mile when compared to Major County, but sits at shallower depths with shallower dips, it has high porosity dolomite and Misener Sandstone development, and has significant hydrocarbon development. The Hunton zone has significantly less CO_2 storage resources than the Ordovician and Arbuckle zones, but it is still a potential reservoir for CCUS.

When looking at the lower Paleozoic reservoirs as a composite, central Oklahoma shows the highest storage resources at depths shallower than 10,000 ft (3,048 m). In central Oklahoma, the Hunton zone, Ordovician sandstones, and the Arbuckle zone are present and have the Simpson-age Oil Creek Formation shales, Sylvan Shale, Woodford Shale, and Pennsylvanian shales that act as seals, respectively.

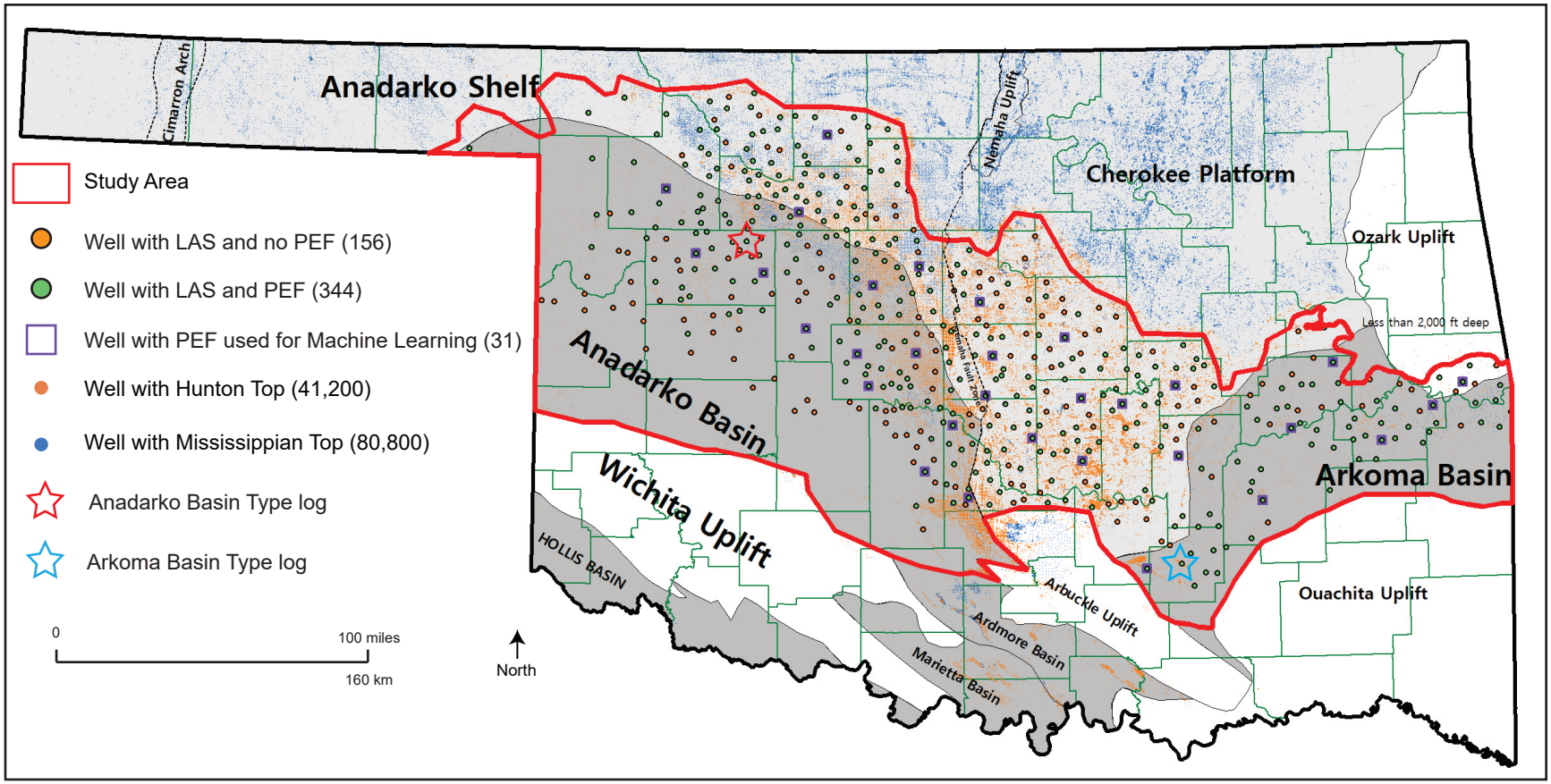


Figure 3.1. Study area and wells with LAS used in the study. Small orange dots are wells with Hunton tops, and the small blue dots are wells with Mississippian tops. Large orange circles are well with LAS and no PEF logs, and the large green circles are wells with LAS and PEF logs. Wells with purple squares were used to train and predict PEF logs for the wells without. Anadarko and Arkoma basin type log locations shown. Geologic Provinces were modified from Northcutt and Campbell, 1995.

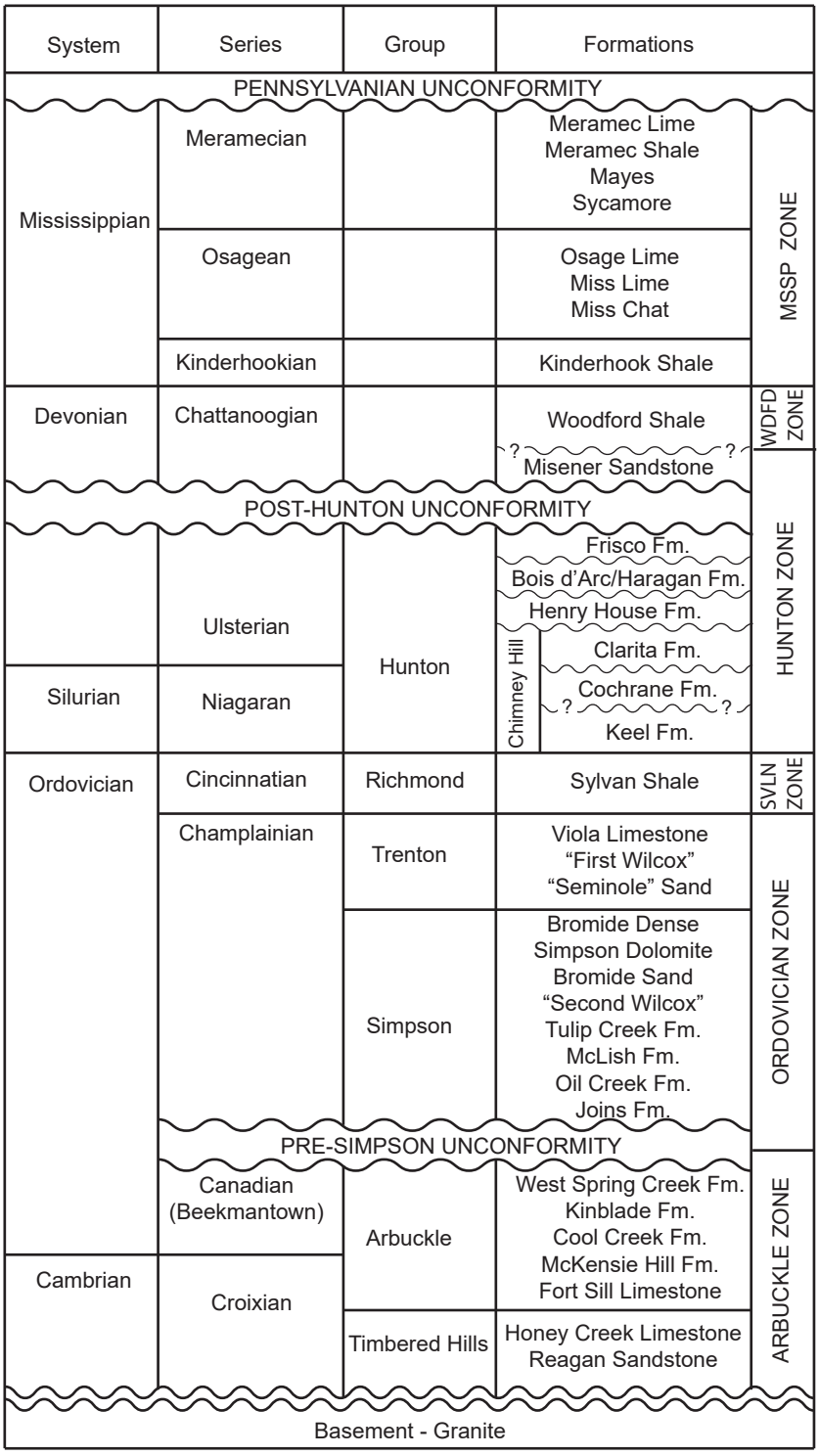


Figure 3.2. Generalized Stratigraphic Column of Oklahoma. Modified from Oklahoma Corporation Commission's General Geologic Sections of Oklahoma and Arkansas, 1975. The top of the Mississippian used for structural modeling is Meramecian in age, and marks the beginning of this stratigraphic column. Correlated formation tops and isopach zones used for structural modeling are labeled.

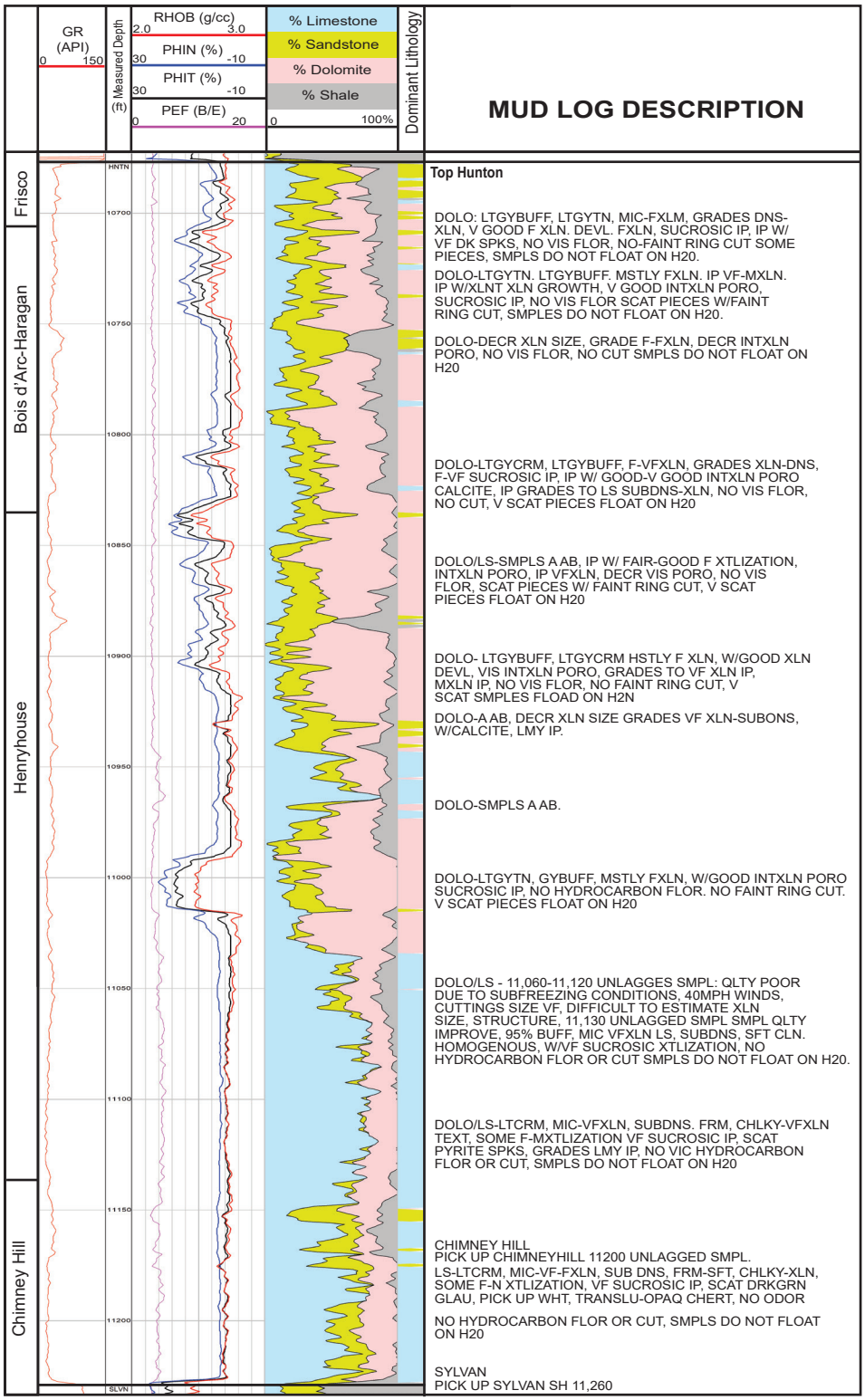


Figure 3.3. Anadarko Basin type log and mudlog descriptions. The Hunton Group formations are labeled on the left. The first column shows GR, followed by the measured depth track. The third column shows RHOB, PHIN, PEF, and PHIT curves from petrophysical analysis. The 4th column shows the mineral percentage curves for each lithology, with the predominant lithology at each depth to the right. The last column is the mudlog sample descriptions.

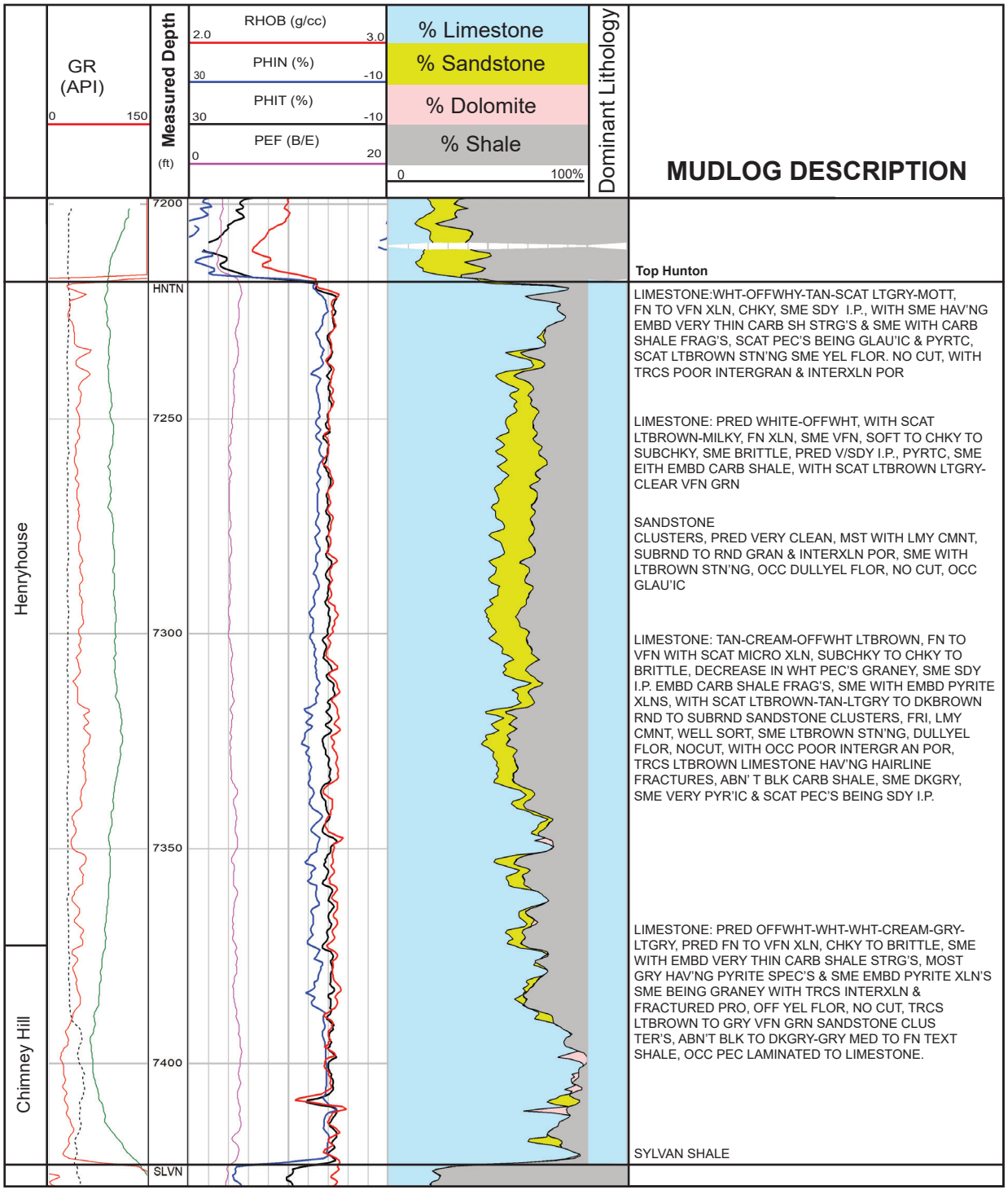


Figure 3.4. Arkoma Basin type log and mudlog descriptions. The Hunton Group formations are labeled on the left. The first column shows the GR, followed by the measured depth track. The third column shows RHOB, PHIN, PEF, and PHIT curves from petrophysical analysis. The 4th column shows the mineral percentage curves for each lithology, with the predominant lithology at each depth to the right. The last column is the mudlog sample descriptions.

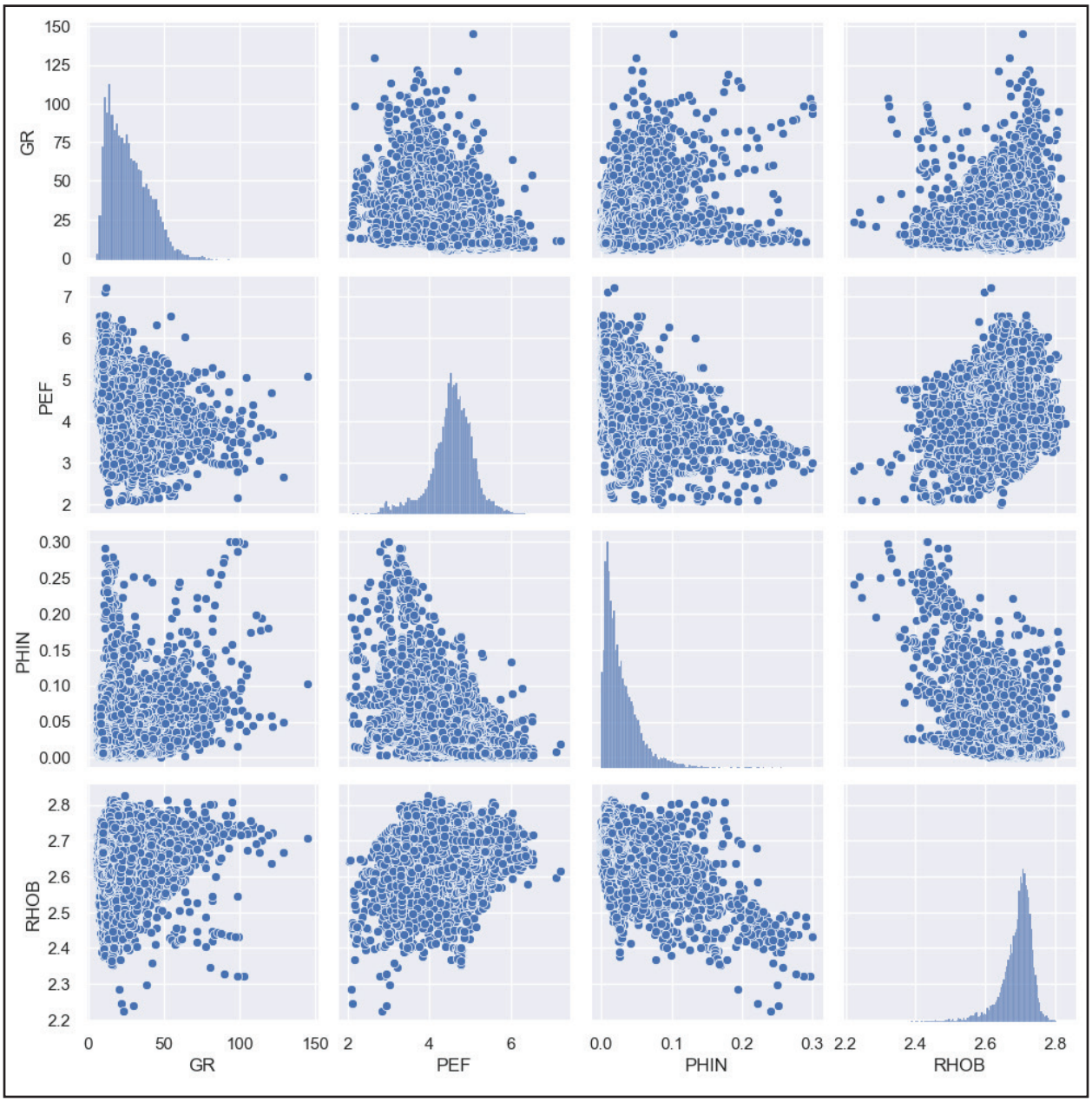


Figure 3.5. Pair plots for GR (0-150 API), PHIN (0-30%), RHOB (2.2-2.8 c/cc) and PEF (2.2-9 barnes) logs for the Hunton zone.

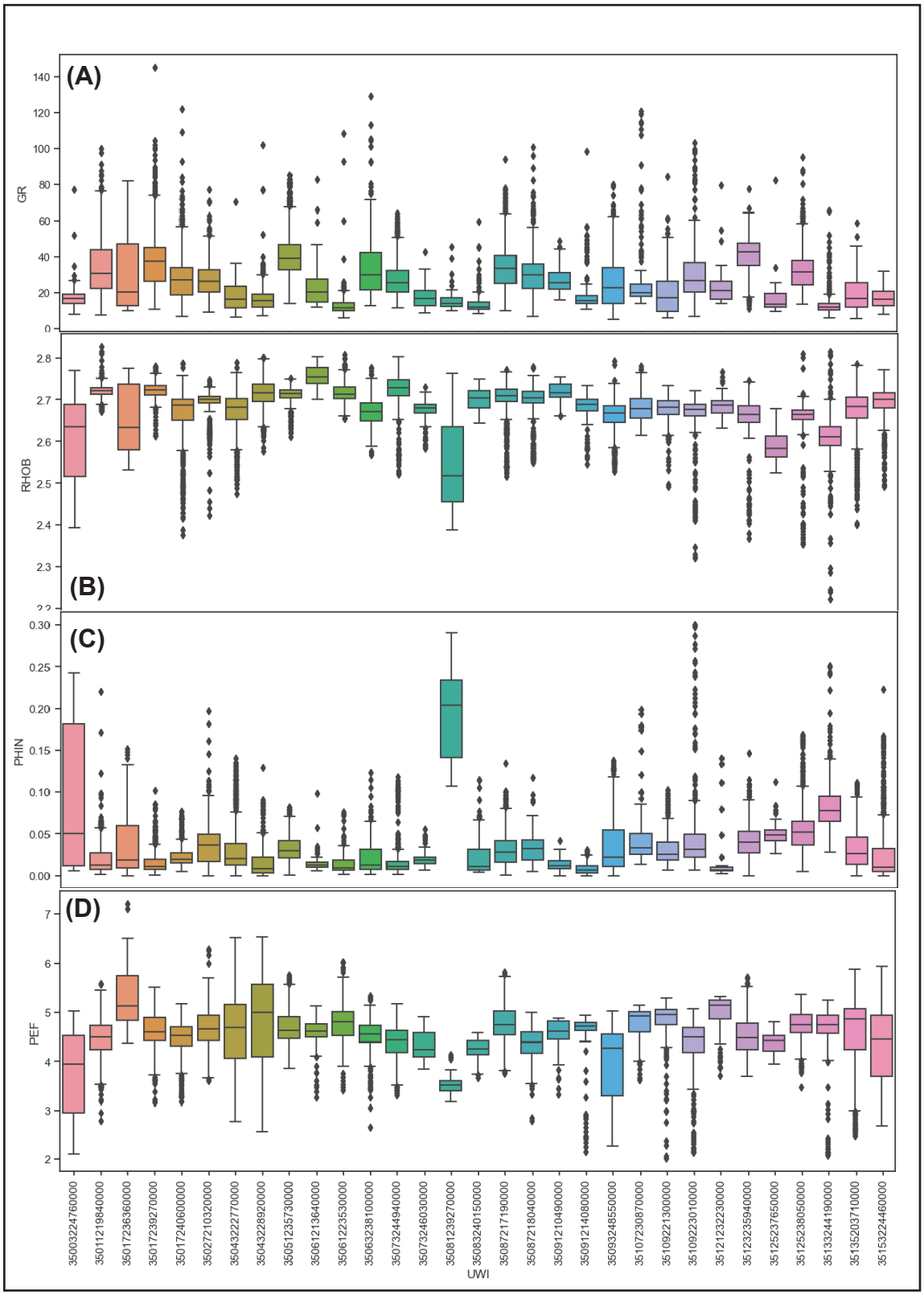


Figure 3.6. Box plots for well logs used in predicting PEF logs. A) GR B) RHOB C) PHIN D) PEF

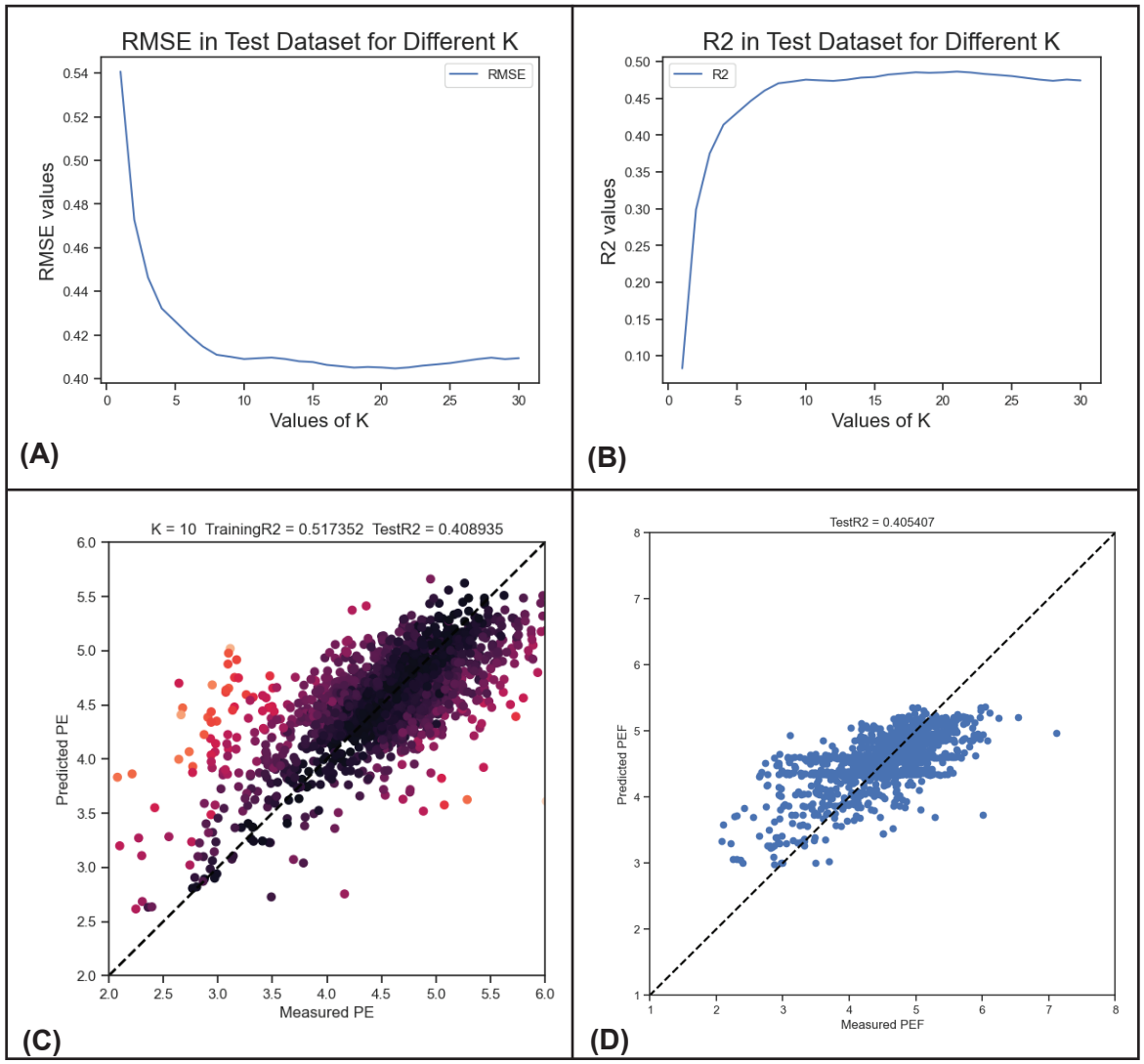


Figure 3.7. A) Root mean square error (RMSE) for K-NN for 1-30 nearest neighbors. B) Coefficient of determination (R2) for 1-30 nearest neighbors. C) PEF vs Predicted PEF for K=10 nearest neighbors using a 15:85 test: train split. D) PEF vs Predicted PEF for the supervised Random Forest model using 5-fold cross validation, 100 estimators, maximum depth of 5, and minimum of 3 data points per leaf.

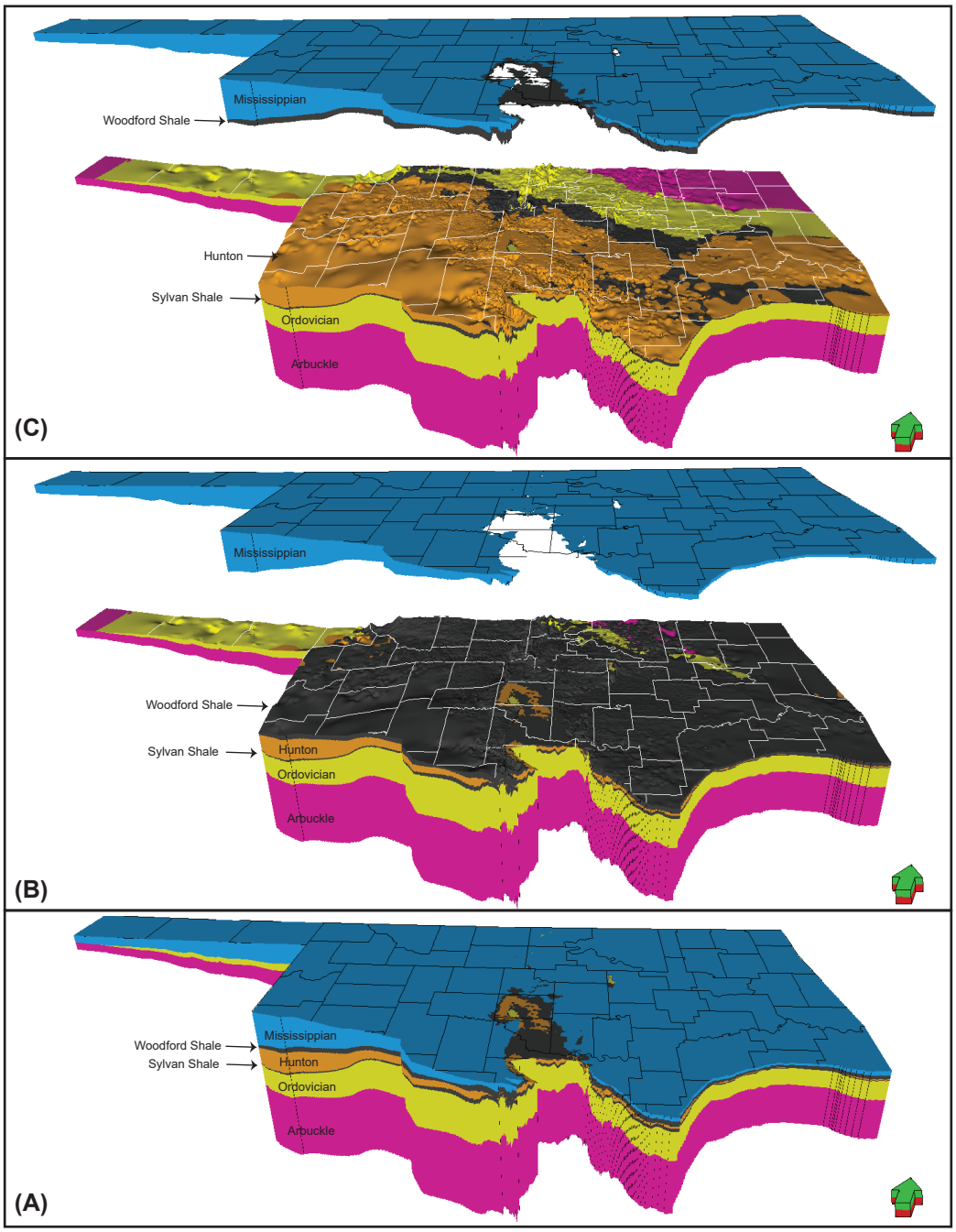


Figure 3.8. A) Mississippian (MSSP zone), Woodford (WDFD zone), Hunton, Sylvan (SVLN zone), Ordovician, and Arbuckle zones flattened on the Mississippian. The top of the Mississippian is an unconformity across the Anadarko shelf and the Cherokee platform. This map is the pre-Pennsylvanian unconformity subcrop map. The Mississippian is present across Oklahoma except in central Oklahoma. B) Same model as 3.8A except the Mississippian has been lifted to reveal the lateral extents of the Woodford Shale. The Woodford Shale and Hunton are not present in the Oklahoma panhandle, and there is a thinning across Noble, Osage, Tulsa, and Wagoner counties. C) Same model as 3.8A and 3.8B except the Woodford has also been lifted to reveal the lateral extent of the Hunton, Sylvan, Ordovician, and Arbuckle zones. This is the post-Hunton unconformity subcrop map.

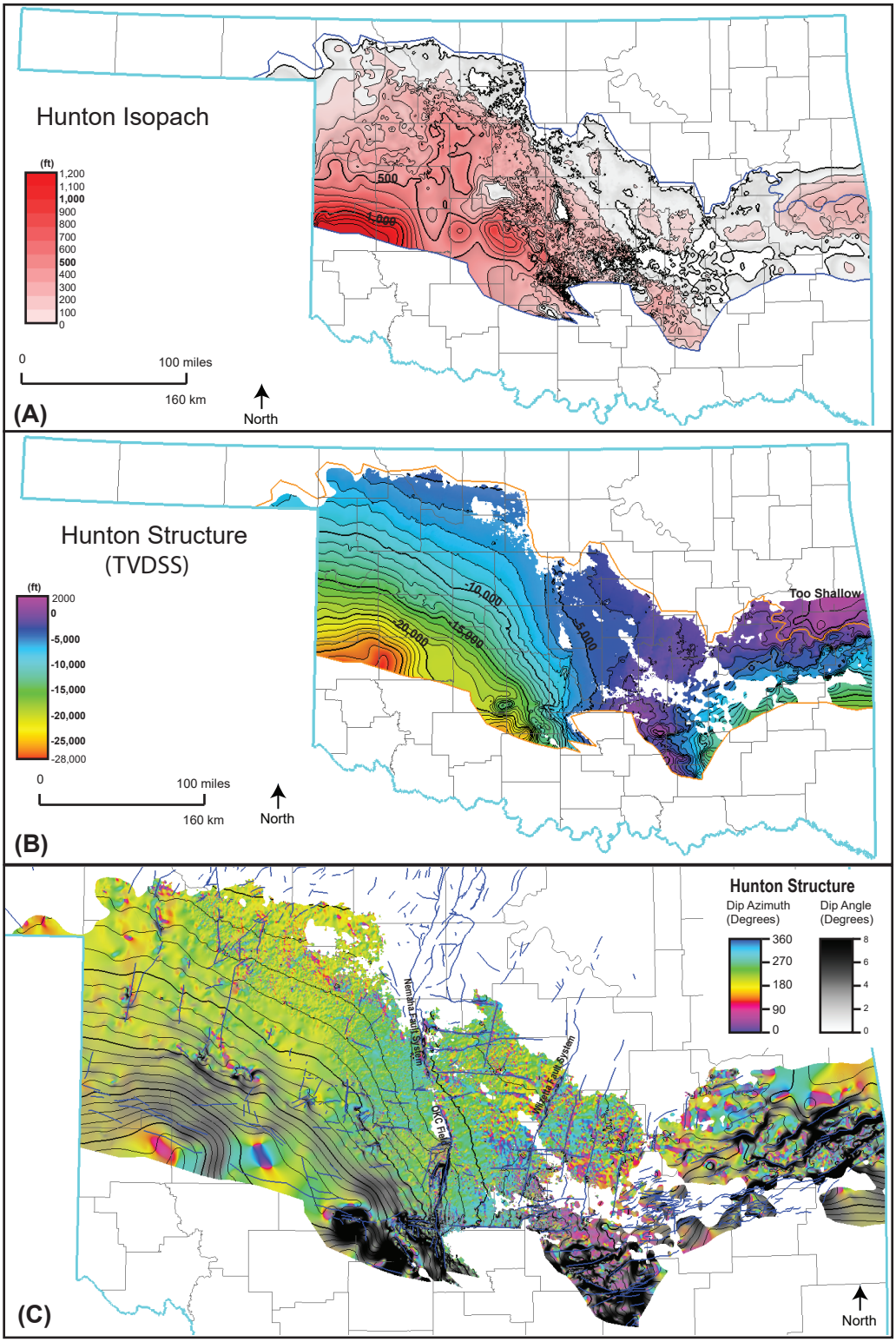


Figure 3.9. A) Hunton zone Isopach. 100 ft (30 m) contour interval, 500 ft (152 m) bold contour interval. B) Hunton Structure map. 1,000 ft (305 m) contour interval, 5,000 ft (1,524 m) bold contour interval. C) Hunton Structure map co-rendered with dip angle and dip magnitude. Faults include the OGS Comprehensive Fault Database (Holloway et al., 2016) and faults identified in this study.

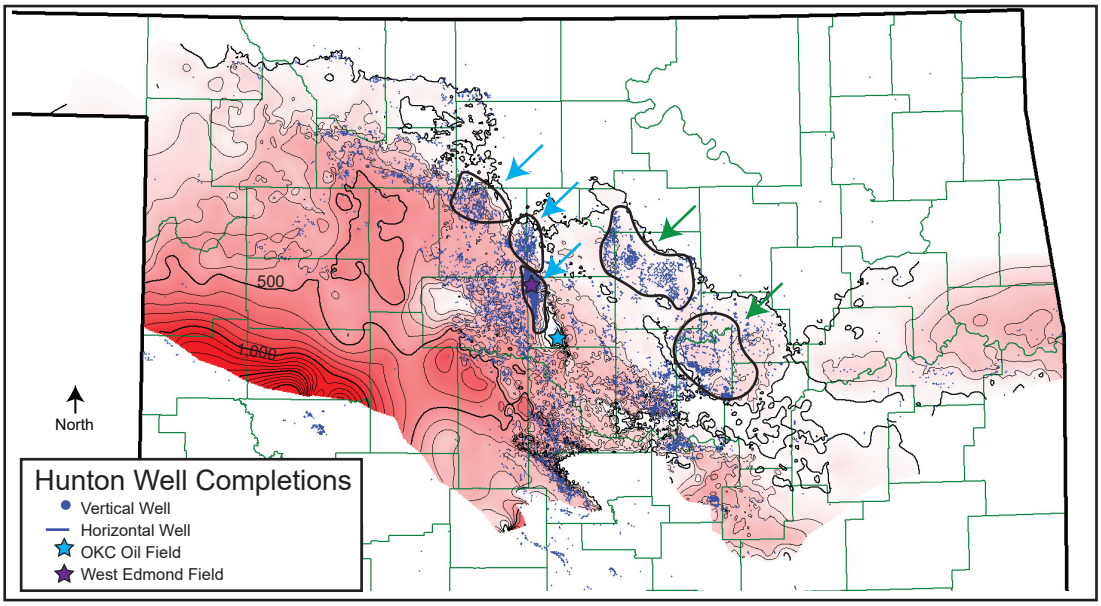


Figure 3.10. Hunton Isopach and all Hunton well completions. The Oklahoma City (OKC) oilfield is marked by the blue star, and the West-Edmond oilfield is marked by the purple star. The OKC oilfield has no Hunton present because it was eroded by the pre-Pennsylvanian unconformity. Blue dots are all vertical wells completed in the Hunton zone, and blue sticks are horizontal wells completed in the Hunton. Because the horizontal wells are hard to see, the polygons highlight areas with recent (post-2000) horizontal Hunton completions. Note, the west Edmond was initially developed by vertical wells but was later drilled horizontally. This same concept was applied to the regions just north and west of the West-Edmond field, blue arrows. Lincoln and Seminole counties also had horizontal development, green arrows.

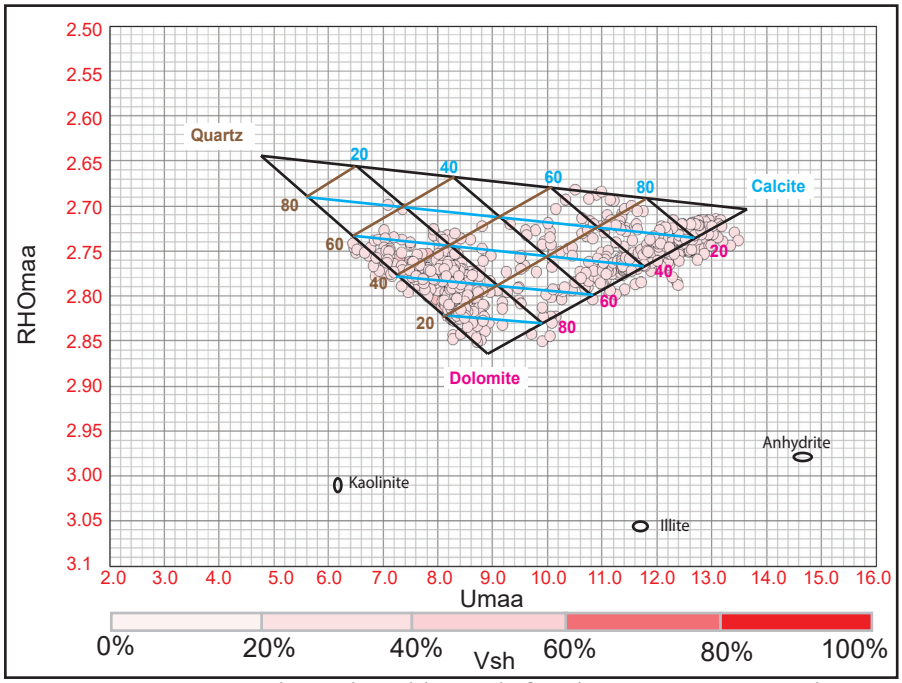


Figure 3.11. RHOmaa - Umaa plot colored by Vsh for the Hunton zone. The Hunton is predominantly calcite (limestone) with lesser amounts of dolomite, quartz (sandstone and silica), and shale.

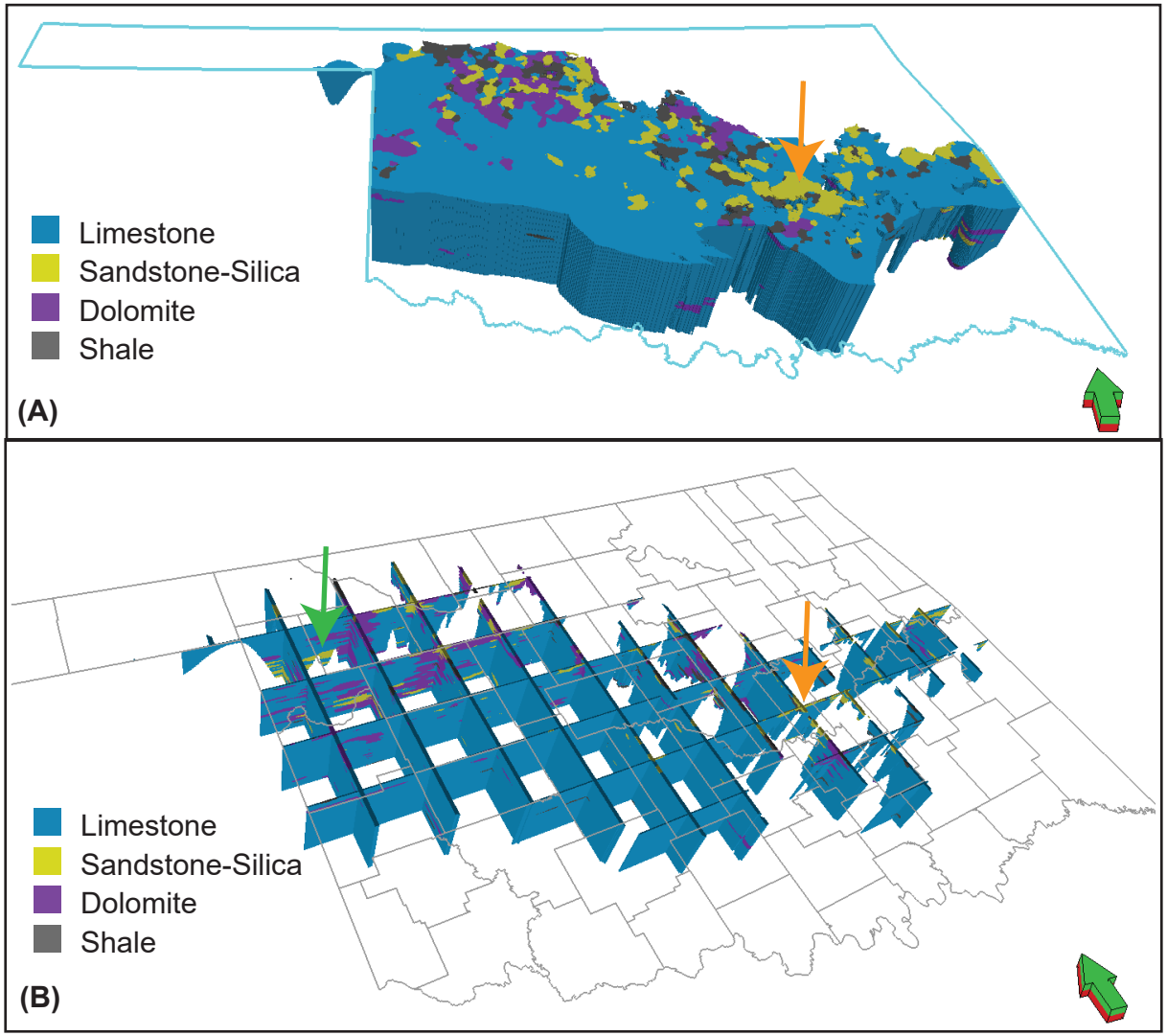


Figure 3.12. A) Lithology Model for the Hunton zone, flattened on the top of the Hunton. Orange arrow pointing to the Misener Sandstone development. B) Fence diagram of the lithology model for the Hunton. Flattened on the top of the Hunton with a 400 vertical exaggeration skipping every 75 lines (roughly 35 miles/56 kilometers). Orange arrow pointing to the Misener Sandstone development, green arrow pointing to the chert development within the Hunton zone.

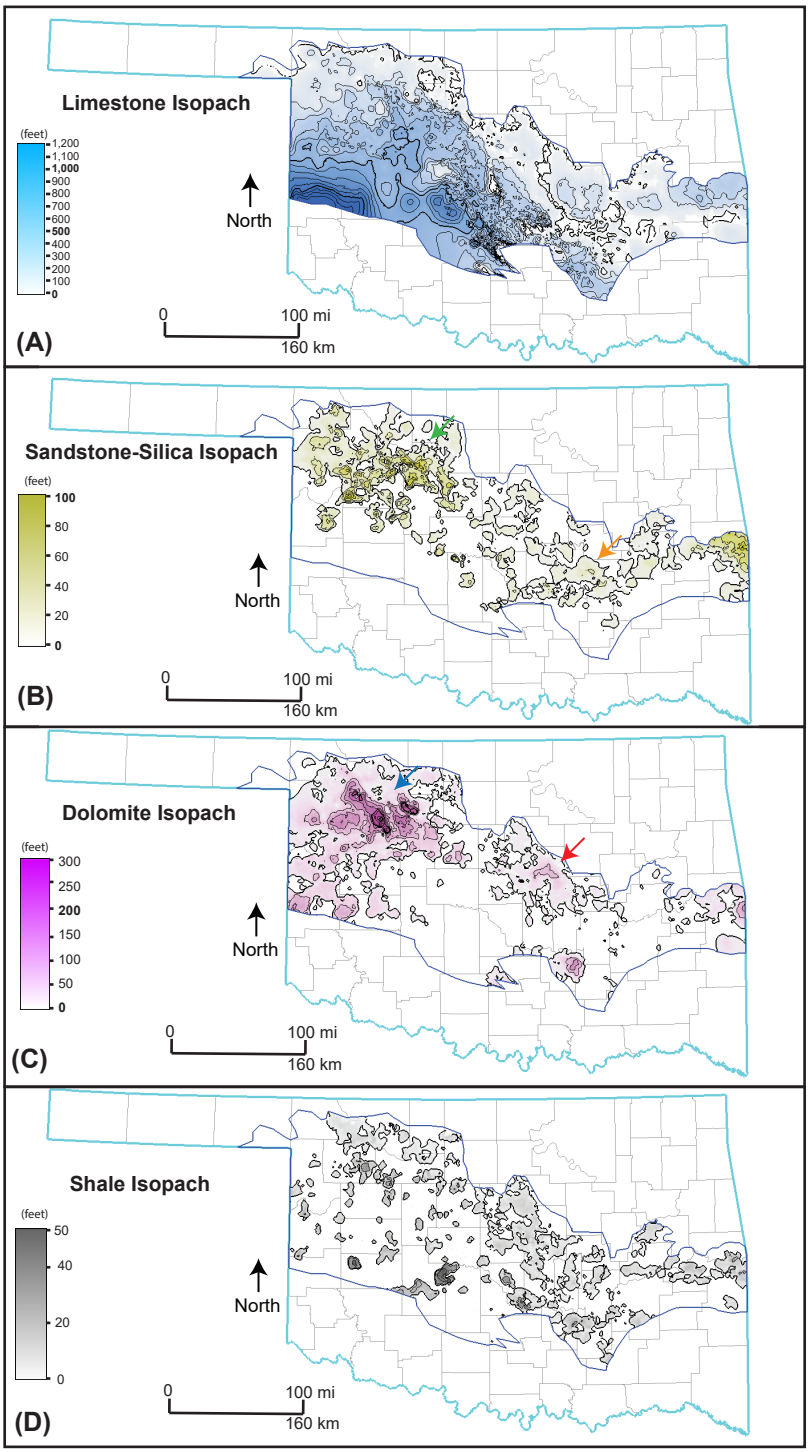


Figure 3.13. Hunton zone lithology thickness for A) Limestone. 100 ft (30 m) contour interval, 500 ft (152 m) bold contour interval. B) Sandstone-Silica. 20 ft (6.1 m) contour interval, 100 ft (30 m) bold contour interval. The orange arrow points to the Misener Sandstone development, and the green arrow points to the chert development within the Hunton zone. C) Dolomite. 50 ft (15 m) contour interval, 200 ft (61 m) bold contour interval. Blue arrow pointing to the north-western Oklahoma dolomite development. Red arrow pointing to the central Oklahoma dolomite development. D) Shale. 20 ft (6.1m) contour interval, 80 ft (24 m) bold contour interval.

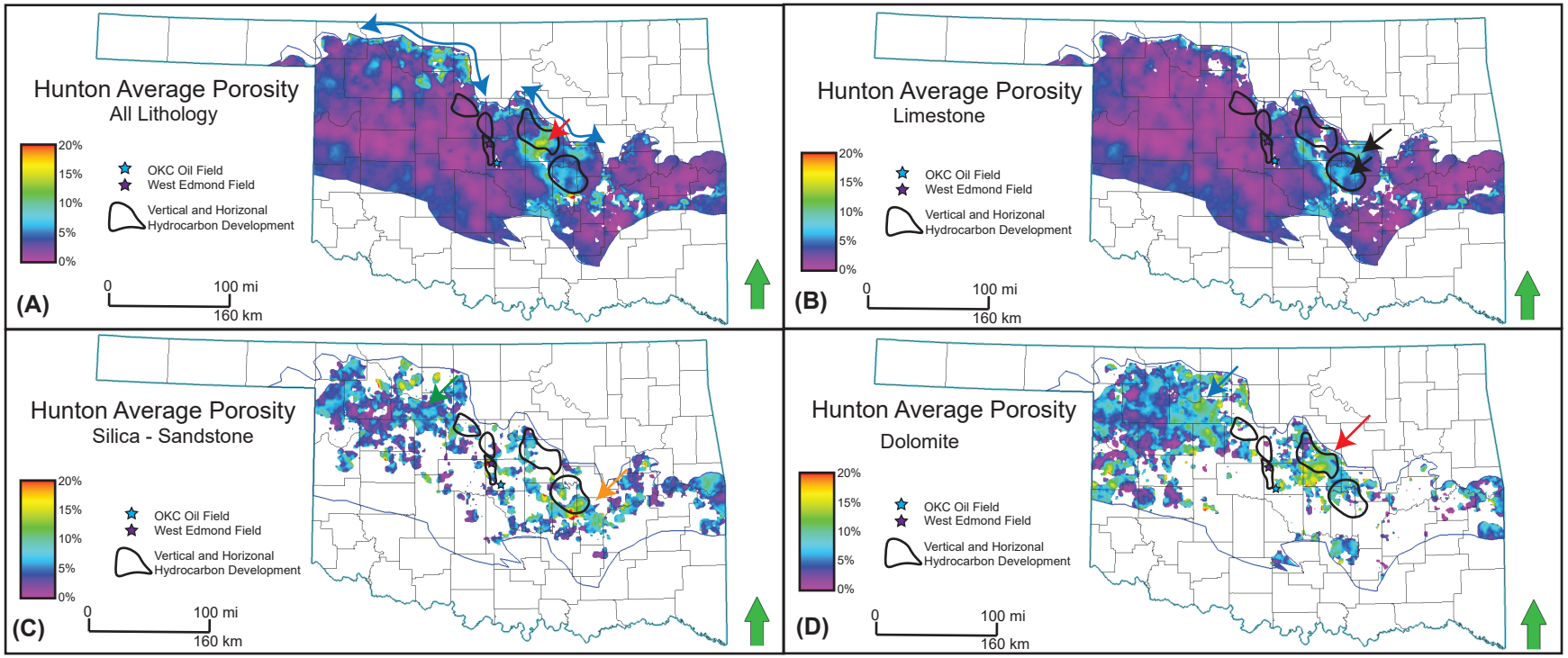


Figure 3.14. A) Hunton zone average porosity. Red arrow pointing to a large area of increased porosity. Blue double-headed arrows point to increased porosity along the Hunton subcrop. Black polygons highlight areas of both vertical and horizontal hydrocarbon development. B) Hunton zone limestone average porosity. Black arrow indicating areas of increased limestone porosity. Black polygons highlight areas of both vertical and horizontal hydrocarbon development. C) Hunton zone silica-sandstone average porosity. The green arrow points to the Chert development area, and the orange arrow points to the Misener Sandstone development. Misener Sandstones have higher porosity than the chert. Black polygons highlight areas of both vertical and horizontal hydrocarbon development. D) Hunton zone dolomite average porosity. The blue arrow highlights the northwest Oklahoma dolomite trend, and the red arrow points to the central Oklahoma dolomite development. Black polygons highlight areas of both vertical and horizontal hydrocarbon development.

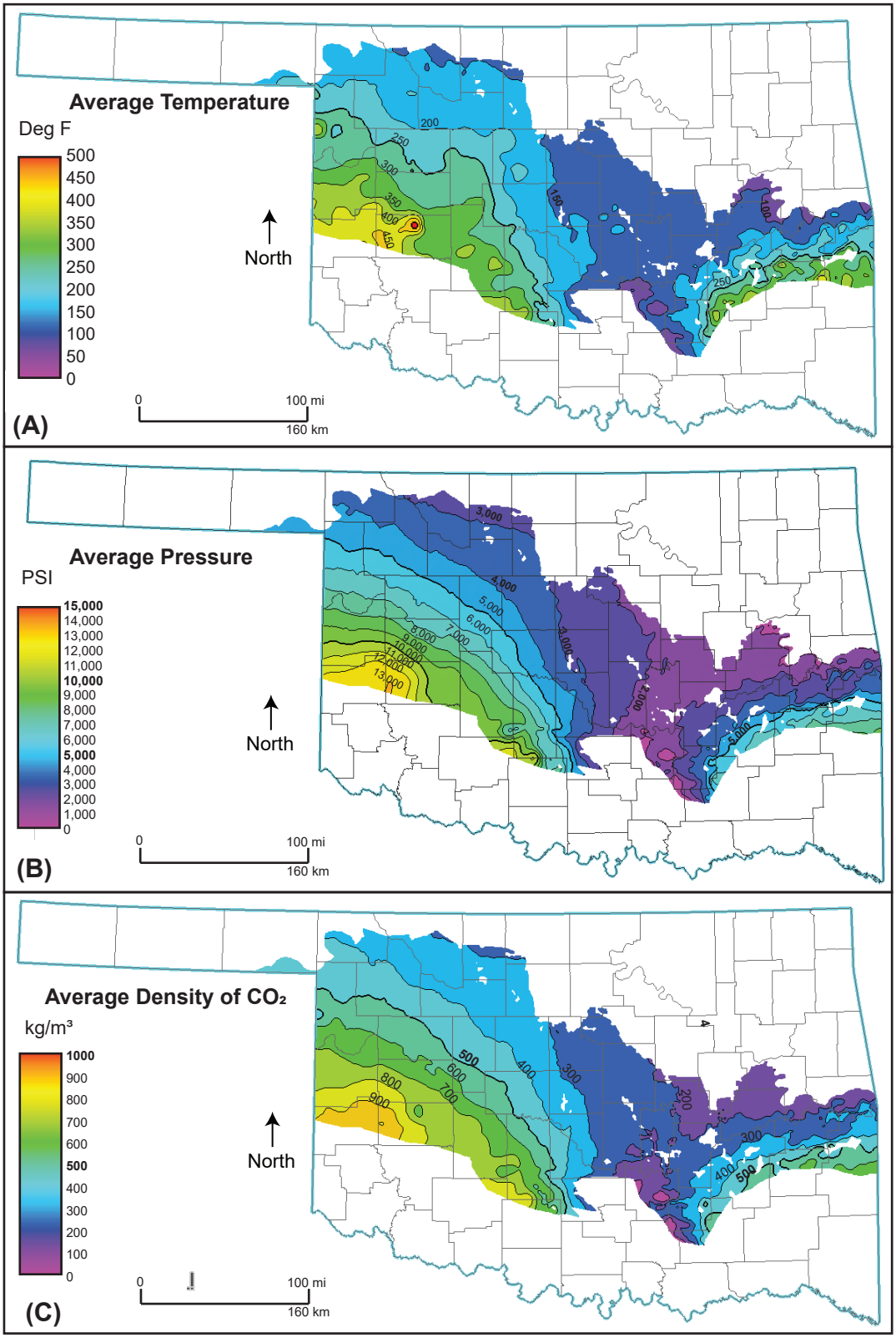


Figure 3.15. A) Average Hunton Temperature map. 50 °F (10 °C) contour interval. B) Average Hunton Pressure map. 1,000 psi (6.89 MPa) contour interval. C) Average density of CO_2 at reservoir temperature and pressure. 100 kg/m³ contour interval.

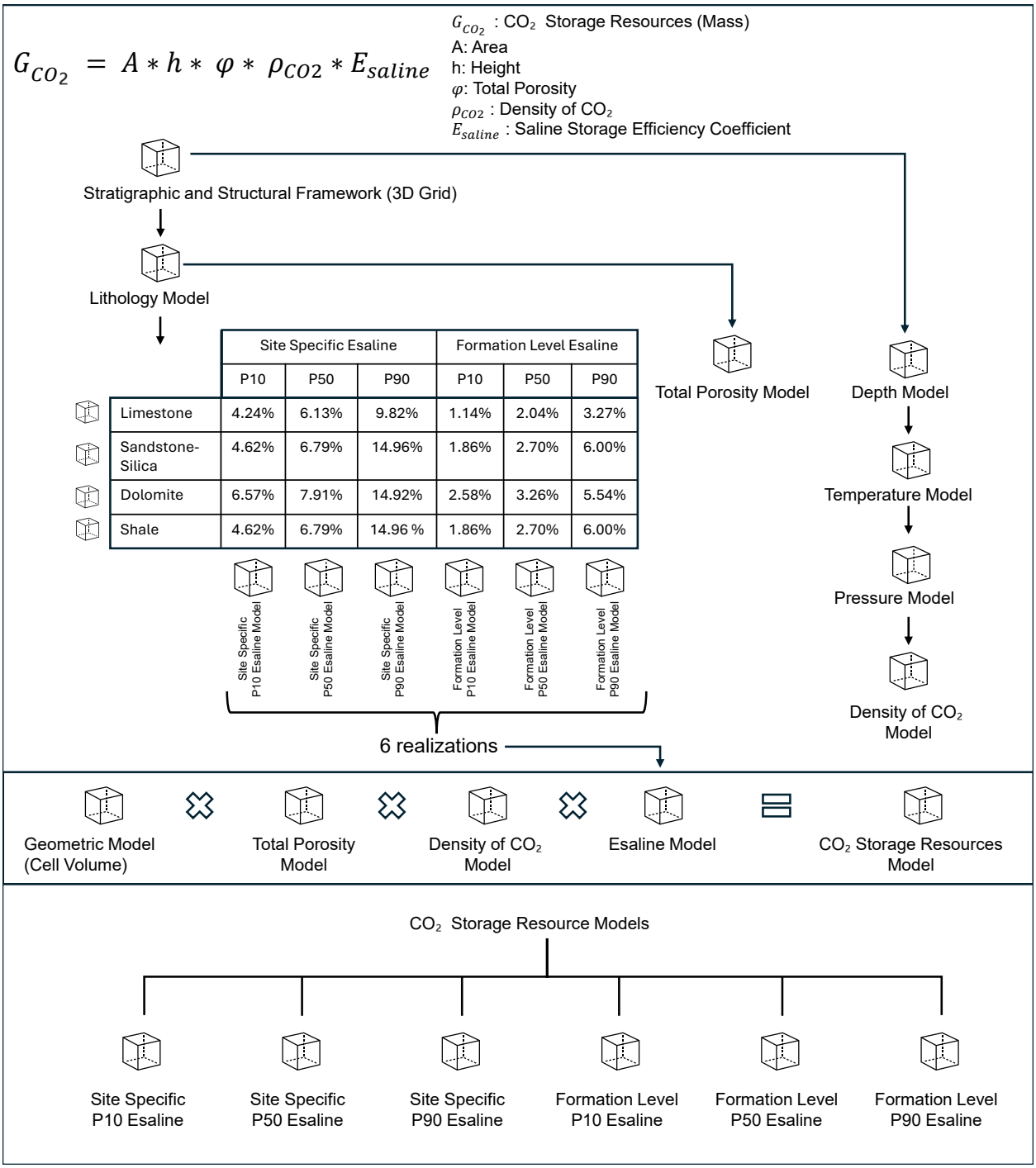


Figure 3.16. CO_2 storage resources modeling workflow.

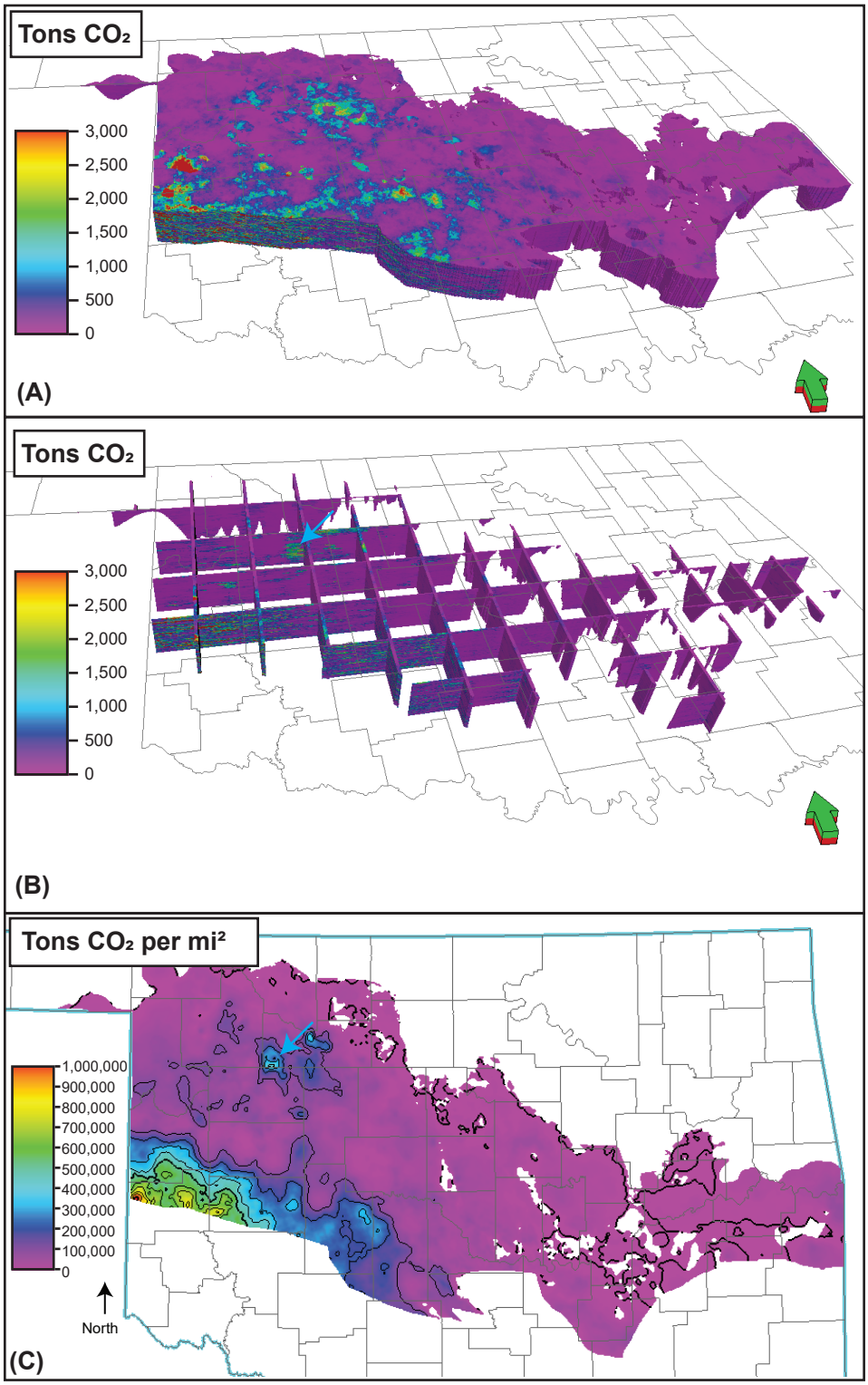
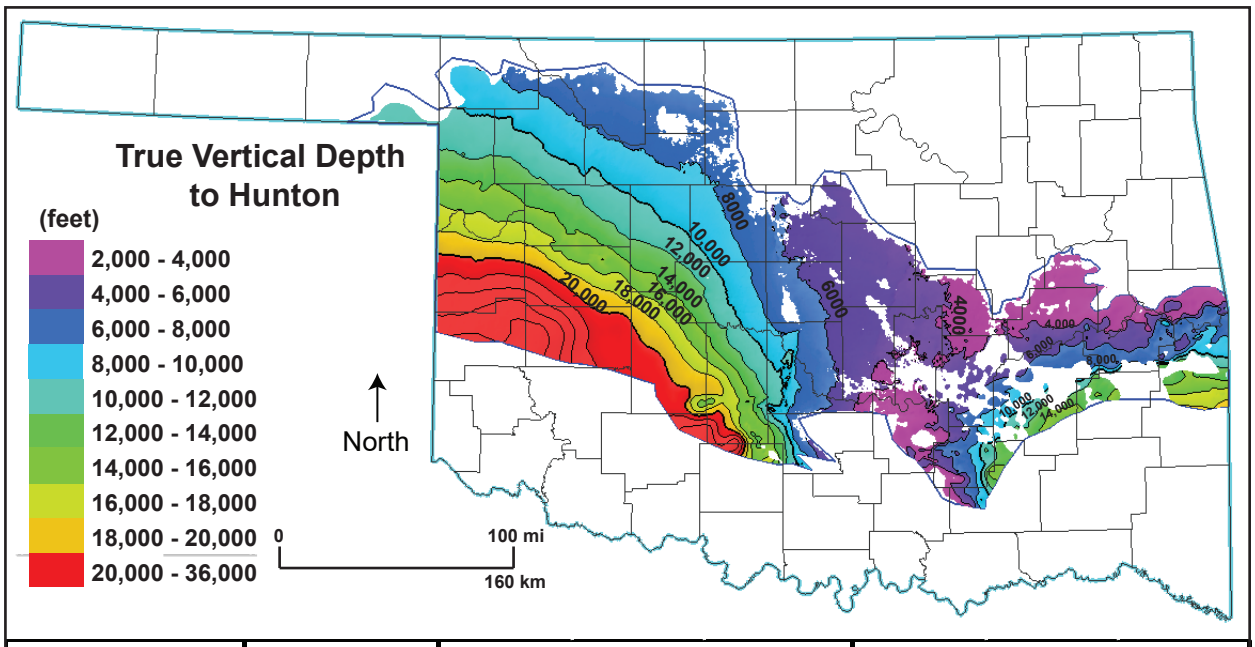


Figure 3.17. CO_2 storage resources models using the P_{50} Esaline values at the formation level. A) Hunton zone Model B) Hunton fence diagram. Blue arrow pointing to the northwest Oklahoma dolomite development showing increased CO_2 storage resources. C) Hunton net-mass map, in tons CO_2 per mi^2. Blue arrow pointing to the northwest Oklahoma dolomite development showing increased CO_2 storage resources.



MD	% of total Hunton Storage resources	Site Specific Mt CO_2			Formation Level Mt CO_2		
		P10	P50	P90	P10	P50	P90
2,000-4,000	1%	46	65	111	16	23	38
4,000-6,000	3%	125	174	299	44	62	105
6,000-8,000	4%	167	233	401	59	83	140
8,000-10,000	9%	338	450	800	124	168	286
10,000-12,000	7%	268	360	629	97	132	222
12,000-14,000	5%	195	268	462	69	96	162
14,000-16,000	6%	251	359	591	86	122	201
16,000-18,000	6%	250	359	584	84	121	197
18,000-20,000	6%	225	322	524	76	109	176
20,000-31,297	51%	2,011	2,882	4,665	676	971	1,566

Figure 3.18. A) Hunton true vertical depth map. 2,000 ft (610 m) contour interval. B) CO_2 storage resources for the entire Hunton zone broken down by 2,000 ft (610 m) intervals. For example, from 4,000 to 6,000 feet depth, the Hunton zone can store between 44-105 Mt of CO_2 using formation level Esaline values, which is 3% of all the storage resources in the evaluated area, highlighted by the dark purple color.

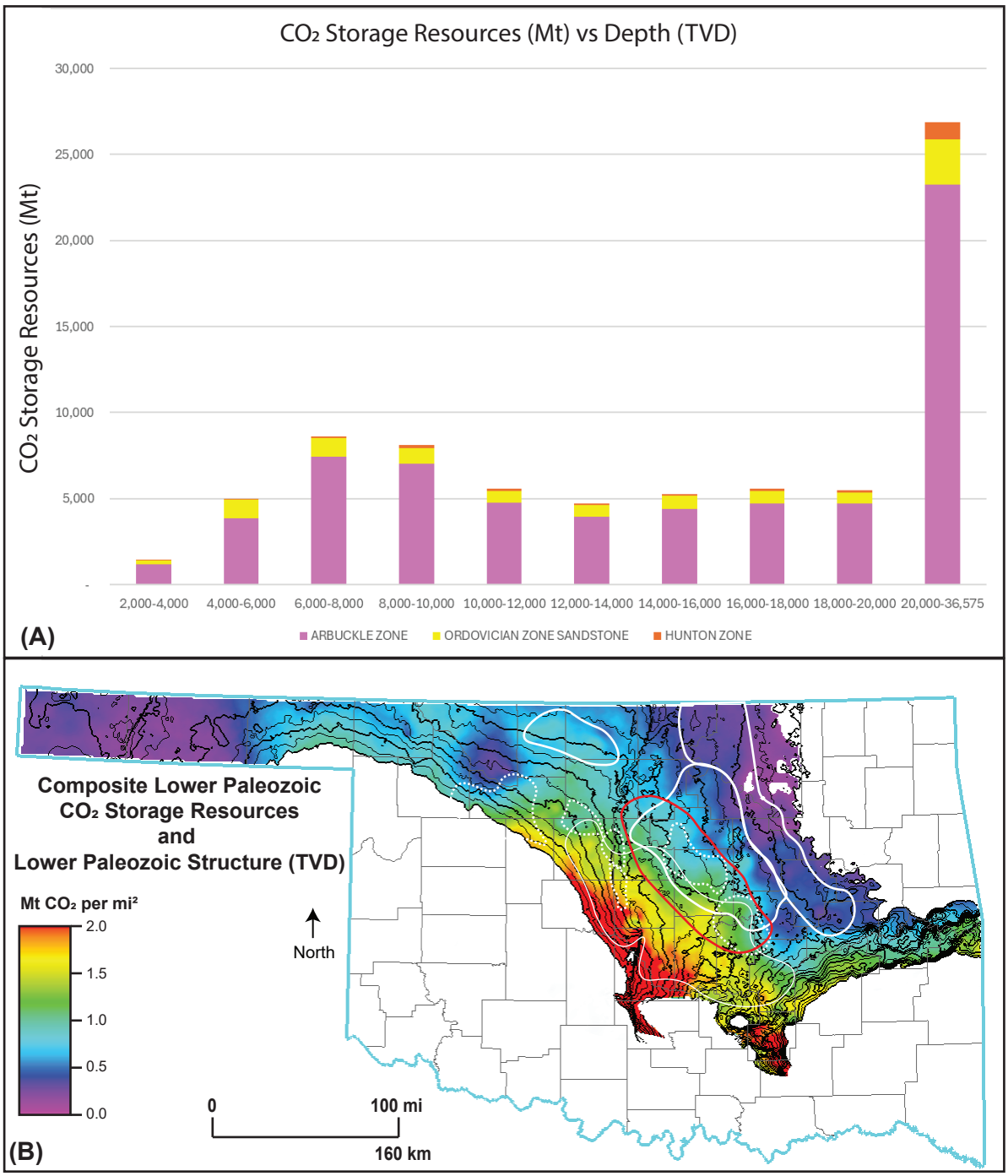


Figure 3.19. A) CO_2 storage resources for the Hunton zone, Ordovician zone sandstones, and Arbuckle zone, broken down by 2,000 ft (610 m) intervals using the P_{50} Esaline storage efficiency coefficients, giving a conservative estimate of CO_2 storage resources. B) CO_2 storage resources for the Lower Paleozoic reservoirs (Hunton zone, Ordovician zone sandstones, and Arbuckle zone) and the Lower Paleozoic composite TVD structure map from 2,000-10,000 ft. Depths deeper than 10,000 ft have been removed. 200 ft (61 m) contour interval, 1,000 ft (305 m) bold contour interval. Thick white outlines show Arbuckle areas of interest, thin white outline shows the Ordovician sandstone area of interest and the white dashed outlines highlight Hunton zone areas of interest. The red polygon shows location of stacked CO_2 storage resource potential.

Tables

Symbol	Term	Range	Description
Terms used to define the entire basin/region pore volume			
A_n/A_t	Net to total Area	0.2 - 0.8	Fraction of total basin/Region are that has a suitable formation present
h_n/h_g	Net to Gross Thickness	0.25 - 0.75	Fraction of total geologic unit that meets minimum porosity and permeability requirements for injection
$\emptyset_{eff}/\emptyset_{tot}$	Effective to Total Porosity Ratio	0.6 - .95	Fraction of total porosity that is effective, i.e. interconnected
Terms used to define the pore volume immediately surrounding a single-well CO_2 injector			
E_A	Areal Displacement Efficiency	0.5 - 0.8	Fraction of immediate area surrounding an injection well that can be contacted by CO_2
E_I	Vertical Displacement Efficiency	0.6 - .9	Fraction of vertical cross section with the volume defined by the area (A) that can be contacted by the CO_2 plume from a single well
E_g	Gravity	0.2 - 0.6	Fraction of net thickness that is contacted by CO_2 as a consequence of the density difference between CO_2 and in-situ brine.
E_d	Microscopic Displacement Efficiency	0.5 - 0.8	Portion of the CO_2 contacted, brine-filled pore volume that can be replaced by CO_2

Table 3.1. Definition of terms used to calculate the Saline Storage Capacity Efficiency, Esaline. From IEA Greenhouse Gas R&D Programme 2009.

Esaline	Site Specific			Formation Level		
	P10	P50	P90	P10	P50	P90
Limestone	4.24%	6.13%	9.82%	1.41%	2.04%	3.27%
Clastics	4.62%	6.79%	14.96%	1.86%	2.70%	6.00%
Dolomite	6.57%	7.91%	14.92%	2.58%	3.26%	5.54%

Table 3.2. Esaline values at the Site Specific and Formation level. From IEA Greenhouse Gas R&D Programme 2009.

	SITE SPECIFIC Esaline Values		
	Hunton - Mt		
	P10	P50	P90
Limestone	3,201	4,628	7,414
Sandstone-Silica	84	123	272
Dolomite	551	664	1,252
Shale	39	58	127
Total	3,876	5,473	9,065

Table 3.3. CO_2 Storage resources for the Hunton calculated with Site Specific Esaline values, broken down by lithology.

	FORMATION LEVEL Esaline Values		
	Hunton - Mt		
	P10	P50	P90
Limestone	1,064	1,540	2,469
Sandstone-Silica	34	49	109
Dolomite	217	274	465
Shale	16	23	51
Total	1,331	1,886	3,094

Table 3.4. CO_2 Storage resources for the Hunton calculated with Formation Level Esaline values, broken down by lithology.

	ARBUCKLE ZONE						ORDOVICIAN ZONE SANDSTONE						HUNTON ZONE						ALL 3 ZONES					
	Mt						Mt						Mt						Mt					
	Site Specific			Formation Level			Site Specific			Formation Level			Site Specific			Formation Level			Site Specific			Formation Level		
MD	P10	P50	P90	P10	P50	P90	P10	P50	P90	P10	P50	P90	P10	P50	P90	P10	P50	P90	P10	P50	P90	P10	P50	P90
2,000-4,000	2,351	2,877	5,486	923	1,180	2,050	391	574	1,259	157	228	506	46	65	111	16	23	38	2,788	3,516	6,855	1,096	1,430	2,594
4,000-6,000	7,631	9,385	17,998	3,000	3,847	6,748	1,850	2,715	5,952	744	1,079	2,391	125	174	299	44	62	105	9,606	12,274	24,249	3,788	4,988	9,243
6,000-8,000	14,711	18,168	34,928	5,784	7,437	13,113	1,874	2,750	6,028	753	1,093	2,421	167	233	401	59	83	140	16,752	21,151	41,357	6,596	8,612	15,675
8,000-10,000	13,903	17,234	33,203	5,465	7,045	12,481	1,537	2,257	4,945	618	896	1,986	338	450	800	124	168	286	15,778	19,940	38,948	6,207	8,109	14,753
10,000-12,000	9,433	11,659	22,402	3,707	4,768	8,407	1,181	1,733	3,796	474	688	1,524	268	360	629	97	132	222	10,882	13,753	26,826	4,278	5,589	10,154
12,000-14,000	7,777	9,630	18,500	3,054	3,933	6,943	1,156	1,697	3,715	464	674	1,491	195	268	462	69	96	162	9,128	11,596	22,676	3,587	4,703	8,595
14,000-16,000	8,738	10,825	20,784	3,429	4,419	7,797	1,260	1,850	4,047	506	734	1,624	251	359	591	86	122	201	10,249	13,033	25,422	4,021	5,275	9,622
16,000-18,000	9,370	11,618	22,298	3,675	4,738	8,363	1,225	1,799	3,936	492	714	1,580	250	359	584	84	121	197	10,845	13,776	26,818	4,252	5,573	10,140
18,000-20,000	9,292	11,522	22,081	3,642	4,695	8,275	1,146	1,682	3,678	460	667	1,476	225	322	524	76	109	176	10,663	13,526	26,283	4,178	5,471	9,927
20,000-36,575	45,808	56,938	109,742	17,994	23,239	41,260	4,562	6,697	14,648	1,831	2,657	5,878	2,011	2,882	4,665	676	971	1,566	52,381	66,517	129,055	20,502	26,866	48,703
TOTAL	129,013	159,855	307,421	50,673	65,301	115,436	16,182	23,754	52,004	6,501	9,430	20,877	3,876	5,473	9,065	1,331	1,886	3,094	149,071	189,081	368,490	58,505	76,617	139,407

Table 3.5. CO_2 storage resources for the Arbuckle zone, Ordovician zone sandstones and Hunton zone broken down by 2,000 ft (610 m) intervals using both the site specific and formation level Esaline storage efficiency factors.

Acknowledgements

I would like to thank Enverus for the well information and well logs, and GVERSE Geographix and Schlumberger's Petrel for the software used in this study. I would also like to thank my doctoral committee members, M. Pranter, H. Bedle, B. Carpenter, and D. Devegowda.

References

Al-Shaieb, Z., P. Medlock, K. Lippert, F. Matthews, and F. Manni, 1993, Overview of Hunton Facies and Reservoirs in the Anadarko Basin: Oklahoma Geological Survey Special Publication 93-4.

Al-Shaieb, Z., J. O. Puckette, A. A. Abdalla, and P. B. Ely, 1994, Megacompartment complex in the Anadarko Basin completely sealed overpressured phenomenon: Basin Compartments and Seals, doi:10.1306/m61588c4.

Amsden, T. W., 1957, Stratigraphy and Paleontology of the Hunton Group in the Arbuckle Mountain Region: Oklahoma Geological Survey Circular 44.

Amsden, T. W., 1960, Hunton stratigraphy, part 6 of Stratigraphy and paleontology of the Hunton Group in the Arbuckle Mountains Region: Oklahoma Geological Survey Bulletin 84, 311 p.

Amsden, T. W., 1975, Hunton Group (Late Ordovician Silurian, and Early Devonian) in the Anadarko Basin of Oklahoma: Oklahoma Geological Survey Bulletin 121.

Amsden, T. W., 1980, Hunton Group (Late Ordovician Silurian and Early Devonian) in the Arkoma Basin of Oklahoma: Oklahoma Geological Survey Bulletin 129.

Amsden, T. W. and G. Klapper, 1972, Misener Sandstone (Middle-Upper Devonian), north-central Oklahoma: American Association of Petroleum Geologists Bulletin, v. 56, p. 2323-2334

Doveton, J. H., 1994, Geologic log interpretation: Tulsa, OK, SEPM.

Enverus Database: <https://www.enverus.com/> (accessed August, 2021).

Fritz, R. D., and P. L. Medlock, 1993, Sequence Stratigraphy of the Hunton Group as Defined by Core, Outcrop, and Log Data: Oklahoma Geological Survey Special Publication 93-4, p. 161–180.

General Geologic Sections of Oklahoma, 1975: <https://oklahoma.gov/content/dam/ok/en/occ/images/og/geocolumn-occ.pdf> (accessed October, 2022).

Holloway, S., A. Holland, and R. Keller, 2016: Oklahoma Geological Survey-Oklahoma Fault Database: <https://www.ou.edu/ogs/data/fault> (accessed April 24, 2023).

Howery, S. D., 1993, A Regional Look at Hunton Production in the Anadarko Basin: Oklahoma Geological Survey Special Publication 93-4.

IEA Greenhouse Gas R&D Programme (IEA GHG), “Development of Storage Coefficients for CO2 Storage in Deep Saline Formations”, October 2009

Johnson, K. S. (ed.), 1993, Hunton Group Core Workshop and Field Trip: Oklahoma Geological Survey Special Publication 93-4.

Johnson, K. S. (ed.), 1996, Platform Carbonates in the Southern Midcontinent, 1996 Symposium: Oklahoma Geological Survey Circular 101.

Johnson, K. S. (ed.), 1999, Silurian, Devonian and Mississippian Geology and Petroleum in the Southern Midcontinent, 1999 Symposium: Oklahoma Geological Survey Circular 105.

Johnson, J. G., Klapper, G. and Sandberg, C. A., 1985, Devonian eustatic fluctuations in Euramerica: Geological Society of America Bulletin, v. 96, p. 567-587.

Kuykendall, M. D. and R. D. Fritz, 1993, Misener Sandstone: Distribution and Relationship to Late/Post-Hunton Unconformities, Northern Shelf, Anadarko Basin: Oklahoma Geological Survey Special Publication 93-4.

Lee, W., 1956, Stratigraphy and structural development of the Salina basin area: Kansas Geological Survey Bulletin 121, 167 p.

Mankin, C. J. (coordinator), 1987, Texas-Oklahoma tectonic region: correlation of stratigraphic units of North America (COSUNA) project: American Association of Petroleum Geologists, Tulsa.

Manni, F. M., 1985, Depositional environment, diagenesis, and unconformity identification of the Chimney Hill Subgroup, in the western Anadarko basin and northern shelf, Oklahoma: Oklahoma State University unpublished M.S. thesis, 129 p.

Medlock, P. L., 1984, Depositional environment and diagenetic history of the Frisco and Henryhouse Formations in central Oklahoma: Oklahoma State University unpublished M.S. thesis, 146 p.

Miller, G., 2017, The History of the WEHLU (West Edmond Hunton Lime Unit) Play from Conventional to Unconventional: <https://www.searchanddiscovery.com/documents/2017/11000miller/ndx_miller.pdf> (accessed , 2024).

Northcutt, R. A., and J. A. Campbell, 1995, Geologic Provinces of Oklahoma: Oklahoma Geological Survey Open File Report 5. http://ogs.ou.edu/docs/openfile/OF5-95.pdf, accessed March 2022

Rottmann, K., E. A. Beaumont, R. A. Northcutt, Z. Al-Shaieb, J. Puckette, and P. Blubaugh, 2000, Hunton Play in Oklahoma (Including Northeast Texas Panhandle): Oklahoma Geological Survey Special Publication 2000-2.

Schlumberger Log Interpretation principles, 1989: Houston, TX, Schlumberger Educational Services.

Shannon, J. P., 1962, Hunton Group (Silurian-Devonian) and Related Strata in Oklahoma: American Association of Petroleum Geologists Bulletin, v. 46.

SMU Node of National Geothermal Data System, Heat Flow and Well Data, n.d.: <http://geothermal.smu.edu> (accessed March, 2023).

Stanley, T. M., 2001, Stratigraphy and Facies Relationships of the Hunton Group, Northern Arbuckle Mountains and Lawrence Uplift, Oklahoma: Oklahoma Geological Survey Guidebook 33.

Taff, J.A., 1902, Atoka folio, Indian Territory: U.S. Geological Survey Geologic Atlas of the United States Folio, GF-79, 8 p., scale 1:125,000

Conclusions

The overarching theme of this dissertation is the spatial distribution of lithology, pore volume and CO_2 storage resources for all reservoirs older than the Devonian for the state of Oklahoma, except the Ardmore, Marietta, and Hollis basins. The oldest, deepest Arbuckle zone sits directly above the crystalline basement and has the largest CO_2 storage resources. It is predominantly a vuggy dolomite and laterally continuous in spatial distribution except in the Southern Oklahoma Aulacogen, where it is predominantly limestone. This zone has been historically used for hydrocarbon production and wastewater disposal, which has led to induced seismicity. Areas without induced seismicity generally coincide with areas that did not have horizontal Mississippian hydrocarbon wells drilled, which were the cause of the increase in produced wastewater production and the need for SWD wells in the Arbuckle Group. Induced seismicity can be mitigated by limiting wastewater injection rates and not injecting directly into crystalline basement. While there is no doubt that there is communication between the Arbuckle and crystalline basement, the lack of induced seismicity above the Arbuckle is a testament to the sealing capabilities of the overlying Simpson Group (Oil Creek Formation shales) that act as seals for the Arbuckle. Additionally, this study suggests that faults that are apparent from induced seismicity (earthquakes that show linear distribution), but unmapped due to lack of hard data (i.e. 2-D/3-D seismic, well log control) would have little vertical offset and would likely have Arbuckle present on both sides of the fault, potentially allowing for fluid flow across. With the exception of the 2011, 5.0 M Prague earthquake in southern Lincoln County that occurred along the Wilzetta fault, there is little induced seismicity associated with the major fault systems of Oklahoma, even though there are high-rate SWD injection wells in the area. While the initial earthquake took place closest to the Wilzetta fault, the subsequent aftershocks and other smaller

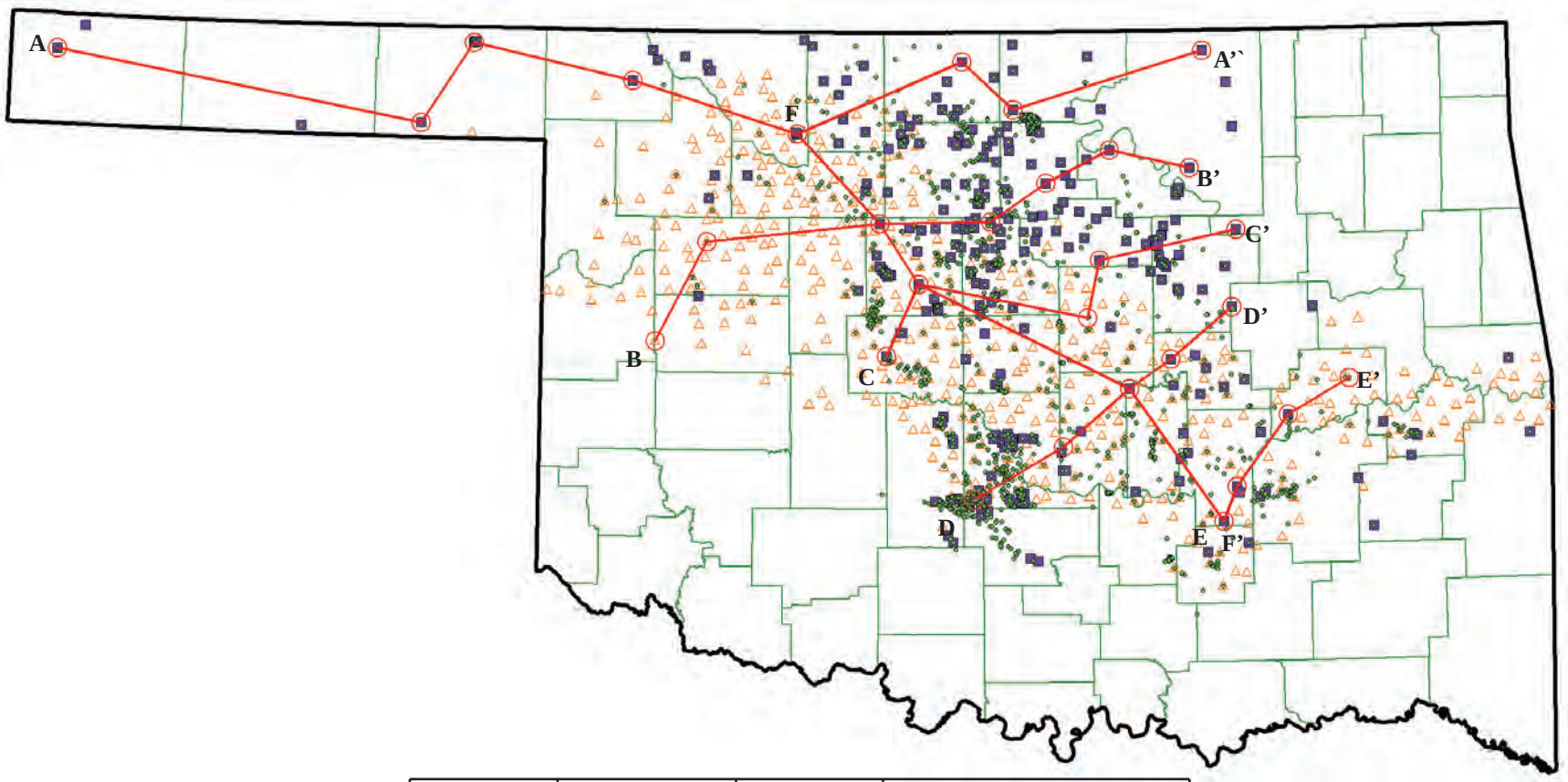
earthquakes over the years illuminate a secondary fault that runs sub-parallel to the Wilzetta fault in the area. The earthquakes do not trend along the main Wilzetta fault.

The second largest reservoir for CO_2 storage is the Ordovician zone, which lies directly above the Arbuckle Group. The Ordovician is predominantly limestone (the Viola Limestone) and sandstone (Simpson, McLish, and Oil Creek sandstones). Dolomites (Simpson Dolomite) are present but not laterally continuous, and the shales are considered seals for hydrocarbon reservoirs and are therefore not considered suitable for CCUS. The injection target for the Ordovician zone would be the Bromide sandstones, sometimes called the "Second Wilcox," which is the most laterally continuous sandstone in the state of Oklahoma. 35% of the total sandstone storage resources for the Ordovician zone are at depths shallower than 10,000 ft (3,048 m) and sit directly above the Arbuckle Group.

The smallest and youngest reservoir evaluated in this dissertation, suitable for CCUS in Oklahoma, is the Hunton zone, which lies directly above the Sylvan Shale. The Sylvan Shale is a regional seal for Ordovician reservoirs, and it extends across most of Oklahoma. The Hunton Group lies below the Woodford Shale, and sometimes the Misener Sandstone can develop at the top of the Hunton zone. The Misener Sandstone was included in the Hunton zone because it is a reservoir lithology and is in direct contact (no seals) with the Hunton. The best porosity and therefore reservoir lithology in the Hunton zone is the dolomite. Major, Woodward, and Dewey counties have an increase in dolomite thicknesses, porosity, and CO_2 storage resources. Another area with increased porosity, shallower depths, and possibly reduced reservoir pressure due to horizontal hydrocarbon production is in Lincoln, Okfuskee, and Seminole counties. Areas with historical hydrocarbon production and waterflooding, like the West Edmond field, could be areas of unusual reservoir pressure.

In conclusion, all 3 of these reservoirs are present across the state, stacked on top of each other and suitable for CCUS. While looking at the lower Paleozoic reservoirs as a composite, central Oklahoma shows the greatest CO_2 storage resources at depths less than 10,000 ft (3,048 m). All three reservoirs are present and accessible from one wellbore. There is Woodford Shale present to seal the thin, dolomitic Hunton Group with Misener Sandstone present. Sylvan Shale below the Hunton seals the lower Ordovician-age Bromide sandstones, which have increased average porosity and thickness in the region. Additionally, the shales in the Oil Creek Formation in the Simpson Group act as seals for the lower Arbuckle zone, which is over 2,000 ft (610 m) thick with the capability to store over 11.9 million barrels of water. Oklahoma's long history of producing and storing hydrocarbons and saltwater in the subsurface has positioned it to be one of the largest carbon hubs in the world.

APPENDIX A



System	Series	Group	Formations	
PENNSYLVANIAN UNCONFORMITY				
Mississippian	Meramecian		Meramec Lime Meramec Shale Mayes Sycamore	MSSP ZONE
	Osagean		Osage Lime Miss Lime Miss Chat	
	Kinderhookian		Kinderhook Shale	
Devonian	Chattanoogian		Woodford Shale	WDFD ZONE
			? Misener Sandstone ?	HUNTON ZONE
POST-HUNTON UNCONFORMITY				
	Ulsterian	Hunton	Frisco Fm. Bois d’Arc/Haragan Fm. Henry House Fm.	
Silurian	Niagaran		Chimney Hill: Clarita Fm. Cochrane Fm. ? ?	
			Keel Fm.	
Ordovician	Cincinnatian	Richmond	Sylvan Shale	SVLN ZONE
	Champlainian	Trenton	Viola Limestone “First Wilcox” “Seminole” Sand	ORDOVICIAN ZONE
		Simpson	Bromide Dense Simpson Dolomite Bromide Sand “Second Wilcox” Tulip Creek Fm. McLish Fm. Oil Creek Fm. Joins Fm.	
PRE-SIMPSON UNCONFORMITY				
	Canadian (Beekmantown)	Arbuckle	West Spring Creek Fm. Kinblade Fm. Cool Creek Fm. McKensie Hill Fm. Fort Sill Limestone	ARBUCKLE ZONE
Cambrian	Croixian	Timbered Hills	Honey Creek Limestone Reagan Sandstone	
Basement - Granite				

Figure A-1. A) Base map showing the regional cross sections A-A' (Figure A-2), B-B' (Figure A-3), C-C' (Figure A-4), D-D' (Figure A-5), E-E’ (Figure A-6) and F-F’ (Figure A-7). Orange triangles are wells with LAS for the Hunton Group, green circles are wells with LAS for the Viola Limestone and Simpson Group, and purple square are wells with LAS for the Timbered Hills and Arbuckle groups. B) Generalized Stratigraphic Column of Oklahoma. Modified from Oklahoma Corporation Commissions General Geologic Sections of Oklahoma and Arkansas. The top of Mississippian used for structural modeling is Meramecian in age, and the beginning of this stratigraphic column.

A

A'

MISSISSIPPIAN FORMATION

ORDOVICIAN ZONE

ARBUCKLE ZONE

CRYSTALLINE BASEMENT

HUNTON ZONE

ORDOVICIAN ZONE

OIL CREEK FORMATION

ARBUCKLE GROUP

ARBUCKLE ZONE

REAGAN SANDSTONE

KINDERHOOK SHALE

WOODFORD SHALE

MISENER SANDSTONE

SYLVAN SHALE

WOODFORD SHALE

SYLVAN SHALE

VIOLA LIMESTONE

Simpson Dolomite

SIMPSON GROUP-BROMIDE SANDSTONES

MISSISSIPPIAN FORMATION

TRIPOLITIC CHERT

TRIPOLITIC CHERT

ORDOVICIAN ZONE

ARBUCKLE ZONE

REAGAN SANDSTONE

CRYSTALLINE BASEMENT

BASEMENT DYKE OR SILL

BASEMENT DYKE OR SILL

Figure A-2.Cross Section A-A', location seen on Figure A-1. West-East cross section from Cimarron County to Osage County across northern Oklahoma, flattened on the Mississippian. The first track shows the color filled GR from 0-150 API, measured depth track, followed by a track showing the PEF from 0-20 barnes and RHOB from 2.0-3.0 g/cc. Mineral percentage curves calculated seen in the next track, and the dominant lithology seen in the last track were generated from methods found in Chapters 2-4 of this study. Color filled gamma-ray between wells.

B

B’

MISSISSIPPIAN FORMATION

KINDERHOOK SHALE

WOODFORD SHALE

HUNTON ZONE

HUNTON GROUP

SYLVAN SHALE

HUNTON ZONE

SYLVAN SHALE

ORDOVICIAN ZONE

SIMPSON GROUP-BROMIDE SANDSTONES

OIL CREEK FORMATION

ARBUCKLE ZONE

CRYSTALLINE BASEMENT

BASEMENT DYKE OR SILL

VIOLA LIMESTONE

SIMPSON GROUP
BROMIDE SANDSTONES

REAGAN SANDSTONE

MISSISSIPPIAN FORMATION

ORDOVICIAN ZONE

ARBUCKLE ZONE

REAGAN SANDSTONE

CRYSTALLINE BASEMENT

Figure A-3.Cross Section B-B', location seen on Figure A-1. West-East cross section from Cimarron County to Osage County across northern Oklahoma, flattened on the Mississippian. The first track shows the color filled GR from 0-150 API, measured depth track, followed by a track showing the PEF from 0-20 barnes and RHOB from 2.0-3.0 g/cc. Mineral percentage curves calculated seen in the next track, and the dominant lithology seen in the last track were generated from methods found in Chapters 2-4 of this study. Color filled gamma-ray between wells.

C

C'

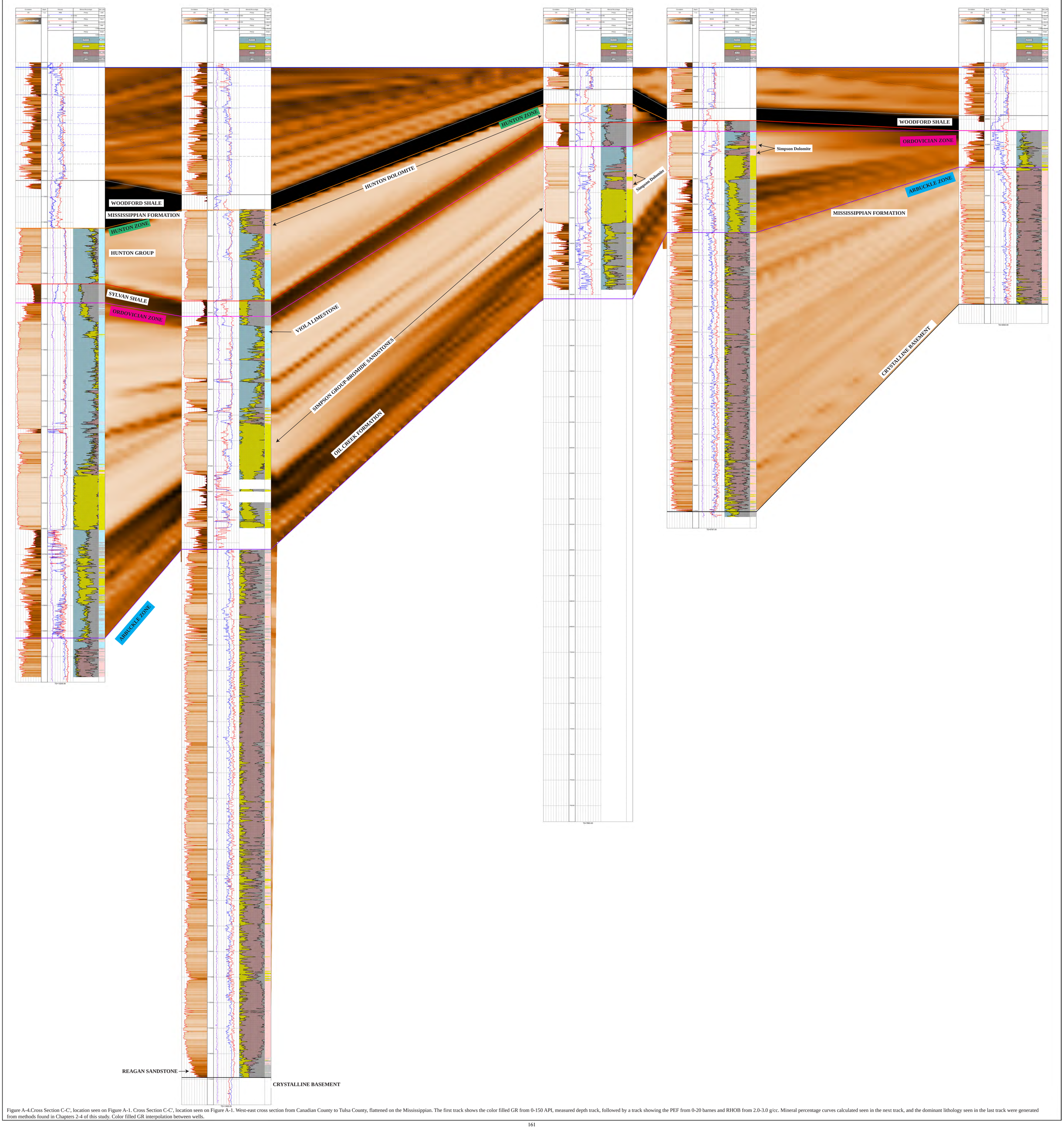


Figure A-4.Cross Section C-C', location seen on Figure A-1. Cross Section C-C', location seen on Figure A-1. West-east cross section from Canadian County to Tulsa County, flattened on the Mississippian. The first track shows the color filled GR from 0-150 API, measured depth track, followed by a track showing the PEF from 0-20 barnes and RHOB from 2.0-3.0 g/cc. Mineral percentage curves calculated seen in the next track, and the dominant lithology seen in the last track were generated from methods found in Chapters 2-4 of this study. Color filled GR interpolation between wells.

D

D’

MISSISSIPPIAN FORMATION

WOODFORD SHALE

HUNTON ZONE

HUNTON GROUP

SYLVAN SHALE

ORDOVICIAN ZONE

VIOLA LIMESTONE

Simpson Dolomite

SIMPSON GROUP-BROMIDE SANDSTONES

OIL CREEK FORMATION

ARBUCKLE ZONE

CRYSTALLINE BASEMENT

REAGAN SANDSTONE

Figure A-5.Cross Section D-D', location seen on Figure A-1. Cross Section D-D', location seen on Figure A-1. Southwest-northeast cross section from southwestern McClain County to Okmulgee County Oklahoma, flattened on the Mississippian. The first track shows the color filled GR from 0-150 API, measured depth track, followed by a track showing the PEF from 0-20 barnes and RHOB from 2.0-3.0 g/cc. Mineral percentage curves calculated seen in the next track, and the dominant lithology seen in the last track were generated from methods found in Chapters 2-4 of this study. Color filled GR interpolation between wells.



Figure A-6. Cross Section E-E', location seen on Figure A-1. Southwest-northeast cross section from southern Hughes County to McIntosh County, flattened on the Mississippian. The first track shows the color filled GR from 0-150 API, measured depth track, followed by a track showing the PEF from 0-20 barnes and RHOB from 2.0-3.0 g/cc. Mineral percentage curves calculated seen in the next track, and the dominant lithology seen in the last track were generated from methods found in Chapters 2-4 of this study. Color filled GR interpolation between wells.

F

F'

MISSISSIPPIAN FORMATION

WOODFORD SHALE

HUNTON ZONE

ORDOVICIAN ZONE

SYLVAN SHALE

OIL CREEK FORMATION

ARBUCKLE ZONE

CRYSTALLINE BASEMENT

Simpson Dolomite

HUNTON GROUP

VIOLA LIMESTONE

SIMPSON GROUP-BROMIDE SANDSTONES

OIL CREEK FORMATION

BASEMENT DYKE OR SILL

REAGAN SANDSTONE

MISSISSIPPIAN FORMATION

WOODFORD SHALE

HUNTON ZONE

SYLVAN SHALE

ORDOVICIAN ZONE

Simpson Dolomite

ARBUCKLE ZONE

REAGAN SANDSTONE

CRYSTALLINE BASEMENT

Figure A-7. Cross Section F-F', location seen on Figure A-1. Northwest-southeast cross section from Harpy County to Hughes County, flattened on the Woodford Shale. The first track shows the color filled GR from 0-150 API, measured depth track, followed by a track showing the PEF from 0-20 barnes and RHOB from 2.0-3.0 g/cc. Mineral percentage curves calculated seen in the next track, and the dominant lithology seen in the last track were generated from methods found in Chapters 2-4 of this study. Color filled GR interpolation between wells.

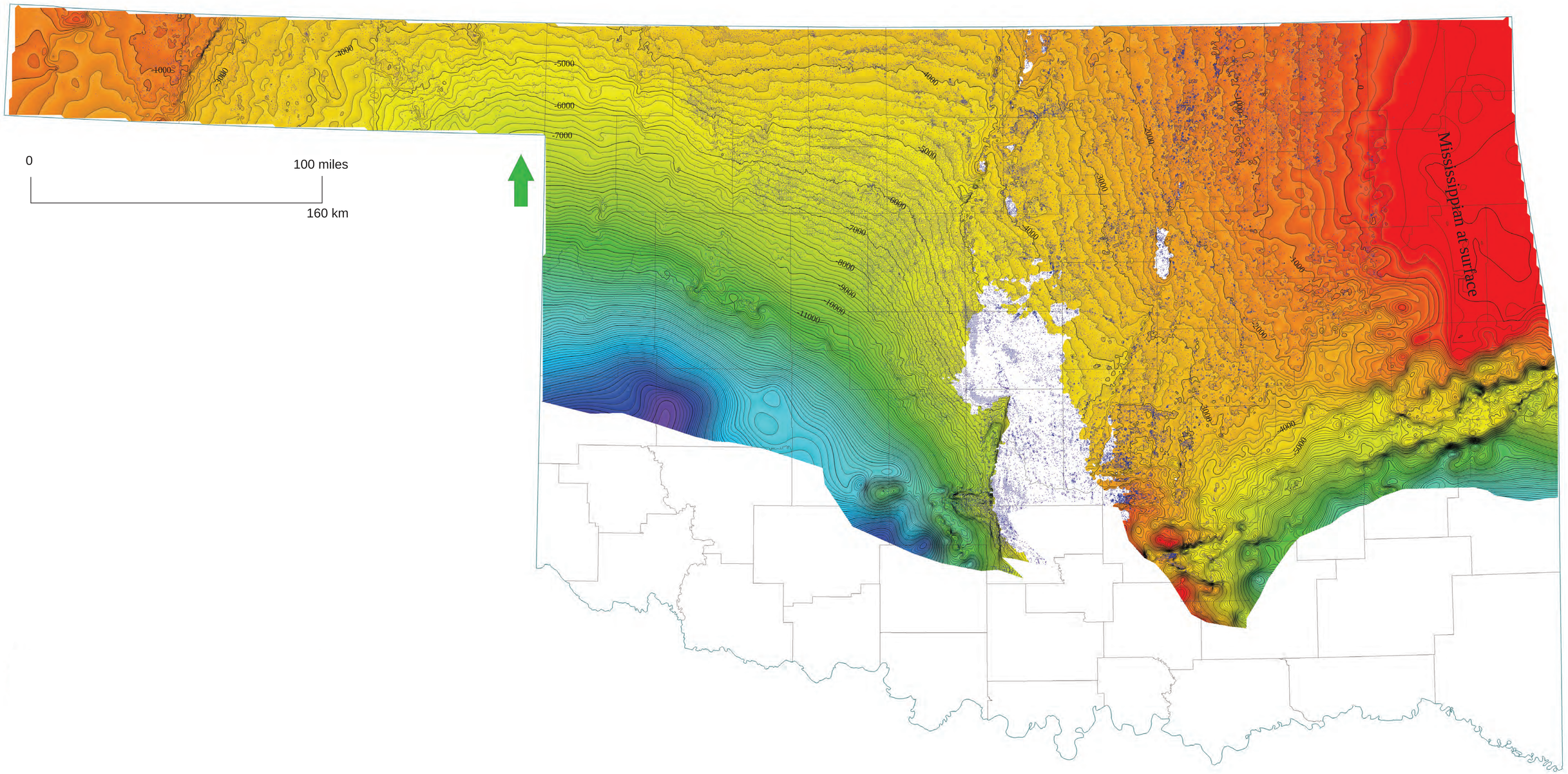


Figure A-8: Mississippian Structure Map. 200 ft contour interval, 1000 ft bold contour interval. Well control shown. The Mississippian Formation (regionally called the Pitkin Limestone and Boone Formation) outcrops at the surface in northeastern Oklahoma.

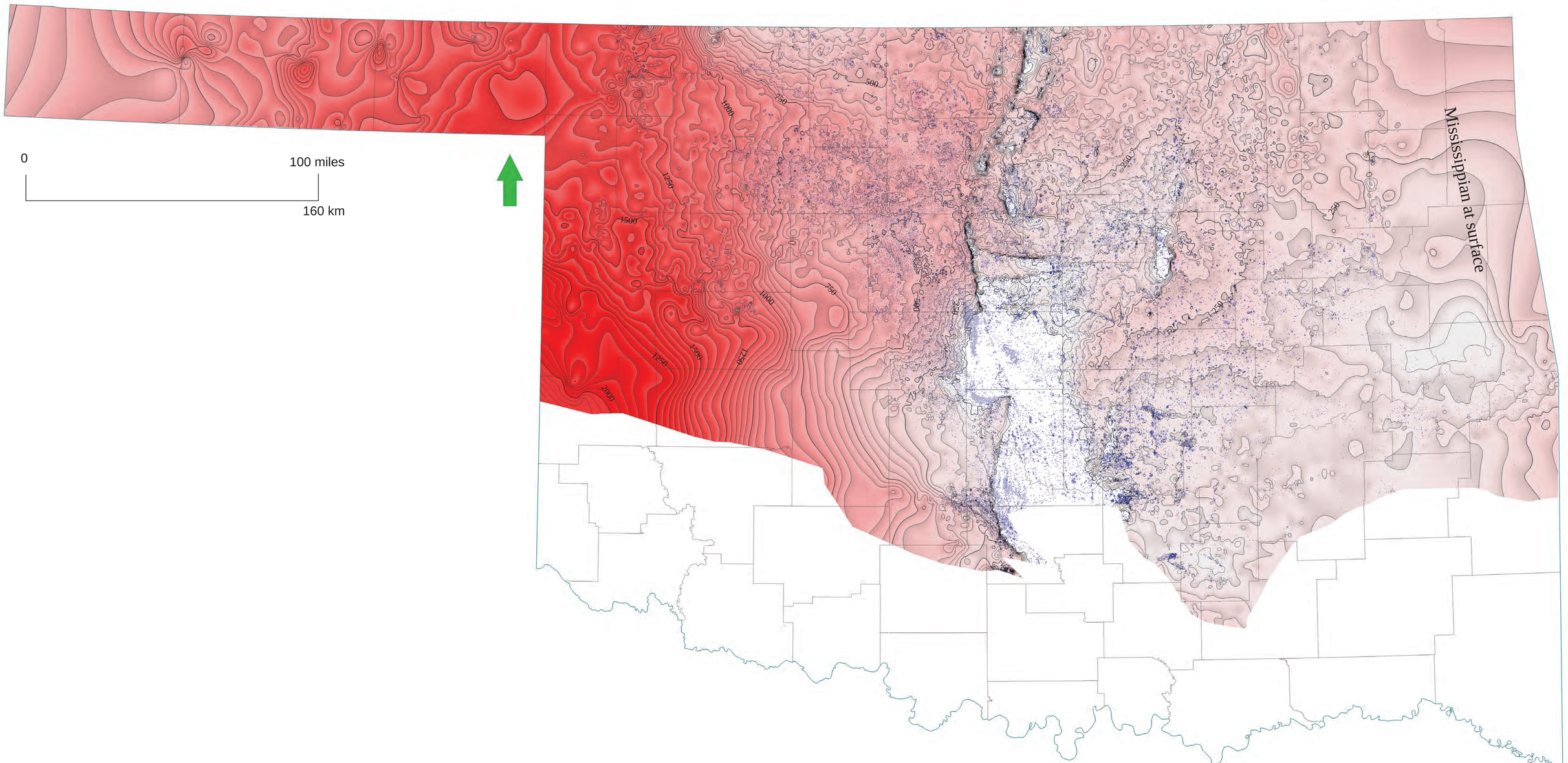


Figure A-9: Mississippian Isopach map. 50 ft contour interval, 250 ft bold contour interval. Well control shown. The Mississippian Formation (regionally called the Pitkin Limestone and Boone Formation) outcrops at the surface in northeastern Oklahoma.

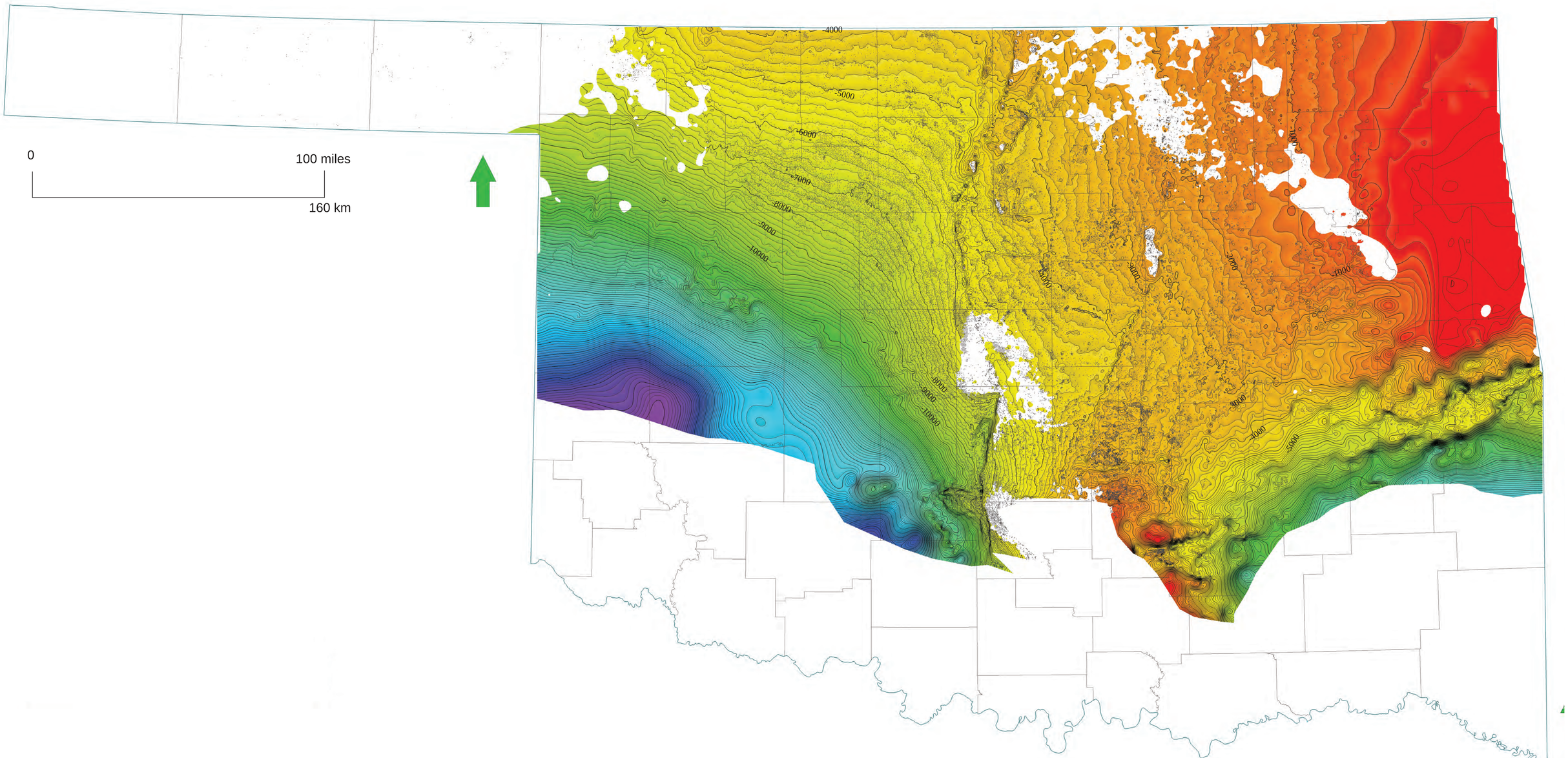


Figure A-10: Woodford Structure map. 200 ft contour interval, 1000 ft bold contour interval. Well control shown.

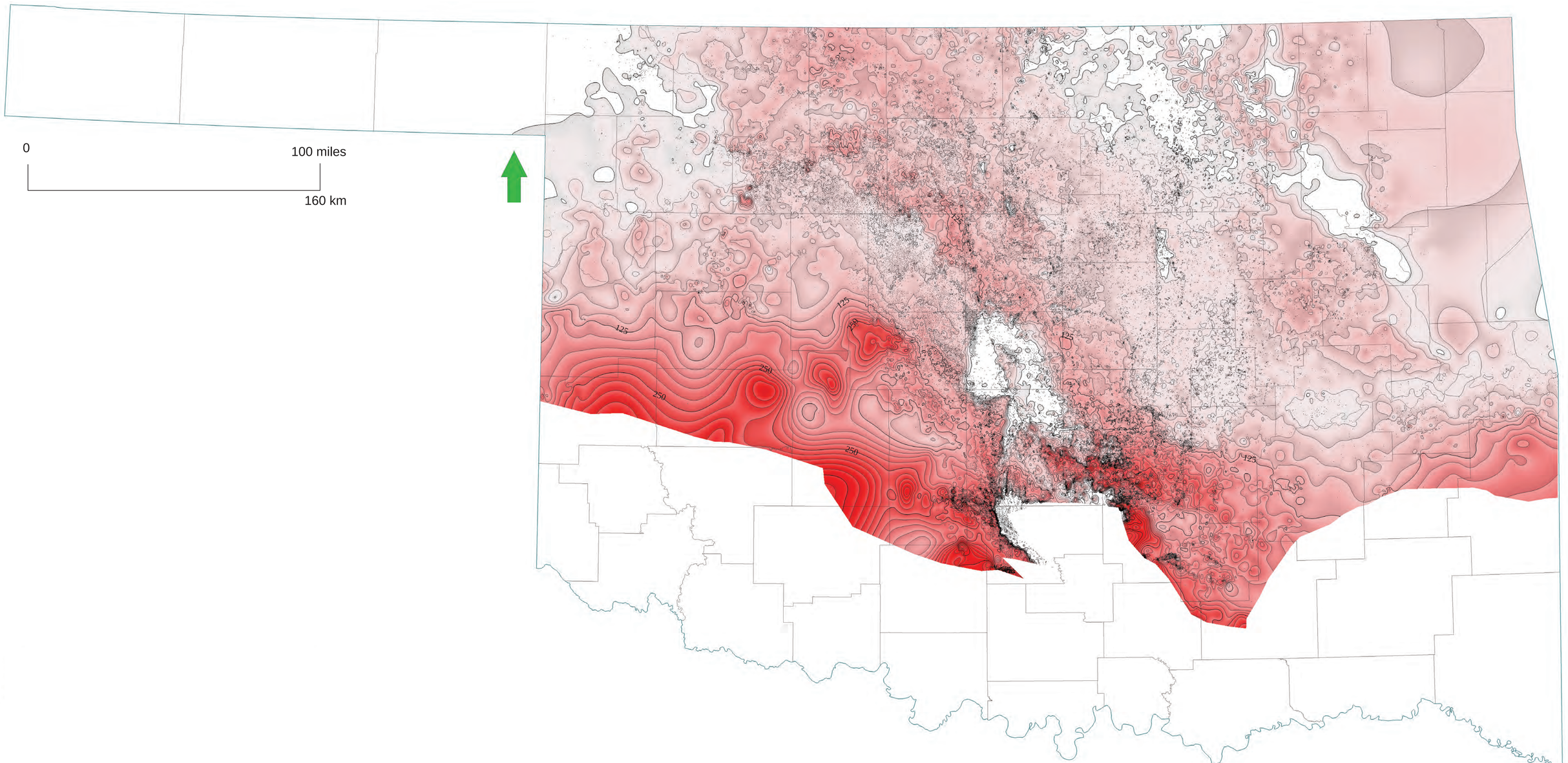


Figure A-11: Woodford Isopach map. 25 ft contour interval, 125 ft bold contour interval. Well control shown.

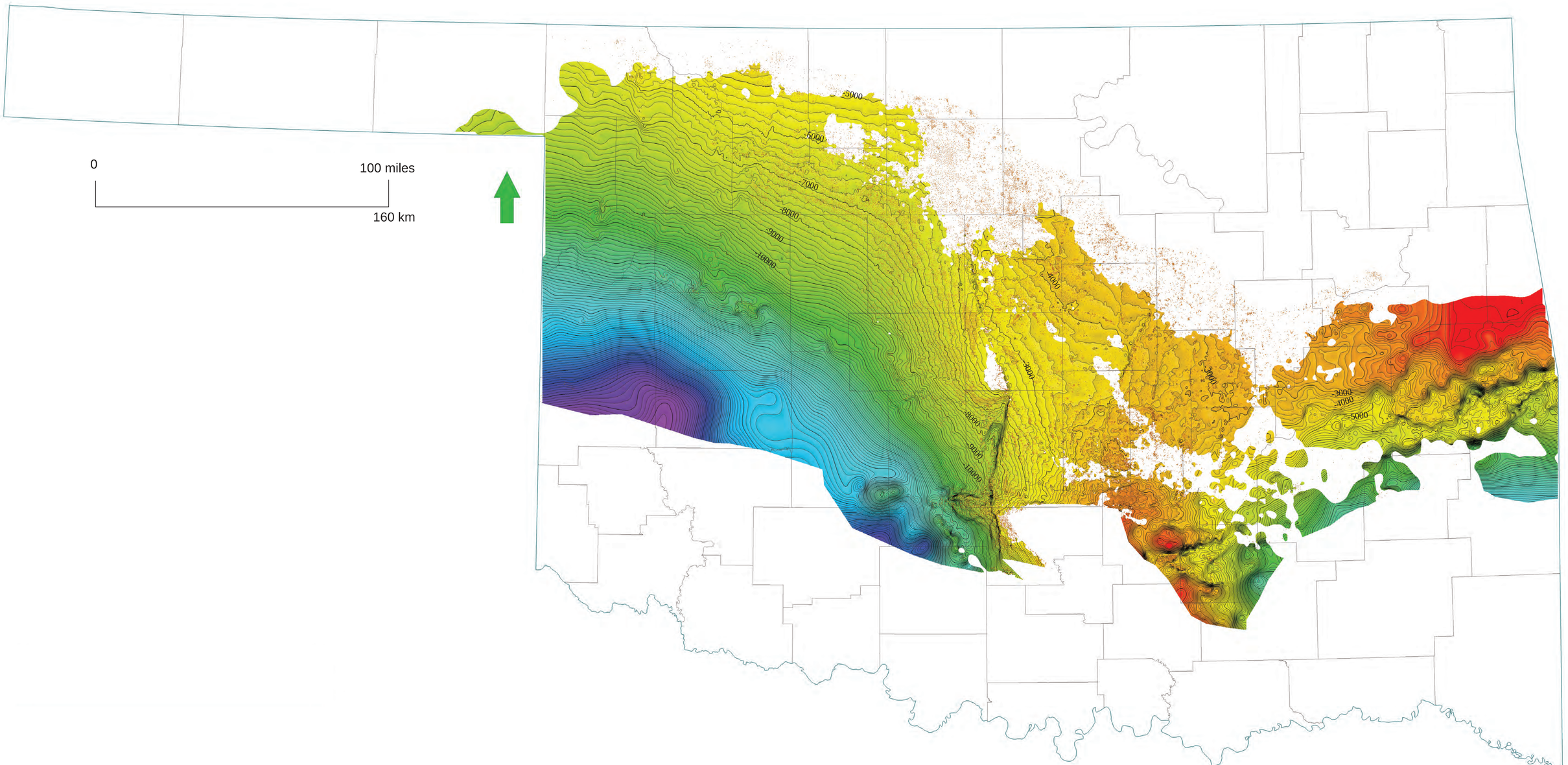


Figure A-12: Hunton Group Structure Map. 200 ft contour interval, 1000 ft bold contour interval. Well control shown.

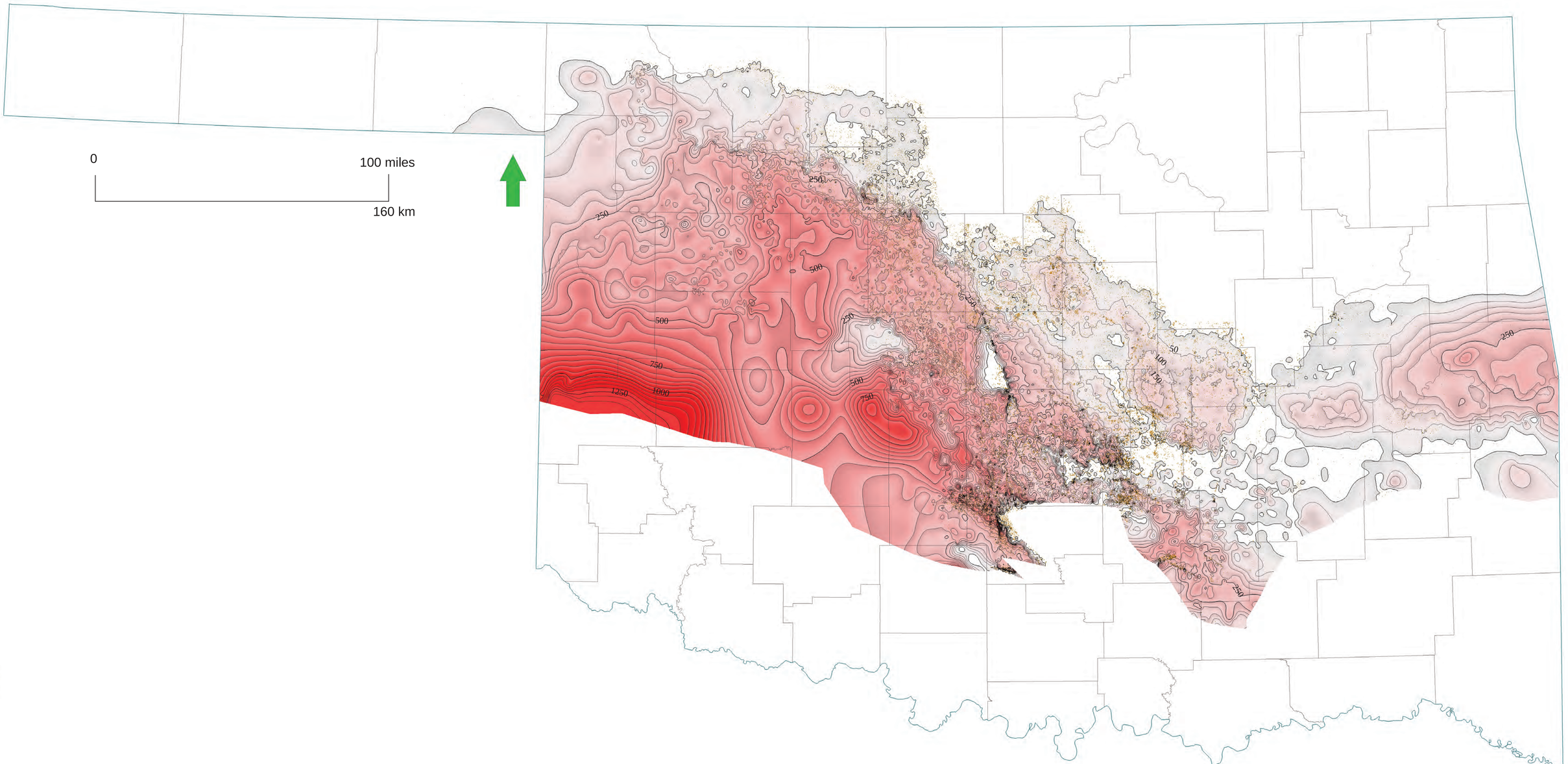


Figure A-13: Hunton Group Isopach map. 50 ft contour interval, 250 ft bold contour interval. Well control shown.

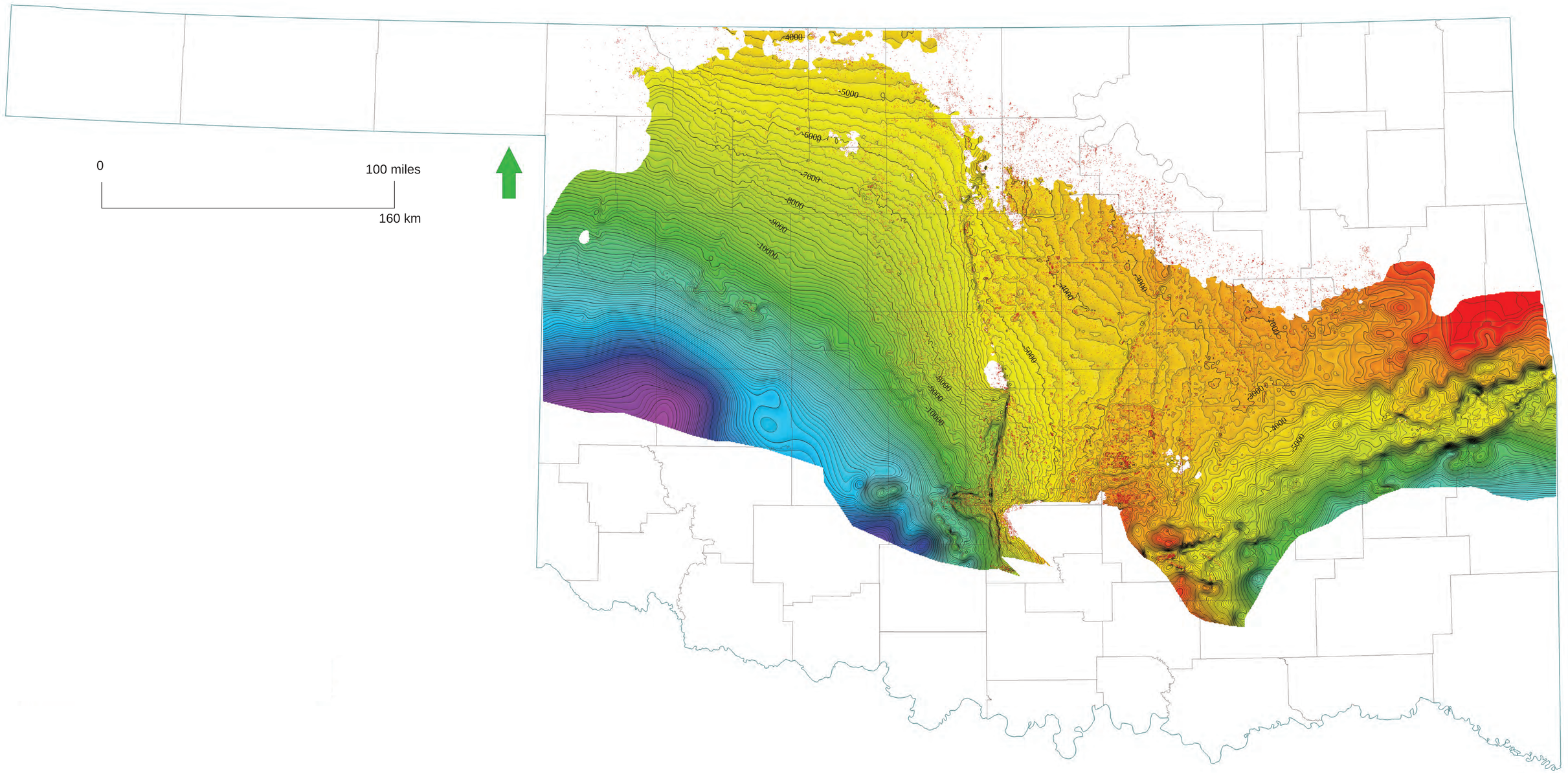


Figure A-14: Sylvan Shale Structure Map. 200 ft contour interval, 1000 ft bold contour interval. Well control shown.

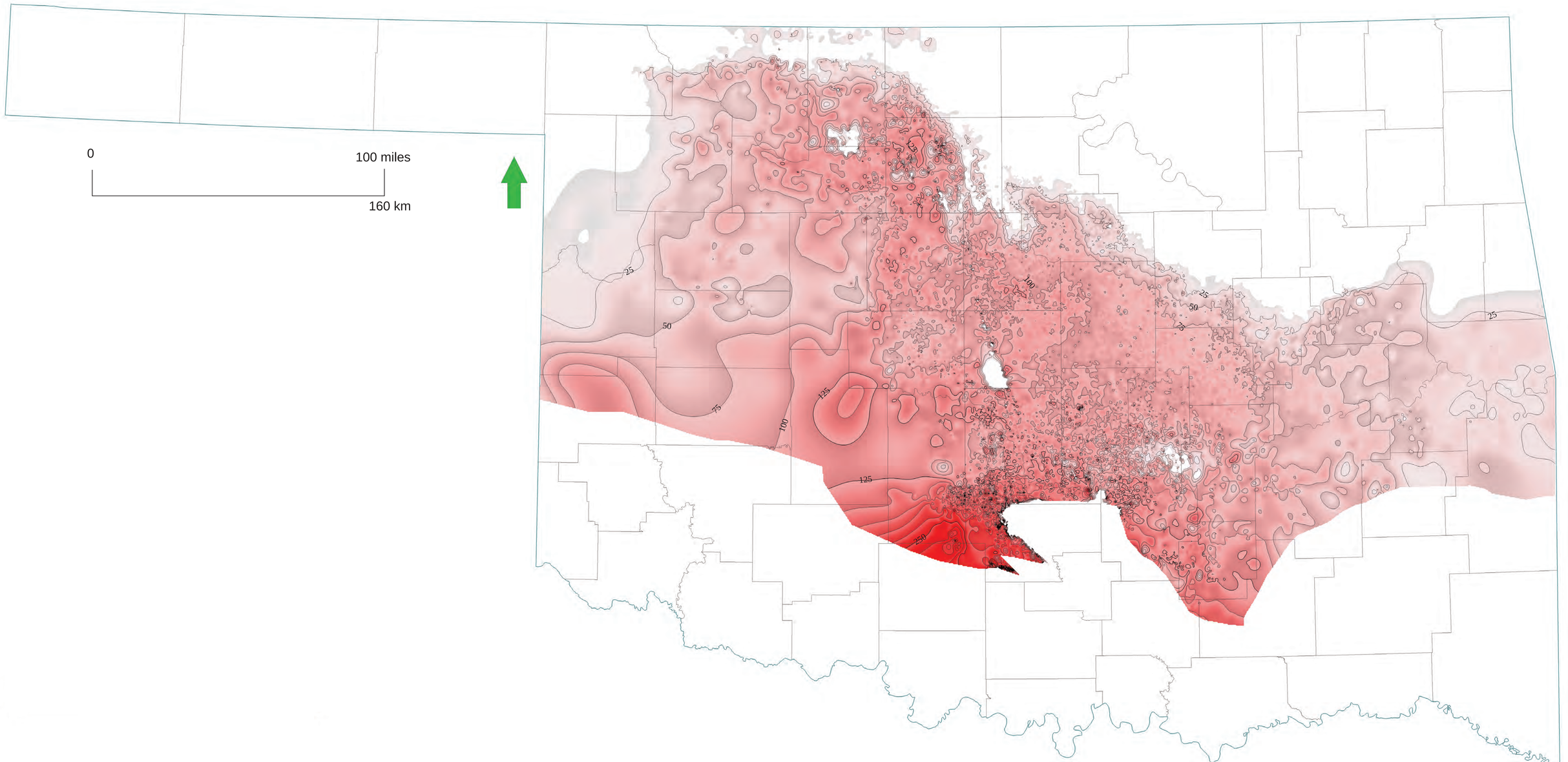


Figure A-15: Sylvan Shale Isopach map. 25 ft contour interval, 125 ft bold contour interval. Well control shown.

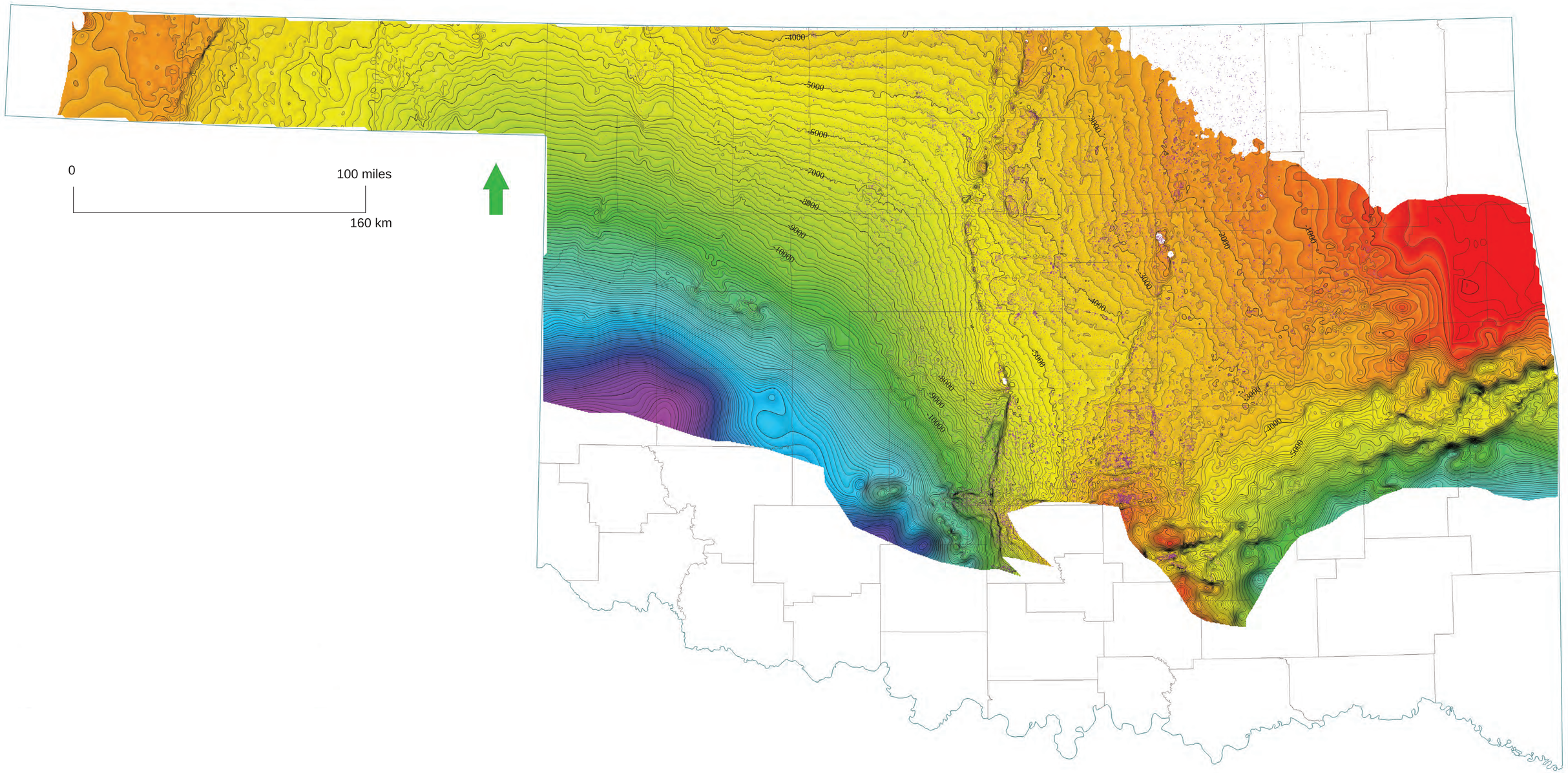


Figure A-16: Viola Limestone (Ordovician) Structure Map. 200 ft contour interval, 1000 ft bold contour interval. Well control shown.

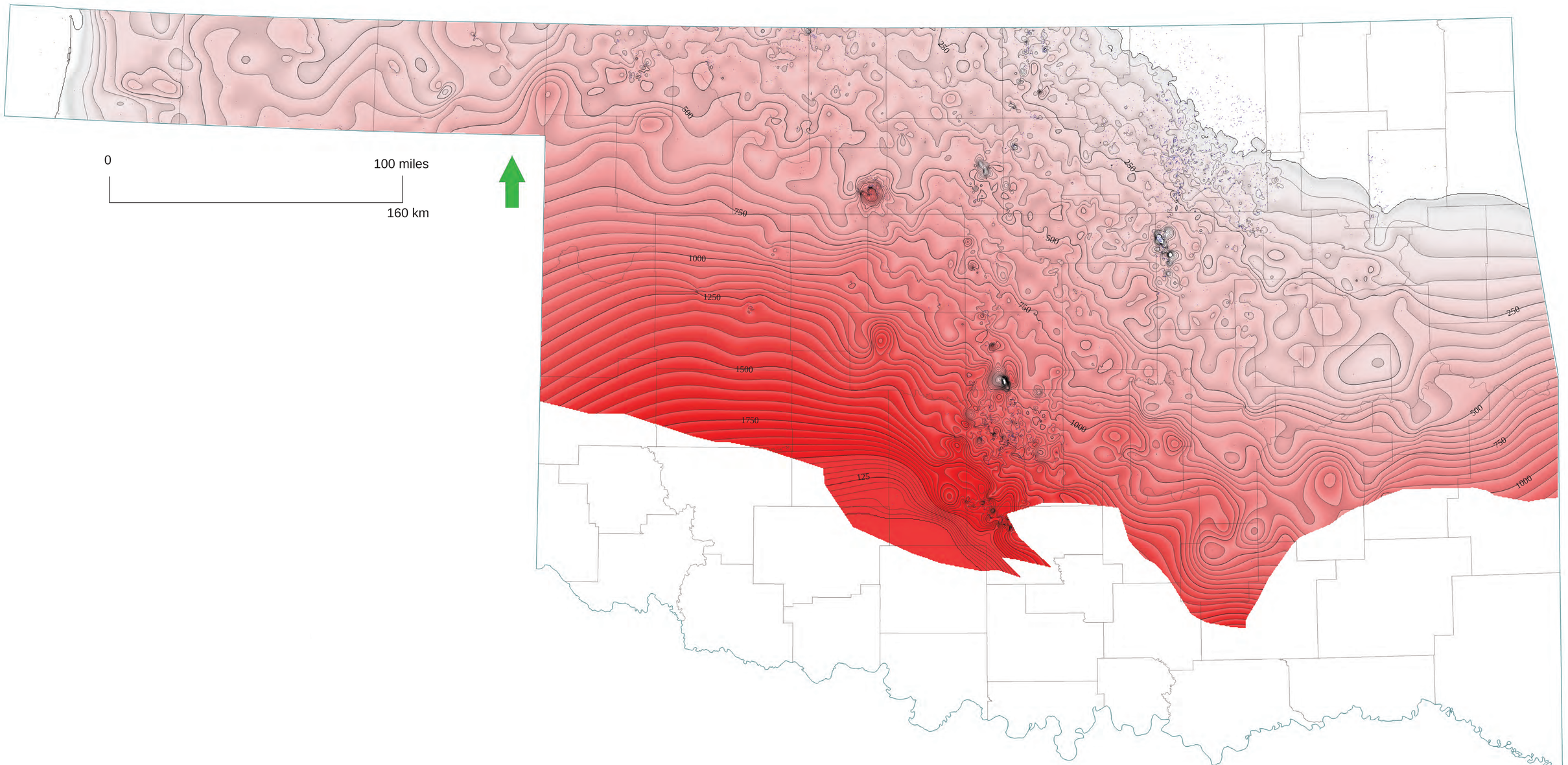


Figure A-17: Ordovician Isopach map. 50 ft contour interval, 250 ft bold contour interval. Well control shown.

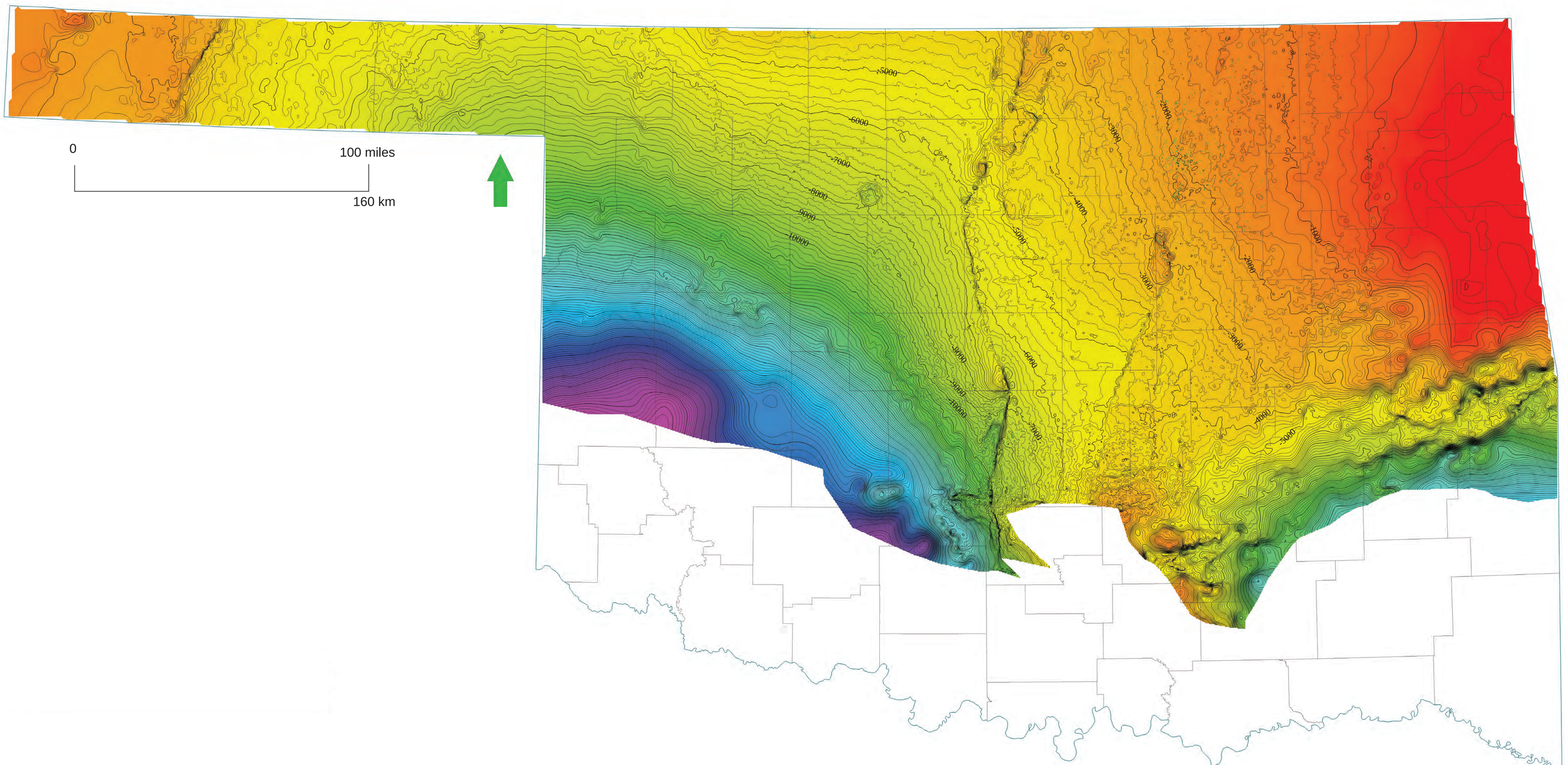


Figure A-18: Arbuckle Group Structure Map. 200 ft contour interval, 1000 ft bold contour interval. Well control shown.

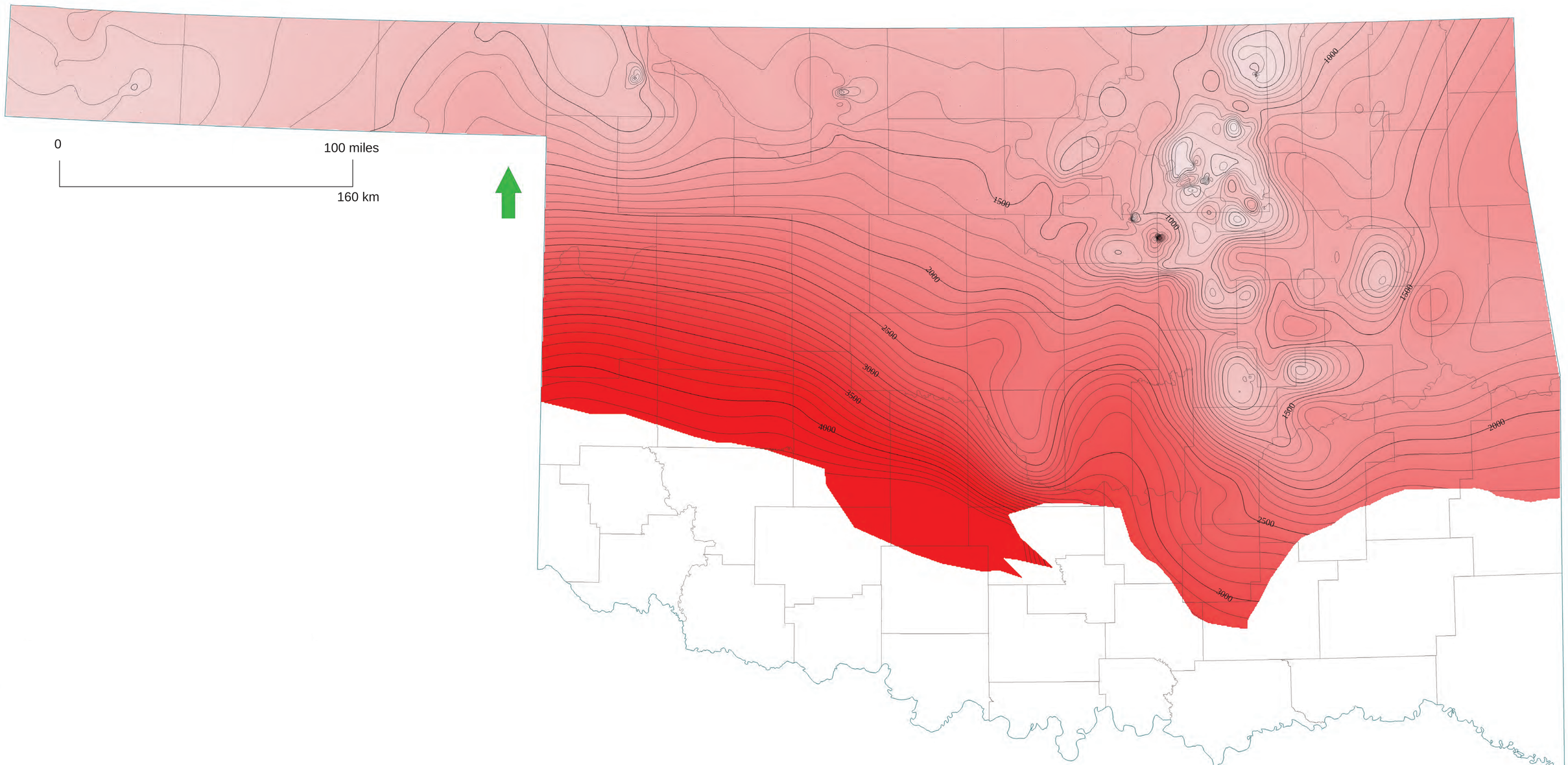


Figure A-19: Arbuckle Isopach map. 100 ft contour interval, 500 ft bold contour interval. Well control shown.

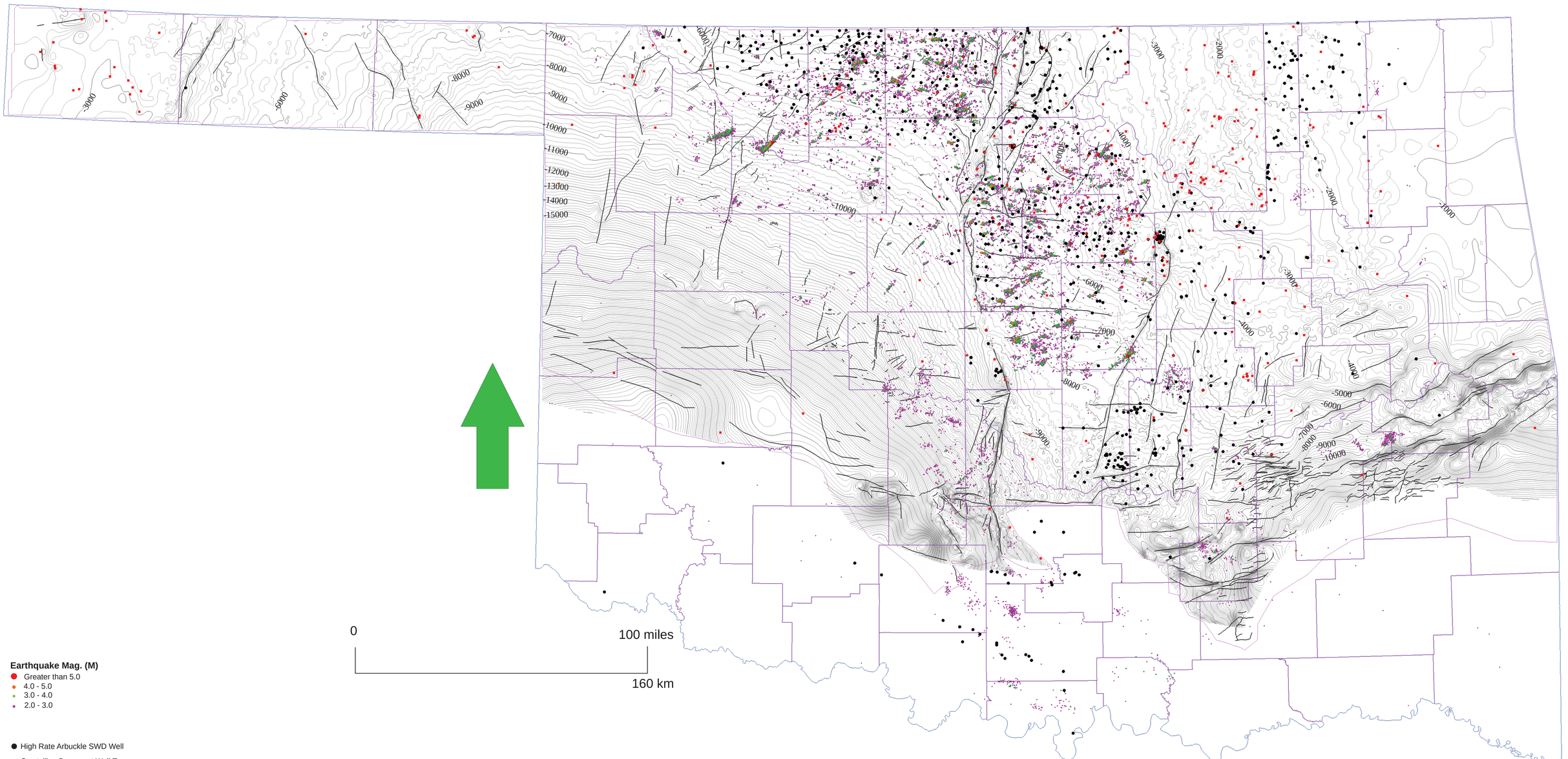


Figure A-20. Crystalline Basement Structure Map and well control (red squares). 200 ft contour interval, 1,000 ft bold contour interval. Faults shown are from the Comprehensive Fault Database (Holloway et al, 2016) for the state of Oklahoma from the OGS and additional interpreted by the author from this study. All Earthquakes from 2011-2013 above 2.0 M. High-rate Arbuckle SWD Injection wells shown.

APPENDIX B:

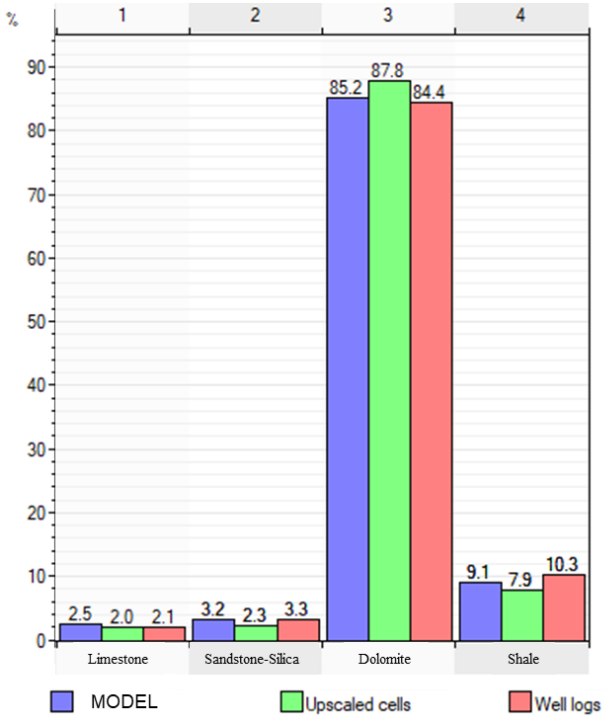


Figure B-1: Lithology model histogram for the Arbuckle zone, Chapter 1.

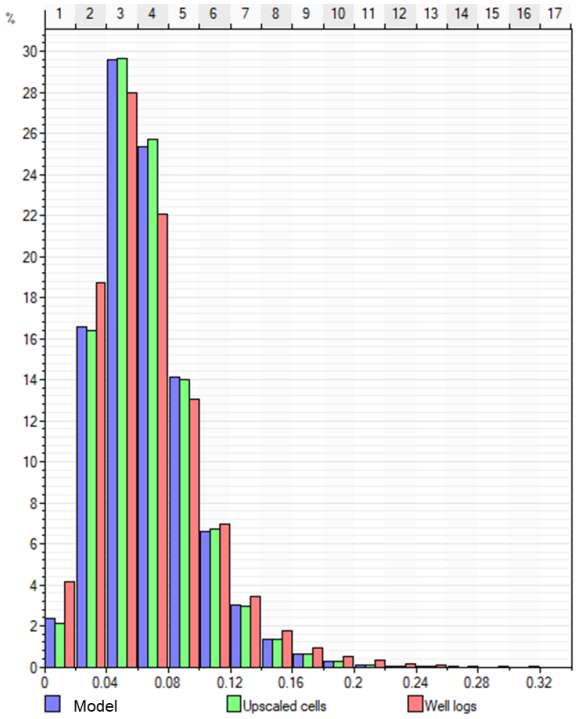


Figure B-2: Porosity model histogram for the Arbuckle zone, Chapter 1.

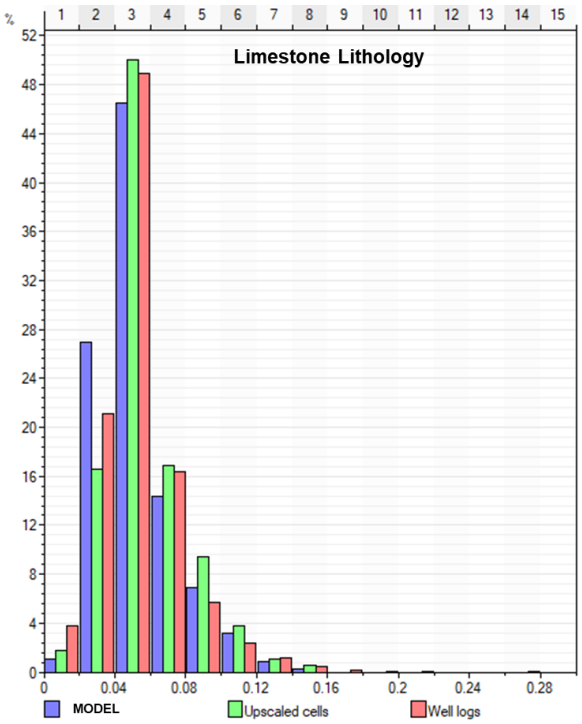


Figure B-3: Porosity model histogram for limestone lithology only, for the Arbuckle zone, Chapter 1.

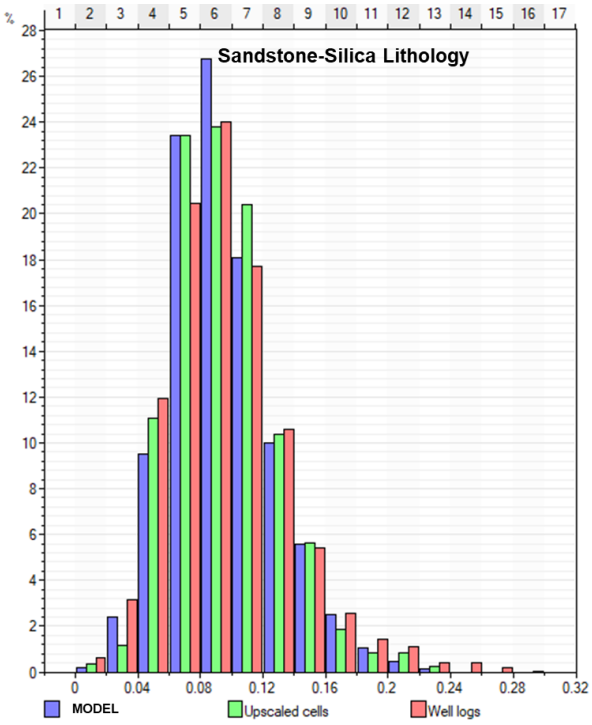


Figure B-4: Porosity model histogram for sandstone-silica lithology only, for the Arbuckle zone, Chapter 1.

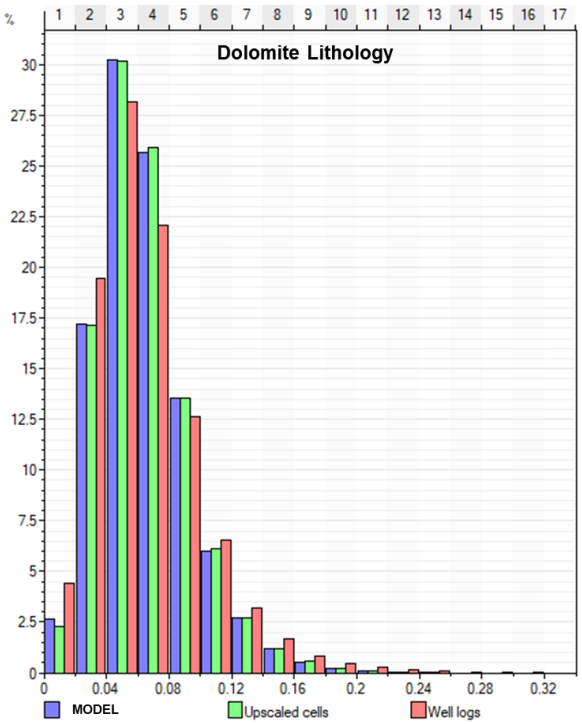


Figure B-5: Porosity model histogram for dolomite only, for the Arbuckle zone, Chapter 1.

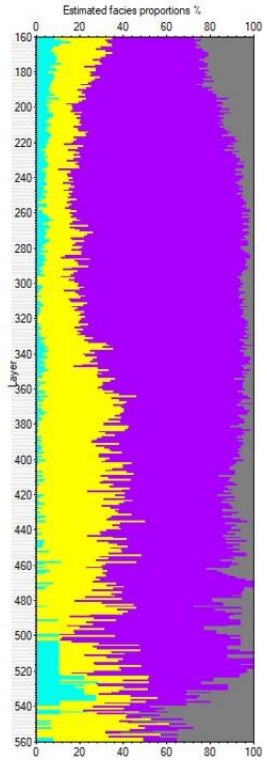


Figure B-6: Vertical Proportion curve for the Arbuckle zone, Chapter 1. Blue is limestone, yellow is sandstone-silica, purple is dolomite and grey is shale.

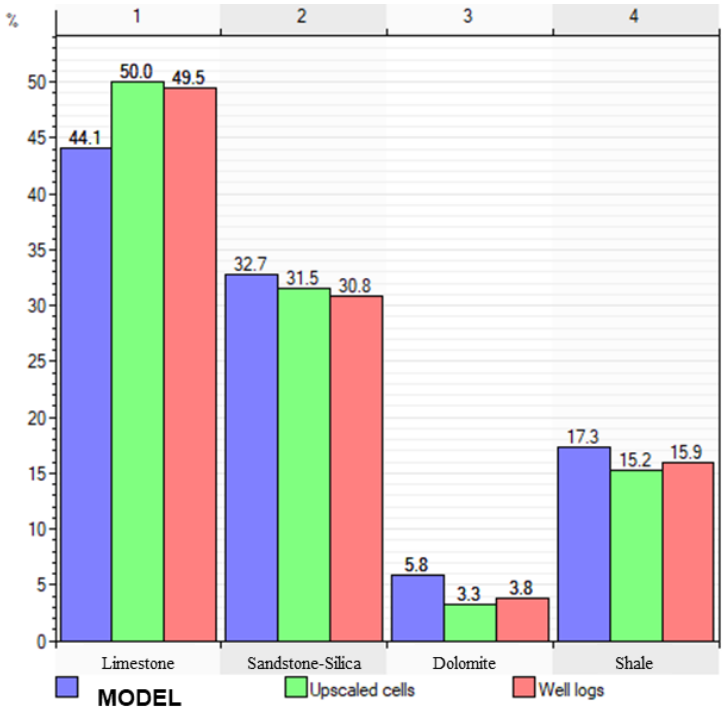


Figure B-7: Lithology model histogram, for the Ordovician zone, Chapter 2.

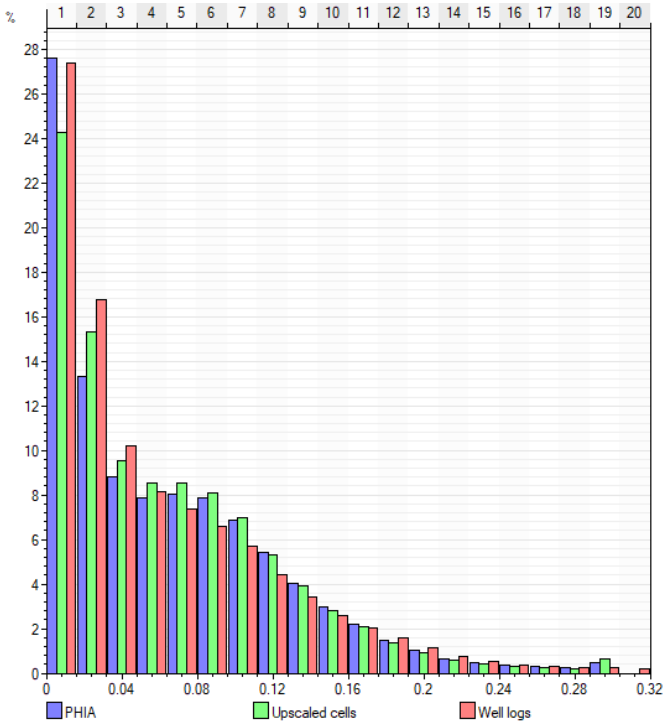


Figure B-8: Porosity model histogram, for the Ordovician zone, Chapter 2.

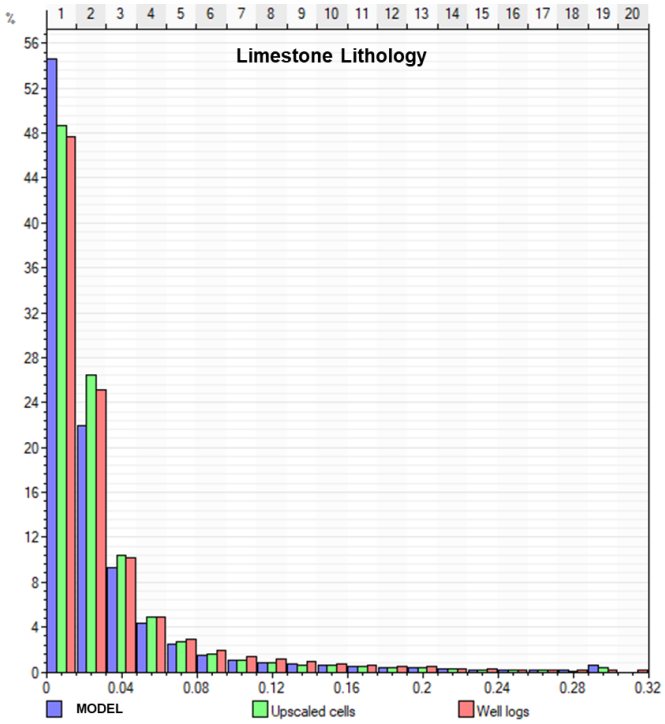


Figure B-9: Porosity model histogram for limestone lithology, for the Ordovician zone, Chapter 2.

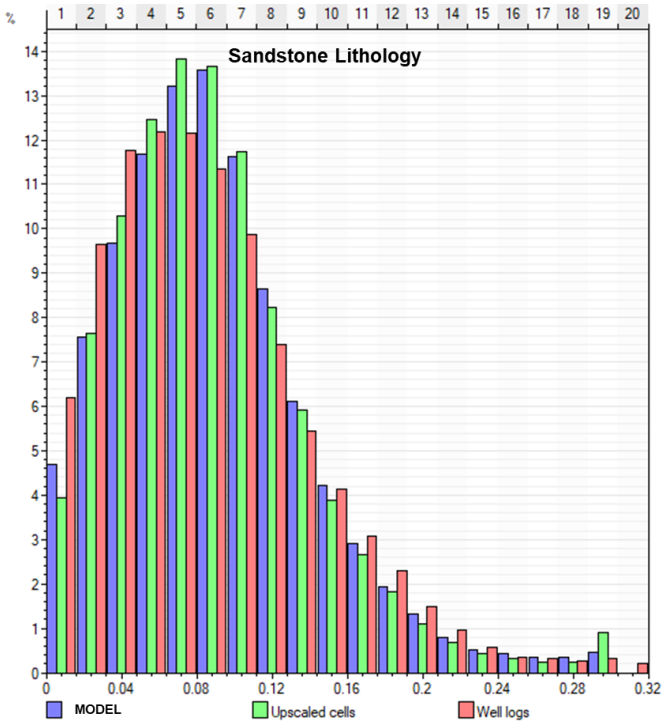


Figure B-10: Porosity model histogram for sandstone lithology, for the Ordovician zone, Chapter 2.

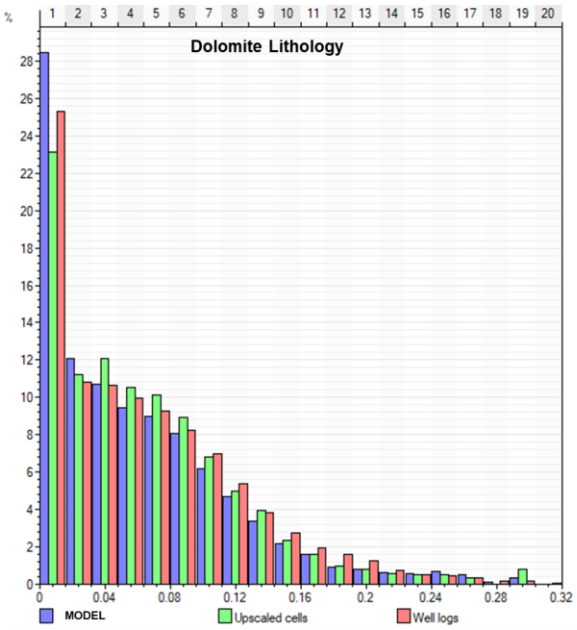


Figure B-11: Porosity model histogram for dolomite lithology, for the Ordovician zone, Chapter 2.

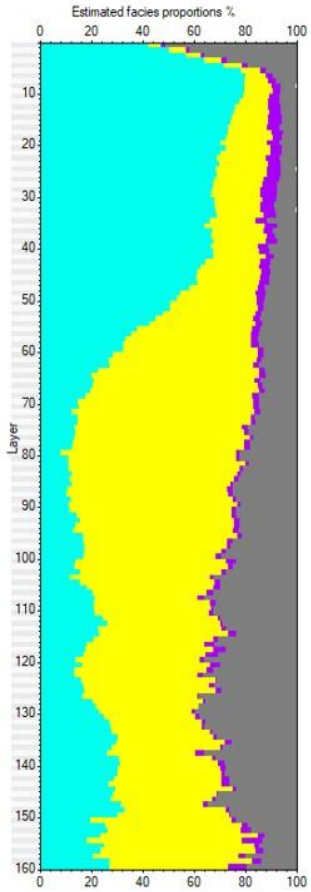


Figure B-12: Vertical proportion curve for the Ordovician zone, Chapter 2.

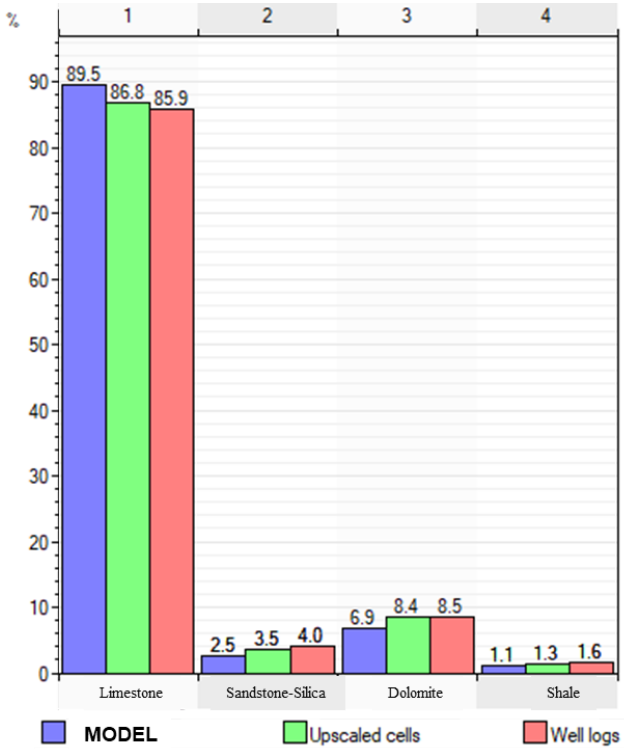


Figure B-13: Lithology model histogram for the Hunton zone, Chapter 3.

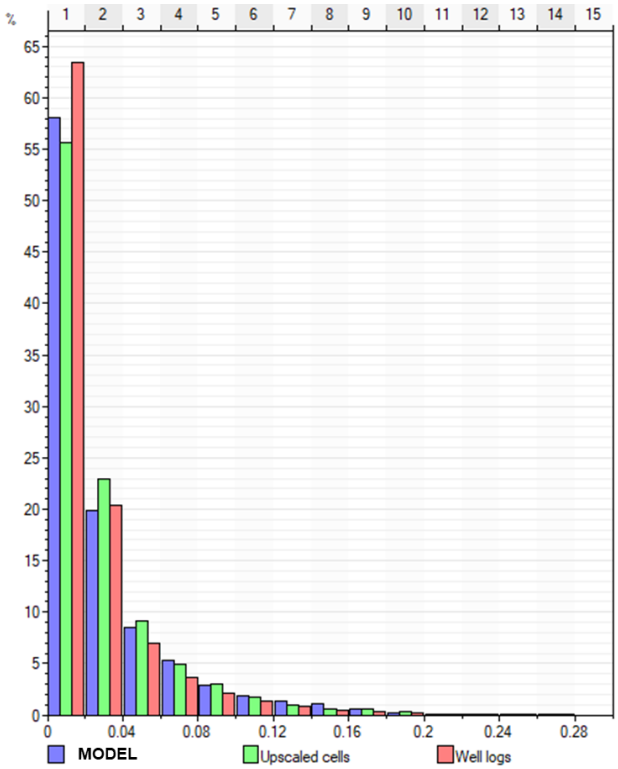


Figure B-14: Porosity model histogram for the Hunton zone, Chapter 3.

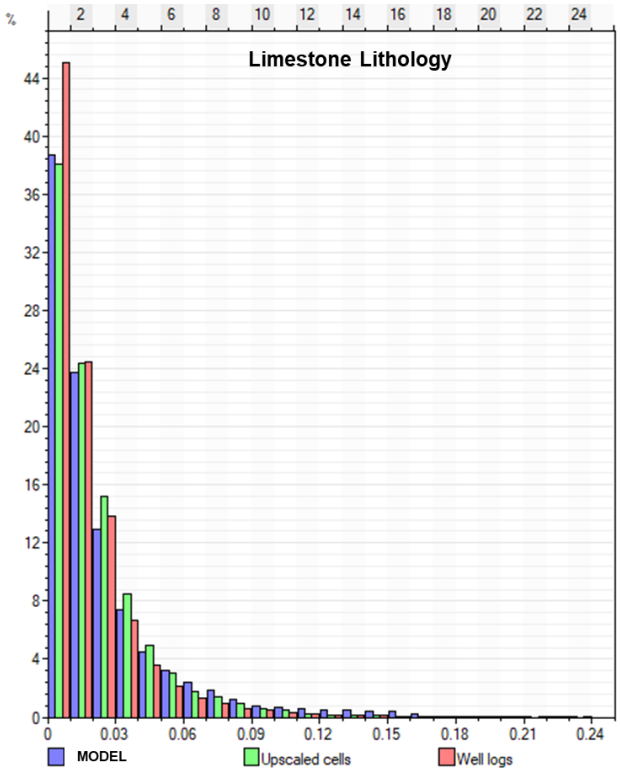


Figure B-15: Porosity model histogram for limestone lithology for the Hunton zone, Chapter 3.

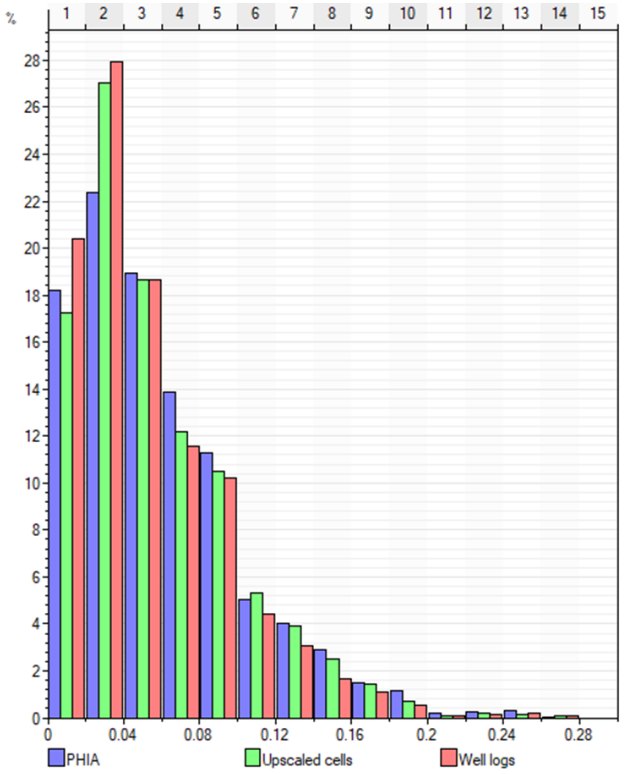


Figure B-16: Porosity model histogram for sandstone-silica lithology for the Hunton zone, Chapter 3.

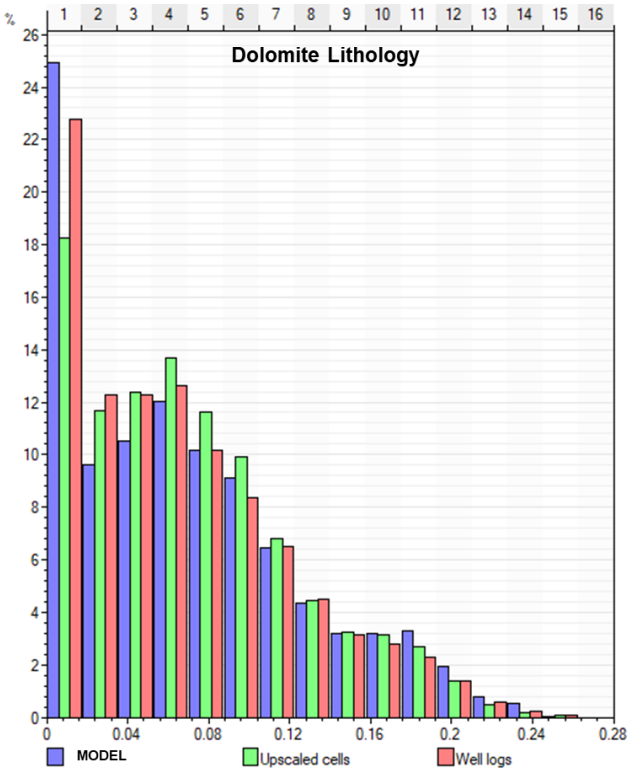


Figure B-17: Porosity model histogram for dolomite lithology for the Hunton zone, Chapter 3.

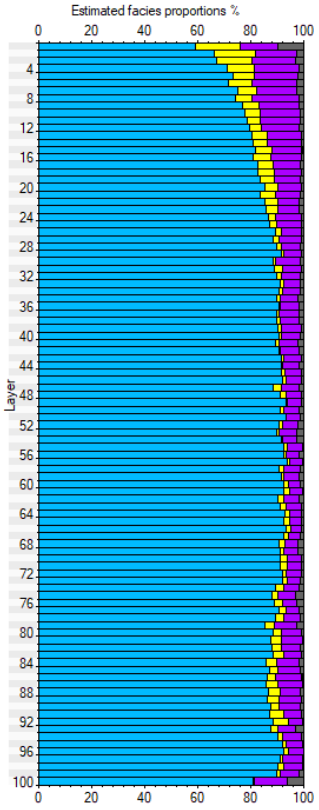


Figure B-18: Vertical proportion curve for the Hunton zone

APPENDIX C:

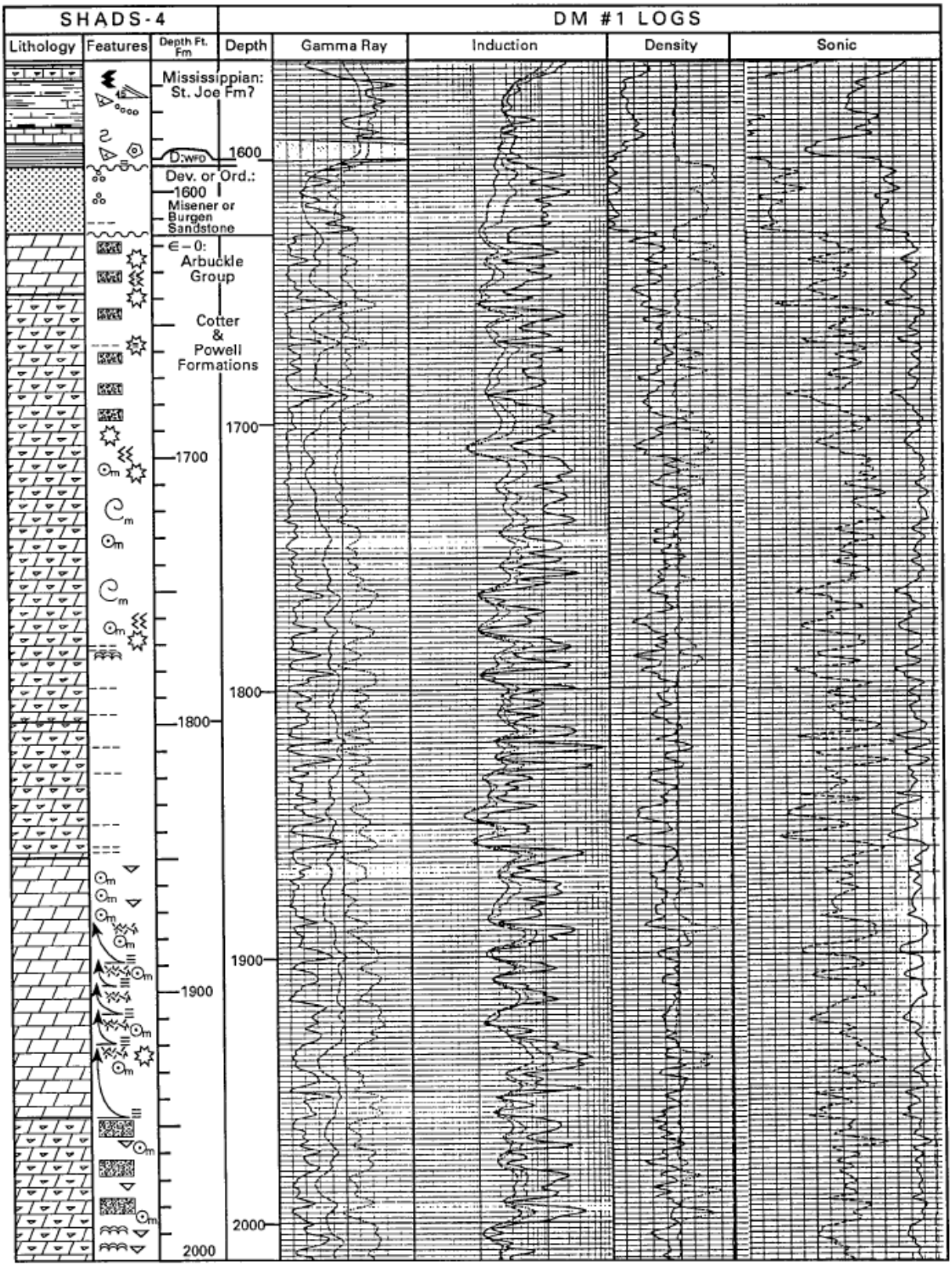

SHADS-4
DM #1 LOGS
Lithology
Features
Depth Ft. Fm
Depth
Gamma Ray
Induction
Density
Sonic
Mississippian: St. Joe Fm?
D;WFD
1600
Dev. or Ord.:
1600
Misener or Burgen Sandstone
∈–0: Arbuckle Group
Cotter & Powell Formations
1700
1800
1900
2000

Figure C-1: SHAD 4 Core description from Derby, 1991.

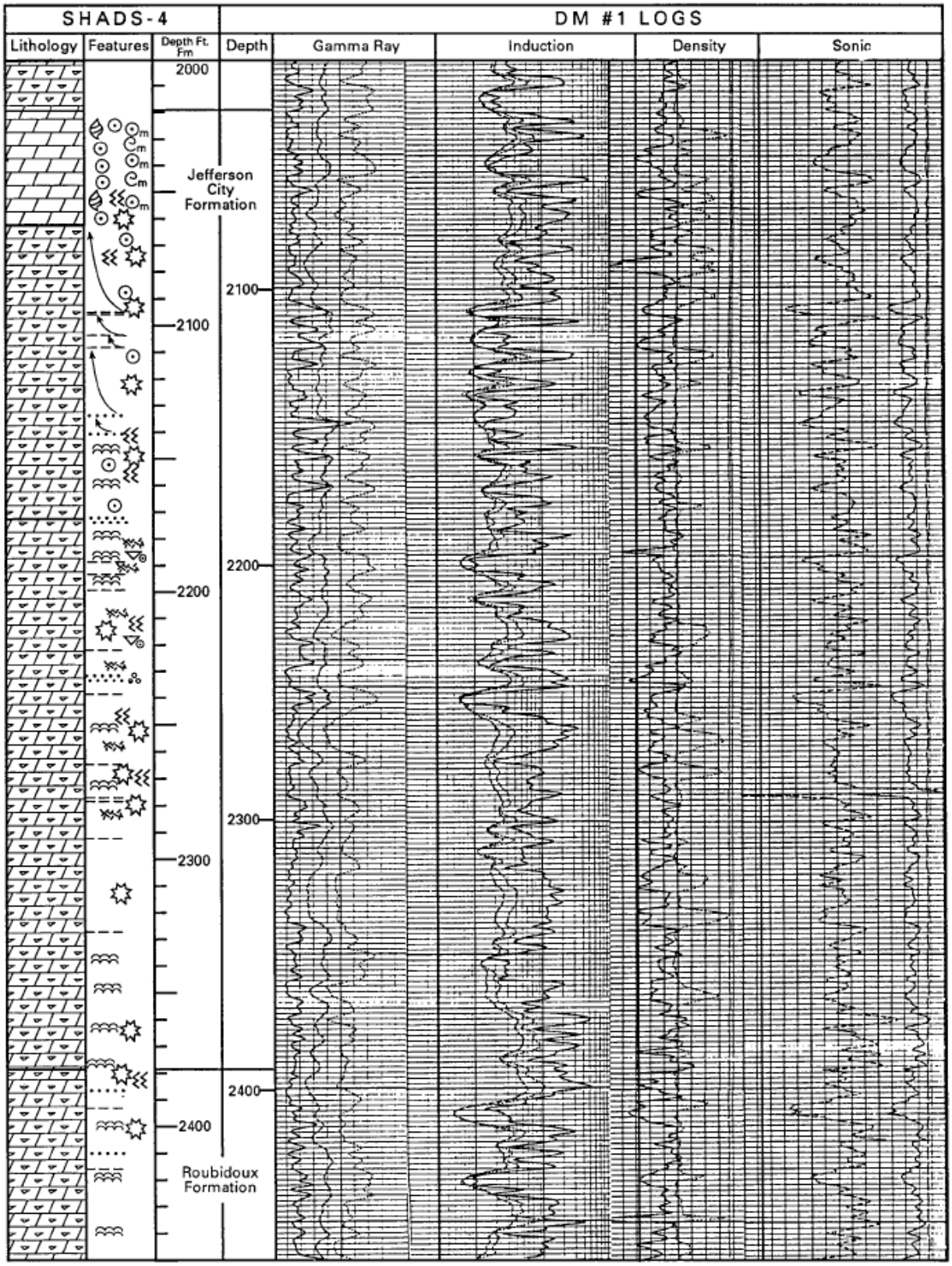


Figure C-1: (continued)

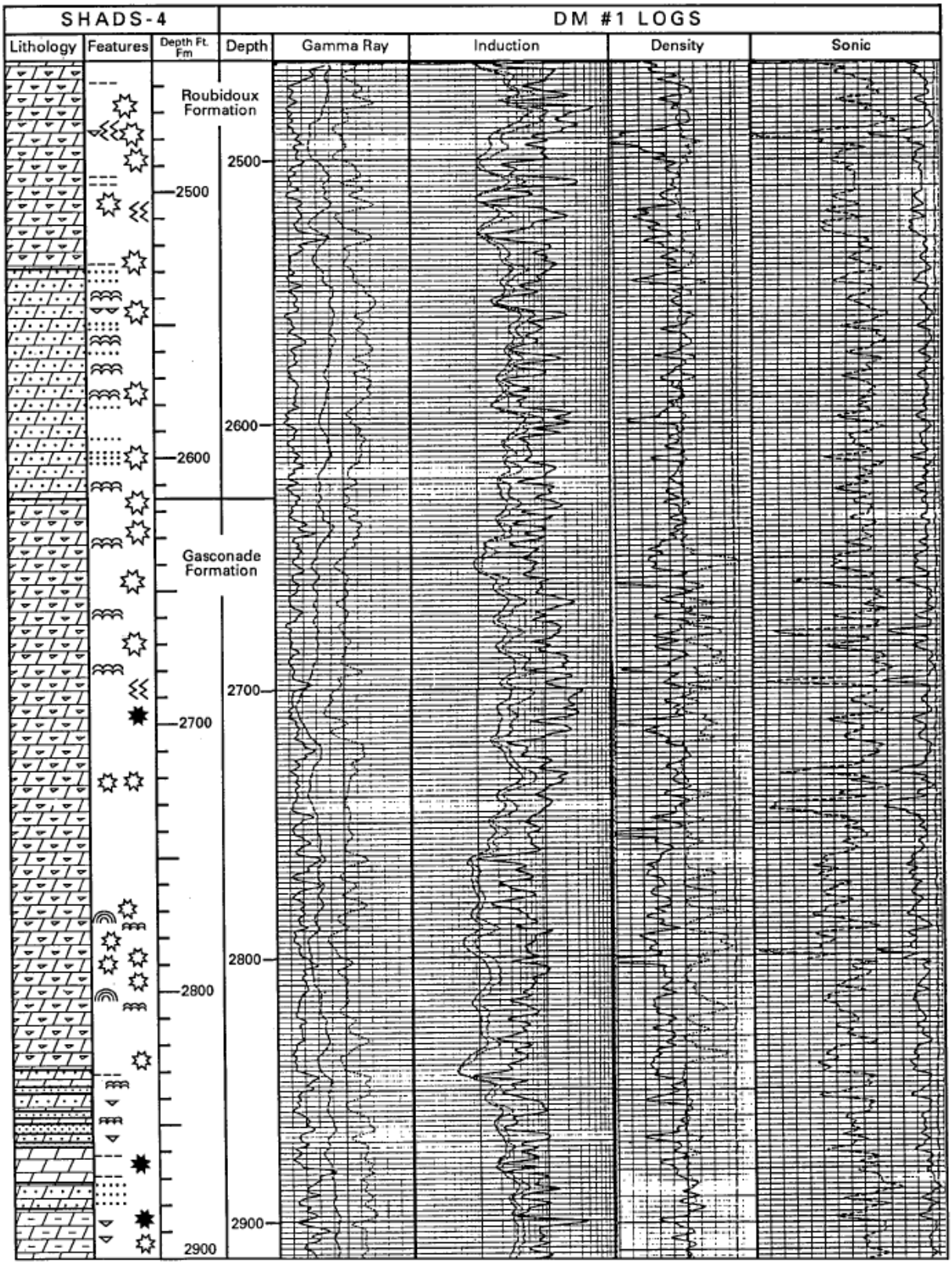


Figure B-1: (continued)

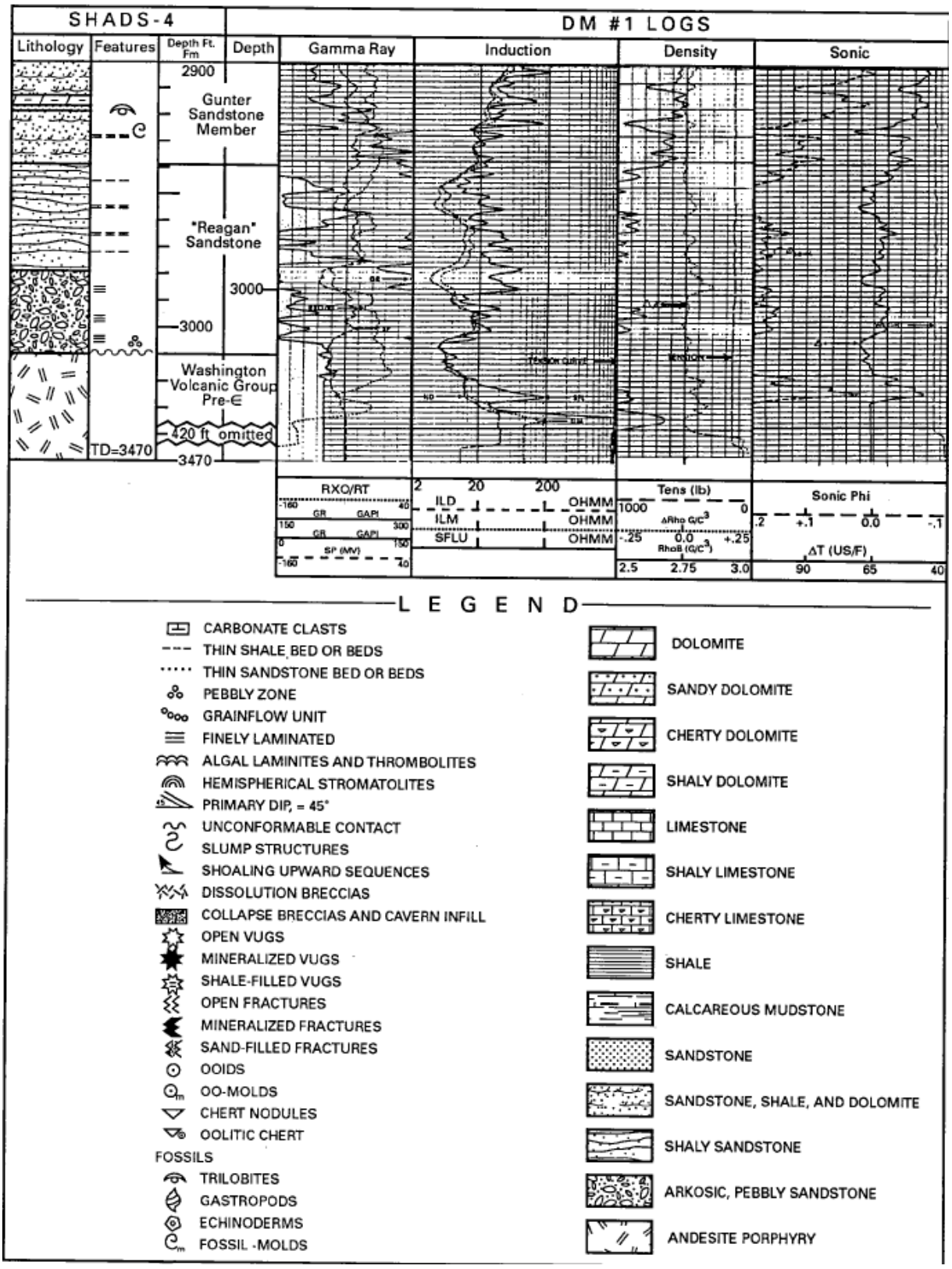


Figure B-1: (continued)



Figure C-2: Shad 4 core photos showing large open vugs. Box. 250 2789-2799

Well	AVG RHOB	AVG DT	AVG PHIN	AVG PHID	AVG PHIS	AVG Secondary Por
35007240850000	2.76	47.4	6%	5%	2%	3%
35007248670000	2.77	51.7	6%	4%	5%	1%
35025210090000	2.77	49.7	5%	4%	4%	1%
35027213910000	2.68	57.2	11%	9%	9%	1%
35027213920000	2.68	54.1	9%	9%	7%	2%
35037287530000	2.62	55.7	13%	13%	8%	4%
35037290940000	2.60	60.8	21%	14%	12%	3%
35037291010000	2.65	57.2	17%	11%	9%	2%
35047241630000	2.76	47.5	6%	5%	2%	3%
35047244030000	2.73	50.3	8%	6%	4%	2%
35047244940000	2.77	52.3	5%	4%	6%	0%
35047245340000	2.75	50.7	6%	5%	5%	1%
35047248140000	2.73	52.0	9%	6%	6%	1%
35047249030000	2.76	49.5	6%	5%	4%	1%
35049239020000	2.66	56.0	6%	11%	8%	2%
35049243260000	2.74	48.0	5%	6%	3%	3%
35051230980000	2.79	47.6	4%	3%	3%	1%
35051231640000	2.75	49.3	5%	5%	4%	2%
35051233760000	2.75	51.5	7%	6%	5%	1%
35051234100000	2.80	47.6	3%	3%	3%	1%
35051234570000	2.74	53.3	8%	6%	6%	0%
35059216240000	2.74	45.2	7%	6%	1%	5%
35063243500000	2.78	48.6	4%	4%	3%	1%
35063243590000	2.75	47.1	3%	5%	2%	3%
35071240240000	2.72	50.2	7%	7%	4%	3%
35071240250000	2.65	51.5	8%	11%	5%	6%
35071248840000	2.70	52.8	8%	8%	6%	2%
35073240810000	2.80	50.0	5%	3%	4%	1%
35073248600000	2.68	55.2	9%	9%	8%	1%
35079206950000	2.79	48.5	6%	3%	3%	1%
35081239070000	2.49	59.1	5%	20%	10%	9%
35087210640000	2.68	63.4	15%	9%	13%	0%
35087212520000	2.67	57.6	11%	10%	9%	1%
35087216840000	2.70	56.7	14%	8%	9%	1%
35087216920000	2.76	50.3	7%	5%	4%	1%
35087217790000	2.70	54.3	7%	8%	7%	1%
35087220030000	2.65	54.3	5%	11%	7%	4%
35091213850000	2.74	51.1	6%	6%	5%	1%
35103240090000	2.70	53.0	9%	8%	6%	2%

35103240380000	2.74	49.7	7%	6%	4%	2%
35103247150000	2.75	53.7	6%	5%	7%	0%
35107233750000	2.67	57.2	10%	9%	9%	1%
35107233760000	2.72	51.3	6%	7%	5%	2%
35107234220000	2.74	56.2	6%	6%	9%	0%
35107234560000	2.73	52.4	10%	7%	6%	1%
35111273680000	2.72	48.5	10%	7%	3%	4%
35113406910000	2.70	53.1	4%	8%	6%	2%
35113409970000	2.75	58.1	7%	5%	10%	0%
35113410500000	2.68	54.8	9%	9%	8%	2%
35121214960000	2.77	51.4	5%	4%	5%	0%
35121228370000	2.79	48.6	5%	3%	3%	1%
35125237090000	2.70	56.6	10%	8%	9%	1%
35125237550000	2.76	50.9	7%	5%	5%	1%
35125239340000	2.62	69.6	21%	12%	18%	0%
35135201380000	2.73	57.2	6%	7%	9%	0%
35143241430000	2.73	58.3	8%	7%	10%	0%
35151219450000	2.78	48.2	5%	4%	3%	1%
35151226020000	2.70	48.8	6%	8%	3%	5%
35153234690000	2.78	49.2	6%	4%	4%	1%
AVERAGE	2.72	52.7	8%	7%	6%	2%

Figure C-3: Secondary (Vugular) Porosity averages for the Arbuckle zone.